Regulation of the activity of the *Escherichia coli* ABC transporter haemolysin B

Inaugural-Dissertation

zur Erlangung des Doktorgrades
der Mathematisch-Naturwissenschaftlichen Fakultät
der Heinrich-Heine-Universität Düsseldorf

vorgelegt von

Sven Reimann
aus Haan

Düsseldorf, April 2017

aus dem Institut für Biochemie
der Heinrich-Heine-Universität Düsseldorf

Gedruckt mit der Genehmigung der
Mathematisch-Naturwissenschaftlichen Fakultät
der Heinrich-Heine-Universität Düsseldorf.

Referent: Prof. Dr. Lutz Schmitt
Korreferent: Prof. Dr. Karl-Erich Jaeger

Tag der mündlichen Prüfung: 16.05.2017

“Nothing in life is to be feared, it is only to be understood.
Now is the time to understand more, so that we may fear less. “

Marie Skłodowska-Curie

Abstract

The toxin haemolysin A (HlyA) is associated with the majority of uropathogenic *Escherichia coli* (UPEC) strains, which cause severe diseases in human. HlyA belongs to the repeats in toxin (RTX) superfamily and is one of the virulence factors, which is secreted by the type 1 secretion system (T1SS) of Gram-negative bacteria. The T1SS nanomachinery is composed of three proteins, the outer membrane protein TolC, the membrane fusion protein haemolysin D (HlyD) and the ATP-binding cassette (ABC) transporter haemolysin B (HlyB). Substrates of the T1SS are transported in an unfolded state across both membranes and without the formation of periplasmic intermediates. Here, the ABC transporter HlyB fulfils a central role during the translocation of the toxin. HlyB is located in the inner membrane of the bacterial cell envelope and it is supposed to energize the translocation mechanism by the consumption of ATP. Therefore, the activity of the protein is supposed to be strictly regulated to prevent futile ATP hydrolysis. Aside from the canonical nucleotide-binding domain and the transmembrane domain, HlyB contains a C39-peptidase like domain (CLD). This additional domain is essential for the secretion process of HlyA, however, its precise role and mechanism is not understood in every detail until now. This doctoral research investigates the regulation of the activity of HlyB and thereby contributes to a more detailed fundamental understanding of the HlyA T1SS translocation machinery.

In order to investigate HlyB *in vitro*, a protocol was established to purify, store and characterise the protein. It could be demonstrated, that the solubilised ABC transporter exhibits a positive cooperativity in ATP hydrolysis. In addition, the CLD of HlyB was analysed in this context and it was found to significantly reduce HlyB basal ATPase activity, whereas it does not affect the substrate-binding affinity. It was concluded that the CLD assumes a regulatory role with an autoinhibitory function.

Furthermore, it was found that HlyB ATPase activity is inhibited or stimulated depending on HlyA concentration and this modulation is generally independent of the secretion signal. By a mutational analysis it was shown that the CLD mediates HlyB ATPase inhibition by an interaction with the substrate. Additional cross-linking experiments suggested that the transmembrane domain also interacts with the substrate and thereby mediating ATPase stimulation. These studies also suppose that both, ATPase inhibition and stimulation, go along with distinct conformational arrangements of HlyB domains.

This doctoral research also deals with the characterisation of the HlyA RTX domain and its influence on the regulation of HlyB. It could be shown that the RTX repeats, a subunit of the RTX domain, interact with the CLD of HlyB and thereby inducing ATPase inhibition. Additionally, it was shown that the most C-terminal RTX repeat is also involved in ATPase stimulation, which might be connected to a predicted α-helical secondary structure located close to this region.

Zusammenfassung

Das Toxin Hämolysin A (HlyA) ist mit einem Großteil uropathogener *Escherichia coli* (UPEC) Stämme assoziiert, welche schwere Erkrankungen des Menschen verursachen. HlyA gehört zu der *repeats in toxin* (RTX) Superfamilie und ist einer der Virulenzfaktoren, die vom Typ 1 Sekretionssystem (T1SS) Gram-negativer Bakterien sekretiert werden. Die T1SS Nanomaschinerie ist aus drei Proteinen zusammengestellt, dem äußeren Membranprotein TolC, dem Membranfusionsprotein Hämolysin D (HlyD) und dem ATP-*binding cassette* (ABC) Transporter Hämolysin B (HlyB). Die Substrate des T1SS werden in einem ungefalteten Zustand und ohne die Ausbildung eines periplasmatischen Zwischenproduktes über beide Membranen transportiert. Hierbei übernimmt der ABC Transporter HlyB eine zentrale Rolle während der Translokation des Toxins. HlyB ist in der inneren Membran der bakteriellen Zellhülle lokalisiert und es wird angenommen, dass es den Translokationsmechanismus durch den Verbrauch von ATP energetisiert. Daher wird postuliert, dass die Aktivität des Proteins strengstens reguliert wird, um sinnlose ATP Hydrolyse zu verhindern. Außer der kanonischen Nukleotidbindedomäne und der Transmembrandomäne, beinhaltet HlyB eine C39-Peptidase ähnliche Domäne (CLD). Diese zusätzliche Domäne ist essentiell für den Sekretionsprozess von HlyA, dennoch ist dessen präzise Rolle und Mechanismus bisher nicht in allen Einzelheiten verstanden. Diese Doktorarbeit erforscht die Regulation der Aktivität von HlyB und trägt dadurch zu einem detaillierteren fundamentalen Verständnis der HlyA T1SS Translokationsmaschinerie bei.

Um HlyB *in vitro* zu erforschen, wurde ein Protokoll etabliert, um das Protein zu reinigen, zu lagern und zu charakterisieren. Es konnte gezeigt werden, dass der solubilisierte ABC Transporter eine positive Kooperativität bezüglich der ATP-Hydrolyse aufweist. Zusätzlich wurde in diesem Kontext die CLD von HlyB analysiert und es wurde festgestellt, dass sie die basale HlyB ATPase Aktivität signifikant reduziert, wohingegen sie die Substrat Bindungsaffinität nicht beeinflusst. Daraus wurde die Schlussfolgerung gezogen, dass die CLD eine regulatorische Rolle mit einer autoinhibitorischen Funktion übernimmt.

Darüber hinaus wurde festgestellt, dass die HlyB ATPase Aktivität in Abhängigkeit von der HlyA Konzentration inhibiert oder stimuliert wird und diese Modulation ist generell unabhängig vom Sekretionssignal. Mittels einer Mutationsanalyse wurde gezeigt, dass die CLD die HlyB ATPase Inhibition durch eine Interaktion mit dem Substrat vermittelt. Zusätzliche *cross-linking* Experimente suggerierten, dass die Transmembrandomäne ebenfalls mit dem Substrat interagiert und dadurch die ATPase Stimulation vermittelt. Diese Studien lassen auch vermuten, dass die ATPase Inhibition und Stimulation mit unterschiedlichen konformationellen Anordnungen der HlyB Domänen einhergehen.

Diese Doktorarbeit handelt auch von der Charakterisierung der HlyA RTX Domäne und deren Einfluss auf die Regulation von HlyB. Es konnte gezeigt werden, dass die RTX *repeats*, eine Untereinheit der

RTX Domäne, mit der CLD von HlyB interagieren und dadurch die ATPase Inhibition induzieren. Zusätzlich wurde gezeigt, dass das C-terminalste RTX *repeat* ebenfalls an der ATPase Stimulation beteiligt ist, was möglicherweise mit einer vorhergesagten α-helikalen Sekundärstruktur in Verbindung steht, welche nahe dieser Region lokalisiert ist.

Table of Contents

List of figures

List of abbreviations

Å	Ångstrom
A. aeolicus	*Aquifex aeolicus*
A. tumefaciens	*Agrobacterium tumefaciens*
aaRS	aminoacyl-tRNA synthetase
ABC	ATP-binding cassette
ACP	acyl carrier protein
ADP	Adenosine diphosphate
Apa	*p*-azidophenylalanine
ATP	Adenosine triphosphate
B. anthracis	*Bacillus anthracis*
B. pertussis	*Bordetella pertussis*
B. subtilis	*Bacillus subtilis*
Bpa	*p*-benzoyl-L-phenylalanine
C. difficile	*Clostridium difficile*
CBB	Coomassie Brilliant Blue
CFTR	cystic fibrosis transmembrane conductance regulator
CHO	Chinese Hamster Ovary
CLD	C39-peptidase like domain
CMC	critical micellar concentration
CP	cytoplasm
csg	curli-specific genes
CU	chaperone-usher
CyaA	adenylate cyclase toxin-haemolysin
DNA	deoxyribonucleic acid
E. chrysanthemi	*Erwinia chrysanthemi*
E. coli	*Escherichia coli*
E. tarda	*Edwardsiella tarda*
e.g.	exempli gratia
EC	Enzyme Commission
EDTA	ethylenediaminetetraacetic acid
eGFP	enhanced Green Fluorescence Protein
EPEC	enteropathogenic *E. coli*

GSP	general secretion pathway
HCD	higher-energy collisional dissociation
HlyA	haemolysin A
HlyA*	HlyA amber variant
HlyA1	N-terminally truncated variant of HlyA
HlyA2	N-terminally truncated variant of HlyA1
HlyB	haemolysin B
HlyC	haemolysin C
HlyD	haemolysin D
IM	inner membrane
IMAC	immobilized metal-ion-affinity chromatography
K. pneumoniae	*Klebsiella pneumoniae*
K_D	dissociation constant
kDa	kilo Dalton
L. lactis	*Lactococcus lactis*
L. monocytogenes	*Listeria monocytogenes*
LMNG	lauryl maltose neopentyl glycol
LPS	lipopolysaccharide
M. jannaschii	*Methanocaldococcus jannaschii*
M. leprae	*Mycobacterium leprae*
M. tubercolosis	*Mycobacterium tubercolosis*
MARTX	multifunctional autoprocessing RTX toxins
MATE	multidrug and toxic compound extrusion
MD	molecular dynamic
MFP	membrane fusion protein
MFS	major facilitator superfamily
µg	microgram
mg	milligram
min	minutes
µl	microlitre
ml	millilitre
µM	micromolar
mM	millimolar
NBD	nucleotide-binding domain
nm	nanometre

NMR	nuclear magnetic resonance
OEP	outer membrane efflux proteins
OM	outer membrane
OMP	outer membrane protein
P. aeruginosa	*Pseudomonas aeruginosa*
P. fluorescens	*Pseudomonas fluorescens*
P. pastoris	*Pichia pastoris*
P. putida	*Pseudomonas putida*
PAGE	polyacrylamide gel electrophoresis
PCAT	C39-peptidase containing ABC transporter
pdb	Protein Data Bank
pI	isoelectric point
PMF	proton motive force
PP	periplasm
pro-HlyA	non-toxic pre-protein
RMSD	root mean square deviation
RND	resistance-nodulation-division
RTX	repeats in toxin
RTX repeats	glycine-rich repeats of the RTX domain
S. aureus	*Staphylococcus aureus*
S. cerevisiae	*Saccharomyces cerevisiae*
S. marcescens	*Serratia marcescens*
SBP	substrate-binding protein
SDS	sodium dodecyl sulphate
SEC	size exclusion chromatography
Sec	general secretory
SMR	small multidrug resistance
SPR	surface plasmon resonance
SRP	signal recognition particle
T1SS	Type I secretion system
T2SS	Type II secretion system
T3SS	Type III secretion system
T4SS	Type IV secretion system
T5SS	Type V secretion system
T6SS	Type VI secretion system

T7SS	Type VII secretion system
T8SS	Type VIII secretion system
Tat	twin arginine translocation
TBS	Tris-buffered saline
TBS-T	TBS with Tween 20
TC	Transporter Classification
TEV	tobacco etch virus
TFA	trifluoroacetic acid
TMD	transmembrane domain
UPEC	uropathogenic *Escherichia coli*
V. cholerae	*Vibrio cholerae*
X. axonopodis	*Xanthomonas axonopodis*
Y. enterocolitica	*Yersinia enterocolitica*

Amino Acids	**Three letter code**	**One letter code**
Alanine	Ala	A
Arginine	Arg	R
Asparagine	Asn	N
Aspartic Acid	Asp	D
Cysteine	Cys	C
Glutamic Acid	Glu	E
Glutamine	Gln	Q
Glycine	Gly	G
Histidine	His	H
Isoleucine	Ile	I
Leucine	Leu	L
Lysine	Lys	K
Methionine	Met	M
Phenylalanine	Phe	F
Proline	Pro	P
Serine	Ser	S
Threonine	Thr	T
Tryptophan	Trp	W
Tyrosine	Tyr	Y
Valine	Val	V

1. Introduction

1.1. Membrane transport

Cells are considered the basic units of life and they are surrounded by a membrane that constitutes the cell envelope. The bacterial membrane is a multilayered structure that protects the organism and assures multiple functions (Glauert *et al.*, 1969). It separates the cellular and extracellular space and enables the bacteria to regulate the exchange of e.g. nutrients with its surrounding. The membrane is impermeable for ions, large molecules or small hydrophilic molecules, while small hydrophobic or neutral compounds such as oxygen can permeate through the envelope (Gouaux *et al.*, 2005). The exchange of further components is enabled by membrane embedded proteins, mediating the transport or facilitated diffusion. In order to pump a compound uphill against its electrochemical gradient, this transport process requires energy. The necessary energy for the transport can be provided by e.g. light, ATP hydrolysis or by the coupling to the transport of a second substrate along a concentration gradient (Boyer, 1997; Lanyi, 2004). Besides transporters, bacterial membranes also contain proteins that are involved in sensing the environmental conditions, locomotion, adhesion, signal transduction or pathogenicity.

1.2. Protein secretion systems

Bacteria can be classified in two major groups depending on the technique of Gram staining (Gram, 1884). Gram-positive bacteria contain a thick peptidoglycan cell wall at the exterior of their membrane comprising multi layers, while Gram-negative bacteria are composed of an inner and outer membrane and a thin peptidoglycan layer in between (Rogers *et al.*, 1980). For most bacteria the composition of the peptidoglycan is strongly conserved (Vollmer *et al.*, 2008a; Vollmer *et al.*, 2008b). Glycan strands are composed of alternating *N*-acetylglucosamin and *N*-acetylmuramic acid residues linked by β-1→4 glycoside bonds. These linear glycan strands are cross-linked by short peptides composed of L-Ala-γ-D-Glu-meso-A2pm (or L-Lys)-D-Ala-D-Ala (A2pm, 2,6-diaminopimelic acid) (Rogers *et al.*, 1980; Vollmer *et al.*, 2008b).

Bacterial membranes are formed by amphiphilic lipids, which are composed in most cases of glycerophospholipids. These contain a glycerol moiety, two fatty acids and a phosphate group with a variable head group. Depending on this composition the glycerophospholipids are for example phosphatidylethanolamin, phosphatidylglycerol, phosphatidylinositol or phosphatidylserine. Also

phosphorus free membrane lipids are common in bacteria, e.g. sulfolipids, glycolipids or diacylglycerol (Sohlenkamp *et al.*, 2016). It is suggested that cells are able to replace phospholipids by phosphorus-free lipids under phosphate starvation or stress (Geiger *et al.*, 1999; Riekhof *et al.*, 2014; Vences-Guzman *et al.*, 2013).

Protein secretion across the cell envelope of both, Gram-positive and Gram-negative bacteria, is a remarkable and essential process. It is important to almost all bacteria and plays a central role in modulating biotic association and interaction between pathogenic or symbiotic bacteria with their eukaryotic hosts. The secreted substrates can be associated with the bacterial outer membrane, they are released into the extracellular space or they are injected into a target cell, depending on the secretion system (Gerlach *et al.*, 2007).

Besides the secretion systems that transport substrates into the extracellular space, bacteria also comprise secretion systems mediating the translocation from the cytoplasm compartment into other compartments of the cell, particularly into or across the inner membrane. Two systems are responsible for this type of protein secretion [reviewed in (Natale *et al.*, 2008)]: the general secretion pathway (Sec pathway) (Danese *et al.*, 1998; Wickner *et al.*, 1991) and the twin-arginine translocation pathway (Tat pathway) (Berks *et al.*, 2005; Robinson *et al.*, 2004). Interestingly in every organism for which a genome has been completely sequenced, homologues of the components of the Sec pathway are present (Cao *et al.*, 2003).

1.2.1. The general secretion pathway

The Sec pathway mediates the transport of unfolded proteins into the periplasmic/endoplasmatic lumen or allows lipid insertion of membrane proteins. The Sec translocon is built of a three-subunit core, which is termed Sec61 in eukaryotes and archaea, and SecYEG in bacteria. The subunits SecY and SecE exhibit significant sequence conservation and are essential for the translocation process (Kudva *et al.*, 2013; Park *et al.*, 2012). Additional to the translocase core units a number of prokaryotes and eukaryotes encode accessory proteins, which are important in the secretion of a vast array of proteins. Some of the Sec apparatus substrates can serve as virulence factors as it is shown for e.g. the Gram-negative bacteria *Vibrio cholerae*, *Klebsiella pneumoniae* and *Yersinia enterocolitica* (Korotkov *et al.*, 2012). To deliver proteins to the Sec translocon bacteria use two different targeting pathways mediated by different proteins (Beck *et al.*, 2000). (i) Proteins that are targeting the periplasm, the outer membrane or the extracellular space are transported by the SecA-dependent pathway, which contain a cleavable signal sequence. Here, the unfolded peptide is kept in a translocation-competent state by cytosolic chaperones, including the trigger factor and tetrameric SecB (Deuerling *et al.*, 2003; Driessen, 2001; Valent *et al.*, 1995). This protein complex is transferred post-translational to SecA, which energises the translocation through the SecYEG translocon by ATP hydrolysis (Driessen, 2001;

Fekkes *et al.*, 1999). (ii) Proteins that are targeting and remaining in the inner membrane interact with the ribosome-bound signal recognition particle (SRP) co-translational (Luirink *et al.*, 2005). This protein complex is targeted to the Sec-translocase and binds to the SRP receptor FtsY, which is located at the SecYEG translocon. The secretion substrate docks onto SecYEG and the membrane integration is supported by the insertase YidC (Beck *et al.*, 2001; Nagamori *et al.*, 2004).

1.2.2. The twin-arginine translocation pathway

The Tat pathway system primarily serves to transport folded proteins across biological membranes (Robinson *et al.*, 2004). The system occurs in the cytoplasmic membranes of most bacteria, archaea and some plants (Muller *et al.*, 2005; Yen *et al.*, 2002). Some post-translational modifications, e.g. the assembly of cofactors can only be done in the cytoplasm prior to the secretion process and not in the extracellular space. This necessity seems to make the Tat system crucial to the organism. Interestingly there are also substrates which highly identical orthologs are transported by both, the Tat and the Sec pathway, depending on the organism (Chen *et al.*, 1996; Harris *et al.*, 2005). In some cases it is still unclear why these proteins are translocated by the Tat pathway, even when the correlating cofactor is assembled after translocation (Sturm *et al.*, 2006). In Gram-negative bacteria the system consists of three subunits: TatA, TatB and TatC (Sargent *et al.*, 1999). The signal peptide of a Tat-secreted protein is bound in *Escherichia coli* by TatB and TatC, which then recruit TatA, together they form the membrane-spanning channel (Muller, 2005). The energy for the translocation process is provided by the proton motif force (PMF). The secretion signal of the transport substrate obtains a pair of arginines in the motif S-R-R at the N-terminus and it is essential for the secretion process (Muller, 2005).

1.3. Gram-negative bacterial secretion systems

In contrast to the pathways that only span the inner membrane (IM), Gram-negative bacteria have evolved macromolecular nanomachineries that span both, the IM and the outer membrane (OM) or the OM only. Secretion systems that span the OM only, depend on the prior substrate transport across the IM. Therefore, these secretion systems are known as Sec- or Tat-dependent protein secretion. To date five double-membrane-spanning secretion systems are identified and classified as the type I secretion system (T1SS), T2SS, T3SS, T4SS and T6SS. The T5SS and machineries that assemble cell surface appendages (type I pili, P pili, curli) only span the OM. In the following these secretion system are described in further detail.

1.3.1. Type I secretion system

The substrates of the bacterial T1SS are of large variety. The secreted products are diverse in size and function and they are associated with nutrient acquisition and virulence. In terms of the architectural composition the T1SS is closely related to the resistance-nodulation-division (RND) family. RND transporters also act as a tripartite system and can be classified into further subfamilies. They transport small molecules out of the cell, e.g. antibacterial compounds and thus mediating an antibiotic resistance [for a detailed review, see Anes *et al.* (2015)]. The T1SS tripartite membrane-spanning system is composed of an IM component, a membrane fusion protein (MFP) and the OM protein channel TolC (Figure 1).

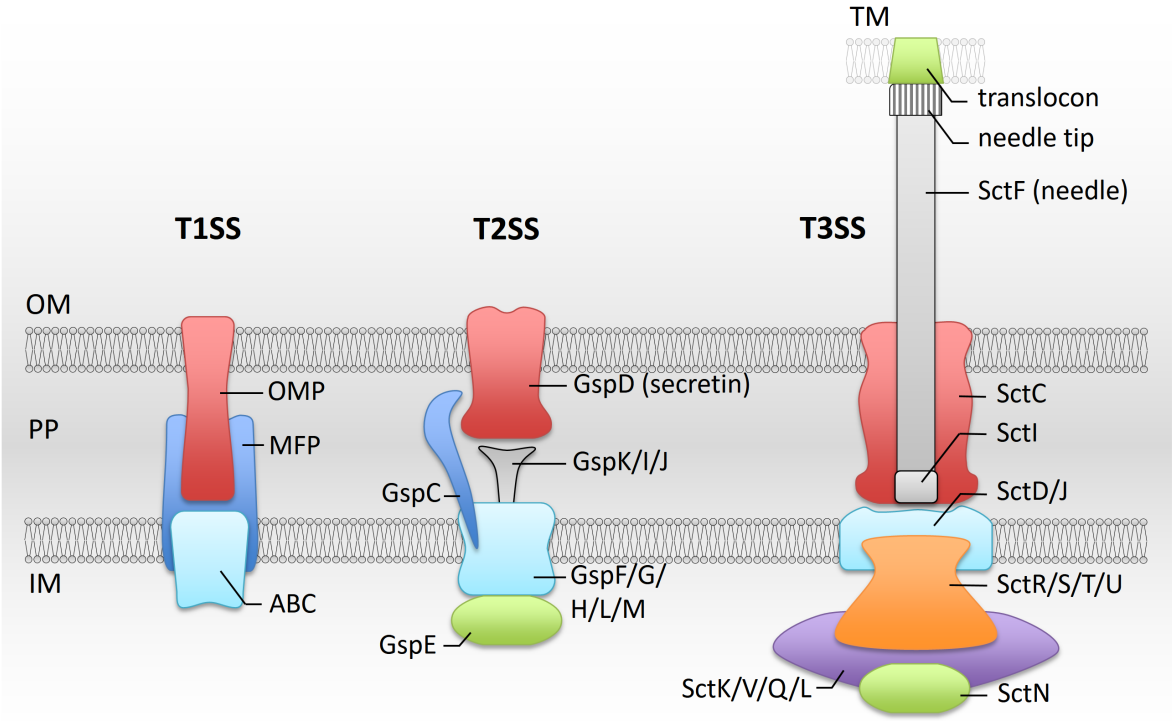

Figure 1. Schematic overview of the structural organisation of the T1SS, T2SS and the T3SS. The type 1 secretion system (T1SS) and the resistance-nodulation-division pumps share the blueprint of an outer membrane protein (OMP), a membrane fusion protein (MFP) and an IM transporter/pump, which energizes the translocation process. The type 2 secretion system (T2SS) can be divided in four compartments: an OM complex (secretin), an IM platform, the cytoplasmic ATPase and the periplasmic pseudopilus. The type 3 secretion system (T3SS) is composed of the so-called 'base' and the 'needle'. The base is composed of the inner and the outer rings, which are connected by the 'neck'. The extended filament ranges into the host cell, while the needle tip mediates host cell contact and adhesion.

The IM component is an ATP-binding cassette (ABC) transporter that functions as a dimer and energises the system by hydrolysis of ATP. The MFP is known to be either pre-associated with the ABC transporter or recruited to it upon substrate interaction (Balakrishnan *et al.*, 2001; Delepelaire, 2004). The trimer TolC forms α-helical channel in the periplasm and a β-barrel channel in the OM that occurs

to open and close upon a twisting motion (Balakrishnan *et al.*, 2001; Bavro *et al.*, 2008; Koronakis *et al.*, 2004).

1.3.2. Type II secretion system

The type II secretion system (T2SS) is localized in the OM and dependent on the Sec or Tat pathway to transport the substrate across the inner membrane (Figure 1). T2SS secrete folded proteins from the periplasm into the extracellular space. In some bacteria the system translocates a single protein, while in others multiple substrates seem to be secreted (Cianciotto, 2005). For example in *Pseudomonas aeruginosa* (Ball *et al.*, 2002), *Pseudomonas putida* (De Vrind *et al.*, 2003) and *Xanthomonas axonopodis* (da Silva *et al.*, 2002) additional T2SS were found that mediate the transport of distinct substrates. The substrates of the T2SS include a broad range of enzymes, e.g. proteases, phosphatases and lipases (Korotkov *et al.*, 2012). Some are crucial for virulence in a mammalian host such as the cholera toxin of *V. cholerae* and the exotoxin A of *P. aeruginosa* (Lu *et al.*, 1996; Sandkvist *et al.*, 1997). The translocon is composed of 12-15 proteins, which are also called the general secretion pathway (Gsp) in *E. coli* (Korotkov *et al.*, 2012). The proteins can be grouped in four parts: an OM complex (secretin), an IM platform, the cytoplasmic ATPase and the periplasmic pseudopilus (Korotkov *et al.*, 2012). The pseudopilus remains within the periplasm in contrast to a pilus that extends into the extracellular space. It is suggested that ATP hydrolysis powers both, the assembly of the pseudopilus and to push substrates across the OM. The OM complex is composed of a multimeric protein, which is called secretin and it is believed to extend into the periplasm connecting with inner membrane components (Korotkov *et al.*, 2011). On the other side the inner membrane platform is composed of at least four proteins and extends into the periplasm to contact the OM complex. A “piston”-like model of the secretion process proposes that a retraction of the pseudopilus pushes the secretion-competent substrate through the outer membrane secretin channel (Hobbs *et al.*, 1993; Korotkov *et al.*, 2012; Shevchik *et al.*, 1997).

1.3.3. Type III secretion system

The double-membrane embedded type III secretion system (T3SS) is found in various pathogenic species such as *Yersinia, Salmonella, Shigella* or enteropathogenic *E. coli* (EPEC) (Galan *et al.*, 2006). It spans both membranes and obtains a “needle”-like apparatus that promotes the “injection” of bacterial effector proteins to the cytoplasm or the membrane of the target eukaryotic cell (Figure 1) (Hu *et al.*, 2015). The translocated substrates remodel the cellular functions and enable the pathogens to establish an infectious niche, however, the precise effects are still being investigated (Angot *et al.*, 2007; Ham *et al.*, 2011; Spano *et al.*, 2013; Tosi *et al.*, 2013). The amount of secreted effector proteins

varies depending on the pathogen (Buttner, 2012; Cornelis, 2006). The translocon is composed of the so-called base and the needle. The base can be subdivided in the two concentric inner rings, which are connected by the so-called neck to the outer rings (Worrall *et al.*, 2016). The inner rings are located in the IM and the outer rings are located in the OM. The needle-filament is a tube-like helical structure with a tip complex and forms a channel from the OM into the interior of the host cell (Kimbrough *et al.*, 2000; Kubori *et al.*, 2000). Typically the needle has a length of 30-70 nm and a width of 10-13 nm (Marlovits *et al.*, 2006; Poyraz *et al.*, 2010). It has been shown that the inner core of the filament is wide enough to channel an unfolded effector substrate (Deane *et al.*, 2006; Demers *et al.*, 2014). The translocation process of the unfolded proteins is highly regulated to ensure the correct hierarchical coordination of each step (Buttner, 2012; Galan *et al.*, 2014; Izore *et al.*, 2011). The information is encoded by the secretion signal, which is located within the N-terminal first 100 residues of the translocated protein (Buttner, 2012; Galan *et al.*, 2014). Specific T3SS chaperones keep the effector protein in secretion-competent state and the chaperone-substrate complex is recognized and transported by the machinery (Parsot *et al.*, 2003). However, little is known about the recognition and transport of the chaperone-substrate complex, the translocation is an ATP-dependent process.

1.3.4. Type IV secretion system

The type IV secretion system (T4SS) is found in Gram-negative bacteria, Gram-positive bacteria and in some archaea (Alvarez-Martinez *et al.*, 2009). It is the most ubiquitous secretion system and one remarkable feature of the T4SS is the ability to secrete single proteins and also DNA into bacterial and eukaryotic cells, mediating the conjugation of plasmid DNA (Bradley, 1980; Durrenberger *et al.*, 1991). Thereby the conjugative pili obtain a special tip, which are suggested to function for cell-to-cell adhesion and establishing the contact to transport single-stranded DNA. All T4SS share an evolutionarily related blueprint, however, the VirB/D4 system of *Agrobacterium tumefaciens* is one of the best-studied (Alvarez-Martinez *et al.*, 2009). Its translocation system is built of 12 different proteins: the translocation apparatus is constructed of six proteins, three ATPases energize the system, the pilus is formed by two proteins and one protein degrades the peptidoglycan layer for pilus biogenesis (Figure 2) (Trokter *et al.*, 2014). Crystal structures of isolated compartments of the T4SS revealed limited insights into the T4SS so far, however, due to the absence of single proteins it was not possible to derive the complete translocation mechanism (Costa *et al.*, 2015). Nevertheless, a study in *A. tumefaciens* using a cross-linking assay, revealed the substrate translocation pathway of the VirB/D4 T4SS (Cascales *et al.*, 2004b). Within the first steps the substrate interacts successively with multiple proteins, which is independent of ATP hydrolysis (Atmakuri *et al.*, 2004). Here, the VirD4 protein is the first interaction partner and recruiting the substrate to the secretion apparatus (Atmakuri *et al.*, 2004). Then the substrate reaches the inner membrane compartments of the translocon and ATP hydrolysis

becomes necessary. Finally, the substrate is transferred to the outer-membrane components and the pili. Interestingly, the membrane-bridging protein VirB10 changes its conformation in response to ATP utilisation and thereby delivering the substrate from the IM to the OM-associated compartment (Cascales *et al.*, 2004a).

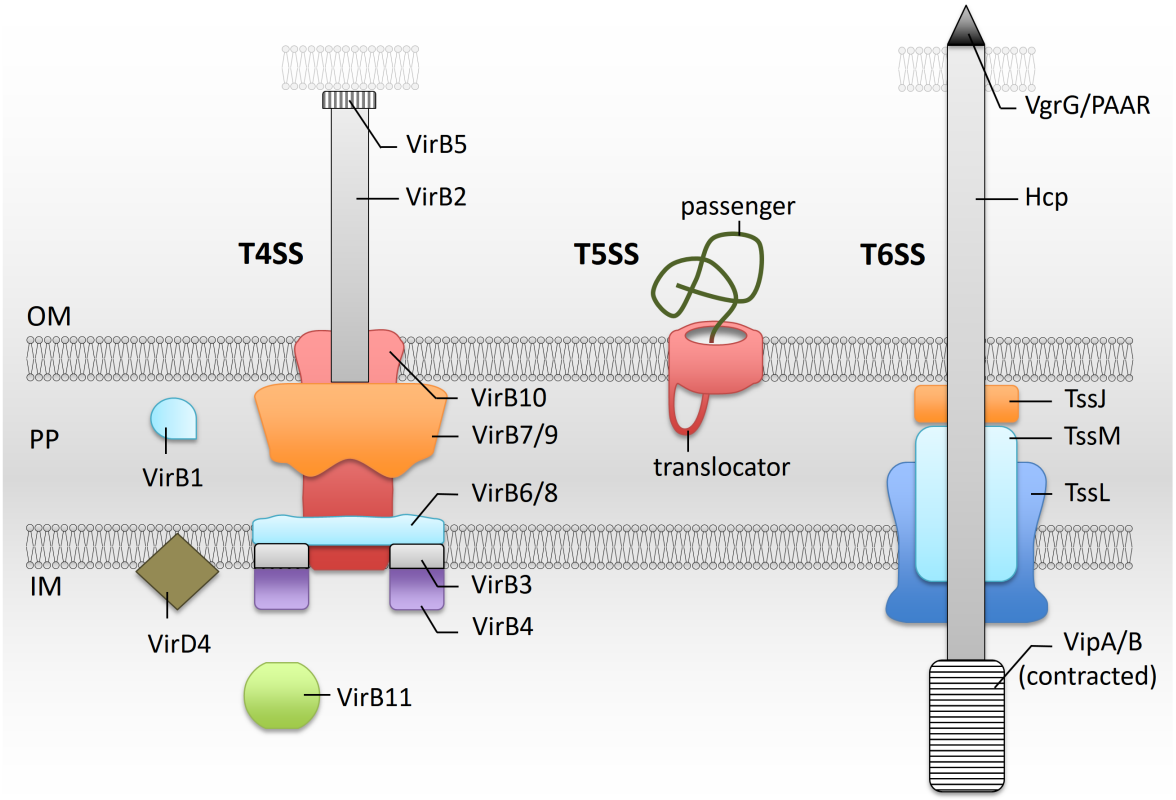

Figure 2. Schematic overview of the structural organisation of the T4SS, T5SS and the T6SS. The type 4 secretion system (T4SS) is built of 12 different proteins that distribute to the translocation apparatus, ATPases, pilus and an enzyme that degrades the peptidoglycan layer. The type 5 secretion system (T5SS) is dependent on the SecYEG translocon (not shown) and is a fused protein composed of the passenger domain and the distinct translocator. The type 6 secretion system (T6SS) is a nanomachine that translocates cell-death mediating effector proteins into the host cell. The apparatus can be subdivided in a membrane-embedded complex spanning from the inner to the outer membrane, and a tail complex that shares an evolutionary origin with the phage injection apparatus.

1.3.5. Type V secretion system

The type V secretion system (T5SS) participates in the translocation of proteins, which are associated with adhesion, colonization, cell mobility, biofilm formation and further virulence factors (Leo *et al.*, 2012). The secretion system is also known as the autotransporter system that mediates the translocation of the substrate through the OM. T5SS proteins have to pass the IM and reach the periplasm prior to the formation of their β-barrel domain, which forms the OM channel. Therefore, these proteins are translocated in an unfolded state by the SecYEG apparatus across the IM and contain the necessary N-terminal Sec signal. The autotransporter protein is a peptide fusion of the secretion

pore and the translocation substrate on one single polypeptide. Therefore, the protein can be divided in two parts: the 'passenger' domain, the domain that is actually translocated through the OM, and the 'translocator', forming the β-barrel pore with a width of about 10 Å (Figure 2) (Ieva *et al.*, 2008). The substrate transport across the OM is ATP independent and energized by the folding of the passenger at the pore exit (Junker *et al.*, 2009). It is known that the passenger domain is secreted through the OM from the C-terminus, however, the exact mechanism is point of investigation (Ieva *et al.*, 2009; Junker *et al.*, 2009). Indeed the T5SS is not a totally self-contained secretion system as expected. Studies demonstrated that chaperones keep the autotransporter polypeptide in an unfolded state within the periplasm and the β-barrel requires the aid of the β-barrel assembly machinery (Bam) (Hagan *et al.*, 2010; Ieva *et al.*, 2011; Roman-Hernandez *et al.*, 2014; Voulhoux *et al.*, 2003; Wu *et al.*, 2005). The T5SSs can be further subdivided into five classes (Leo *et al.*, 2012): (type Va) autotransporter-secretion, (type Vb) two-partner secretion, (type Vc) trimeric autotransporter secretion, (type Vd) fused two-partner secretion and (type Ve) inverted autotransporter-secretion.

1.3.6. Type VI secretion system

The type VI secretion system (T6SS) is a contractile nanomachine that translocates protein effectors to prokaryotic and eukaryotic cells (Russell *et al.*, 2014). A cell-cell contact dependent process triggers a contraction of the system and the delivery of lethal effectors across the target membrane, primarily resulting in the death of the target cell (Hood *et al.*, 2010; Russell *et al.*, 2011). This proximity-dependent defense system against competitors extends the additional repertoire of bacterial released agents such as bacteriocins and antibiotics. The T6SS gene clusters vary depending on the organism. The *evp* and the *hsi-2* gene clusters from *Edwardsielle tarda* and *P. aeruginosa* obtain 16 genes, while the gene cluster in *Serratia marcescens* obtains 38 genes (Cascales, 2008; Murdoch *et al.*, 2011). However, 13 of these appear to be conserved in all T6SS (Green *et al.*, 2016; Russell *et al.*, 2014). The system is the most recent discovered secretion system and there is still much to learn about. The general blueprint can be divided in two main complexes (Figure 2): (i) the membrane-embedded complex built of three membrane-associated subunits and spanning from the IM to the OM (ii) a tail complex that shares an evolutionary origin with the phage injection apparatus (Basler *et al.*, 2012). It is suggested that even the mechanism of the T6SS follows the contraction mechanism of phage tails (Basler *et al.*, 2012; Kudryashev *et al.*, 2015). The actual secretion model proposes three main steps: assembly, contraction and disassembly. The assembly starts with the formation of the membrane-embedded complexes and the elongation of the cytoplasmic tubular structure. Upon contact with a target cell the sheath contracts and ejects the internal tube towards the extracellular space. The contracted sheets are then disassembled by a distinct ATPase and recycled again during the assembly step (Zoued *et al.*, 2014).

1.3.7. Type VII secretion system

The envelope of mycobacteria is composed of a plasma membrane that is equivalent to the IM of Gram-negative bacteria, a periplasm that contains peptidoglycan and arabinogalactan, and an OM with a coat of mycolic acids, which is therefore called the mycomembrane (Houben *et al.*, 2014). The mycolic acids form a hydrophobic and waxy coat, which mediates a strong persistence against antimicrobial enzymes, chemicals and mechanic stress (Houben *et al.*, 2014). Mycobacteria such as *Mycobacterium tuberculosis* and *Mycobacterium leprae* belong to the *Corynebacteriales,* which are characterised by the presence of the mycolic acids in their cell envelope (Goodfellow *et al.*, 2015). Originally the type VII secretion system (T7SS) was identified in 2003 in *M. tubercolosis* and called the ESX-1 system (Stanley *et al.*, 2003). The secreted products were called EsxA and EsxB or initially designated as ESAT-6 and CFP-10, respectively. It has been shown that some of these Esx proteins are also functionally secreted in *Staphylococcus aureus*, *Listeria monocytogenes*, *Bacillus anthracis* and *Bacillus subtilis* (Anderson *et al.*, 2011; Baptista *et al.*, 2013; Burts *et al.*, 2008; Burts *et al.*, 2005; Garufi *et al.*, 2008). The T7SS apparatus and in some cases also their substrates are encoded in a linked gene cluster. In general five proteins are encoded that form the core channel and a membrane protease, which is involved in substrate processing (Solomonson *et al.*, 2013). Furthermore, an ATPase and a chaperone that guides the substrate to the translocon are located within the cytosol (Korotkova *et al.*, 2014). The steps that mediate the substrate through the periplasm are not known and further components that facilitate the transport through the mycomembrane still has to be identified.

1.3.8. Type VIII secretion system / nucleation-precipitation pathway

The type VIII secretion system (T8SS) is also called the nucleation-precipitation pathway and contributes to the production of curli fibers at the cell surface. Curli fibers are filaments built of non-covalent bound subunits and belong to the class of amyloids (Chapman *et al.*, 2002; Zhou *et al.*, 2012). Amyloids are commonly known for causing human diseases by protein misfolding, but they are further suggested to regulate hydrophobicity during fungal reproduction or transcriptional regulation in a variety of organisms (Badtke *et al.*, 2009; Blanco *et al.*, 2012; Breydo *et al.*, 2012; Fowler *et al.*, 2007; Irvine *et al.*, 2008; Zuccato *et al.*, 2010). Curli are known to contribute to biofilm formation and interactions with the host immune system and thereby protecting the bacteria (Hammar *et al.*, 1995; Olsen *et al.*, 1989). The tightly-ordered packing of the subunits confers a resistance against degradation by enzymes or the decomposition by sodium dodecyl sulphate.

E. coli obtains two operons that encode curli-specific genes (*csg*) for the structural components (*csgBAC*) and the assembly apparatus (*csgDEFG*) (Chapman *et al.*, 2002). The curli subunits are CsgA and CsgB, which engage a ratio of approximately 20:1 (CsgA : CsgB) *in vivo* (White *et al.*, 2001). Initially,

the major subunit CsgA is secreted into the periplasm by the SecYEG apparatus. Then, the T8SS translocates CsgA into the extracellular space where it builds the amyloid structure together with the nucleator subunit CsgB. The T8SS apparatus consists of three proteins, the soluble accessory factors CsgE and CsgF, and the lipoprotein transporter CsgG. Latter forms a 36-stranded β-barrel in the OM with a channel opening in the periplasm of 9 Å in diameter. CsgE forms an adapter in the periplasm, binds to the CsgG periplasmic domains and creating a large cage. The unfolded curli subunit CsgA would fit in this periplasmic cage and it is suggested that hereby an entropy gradient is created, facilitating the diffusion into the extracellular space. The roles of further proteins in this context remains unclear, however, they are suggested to be involved in stimulating the assembly of CsgA at the outside of the cell (Nenninger *et al.*, 2009). Also the order of assembly of the secretion complex and the incorporation of the curli subunits into curli fibers have to be investigated.

1.3.9. Chaperone-usher pathway

The assembly and the secretion of pili is mediated by the chaperone-usher (CU) pathway. The pili are anchored in the outer bacterial membrane by their distinct machinery, the usher, and extend from the surface as fibres with a length in micrometre scale. They mediate host cell recognition and the attachment to urinary tract epithelium (Lillington *et al.*, 2015). With these properties they contribute to pathogenicity and biofilm formation (Wright *et al.*, 2007). P pili and type 1 pili are the best-characterised CU pili systems and exhibit helical rod-like shapes. The subunits of the pilus are secreted through the inner membrane by the SecYEG apparatus in an unfolded state (Jones *et al.*, 1997). Upon reaching the periplasm the subunit folding is catalysed by chaperones with the 'Donor Strand Complementation' mechanism. The outer membrane protein, the usher, catalyses the subunit polymerisation and mediates the pilus secretion. The elongation of the P pilus proceeds until the termination subunit binds to the usher (Verger *et al.*, 2006). The termination of the type I pilus assembly system is unknown so far.

1.4. The ATP-binding cassette transporter superfamily

The ABC transporter superfamily of genes describes both uptake and efflux transport systems, which were separated once in history probably before the differentiation of prokaryotes and eukaryotes (Saurin *et al.*, 1999). ABC transporters can be found across all three kingdoms of life: archaea, eukaryota and bacteria (Ames *et al.*, 1990; Higgins, 1992). In general, transporters of this superfamily are composed of two integral transmembrane domains (TMDs) and two cytoplasmic nucleotide-binding domains (NBDs). In eukaryotic organisms these modules are generally fused,

yielding in a single polypeptide chain. In contrast, bacterial ABC transporters follow an individual domain blueprint (Higgins, 1992). Additionally to TMDs and NBDs, uptake systems obtain usually an extracytoplasmic substrate-binding protein (SBP). In Gram-negative bacteria the SBP is localised in the periplasm, while it can be encoded as a separate protein or fused to the ABC importer (Neu *et al.*, 1965; van der Heide *et al.*, 2002). In Gram-positive bacteria and archaea SBPs are membrane-attached via a lipid-anchor, a transmembrane peptide or the receptor is fused to the TMDs (Berntsson *et al.*, 2010; van der Heide *et al.*, 2002). Transport processes are energized by ATP hydrolysis within the NBDs, which dimerize in a characteristic head-to-tail arrangement upon ATP-binding (Al-Shawi, 2011). The nucleotide-binding-sites of both NBDs sandwich the ATP at the dimer interface.

Bacterial transporters belong to at least 300 different families. These can be categorized depending on their properties such as energy source, substrates and transmembrane regions (Sun *et al.*, 2014). The Transporter Classification (TC) database is analogous to the Enzyme Commission (EC) system, except that it incorporates both, functional and phylogenetic information of transporter proteins (Saier *et al.*, 2016). Thereby it uses the integral membrane protein/domain to classify the ABC transporter system into families (Saier, 1994, 2000). Probably the five largest of these families are: the major facilitator superfamily (MFS), the resistance-nodulation-division (RND) family, the multidrug and toxic compound extrusion (MATE) family, the small multidrug resistance (SMR) family and the ATP-binding cassette (ABC) superfamily (Piddock, 2006; Poole, 2007; Putman *et al.*, 2000).

The ABC superfamily is further subdivided into ABC exporters and importers. ABC exporters are divided into the three different, evolutionary distinct superfamilies that are called ABC1, ABC2 and ABC3 (Wang *et al.*, 2009). Furthermore, ABC importers are believed to be almost exclusively of the ABC2-type superfamily, however, they differ completely in their principal function. ABC importers have been divided into two classes depending on the transport mechanism: Type I importers translocate the substrate with an alternating access mechanism that is also driven by the substrate. Type II importers interact with the substrate even in a nucleotide-free state, while hydrolysis energises an inward-facing conformation. A third importer sub-superfamily is called the ECF system, which lacks an extracytoplasm receptor and it is specialised for abundant substrates such as vitamins, minerals and small molecules (Slotboom, 2014).

1.4.1. Transmembrane domains

In contrast to the NBD of ABC transporters, the TMD displays a low level of homology, likely reflecting the variety of transported substrates. The ‘typical’ ABC exporter exhibits 12 transmembrane-spanning α-helices, which form the transport pathway of the substrate (Locher, 2009). The α-helices are arranged in two bundles of each six and shaping a tunnel that is opened to one side. Crystal structures of several transporters revealed a common ABC exporter fold. Here, each TMD monomer is formed by

a smaller lobe composed of two transmembrane segments and a bigger lobe composed of four transmembrane segments (Dawson *et al.*, 2006; Dong *et al.*, 2005; Lin *et al.*, 2015; Ward *et al.*, 2007). Both lobes form a V-shaped conformation that results in a pseudo-symmetry of the dimer. The catalysis at the NBDs trigger an extensive structural reorganisation within the TMDs that changes the cavity-opening built by the α-helices within the membrane from one side to the other (Becker *et al.*, 2010; Dawson *et al.*, 2006; Dong *et al.*, 2005; Ward *et al.*, 2007; Zou *et al.*, 2009). This step also changes the affinity to the substrate from a high-affinity to a low-affinity binding site (Dawson *et al.*, 2007; Doshi *et al.*, 2013).

Those TMDs that are not directly coupled to their NBDs feature α-helices, which are located at the transmission interface between the NBD and the TMD. This 'coupling helix' extends from the transmembrane-embedded domain into the cytoplasm by 25-40 Å and runs parallel to the plane of the membrane. The NBD contributes to the transmission interface primarily through a groove on the interaction surface formed by amino acids located around the Q/X-loop (Figure 3). Moreover, the exporter Sav1866 shows a domain swapped interaction of TMD A with NBD B and *vice versa*, while in contrast e.g. the importer BtuCD shows no swapping (Becker *et al.*, 2010; Locher *et al.*, 2002). ABC importers and exporters deviate in this aspect and thereby maybe referring to different transport mechanisms. A unique feature of ABC importers that is considered to be a signature motif, is the so-called 'EAA' motif sequence of 15-20 amino acids residues in the coupling helix (Wen *et al.*, 2011). Type I importers are structurally represented by the molybdate transporter ModBC, they mediate the uptake of relatively small compounds and contain typically 12 transmembrane-spanning α-helices (Gerber *et al.*, 2008; Hollenstein *et al.*, 2007). In each TMD they are grouped in five and an extra N-terminal helix that is closely located to the other TMD (Locher, 2009). Type II importers are generally represented by the blueprint of BtuCD that contains 20 transmembrane helices and mediate the transport of bigger molecules (Korkhov *et al.*, 2012).

1.4.2. Nucleotide-binding domains

Chemical energy is transferred to mechanical energy by the NBD of ABC transporters and thereby often referred as the engine or motor domain. The NBD can be divided in a RecA-like subdomain and a helical subdomain, which harbour several conserved motifs that are involved in ATP binding and hydrolysis (Figure 3) (Schneider *et al.*, 1998): the '**Walker A**' ('P-loop'; GxxGxGKS/T, consensus motif where x is any amino acid) binds the nucleotide and γ-phosphate, the '**Walker B**' (ϕϕϕϕDE, consensus motif where ϕ means any hydrophobic amino acid) contains a conserved glutamate that is involved in the nucleophilic attack on ATP via a water molecule, the '**Signature motif**' ('C-loop' or 'LSGGQ motif') is the hallmark of ABC proteins and contacts the nucleotide and γ-phosphate, the '**A-loop**' (a conserved aromatic residue) interacts with the adenine ring of a bound nucleotide (Ambudkar *et al.*, 2006), the

'**D-loop**' (SALD, consensus motif) is involved in the cross-dimer interaction of the NBDs, the '**H-loop**' (a conserved histidine) is suggested to bind the γ-phosphate and acts as a base for water (Zaitseva *et al.*, 2005a), the '**Pro-loop'** (conserved proline), connects lobe I and lobe II of the NBD (Schmitt *et al.*, 2003); the '**Q-loop**' (a conserved glutamine) binds the γ-phosphate and is involved in the TMD interaction, the '**X-loop**' (TEVGERG, consensus motif) is only found in ABC exporters and involved in TMD interaction (Dawson *et al.*, 2006).

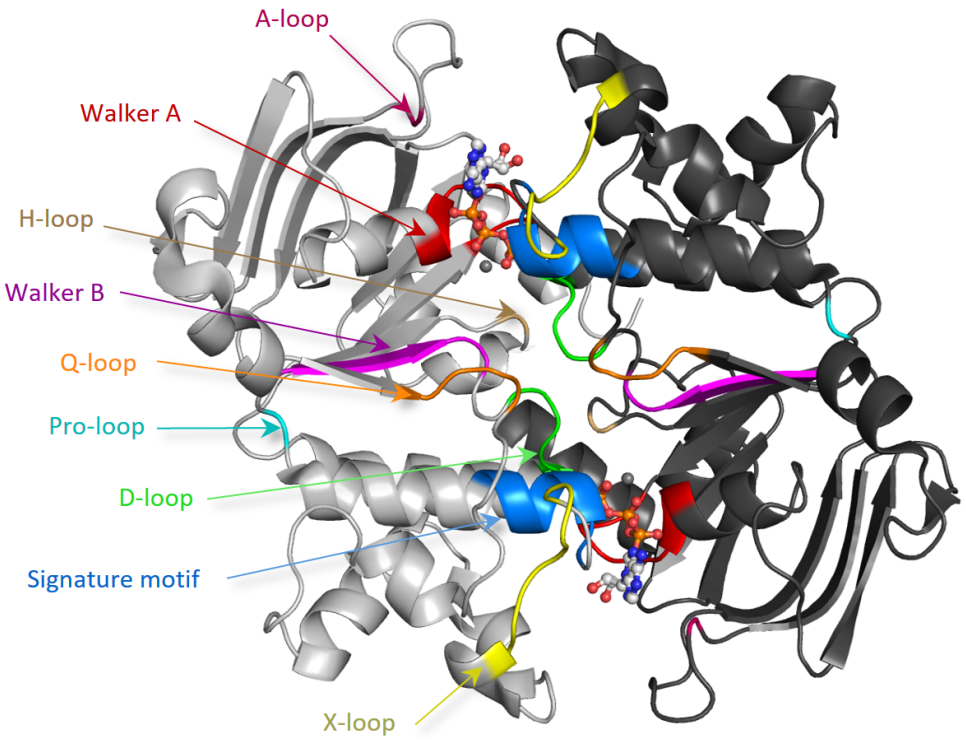

Figure 3. Structural overview of the haemolysin B NBD dimer and the conserved motifs. Ribbon representation of the three-dimensional structure of the haemolysin B NBD dimer with ATP/Mg2+ in the domain interface (each monomer in grey or black). The conserved motifs are highlighted by colors and labelled appropriately (Guo *et al.*, 2006; Zaitseva *et al.*, 2005a). At the NBD dimer interface ATP and Mg^{2+} are represented by spheres (PDB entry 1XEF).

Typically two NBDs arrange the nucleotide-binding sites in a 'head-to-tail' conformation and thereby sandwiching the ATP molecule(s) by the Walker A of one domain and the signature motif by the other domain and vice versa (Figure 3) (Dawson *et al.*, 2006, 2007; Zaitseva *et al.*, 2005a). Hereby two ATP molecules can be bound by an NBD dimer and provides the basis of cooperativity in ATP binding and hydrolysis (Davidson *et al.*, 1996; Senior *et al.*, 1998).

1.4.3. Mechanisms of ATP hydrolysis

The NBDs share a strongly conserved architecture, independent of the functional divergences of ABC transporters and DNA maintenance ATPases (Hopfner *et al.*, 2003). Crystallographic analysis of NBDs

showed a bilobal structure (Hung *et al.*, 1998; Jones *et al.*, 1999b; Procko *et al.*, 2006; Smith *et al.*, 2002; Zaitseva *et al.*, 2006). The larger lobe is related to a subdomain of RecA-like ATPases and contains the Walker A, Walker B, D-loop and H-loop. Therefore, it is called the core subdomain. The second subdomain, which is structurally more diverse and 'helical' is called the helical subdomain or α subdomain and contains the ABC transporter specific signature sequence (Karpowich *et al.*, 2001). The Q-loop and the Pro-loop connect these subdomains flexibly (Yuan *et al.*, 2001). The hydrolysis substrate is ATP, which is cleaved at the phosphoanhydride of the β-γ phosphodiester bond that stores 57 kJ/mol Gibbs free energy (Berg *et al.*, 2002).

Two models of ATP hydrolysis are commonly discussed for ABC transporters. The first is called the ATP 'Processive Clamp' (Chen *et al.*, 2003; Janas *et al.*, 2003) or also the 'Switch' model (Figure 4) (Higgins *et al.*, 2004a; Zaitseva *et al.*, 2006). The model assumes that the NBD dimer switches between two states. The ATP molecules are bound at the dimer interface of the NBDs and induce a symmetric 'closed' dimer (Figure 4 D). The ATP hydrolysis occurs in both substrate binding sites and subsequently the NBD dimer dissociates to unliganded 'open' conformation (Figure 4 A). This opened state assumes the separation of the dimers, building a gap with a distance of about 20-30 Å and the release of ADP/Pi.

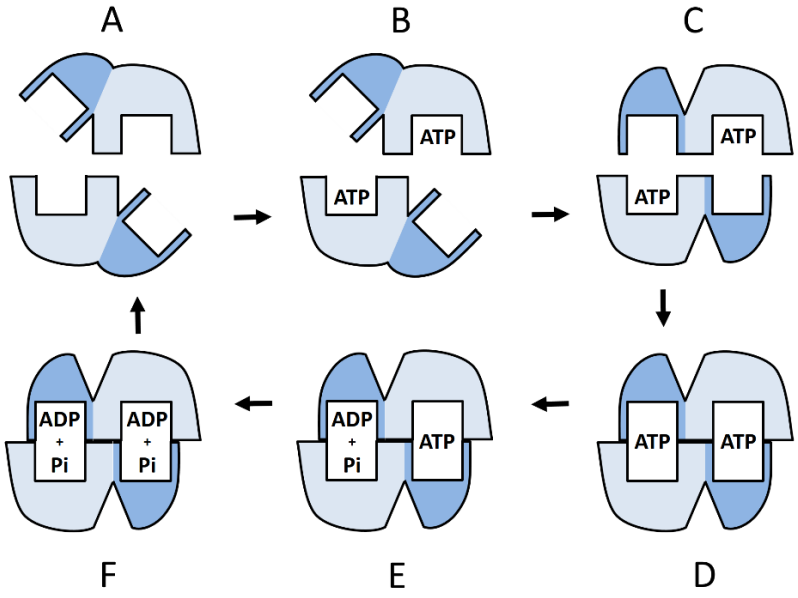

Figure 4. ABC Switch Model (adapted from Jones *et al.* (2013)). The NBD monomers are separated in the large core subdomain (magenta) and the smaller helical subdomain (cyan). (A) The NBDs in the 'resting state' are separated and (B) each bind ATP to the core subdomain. (C) This binding induces a rotation of the helical subdomain and (D) the formation of the 'closed' dimer. (E, F) ATP is hydrolysed processively and results in the opening and releasing of the ADP/Pi.

These described conformational changes are mediated to the TMDs, as described above, and induce the formation of an inward-facing and an outward-facing conformation, respectively.

The second model assumes that both NBDs remain in contact during the hydrolysis of ATP and is called the 'Constant Contact Model' (Jones *et al.*, 2007, 2009). The main feature of this model assumes an alternating hydrolysis of ATP at each site, while the other site releases and exchanges the nucleotide (Figure 5). Concerning this model a number of variants are discussed that base on biochemical and biophysical studies or crystal structures. Several studies assume an intermediate state that has bound two ATP molecules simultaneously (Loo *et al.*, 2010; Sauna *et al.*, 2007; Siarheyeva *et al.*, 2010; Verhalen *et al.*, 2011) while other assume a model, which does not prospect this state, as described here (Jones *et al.*, 2007). The latter model also proposes a rotation of the core subdomain that is predicted by molecular dynamics simulations and structural data (Jones *et al.*, 2009, 2011; Khare *et al.*, 2009; Wen *et al.*, 2011; Yuan *et al.*, 2001; Zaitseva *et al.*, 2006).

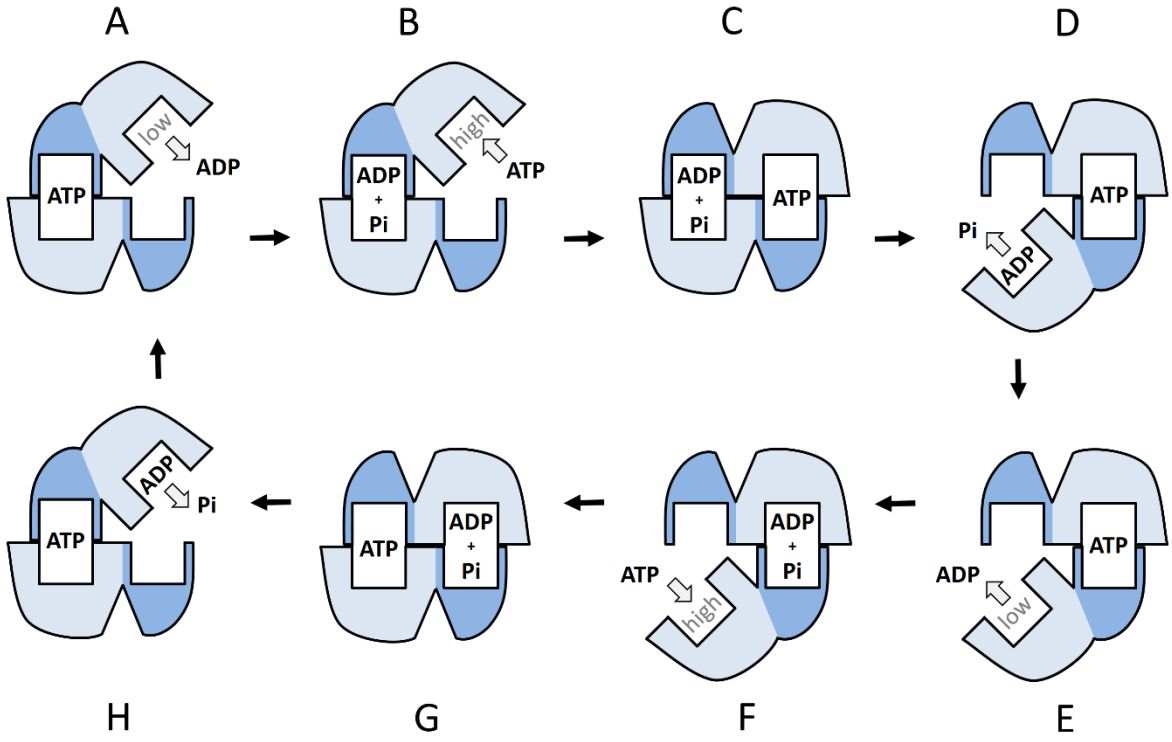

Figure 5. Constant Contact Model (adapted from Jones *et al.* (2013)). The NBD monomers are separated in the large core subdomain (red) and the smaller helical subdomain (blue). (A, E) ATP is bound in one dimer site, while the other releases ADP. (B, F) The ATP hydrolysis in one dimer site increases the affinity for ATP in the core subdomain. (C, G) The binding of ATP closes the NBD dimer on the second site. (D, H) The first dimer site opens by rotation of the core subdomain, which is induced by the occlusion of ATP on the second dimer site. Subsequently Pi is released.

ATP hydrolysis energizes the translocation of substrates across a membrane, however, the amount of ATP molecules needed for the translocation of one substrate has been only quantified for a couple of systems. For example two ATP molecules are consumed for the translocation of one substrate in the cases of the glycine-betaine or maltose importer from *E. coli* (Mimmack *et al.*, 1989) and in the case of

OpuA from *Lactococcus lactis* (Patzlaff *et al.*, 2003). In comparison the Sec pathway has been shown to translocate 20-30 amino acids upon hydrolysis of one ATP molecule (Schiebel *et al.*, 1991; Uchida *et al.*, 1995).

1.4.4. Accessory domains

Some ABC transporters contain an additional domain to the four core-domains, which are two NBDs and two TMDs. This domain obtains different functions such as regulation or catalysis and can be located extrinsic or intrinsic to the membrane. Biemans-Oldehinkel *et al.* (2006a) categorized the accessory domains in four groups: (i) extracytoplasmic domains (ii) membrane-embedded domains (iii) cytosolic regulatory domains and (iv) cytosolic catalytic domains. In the following these groups are described by examples in further detail:

(i) Extracytoplasmic domains: These domains are found in members of the ABCA family and further examples are the extracellular N-terminal domain of ProW from *E. coli* and the SBDs or proteins from ABC importers. In the case of the ABCA family these domains contain *N*-glycosylation sites, which seem to modulate the expression levels (Bungert *et al.*, 2001). ProW is part of the proline and glycine betaine transport system (ProU) and here the function of the additional domain is unknown so far.

(ii) Membrane-embedded domains: In addition to the core TMSs of TMDs many ABC transporters harbour further TMSs that can be considered as accessory membrane-embedded domains and they are generally less conserved (van der Heide *et al.*, 2002). In most cases the function of the additional domain is unknown. However, in the case of the TAP translocation machinery the function of the additional domain could be revealed. TAP is a heterodimer, which translocates antigenic peptides from the cytosol into the endoplasmic reticulum lumen where they are bound to MHC I molecules. The extra domain of TAP are suggested to mediate the assembly of the macromolecular peptide (Bangia *et al.*, 1999; Lehnert *et al.*, 2016; Leonhardt *et al.*, 2005; Noll *et al.*, 2017).

(iii) Cytosolic regulatory domains: Once an ABC transporter is expressed it also has to be regulated in its activity, e.g. a cytosolic regulatory domain. In the case of the maltose/dextrin transporter the C-terminal domain of MalK regulates uptake activity dependent on the binding of the regulator molecule IIA^{glc} (Bohm *et al.*, 2002; Dean *et al.*, 1990; Nelson *et al.*, 1984). It senses the presence of glucose and activates the transporter whether this source is exhausted.

In the case of the osmoregulatory ABC transporter OpuA, the regulatory domains constitute a sensor that switches the transporter activity upon interacting with the charged membrane surface and the cytoplasmic ionic strength (Biemans-Oldehinkel *et al.*, 2006b). An increasing ionic strength can be the consequence of a decreasing cell volume, which is induced by a shift in medium osmolality. Then, the activated transporter imports glycine betaine, which triggers the influx of water and protects the cell from plasmolysis (van der Heide *et al.*, 2000).

Another well-known example is the cystic fibrosis transmembrane conductance regulator (CFTR). It is a member of the ABC transporter family and channels chloride ions through a membrane (Liu *et al.*, 2017). The transporter activity is regulated by a phosphorylation dependent mechanism of the R-domain (Dahan *et al.*, 2001; Gadsby *et al.*, 1999; Rich *et al.*, 1991).

(iv) Cytosolic catalytic domains: Many bacteriocins are synthesized as prepeptides and contain a GG-motif, which is proposed as LSXXELXXIXGG, where X can be any amino acid (Havarstein *et al.*, 1994). This motif is recognized by the correlating ABC transporter, which comprises a specific N-terminal catalytic C39-peptidase domain (Havarstein *et al.*, 1995). This regulatory domain contains the conserved cysteine and histidine motifs that are responsible for recognition and cleavage of the transport substrates at the GG-motif. Thereby the bacteriocin matures in its active conformation.

The N-terminal additional domains of T1SS ABC transporters were also subdivided into three distinct groups by Kanonenberg *et al.* (2013). The classification considers the function of the additional domain and the substrate being translocated. The first group harbours the above described C39-peptidase containing ABC transporters (PCATs), which are found e.g. in the bacteriocin secretion system of Gram-positive bacteria and the microcins T1SS of Gram-negative bacteria (substrates < 10 kDa) (Figure 6 I) (Lin *et al.*, 2015).

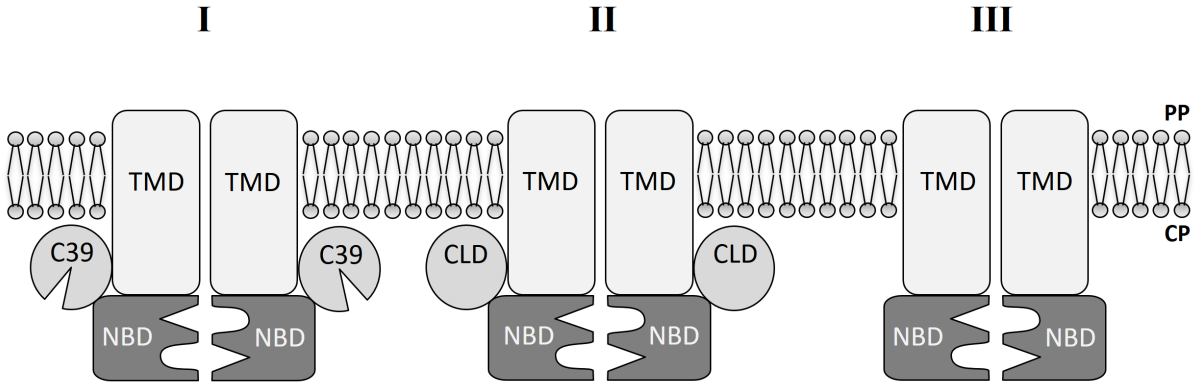

Figure 6. Schematic domain architecture of T1SS ABC transporters. The ABC transporters involved in T1SS were classified depending on the N-terminal additional domain and the transported substrate (Kanonenberg *et al.*, 2013). Besides the canonical nucleotide-binding domain (NBD) and the transmembrane domain (TMD), group I contains a C39 peptidase domain (C39) that cleaves the substrate N-terminal leader peptide. Group II comprises an additional C39-peptidase like (CLD) domain, which function is not completely understood. Group III comprises the canonical architecture and harbours no additional domain.

The second group contains ABC transporter with a C39-peptidase like domain (CLD), which in contrast has no proteolytic activity, however, it is still essential for secretion, at least shown for the substrate haemolysin A (HlyA) (Figure 6 II) (Lecher *et al.*, 2012). In general it was observed that the substrates of

CLD containing ABC transporters are larger (> 55 kDa) and they are members of the RTX toxin family (Kanonenberg *et al.*, 2013; Lecher *et al.*, 2012).

The third group harbours no additional N-terminal domain and translocates substrates, which are small in comparison to RTX proteins (Figure 6 III) (Delepelaire, 2004; Holland *et al.*, 2003). One well-known substrate belonging to this group is HasA, a 19 kDa iron scavenger protein secreted by *S. marcescens* (Letoffe *et al.*, 1994). The protein does not contains any RTX repeats, however, it obtains "primary anchor site" that also interact with the cognate ABC transporter (HasD) and it requires the general chaperone SecB (Delepelaire *et al.*, 1998; Masi *et al.*, 2010).

1.5. The haemolysin A type I secretion system

A T1SS is composed of three membrane proteins, an ABC transporter, a MFP and an outer membrane protein (OMP). Together these proteins secrete a substrate in one step across two membranes, without the formation of a periplasmic intermediate. The C-terminal secretion sequence of the transport substrate is not cleaved during the translocation process (Thomas *et al.*, 2014b). Probably the best-studied secretion system in this family is the HlyA T1SS from *E. coli*, which is described in the following in further detail.

1.5.1. The outer membrane factor – TolC

TolC is a member of the outer membrane efflux proteins (OEP) family or also referred as outer membrane factor (OMF) family. Members of this family are found in the context of the ABC-, the RND and the MFS superfamilies. The structure of TolC was solved and revealed a 140 Å long single channel, which is shaped by a 12-stranded β-barrel and α-helical domain (Figure 7 A) (Koronakis *et al.*, 2000). The homotrimer is anchored in the outer membrane by the β-barrel domain and extends about 100 Å into the periplasm. Here, the α-helical domain comprises an equatorial part that contains mixed α-helical and β-sheet elements (Koronakis *et al.*, 2000). The conduit formed by TolC is water-filled with a diameter of 35 Å and the cavity is one of the largest know so far, with a volume of about 43,000 $Å^3$ (Figure 7 B) (Andersen *et al.*, 2001). TolC is synthesized in the cytoplasm and obtains an N-terminal signal peptide, recruiting the Sec apparatus that mediates the transport of the unfolded peptide into the periplasm (Danese *et al.*, 1998). It is known that the assembly of TolC as well as other OMFs is facilitated by the BamABCDE complex, however, the very final steps of TolC assembly and membrane insertion remain ambiguous (Charlson *et al.*, 2006; Jain *et al.*, 2007; Malinverni *et al.*, 2006; Voulhoux *et al.*, 2003; Werner *et al.*, 2005; Wu *et al.*, 2005). The closed periplasmic pore of TolC has a width of 3.5 Å, which is even to small for the passage of ions (Figure 7 C) (Koronakis *et al.*, 2000).

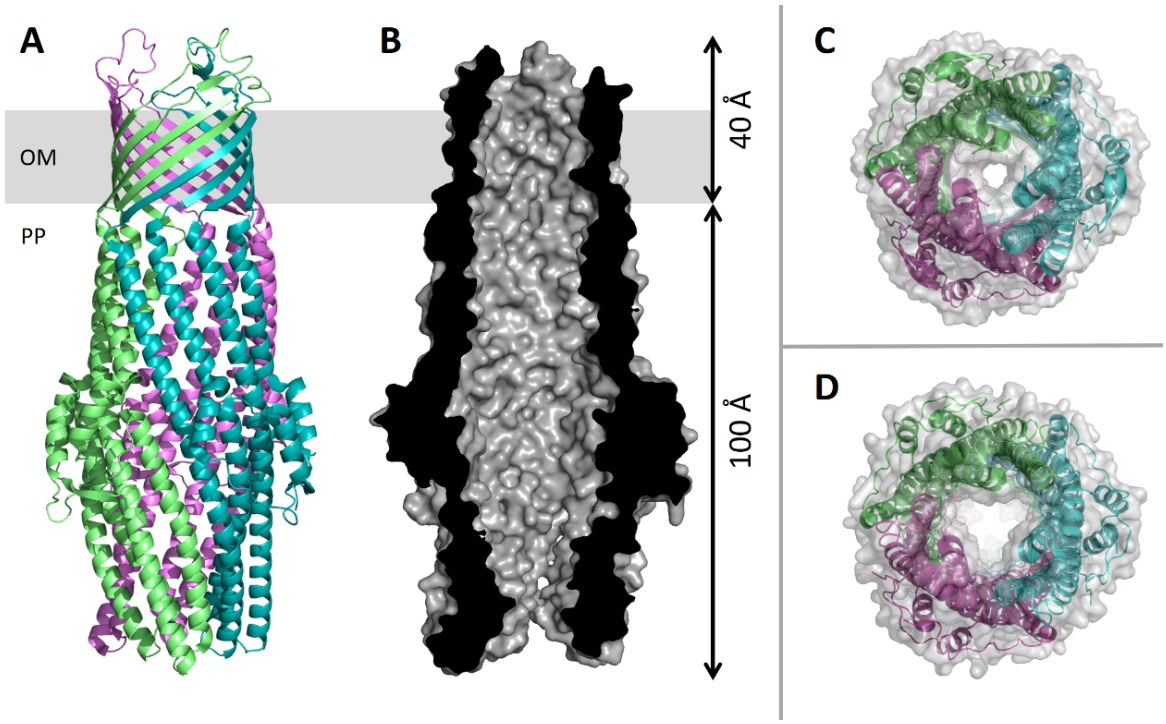

Figure 7. The periplasmic entrance of TolC (adapted from Lenders *et al.* (2013)). (A) Ribbon representation of the TolC homotrimer from a side view. Every monomer is indicated by a different colour (PDB entry: 1EK9). (B) Surface representation of TolC sliced in the axis of the channel pore (PDB entry: 2XMN). (C) Surface (grey) and ribbon (colors) representation of the closed periplasmic entrance of TolC, viewed from the periplasm in direction of the OM (PDB entry: 1EK9). (D) Surface (grey) and ribbon (colors) representation of the opened periplasmic entrance of TolC, viewed from the periplasm in direction of the OM (PDB entry: 2XMN). OM, outer membrane; PP, periplasm.

The opening mechanism of TolC is proposed to go along with a conformational reorganisation of the coiled-coil α-helices, which open the pore in the periplasm by twisting the gate in an iris-like motion (Figure 7 D) (Koronakis *et al.*, 2000).

1.5.2. The membrane fusion protein – HlyD

The membrane fusion protein haemolysin D (HlyD) of the HlyA T1SS has a size of 53 kDa and so far no complete structural data of HlyD are available (Wagner *et al.*, 1983). Kim *et al.* revealed the crystal structure of a fragment that contains about 60 % of the amino acids and lacks the N-terminal and C-terminal parts (Kim *et al.*, 2016). It is suggested that HlyD forms trimers (Thanabalu *et al.*, 1998) or hexamers (Kim *et al.*, 2016; Lee *et al.*, 2012), however, a dimer of trimers is very likely, since it would fit the overall stoichiometry of the translocon. A comparison with the structure of the analogous MexA and a topological analysis predicts a location of HlyD in the cytoplasm, IM and periplasm. It is suggested that the N-terminal part of HlyD extends into the cytoplasm and a single transmembrane segment anchors the protein in the IM. The periplasmic part of HlyD is predicted to form α-helices and a large β-strand helical domain (Higgins *et al.*, 2004b; Schulein *et al.*, 1992; Wang *et al.*, 1991). The explicit

roles of HlyD during the translocation process have not been revealed, however, the protein is essential for secretion. It is suggested that the MFP is involved in specific interactions with the ABC transporter and the OMP, while it provides the interconnection of these two components. It is also suggested that HlyD participates in the recognition of the transport substrate HlyA, most likely together with the ABC transporter (Balakrishnan *et al.*, 2001). In this study, Balakrishnan *et al.* deleted the N-terminal 45 residues of HlyD and also showed that TolC was not 'recruited' anymore. Taken together the results of numerous mutagenesis studies envisage a more complicated role of HlyD than just connecting the ABC transporter and the OMP.

1.5.3. The ABC transporter – HlyB

The inner membrane component of the HlyA T1SS is the ABC transporter haemolysin B (HlyB). It comprises one canonical TMD and NBD in each monomer. In addition, HlyB contains a third domain at the very N-terminus, which is called the CLD (C39-peptidase like domain) (Lecher *et al.*, 2012; Lecher *et al.*, 2011). To date the structure of the isolated NBD was resolved by X-ray crystallography (Schmitt *et al.*, 2003; Zaitseva *et al.*, 2005a; Zaitseva *et al.*, 2006) and the structure of the isolated CLD was resolved by NMR (Lecher *et al.*, 2012).

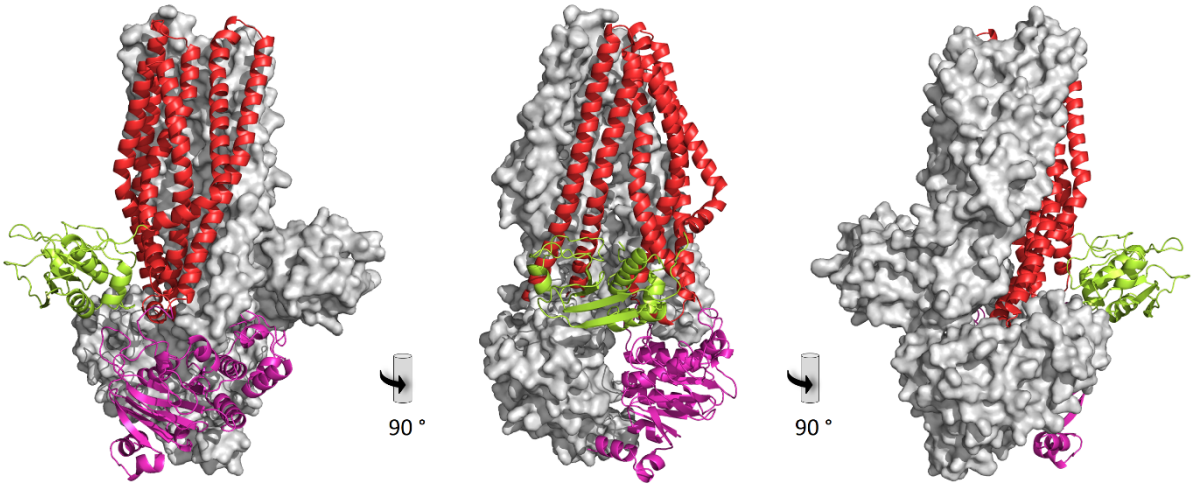

Figure 8. Model of the HlyB dimer based on the bacteriocin transporter PCAT1. The model of HlyB was predicted using Phyre2 (Kelley *et al.*, 2015). The images show the same model from a different perspective. One monomer surface is shown in grey and the other monomer is shown in a ribbon representation and colored in green (CLD), red (TMD) and magenta (NBD).

Since no structural data of the complete ABC transporter HlyB are available and to imagine the localisation of the three domains, Figure 8 shows a model of a HlyB dimer based on PCAT1 (PDB entry 4RY2). The model was predicted by the application of the Phyre2 server (Kelley *et al.*, 2015). An alignment by PyMOL of the model with the HlyB-NBD crystal structure returned a Cα root mean square

deviated (RMSD) of 2.2 Å for 223 aligned residues of 241. Additionally an alignment of the model with HlyB-CLD NMR structure returned a Cα RMSD of 1.8 Å for 110 aligned residues of 138 in total.

The CLD is composed of 123 amino acids and the overall structure of this N-terminal additional domain can be divided in two subdomains. The core subdomain consists of six β-sheets that are flanked by two α-helices, while the minor N-terminal part comprises three α-helices (Figure 9 A) (Lecher *et al.*, 2012). Lecher *et al.* also specified crucial variations that abolished the catalytic activity of the CLD. A comparison to the similar ComA-PEP C39 peptidase, revealed the presence of a tyrosine instead of the essential cysteine (Wu *et al.*, 2004). In addition, the essential histidine of the putative catalytic site is flipped by 180 ° (Lecher *et al.*, 2012). So far the distinct functional role of the CLD remains ambiguous, however, it is essential for the secretion of HlyA and it reveals a sequence homology of 42 % to C39 peptidases (Lecher *et al.*, 2012). These peptidases are found at the N-terminal part of bacteriocin and microcin transporters, where they cleave the premature substrates at the conserved GG-motif (Kotake *et al.*, 2008).

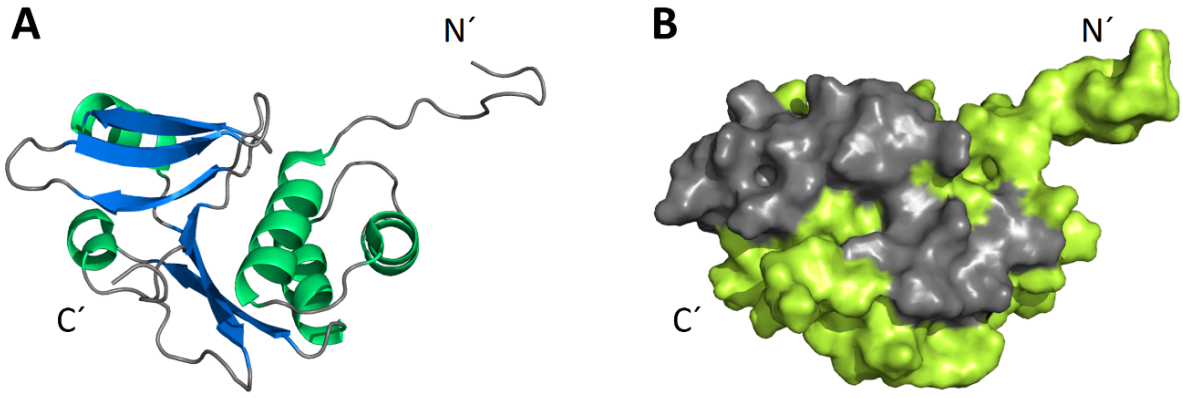

Figure 9. Structural overview of the CLD of HlyB and suggested binding sites with HlyA. (A) The three-dimensional structure of the CLD of HlyB determined by NMR (Lecher *et al.*, 2012) (PDB entry 3ZUA). Secondary α-helical structures are colored in green and β-sheets are colored in blue. (B) Chemical shift perturbation experimental results are transferred onto the structure of the CLD. Proposed interacting amino-acids are colored in black, while non-interacting regions are colored in yellow (Lecher *et al.*, 2012).

In contrast, HlyA does not contain such a GG-motif and it is not cleaved during or after the transportation process, however, the substrate was shown to interact with the CLD in an exclusively unfolded state (Lecher *et al.*, 2012). The interacting amino acids of the CLD were detected by chemical shift perturbation experiments and in comparison to the ligand-binding region of ComA-PEP, they are located at the opposite site of the ComA-PEP catalytic centre (Figure 9 B) (Lecher *et al.*, 2012).

The NBD of ABC transporters is a well conserved domain and energises the translocation process by ATP hydrolysis. The functional HlyB dimer assembles upon ATP binding and building the active

conformation (Schmitt *et al.*, 2003; Wang *et al.*, 1991; Zaitseva *et al.*, 2005b; Zaitseva *et al.*, 2006). The distinct mechanistics of HlyB ATP hydrolysis were further analysed by Zaitseva *et al.*. A substitution of the conserved histidine to alanine (H662A) in the isolated HlyB-NBD abolished ATPase activity, while preserving the ability to bind ATP. A heterodimer of the ATPase-deficient mutant and the wild-type protein was still able to hydrolyse ATP and suggested a sequential (two-cylinder engine) mechanism (Zaitseva *et al.*, 2005b). This finding was underlined one year later with a detailed study, revealing a structural asymmetry within the dimer (Zaitseva *et al.*, 2006). Such as the CLD, the NBD is also in the focus of studies that investigate its distinct interaction with the transport substrate and the subsequent precise regulation and communication of the translocon. Several mutational analysis of HlyB were performed by different laboratories and are well summarised by Holland *et al.* (2016). Further results by surface plasmon resonance suggest a distinct interaction of the C-terminal fragment of HlyA and the isolated NBD, which is strikingly dependent on the secretion signal and the concentration of ATP or ADP (Benabdelhak *et al.*, 2003). Taken together with the hypothetical functions of the CLD, these results emerge a complex picture of the interaction pattern between HlyA and the HlyB ABC transporter.

1.5.4. Interactions of the HlyA T1SS components

Beginning at the outer membrane factor TolC, which three-dimensional structure is solved and studied for many years, the channel-forming protein is suggested to rest in a closed conformation. The structure of TolC shows a tightly closed pore in the periplasm, which is even small enough to hinder the passage of ions (Eswaran *et al.*, 2003; Koronakis, 2003). The opening mechanism of TolC is proposed to go along with a conformational reorganisation of the coiled-coil α-helices and twisting the gate in an iris-like motion (Koronakis *et al.*, 2000). Therefore, a signal is necessary to trigger the opening of the channel, which is supposed to be a substrate interaction with the inner membrane complex. Studies of the AcrAB-TolC translocon by cryoEM pointed to quaternary structural changes in AcrB that are communicated to AcrA, which repacks and trigger the opening of TolC (Wang *et al.*, 2017).

The structural differences of drug efflux pumps and especially of their TMDs, make it unlikely that in general the inner membrane transporter interacts directly with TolC. Therefore, each system has to be investigated individually and only little structural information is available for the inner membrane complex of the HlyA T1SS. Nevertheless, several models have in common that the MFP binds TolC in a six to three stoichiometry (Janganan *et al.*, 2011; Su *et al.*, 2011; Tikhonova *et al.*, 2009; Tikhonova *et al.*, 2011; Xu *et al.*, 2011a). In general the α-helical hairpins of the MFPs interact with TolC by surrounding the tip of the OMP or by interacting in a tip-to-tip manner (Kim *et al.*, 2010; Wang *et al.*, 2017; Xu *et al.*, 2010; Xu *et al.*, 2011b).

Cross-linking experiments showed that the inner membrane complex of the HlyA T1SS, composed of HlyB and HlyD, is assembled even in the absence of the transport substrate (Thanabalu *et al.*, 1998). Deletions of the N-terminal, cytoplasmic part of HlyD abolished the formation of cross-linking products to HlyA and TolC (Thanabalu *et al.*, 1998). This suggests that the HlyA to HlyD interaction is a crucial signal in the subsequent 'recruitment' of the OMP TolC. The same study also demonstrated that this 'recruitment' is independent of HlyB ATPase activity (Thanabalu *et al.*, 1998). Furthermore, surface plasmon resonance experiments showed that the interaction of the HlyA secretion signal to the HlyB NBD is diminished upon ATP binding or hydrolysis (Benabdelhak *et al.*, 2003). This strongly suggests HlyB to energize the translocation after TolC completes the full translocon. Recent studies with an eGFP-HlyA fusion protein also clearly demonstrated a vectorial transport with the C-terminus of HlyA leaving the translocon first at the extracellular site (Lenders *et al.*, 2015). Lenders *et al.* also determined the secretion rate of HlyA to 16 amino acids per transporter and second (Lenders *et al.*, 2016).

1.6. The RTX protein – HlyA

Gram-negative bacteria secrete toxins, hydrolytic enzymes or surface-bound proteins via the type 1 secretion system across the cell envelope (Holland *et al.*, 2005). One of these proteins is haemolysin A (HlyA), which was discovered in the 1980s in uropathogenic *E. coli* strains (Welch *et al.*, 1981). This toxin of about 110 kDa is affecting pore formation in the target cell membrane and belonging to the 'repeat in toxins' (RTX) family (Ludwig *et al.*, 1991; Welch *et al.*, 1992). The common feature of RTX proteins is their translocation via the T1SS and glycine- and aspartate-rich nonapeptide repeats binding calcium ions.

RTX cytotoxins can be divided in two families, the multifunctional autoprocessing RTX toxins (MARTX) and the pore-forming leukotoxins (Linhartova *et al.*, 2010). HlyA belongs to the latter mentioned family, which share (i) the activation by acylation of lysine residues, (ii) a hydrophobic domain, (iii) the export by T1SS and (iv) binding of calcium ions within the repeat motif (Linhartova *et al.*, 2010). Historically RTX toxins were separated in haemolysins and leukotoxins due to a target 'limitation' of haemolysins. More recent studies found that even those target leukocytes and thereby making this differentiation obsolete (Lally *et al.*, 1997; Linhartova *et al.*, 2010; Welch, 1991).

HlyA is expressed as a variant, which is lytically inactive (pro-HlyA). Prior to its secretion the protein is acylated at two internal lysine residues at positions 564 and 690 (Figure 10) (Lim *et al.*, 2000). The acylation process is performed by the acyltransferase HlyC together with the acyl carrier protein (ACP) in the cytoplasm (Issartel *et al.*, 1991). The fatty acids carried by ACP are various, including the palmitic (C16:0) and palmitoleic (C16:1) (Issartel *et al.*, 1991; Trent *et al.*, 1998). However, HlyC selectively (about 68 %) mediates the linkage of myristic acid (C14:0) to pro-HlyA *in vivo* (Lim *et al.*, 2000). The

toxicity of HlyA is mediated by the ability to form pores within a broad range of membranes. The precise mechanism of the pore formation and interactions is poorly understood.

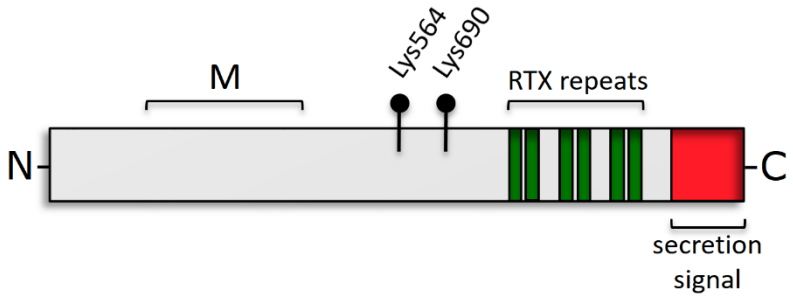

Figure 10. Schematic overview of HlyA variants (taken and adapted from Reimann *et al.* (2016)). (A) The HlyA elongated protein with a size of 110.5 kDa and (M) the putative membrane insertion domain, two lysine residues that are acylated, (RTX repeats) six nonapeptide repeats that bind Ca2+ ions and the C-terminal secretion signal.

In the case of HlyA the N-terminal hydrophobic 'membrane insertion domain' is assumed to contain nine amphipathic α-helices (Hyland *et al.*, 2001). However, two steps appear to be essential, a reversible adsorption of the toxin by electrostatic forces and an irreversible membrane insertion (Bakas *et al.*, 1996; Ostolaza *et al.*, 1997).

The RTX specific repeats bind calcium ions at the outside of the cell and appear to trigger the folding of the protein into the active conformation (Simpson *et al.*, 2011). The repeats obtain the consensus sequence GGxGxDxUx, where 'x' represents any amino acid and 'U' represents a large hydrophobic amino acid. HlyA obtains six RTX repeats that contain the strict consensus sequence (Uniprot: P08715) (Figure 10). However, depending on the stringency of the motif, between 6 and 17 nonapeptide repeats can be assigned to the toxin, located at the C-terminal part of the protein (Linhartova *et al.*, 2010; Thomas *et al.*, 2014b). The exact function of this domain is currently not fully resolved. It is suggested that calcium ions bind to the repeats in a 1:1 ratio and the region takes on a stabilised β-roll structure (Bumba *et al.*, 2016; Felmlee *et al.*, 1988; Linhartova *et al.*, 2010; Ludwig *et al.*, 1988; Rhodes *et al.*, 2001; Rose *et al.*, 1995; Sanchez-Magraner *et al.*, 2010; Sanchez-Magraner *et al.*, 2007; Schindel *et al.*, 2001). The first residues of each motif form a turn and the remaining part builds a short β-strand. The backbone carbonyl groups of the glycine residues and the side chains of aspartate residues of two different RTX repeats coordinate one calcium ion (Baumann *et al.*, 1993). The repetitive arrangement of this structure then forms the β-roll. A recent study also assumes the binding of calcium ions at the outside of the cell to trigger the translocation of the peptide in a 'push-ratchet'-kind of way (Bumba *et al.*, 2016).

The C-terminal secretion signal of HlyA is localised in the last 60 amino acids (Gray *et al.*, 1989; Gray *et al.*, 1986; Kenny *et al.*, 1991; Kenny *et al.*, 1992). A closer view reveals clusters of charged amino acids,

uncharged amino acids, hydroxylated amino acids and an aspartate box (Holland *et al.*, 1990). Further analysis of the secondary structure also predicts two helical parts (Koronakis *et al.*, 1989). Although the exact translocation mechanism of HlyA is still unknown, the secretion rate of HlyA could be quantified to about 16 amino acids per transporter and second (Lenders *et al.*, 2016). Finally, in comparison to other RTX-proteins no universal conservation was found so far and the exact mode of secretion signal recognition is currently unknown.

2. Aims

The HlyA T1SS of *E. coli* is one of the best-studied protein secretion systems. The toxin HlyA is a member of the RTX superfamily and associated with the majority of uropathogenic *E. coli* strains (Foxman, 2002). The toxin is able to lyse cell tissues and thus enabled to enter the blood stream of the host (Brooks *et al.*, 1980). The bacterial translocation machinery of HlyA is composed of three proteins, which are located in the inner and the outer membrane of the cell. The channel forming protein TolC is localised in the outer membrane and extends into the periplasm. The inner membrane harbours the membrane fusion protein HlyD and the ABC transporter HlyB. This tripartite nanomachinery translocates HlyA in an unfolded state across both membranes into the extracellular space, where the toxin folds upon calcium ion binding to the RTX repeats (Bakkes *et al.*, 2010; Baumann *et al.*, 1993; Welch, 2001).

The ABC transporter of the HlyA T1SS is supposed to energize the machinery by ATP hydrolysis. In order to prevent futile consumption of energy storing ATP, this process is assumed to be highly regulated. Although the system is investigated since many years, the aspect of HlyB ATPase activity regulation and the role of its N-terminal domain remain to be answered. Besides the canonical nucleotide-binding domain and the transmembrane domain, HlyB obtains the additional C39-peptidase like domain (CLD), which assumes an unknown function (Lecher *et al.*, 2012). So far, only the isolated nucleotide-binding domain or the isolated CLD of HlyB were studied and little is known about the complete ABC transporter protein (Zaitseva *et al.*, 2005a; Zaitseva *et al.*, 2005b; Zaitseva *et al.*, 2006). Therefore, one aim of this thesis was a biochemical characterisation of the solubilised and purified ABC transporter and the identification of the function of the CLD.

The nucleotide-binding domain and the CLD of HlyB were found previously to interact independently with HlyA, anyway, little is known about the mechanistic terms of these interactions (Benabdelhak *et al.*, 2003; Lecher *et al.*, 2012). Therefore, another aim of this thesis was the biochemical characterisation of HlyB upon interacting with the transported substrate.

Until now, the RTX repeats of HlyA are only known to bind calcium ions at the outside of the cell and thereby inducing the folding of the protein (Baumann *et al.*, 1993; Welch, 2001). After successfully identifying the RTX repeats also to interact with the CLD, the final aim was to investigate their contribution to the secretion process.

3. Publications

3.1. Chapter I

Title: Molecular insights into type I secretion systems

Authors: Michael H.H. Lenders [a], Sven Reimann [a], Sander H.J. Smits and Lutz Schmitt
[a]: These authors contributed equally to this article.

Published in: *Biological chemistry* (2013)
Impact factor: 2.689

Proportionate work on this publication: writing of the manuscript

DE GRUYTER DOI 10.1515/hsz-2013-0171 — Biol. Chem. 2013; 394(11): 1371–1384

Review

Michael H.H. Lenders[a], Sven Reimann[a], Sander H. J. Smits and Lutz Schmitt*

Molecular insights into type I secretion systems

Abstract: Type 1 secretion systems are one of the main machineries in Gram-negative bacteria involved in the secretion of a wide range of substrates from the cytoplasm across the inner and outer membrane in one step to the extracellular space. The range of substrates varies from small proteins up to large surface layer proteins of about 900 kDa. Most of the substrates have a non-cleavable C-terminal secretion signal and so-called GG repeats that are able to bind calcium ions. The translocator complex is composed of a trimeric outer membrane protein that provides a pore in the outer membrane. A multimeric membrane fusion protein spans the periplasm and forms a continuous channel connecting the outer membrane protein with a dimeric ATP-binding cassette transporter in the inner membrane. The ATP-binding cassette-transporter is thought to form a channel through the inner membrane and energizes the transport process. This review will provide a detailed view of the components of the translocator and will summarize structural as well as functional data.

Keywords: ATP-binding cassette (ABC)-transporter; ATPase; haemolysin A; membrane fusion protein; outer membrane protein; type 1 secretion.

[a]These authors contributed equally to this article.
***Corresponding author: Lutz Schmitt,** Institute of Biochemistry, Heinrich Heine University, Universitätsstraße 1, D-40225 Düsseldorf, Germany, e-mail: Lutz.Schmitt@hhu.de
Michael H.H. Lenders, Sven Reimann and Sander H. J. Smits: Institute of Biochemistry, Heinrich Heine University, Universitätsstraße 1, D-40225 Düsseldorf, Germany

Introduction

A broad range of morphologically diverse bacteria are known to secrete proteins to the exterior (Pugsley and Schwartz, 1985). The type 1 secretion system (T1SS) has evolved in Gram-negative bacteria to secrete substances in one step from the cytoplasm across both the inner and outer membrane, without any periplasmic intermediate. This mechanism of secretion is independent of the Sec-mediated pathway (Schatz and Beckwith, 1990).

The transport complex itself contains three specific components, which interact with each other and build up the secretion apparatus (Letoffe et al., 1996; Thanabalu et al., 1998). Two proteins are located in the inner membrane, an ATP-binding cassette (ABC) transporter and a membrane fusion protein (MFP). The third component is a protein residing in the outer membrane, which has therefore been called an outer membrane protein (OMP). This forms a channel from the periplasm to the extracellular medium. Components of T1SSs reside in the membranes of the bacterial envelope. Most substrates of T1SSs contain a non-cleavable C-terminal secretion signal, which upon interaction with their ABC transporter initiates assembly of the whole transport complex (Letoffe et al., 1996; Thanabalu et al., 1998).

The importance of the T1SS is demonstrated by its numerous transport substrates, which vary from small proteins like the hemophore HasA (19 kDa) to huge surface layer proteins up to 900 kDa in size (Letoffe et al., 1994; Hinsa et al., 2003; Satchell, 2011). Other transported substrates include adenylate cyclases, lipases and proteases. One of the best-characterized T1SSs and the first to be identified is the hemolysin A (HlyA) secretion machinery of *Escherichia coli*. HlyA is found in most uropathogenic strains and was discovered in the early 1980s (Springer and Goebel, 1980; Welch et al., 1981, 1983; Mackman and Holland, 1984). Therefore it represents one of the paradigms of T1SSs.

Despite extensive research on the system, many aspects are still controversial. In this review we gather together existing results regarding the following questions:

- Does substrate folding take place prior or after the transport process?
- Which parts of the substrate and the components of the transport complex interact with each other?
- What is the specific function of the components of the translocon during assembly and transport?

Furthermore, we will speculate about the transport mechanism in the light of the questions raised above.

Components of the type 1 secretion system

The outer membrane protein

An OMP is an essential part of the T1SS and knock-out mutants lead to secretion deficient bacterial strains (Wandersman and Delepelaire, 1990). Members of this family include TolC, PrtF, CyaE and LipD (Delepelaire, 2004). TolC is the best-characterized protein of this family, since in addition to biochemical and functional studies, the structure of TolC in the closed and 'sequential open state' is known (Koronakis et al., 2000; Pei et al., 2011). Here, the 'sequential open state' describes the structure of the partially open periplasmic gate of TolC. Furthermore, secretion-deficient mutants were used to identify crucial amino acids, cross-linking studies investigated the closed state of the pore in great detail and conductance experiments of the transition states with a 'sequentially open' state of TolC resulted in a detailed picture of the protein's function (Vakharia et al., 2001; Andersen et al., 2002; Eswaran et al., 2003). TolC is not only involved in protein transport through the T1SS of Cva and Hly but is also an essential part of multiple drug efflux systems in *E. coli* such as Acr, Mac and Emr (Koronakis et al., 2004).

The homotrimeric TolC is 140 Å in length, as shown in Figure 1A, from its periplasmic tip region to the extracellular loops of its β-barrel, and builds a continuous channel that spans the outer membrane and extends to a large extent into the periplasmatic space. The β-barrel measures 40 Å in the outer diameter and consists of four β-strains per monomer, which form a hollow cylindrical shape. A 100 Å tunnel formed by 12 α-helices follows the β-barrel and expands into the periplasm. These helices are packed laterally with two neighboring helices building an α-barrel, see Figure 1A (Koronakis et al., 2000). The interaction between two neighboring helices is stabilized by so called 'knobs-into-holes' packing (Koronakis et al., 2004). Here, the intermeshing of side chains stabilizes the assembly of the 12 laterally packed helices of the α-barrel (Koronakis et al., 2004). The accessible interior diameter of the water-filled pore is 20 Å (35 Å for the outer diameter), see Figure 1A and B. The periplasmic end formed by densely packed coiled coils is closed and only 3.5 Å in diameter. This is too small to allow passage of even ions, see Figure 1C (Delepelaire, 2004). Salt bridges and hydrogen bonds stabilize this closed conformation. The most important amino acids of the closed conformation are T152, D153, Y362 and R367, which are located in the coiled coil region at the periplasmic end of the pore. Conductivity experiments showed that the mutation of these amino acids to alanine resulted in a partly opened conformation of TolC (Andersen et al., 2002). The structure of the Y362F and R367S double mutant showed an enlarged periplasmic entrance of the protein (Figure 1D) due to a weakening of the ionic interactions between the monomers (Pei et al., 2011).

It is proposed that upon opening, TolC undergoes an 'iris-like motion' of the inner α-helical coiled coils around the outer coiled coils at the periplasmic ends of the α-barrel (Eswaran et al., 2003). Cross-linking studies have suggested that an untwisting of the 'entrance helices' is necessary for TolC-dependent substrate secretion (as in the case of the hemolysin T1SS), but not for TolC recruitment (Eswaran et al., 2003). Data from TolC mutants that form only open state structures emphasized this iris-like motion of the inner α-helical coiled coils (helices H7/H8). Helix H7 moves around helix H8 and together they move around the outer coiled coils (helices H3/H4) at the periplasmatic ends (Bavro et al., 2008; Pei et al., 2011). These structures highlight an increasing distance between the inner α-helical coiled coils from 12.2 Å in wild type TolC to 18.9 Å and 21.3 Å in the TolC mutants (Figure 1C and D). This increasing distance results in an increased conductivity ranging from 80 pS in wild type TolC to 370 pS and 1000 pS in the TolC mutants (Pei et al., 2011).

In all T1SSs, TolC or other OMPs in the active pore interact with a membrane fusion protein (Letoffe et al., 1996; Thanabalu et al., 1998). So far, direct interactions between OMPs and the cognate ABC transporter yet to be observed in T1SS and probably do not exist. In contrast, in the Acr multidrug efflux pump system TolC directly interacts with the secondary transporter AcrB (Tamura et al., 2005). Cross-linking experiments of cysteine residues introduced by site-directed mutagenesis showed that the transporter forms a complex by transient tip-to-tip interaction with TolC. In addition, structural data derived from the open state of TolC identified a binding groove for interaction with the membrane fusion protein AcrA (Bavro et al., 2008; Pei et al., 2011). This is also in line with cross-linking studies of site-specific TolC and AcrA cysteine variants (Lobedanz et al., 2007). The binding groove is located between the lower α-helical barrel of TolC and the N-terminal α-helix of the AcrA coiled coil. As mentioned above, the α-helical domain of MFPs, especially the α-hairpin, seems to be essential for interaction with TolC (Stegmeier et al., 2006; Kim et al., 2010). The open state structure of TolC allows us to speculate that a larger interaction interface with the N-terminal α-helix of the MFP could be possible (Pei et al., 2011).

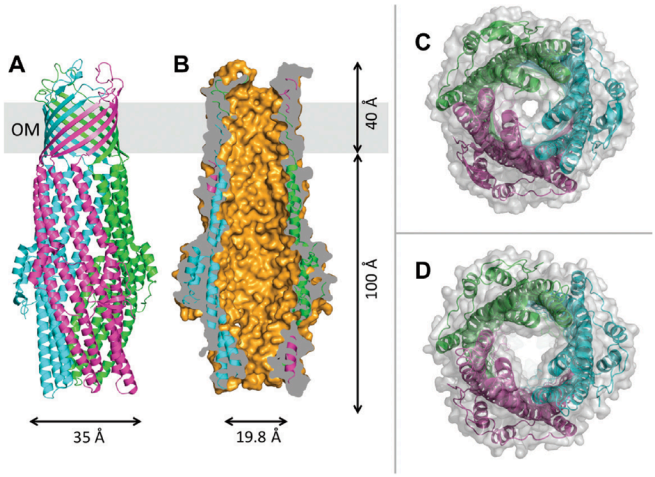

Figure 1 Structural overview of TolC.
(A) Cartoon representation of the side view of the TolC homotrimer in its closed state. The different monomers of TolC are highlighted in green, cyan and magenta. (B) A cross-section side view of a space-filling model of the TolC trimer shows a near-continuous channel from the β-barrel in the outer membrane (OM) to the periplasmic entrance of the α-barrel. The gray surface highlights the cross-sectional area in combination with a cartoon representation of the side view of the TolC homotrimer. The bright orange surface shows the inner and outer surface of the part of TolC (the black arrows indicate the dimensions of TolC). (C) View through the closed pore towards the periplasmic entrance of the α-barrel. Monomers are highlighted in green, cyan and magenta. To illustrate the closed conformation, the shape of the surface of TolC is shown in transparent gray panels (A, B and C are based on Protein Data Bank entry 1EK9). (D) View through a sequential open state of the pore towards the periplasmic entrance of the α-barrel. The monomers are highlighted in green, cyan and magenta. To illustrate the sequential open conformation, the shape of the surface of TolC is shown in transparent gray panels (D is based on Protein Data Bank entry 2XMN).

Molecular dynamic simulation of TolC indicated the possibility of a more complex pattern of conformational movements. In particular, a peristaltic motion in the periplasmatic domain that may facilitate transport of the substrates through the tunnel was proposed. Furthermore, movement was observed in coarse-grained simulations and two putative gate regions, located at either end of the protein, were identified. However, additional simulation of TolC also suggested that the cylindrical shape of the β-barrel represents a crystallographic artifact. After 2 nanoseconds of simulation, the barrel changed its shape to that of a more triangular prism. This conformation was also observed in the crystal structure of the functional TolC homolog OprM (Akama et al., 2004a; Vaccaro et al., 2008).

The membrane fusion protein

Bacterial MFPs are a highly diverse group in terms of structures and mechanisms (Zgurskaya et al., 2009). MFPs are involved in many multicomponent transport systems such as T1SSs or multidrug efflux systems. The transporter components of these systems are members of the resistance-nodulation-cell division, ABC or major facilitator superfamilies. So far, no structures of any MFPs involved in T1SS are available, but structures of analogous proteins involved in multidrug resistance, such as AcrA (Higgins et al., 2004) or MacA, have been reported. Several structures for other MFPs are also available, like CusB or MexA, which will not be discussed in detail here (Akama et al., 2004b; Su et al., 2009). AcrA and MacA are part of tri-partite multidrug efflux pumps. AcrA interacts with a transporter of the resistance-nodulation-cell division family and MacA interacts with an ABC-transporter. All MFPs share a highly conserved C-terminal part, whose structure is not resolved in the crystals. It has however been shown that this part of the molecule is essential for the secretion process of the transport complex (Schulein et al., 1994).

In contrast to the lipid anchor of AcrA and a single transmembrane spanning helix of MacA, MFPs of T1SSs contain a single transmembrane-spanning helix and a cytoplasmic tail (Figure 3 shows this part as a circle). In the case of the hemolysin T1SS, it has been demonstrated that the MFP hemolysin D (HlyD) directly interacts with the transport substrate and that its presence is essential for the assembly of the secretion complex and for the

secretion process itself (Balakrishnan et al., 2001). In contrast, co-precipitation experiments of other T1SSs such as HasE or PrtE indicated no direct interaction of the MFP with the substrate (Letoffe et al., 1996).

Most MFPs, including those of T1SSs, contain an α-helical domain (Johnson and Church, 1999). In the case of AcrA and MacA, this α-helical domain, especially the α-hairpin, is essential for interaction with TolC (Kim et al., 2010; Xu et al., 2010, 2011b). Mutants of the α-hairpin of the α-helical domain in HlyD disturbed this interaction (Lee et al., 2012). The MFPs of T1SSs are also involved in folding substrates into their native conformation. In the case of hemolysin and colicin V, amino acid substitution of MFPs resulted in reduced transport efficiencies associated with incorrectly folded substrates in the extracellular space (Hwang and Tai, 1999; Pimenta et al., 2005).

In vivo experiments showed that AcrA, MexA and HlyD can be cross-linked, resulting in the detection of dimers or trimers (Zgurskaya and Nikaido, 2000; Balakrishnan et al., 2001; Nehme and Poole, 2007; Zgurskaya et al., 2009). These results were obtained in the absence of the transporter and TolC (Zgurskaya et al., 2009). Recent models, however, propose higher-order oligomeric states. Thus, AcrA may form hexamers, as derived from electron microscopic studies (Xu et al., 2011a). MacA forms stable hexamers in solution that were also obtained inside the crystals (Yum et al., 2009). Studies using surface plasmon resonance spectroscopy also showed that MFPs are prone to oligomerization. In the case of MacA, stable oligomers were formed and survived for more than 3 minutes. The oligomers of EmrA were formed with low-micromolar affinity, whereas AcrA oligomerization requires non-physiological protein concentrations (Tikhonova et al., 2009). The data demonstrate decreasing stability of MFP oligomers in the order MacA, EmrA, AcrA. Furthermore, the stability of the MFP–TolC complex was correlated with the same order of stability as MFP oligomers. These authors assumed that the dynamic nature and variations in MFP oligomerization correlates with structural particularities of the respective IM transporters.

The ABC transporter

ABC transporters are ATP-dependent primary transporters. They are found in archeae, prokaryotes and eukaryotes and are able to transport a broad range of substrates across biological membranes (Higgins, 1992). The general ABC transporter blueprint includes two hydrophobic transmembrane domains (TMDs) and two highly conserved hydrophilic nucleotide-binding domains (NBDs, Figure 2). The NBDs supply the energy needed for transport by nucleotide binding, Mg^{2+} coordination and/or hydrolysis (Oswald et al., 2006). All components of the ABC transporter can be found as a four-domain polypeptide or assembled from up to four subunits encoded by different genes into a stable complex (Kerr, 2002; Davidson et al., 2008; Zolnerciks et al., 2011).

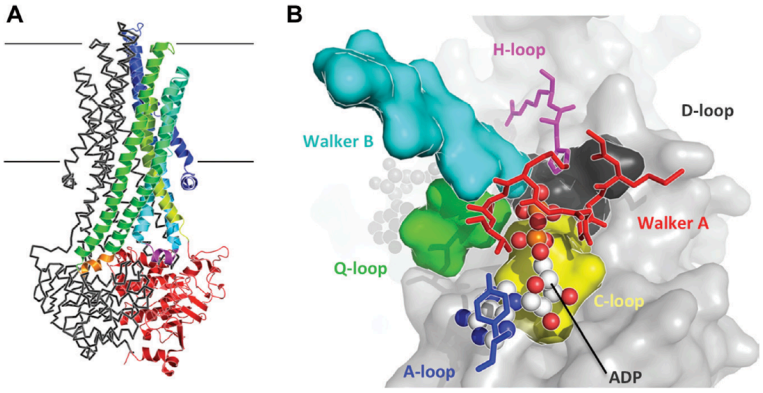

Figure 2 Spatial arrangement of an ATP-binding cassette exporter and structural features of the ATP-binding cassette exporter nucleotide-binding domains (NBDs).
(A) Structure of Sav1866 from *Saccharomyces aureus* with bound ADP (Protein Data Bank entry 2HYD) and for clarity with one monomer colored dark gray. The other monomer's transmembrane domains are colored in blue, cyan, yellow and green, while the corresponding NBD is colored red. Coupling helix 1 (purple helix) is thought to make contact with both NBDs during formation of the nucleotide sandwich. Coupling helix 2 (orange helix) is always domain-swapped to interact with the opposing NBD. (B) Close-up view of the gray NBD and the sandwiched ADP molecule. Directly involved conserved motifs are colored as follows: Walker A, red; Q-loop, green; H-loop, purple; Walker B, cyan; A-loop, blue; C-loop, yellow; D-loop, black.

In consideration of the NBD's crucial role in transforming chemical energy to mechanical movement translocation, it is not surprising that the primary sequence of NBDs is highly conserved (Seeger and van Veen, 2009). Each NBD consists of two subdomains with several highly conserved motifs (Figure 2). Thus, for example, the α-helical subdomain carries the ABC signature motif (also called the C-loop) represented by the sequence motif LSGGQ (Ames et al., 1992). This motif is the hallmark of the ABC transporter superfamily. The catalytic subdomain contains six conserved motifs (Walker A, Walker B, Q-loop, A-loop, H-loop, and D-loop). For detailed reviews on the function of each motif see, Oswald et al. (2006) or Seeger and van Veen (2009). In contrast to these motifs conserved in all ABC transporters (exporters and importers), the X-loop (consensus sequence TEVGERG) is only found in ABC-exporters and appears to be involved in interdomain communication and cross-talk between the NBD and the TMD (Dawson and Locher, 2006).

Several structural studies have shown that NBDs act as functional dimers, such as MJ0796, an uncharacterized ABC transporter (Smith et al., 2002), MalK the ATPase subunit of the maltose transporter (Chen et al., 2003) and the NBD of HlyB (Schmitt et al., 2003; Zaitseva et al., 2006). Furthermore, an oligomeric active conformation was confirmed through the dependence of ATPase activity on HlyB–NBD concentration (Zaitseva et al., 2006). Further analysis suggested an ATP-induced dimerization, emphasizing the role of the dimer as the active form of the enzyme (Zaitseva et al., 2005). Thus, two NBDs form a functional unit, enclosing two nucleotide-binding sites at their interfaces. These cavities form a 'nucleotide sandwich' (Smith et al., 2002) with a 'head-to-tail' arrangement of the NBDs. This arrangement was first predicted by Jones and George (1999), subsequently verified in the MalK structure (Chen et al., 2003) and finally confirmed via the structure of the multidrug ABC transporter Sav1866 by Hollenstein et al. (2007).

In contrast to the NBD, the ABC-TMDs vary greatly in sequence, architecture and the number of transmembrane helices. Most ABC exporters exhibit six α-helices per TMD, which extend as intracellular loops into the cytoplasm. Consequently, the NBD is about 25 Å away from the membrane. The 'coupling helices' are postulated to be involved in the transmission of crucial conformational changes from the NBDs to the TMDs. In the case of ABC exporters, coupling helix 1 is flanked by transmembrane helices 2/3, and is thought to make contact with both NBDs (Figure 2A, purple helix). Coupling helix 2 is flanked by transmembrane helices 4/5, is always domain-swapped, and interacts with the opposing NBD (Figure 2A, orange helix) (Dawson and Locher, 2006). In contrast, ABC importers contain between five (MetI) (Hollenstein et al., 2007; Oldham et al., 2007; Kadaba et al., 2008) and ten (BtuC) (Locher et al., 2002; Pinkett et al., 2007) α-helices per TMD, occasionally containing an additional N-terminal transmembrane helix that is domain swapped to the other TMD. Furthermore, ABC importers possess only one coupling helix, coupling helix 1, while coupling helix 2 is absent.

In the case of T1SS, secretion-defective HlyA mutants with an altered C-terminal secretion signal could be complemented by mutations within the corresponding ABC transporter HlyB (Zhang et al., 1993). These experiments demonstrated that ABC transporters recognize and bind to the cognate transport substrate. Surface plasmon resonance studies of the HlyB-NBD and HlyA provided further evidence for a specific interaction of the C-terminal 50 residues of the substrate with its ABC transporter (Benabdelhak et al., 2003). This highlights the fact that the NBD plays a crucial role in substrate recognition. In this T1SS, functional analysis of hybrid transporters formed by PrtD, PrtE and PrtF with HasD, HasE and TolC, respectively, demonstrated *in vivo* that the ABC transporter is responsible for recognition of the substrate (Binet and Wandersman, 1995). Moreover, the transporter might even be involved in 'protecting' the substrate as shown in the case of HlyB. Here, the canonical composition of four modules (two TMDs and two NBDs) is supplemented by an additional N-terminal extension of 123 amino acids, called the 'C39-like domain' (CLD). The CLD is indispensible for secretion and binds exclusively the unfolded state of the Repeats in Toxins (RTX) domain of HlyA (Lecher et al., 2012). As no known chaperone is likely involved in protecting unfolded HlyA inside the cell (Holland et al., 2005), the CLD of HlyB is thought to fulfill this role (Lecher et al., 2012). In parallel to binding the transport substrate, an ABC transporter seems to play a crucial role in recruitment of the other components of the transport complex, a process that is only initiated in the presence of the signal sequence of the substrate. In the case of HasA lacking the C-terminal secretion signal, the protein – as expected – is not secreted. However, assembly of the transport complex still takes place (Cescau et al., 2007). Further investigations using substrate affinity-chromatography revealed an ordered recruitment of the transport complex. Thus, the substrate initiates this process while interacting with the ABC transporter, which in turn interacts with the membrane fusion protein. Finally, the outer membrane factor is engaged (Letoffe et al., 1996) to complete the transport pathway.

The role of ABC transporters in the assembly of a functional complex also depends on ATP, as shown in the case of HlyB (Thanabalu et al., 1998) and MacB, an ABC transporter and founding member of the macrolide exporter family. MacB interaction with the corresponding membrane fusion protein was also observed in the presence of ATP (Lu and Zgurskaya, 2012), which suggested that binding of ATP initiates transport complex recruitment (Thanabalu et al., 1998). Further ATP hydrolysis energizes substrate transport (Koronakis et al., 1993, 1995; Letoffe et al., 2001). ATP also appears to compete with the secretion signal of HlyA for binding to the HlyB-NBDs complex release, as shown by surface plasmon resonance spectroscopy for the hemolysin system (Benabdelhak et al., 2003). Further studies validate the importance of ATP as they have shown that complex release only occurs in the presence of an intact Walker B motif (Masi and Wandersman, 2010).

Signals affecting secretion

Transport substrates of T1SS share several common denominators. The secretion signal is usually located at the C-terminal end (last 50–60 C-terminal amino acids) and is not cleaved during transport (Nicaud et al., 1986; Mackman et al., 1987; Jarchau et al., 1994). Its presence is necessary and sufficient for secretion (Gray et al., 1986; Stanley et al., 1991; Kenny et al., 1994). Therefore, the secretion signal has been fused to non-secretable proteins, which consequently become substrates of T1SS. Nevertheless, the sequence reveals no clear consensus, suggesting that the secondary structure is the recognition motif (Wolff et al., 1994; Zhang et al., 1995). The secretion signal seems to consist of two α-helices bridged by a linker peptide and followed by an unstructured and flexible region (Hui et al., 2000; Hui and Ling, 2002).

Some transport substrates like HasA are secretion-competent while containing only this secretion signal, whereas other substrates contain additional motifs (Finnie et al., 1998; Delepelaire and Wandersman, 2003). Most secreted proteins of T1SSs belong to the RTX family. These are characterized by glycine-rich repeats located close to the secretion signal and giving rise to the name RTX (Strathdee and Lo, 1989). Nearly all members of this family are secreted by T1SS and have distinctive repeats with the consensus sequence GGxGxDxxx (GG repeat), where x can be any amino acid (Ludwig and Goebel, 1999; Linhartova et al., 2010). A sequence analysis of bacterial genomes revealed that GG repeats containing proteins vary greatly in size (from 78 to 8682 residues), nearly all of them have an acidic isoelectric point (pI) and contain very few or no cysteines (Delepelaire, 2004). The parallel β-roll or β-sandwich structure appears to promote folding into the active conformation by binding of calcium ions to these nonapeptide repeats (Rose et al., 1995; Rhodes et al., 2001). Folding is induced outside of the cell, because of the low intracellular calcium concentration (<100 nM) (Gangola and Rosen, 1987; Ludwig et al., 1988; Jones et al., 1999).

Type 1 secretion occurs in an unfolded state

If we consider that the interior diameter of TolC is 20 Å in size (Koronakis et al., 2004), which is comparable to the width of two α-helices oriented parallel or antiparallel to each other, the question arises of how proteins of up to 900 kDa in size can be secreted through such a small pore. One possibility could be that secretion occurs in an unfolded conformation across both membranes of Gram-negative bacteria. Evidence for translation of unfolded substrates has been obtained, for example, for HlyA (Bakkes et al., 2010) and HasA (Debarbieux and Wandersman, 2001).

At least one T1SS relies on SecB interaction. Research investigating HasA secretion has revealed a direct dependency of HasA secretion on the presence of SecB (Delepelaire and Wandersman, 1998; Sapriel et al., 2003). It has been shown that SecB keeps HasA in transport-competent, unfolded or at least loosely-folded state. However, in the case of the hemolysin T1SS, SecB is not involved in secretion (Bakkes et al., 2010). Furthermore the C-terminal 60 amino acids of T1SS substrates are indispensable for secretion (Mackman et al., 1987; Stanley et al., 1991; Gentschev et al., 1995; Chervaux and Holland, 1996). Second, Bakkes et al. (2010) showed that folding rates dictated secretion level; slow folding proteins, forming unfolded intermediates, resulted in higher secretion levels in contrast to fast folding proteins. Taking this into account, we have been able to impose secretion of non-native T1SS substrates, for example, the maltose binding protein. Slow folding mutations affected the speed of folding but not the refolding velocity or functionality of the mature maltose binding protein (Bakkes et al., 2010). Another example emphasizing the importance of folding rate in the promotion of secretion was a fusion of a C-terminal fragment of HlyA containing the secretion signal with the cytosolic eukaryotic intestinal fatty acid binding protein. Again, only a

slow-folding mutant could be secreted, in contrast to the wild-type protein (Schwarz et al., 2012). Following secretion and folding, the slow folding mutant was biologically active, showing the same binding affinity for DAUDA, a fluorescence fatty acid analog, as the wild type (Schwarz et al., 2012).

Transport mechanism of type 1 secretion system

The exact mechanism and assembly of T1SS is not understood and many questions remain unanswered. For example how do T1SSs transport their substrate in an energetically favorable way? How much ATP is used for one secretion cycle? Are there any other energy sources that favor the secretion process? Is the N-terminal end or the C-terminal part secreted first?

This leads to another question, namely what is the role of the secretion signal? Is the secretion signal responsible for dissociation of the type 1 translocon, its assembly or both? What prevents large substrates like RTX toxins that are secreted in an unfolded form from being degraded in the cell? Finally, do the MFP and OMP also have a direct function during secretion or are they only involved in forming the tunnel-channel that spans both membranes?

We cannot answer these questions in this review but at least we want to summarize possible mechanisms and try to answer the questions based on today's knowledge.

Energizing type 1 secretion system transport

The stoichiometry of ATP consumption during the transport process of an ABC transporter has been characterized. In the case of the ABC importer OpuA from *Lactococcus lactis* (Patzlaff et al., 2003) and the maltose and glycine-betaine import system of *E. coli* (Mimmack et al., 1989), two ATP molecules are hydrolyzed during one transport cycle. In contrast, TAP1/2 or CFTR hydrolyses only one ATP during transport cycle (Chen et al., 2004; Zhou et al., 2006).

In the case of T1SS, the number of ATP molecules consumed per transport cycle is unknown. For proteins of up to 900 kDa such as LapA in *Pseudomonas fluorescens* (Hinsa et al., 2003) it seems, at first glance, impossible that only two ATP molecules are required to energize this process. In comparison, the Sec pathway consumes one ATP per 20–30 amino acids translocated (Schiebel et al., 1991; Uchida et al., 1995). Such an iterative ATP hydrolyzing process for energizing the transport of T1SS has not been confirmed so far.

The question is how T1SSs manage to energize the transport process. It was reported that the proton motive force (PMF) is partly involved in the early stages of HlyA translocation. HlyA secretion was inhibited if the membrane potential and the proton gradient of the PMF collapsed. Furthermore, selective depletion of the proton gradient also blocked successful secretion (Koronakis et al., 1991).

Most of the T1SS substrates have an isoelectric point below 5 (Delepelaire, 2004). This indicates that substrates have an overall negative charge within the cell, resulting in a charge gradient across the membrane. Furthermore, the concentration of the substrate inside the cell is much higher than in the extracellular space. A concentration gradient and the PMF facing outward might allow diffusion across the cell wall and both membranes.

During transport, as deduced from crystal structures of putative intermediates, an ABC transporter occurs in at least two different conformations. The inward-facing conformation represents a state of the ABC transporter open to the cytoplasm, while the outward-facing conformation is open to the periplasm. Some evidence indicates that the alternative conformations have different binding affinities (Martin et al., 2001). The inward facing conformation may have a higher binding affinity in comparison to the outward facing conformation. Therefore, the inward facing conformation binds the substrate, whereas the outward facing conformation promotes the release of the substrate into the extracellular space. Importantly, this mechanism could also prevent the reverse transport of the substrate. This mechanism is effective for small proteins, but the question arises as to how this can be directly transferred to mechanisms of higher polypeptides.

Another driving force for the type 1 secretion process could be linked to the glycine-rich repeats found in most T1SS substrates (Delepelaire, 2004). The amount of the repeats correlates with the size of the protein and occurs mainly with one repeat for every 6–12 kDa (Delepelaire, 2004; Linhartova et al., 2010). As mentioned above, these repeats bind Ca^{2+} ions and induce folding of the protein. Inside bacterial cells, the Ca^{2+} concentration is around 100 nM (Jones et al., 1999), which will prevent folding. After secretion, the proteins start folding in the extracellular space where the Ca^{2+} concentration is much higher. The Ca^{2+}-induced folding of the proteins could involve an inherent driving force, which 'pulls' the protein through the transporter. Such a pulling mechanism is mentioned

by Linhartova et al. (2010) and is supported by various experimental data from the hemolysin T1SS. The folding of the proteins would also prevent transport in the opposite direction, because folded proteins are too large to re-enter the TolC pore.

The role of the secretion signal

As mentioned above, many results concerning different T1SSs demonstrate that the C-terminal secretion signal of the substrates is required for secretion and directly effect the catalytic cycle of the NBDs of the ABC transporter. However, the impact appears to vary depending on the effect of the signal sequence on catalytic activity between different T1SSs. In the case of HasA, the secretion signal seems to be responsible for HasD-driven ATP hydrolysis and dissociation of the translocation complex (Masi and Wandersman, 2010). Data for the T1SS metalloproteases PrtB and PrtG of *Erwinia chrysanthemi* suggest that *in vitro* the secretion signal inhibits the ATPase activity of the ABC transporter PrtD (Delepelaire, 1994). These results lead to two fundamentally different mechanisms of how the secretion signal controls secretion. Does the secretion signal induce ATP binding/dimerization of the NBDs and thus induce secretion by switching the transporter from an inward- to an outward-facing conformation (activating model) concomitant with ATP hydrolysis? Or does the secretion signal trigger ATP-hydrolysis of the ABC transporter only at the last stage, leading to substrate release on the surface and dissociation of the secretion complex (terminating model)?

Figure 3 highlights how an 'activating model' could work. First, binding of ATP and the secretion signal of the substrate induce dimerization of the NBDs and simultaneously trigger recruiting of TolC to the secretion complex. In a second step, the ABC transporter changes the conformation of the TMDs to open up the transport pathway,

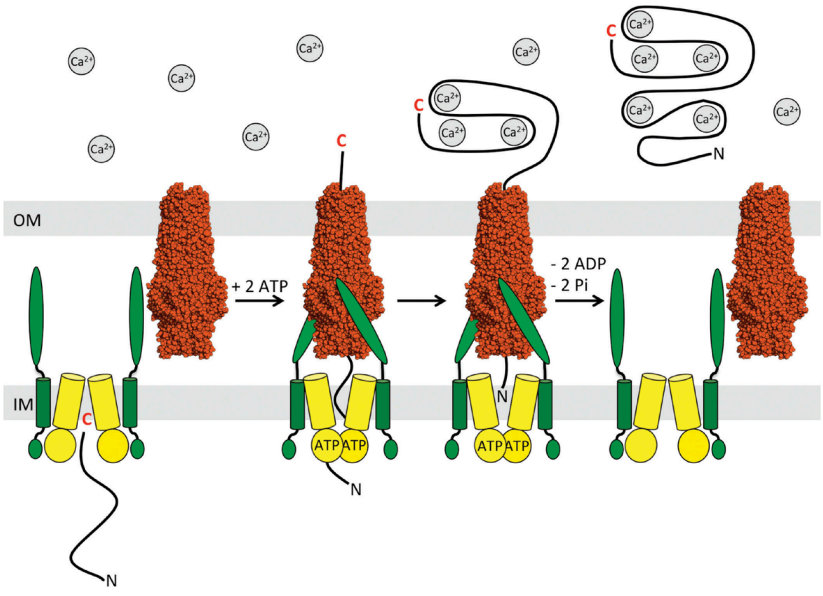

Figure 3 Possible steps of an activating type 1 secretion system pathway.
In the first step the outer membrane (OM) TolC (shown in side view as orange spheres and based on Protein Data Bank entry 1EK9), in the presence of the transport substrate, is recruited by the MFP and the ATP-binding cassette (ABC) protein (highlighted in green and yellow, respectively) located in the inner membrane. The oligomeric state of the membrane fusion protein (MFP) is unknown so far but to ensure a better overview only two MFPs are shown. TolC recruitment is mediated by binding of the substrate secretion signal to the two IM proteins, ATP-binding cassette transporter and MFP. Simultaneously, the binding of the secretion signal initiates ATP binding by the ABC transporter. The resulting conformational changes in the transmembrane domains of the ATP-binding cassette transporter displace the C-terminus of the unfolded substrate into the translocator. Third, the substrate is 'pulled' through the translocator by progressive folding in the calcium-rich extracellular space (calcium ions highlighted as gray dots). When the substrate passes completely through the translocator, it is presumed that this triggers ATP hydrolysis of both ATP molecules and will reset the transporter to its initial state. Finally, the transport complex dissociates and releases ADP and free phosphate into the cytoplasm. The fully folded substrate then diffuses into the extracellular space.

with the secretion signal leading the way into and through the transenvelope channel. In a third step, the substrate translocates progressively to the extracellular space, where folding and finally dissociation from the complex takes place. In a fourth step, the release of the substrate is in some way detected by the transporter and ATP-hydrolysis is triggered, which resets the transporter (switching from an outward- to an inward-facing conformation). This results in the disassembly of the whole secretion complex. Despite this, a detailed mechanism initiating ATP-hydrolysis is so far still unclear.

A 'terminating model' of protein secretion for type 1 secretion of HasA has also been proposed. Transport has to be initiated by a so-far unknown factor and leads to binding of ATP and the substrate. The substrate is bound by N-terminal 'anchors' to the ABC transporter and leads to the recruitment of the other subunits of the transport complex (Masi and Wandersman, 2010). Through ATP-binding, dimerization of the NBDs is induced, which leads to a switch of the transporter from an inward- to an outward-facing conformation. In the following step, the substrate is secreted with its N-terminus first and traverses the transport channel to the extracellular space. Finally, interaction of the C-terminal secretion signal induces ATP hydrolysis, which resets the transporter to an inward-facing conformation, releases the secreted protein and dissembles the translocation complex.

The main difference between the models is the orientation of the substrate during secretion, the C-terminal signal sequence either leading the way through the translocator or being the last to enter the channel. In favor of the activating model is the fact that many fusion proteins are secreted by the hemolysin T1SS (Mackman et al., 1987; Kenny et al., 1991; Blight and Holland, 1994; Gentschev et al., 2002; Bakkes et al., 2010; Schwarz et al., 2012). These proteins are fused at their C-terminus to a fragment of HlyA that contains the secretion signal. The secretion process can therefore only start after translation of the secretion signal. Furthermore, the isolated secretion signal of HlyA can be secreted autonomously by the T1SS (Jarchau et al., 1994) and contains all information for secretion.

In the case of HasA, multiple upstream regions of the primary sequence (anchoring sequences) appear to interact with the ABC transporter HasD (Masi and Wandersman, 2010). Other authors propose that the secretion signal is important for the dissociation of the secretion complex by affecting the catalytic cycle of the NBDs (Cescau et al., 2007). For these reasons, the 'terminating model' would be more appropriate in the case of HasA.

What protects unfolded intracellular type 1 secretion system substrates from degradation?

Several different experiments indicate that T1SS substrates are secreted in an unfolded state (Debarbieux and Wandersman, 2001; Bakkes et al., 2010). As mentioned above, the resulting question is what prevents the unfolded substrates from degradation?

In the case of the hemolysin T1SS, the ABC transporter contains a N-terminal appendix (CLD), with extensive identity to C39 proteases. The structure of the isolated domain was solved by nuclear magnetic resonance spectroscopy (Lecher et al., 2011). In contrast to regular C39 proteases like ComA from *Streptococcus pneumonia* (Ishii et al., 2010), the catalytic triad is degenerated and there is no enzyme activity. The CLD interacts with HlyA and is specifically required for secretion. Pull-down assays have indicated a specific interaction of the CLD with unfolded HlyA but not with its folded conformation (Lecher et al., 2012). Thus, the CLD interacts inside the cell with unfolded HlyA, perhaps acting as a chaperone to protect HlyA from degradation.

The N-terminal CLD is not present in all ABC transporters of T1SSs. How do other systems without a CLD manage to protect the unfolded substrate against degradation? For HasA, a small protein with no GG repeats, SecB was clearly shown to be required for HasA secretion (Delepelaire and Wandersman, 1998; Sapriel et al., 2003; Wolff et al., 2003). However, the question remains as to how other T1SSs that are SecB-independent like Prt (Delepelaire and Wandersman, 1998) and do not contain a CLD manage to stabilize their intracellular substrates.

Function of membrane fusion protein and outer membrane protein components of the translocator

MFPs and OMPs assemble to form a continuous channel together with the ABC transporter, which crosses both membranes and allows secretion of this cognate protein. Nevertheless, studies of random point mutations in MFPs, in particular HlyD (Pimenta et al., 2005) and CvaA (Hwang and Tai, 1999) and in OMPs, notably TolC (Vakharia et al., 2001), resulted in incorrect folding of the substrates, although these were secreted in normal amounts. In the case of TolC, six mutants were identified that had normal secretion levels but reduced hemolytic activity (Vakharia et al., 2001). The activity of secreted HlyA could be restored by de- and renaturating *in vitro*. Time-course experiments

in this study showed that HlyA is secreted more slowly in the mutants. This may point to a role of TolC in interacting with HlyA, thereby altering its correct folding (Delepelaire, 2004).

Specific mutants in MFPs resulted in similar phenotypes. In the case of HlyD, specific mutations in the periplasmic part of the protein resulted in reduced hemolytic activity of secreted HlyA (Pimenta et al., 2005). The amount of HlyD and HlyA in the mutants was similar to that of the wild type and the hemolytic activity of HlyA could be restored as in the case of TolC mutants by de- and renaturating *in vitro* (Pimenta et al., 2005). Another interesting aspect is that the hemolytic activity of these HlyD mutants is reduced by increasing the extracellular Ca^{2+} concentration. The exact role of Ca^{2+} is not completely understood and is highly speculative to the extent that it affects the formation and stable packing of the HlyD molecules and results in an aberrant movement of HlyA through the translocator (Pimenta et al., 2005).

Conclusion

The T1SS is one of the most important systems for the one-step secretion of substrates in Gram-negative bacteria, as shown by their ubiquitous occurrence and wide substrate range. Furthermore, the transport system is fascinating due to its simple arrangement of three components, enabling an energetically-favorable transport process over a huge distance. Current biochemical and structural data from T1SSs allow only an overview of the transport process. One of the most challenging and crucial aspects will be the investigation of the interaction of all translocator components. Further structural analysis will be essential to gain a better understanding of the transport mechanism and especially the key role of the ABC transporter.

Acknowledgments: We thank all members of the Institute of Biochemistry, Heinrich-Heine-Universität Düsseldorf, for helpful and very fruitful discussions. We gratefully acknowledge support (and training) from the International NRW Research School BioStruct, granted by the Ministry of Innovation, Science and Research of the State North Rhine-Westphalia, the Heinrich-Heine-University Düsseldorf, and the Entrepreneur Foundation at the Heinrich-Heine-University of Düsseldorf. Apologies to all our colleagues who contributed to our current understanding of T1SS but were not referenced due to space limitations.

Received May 6, 2013; accepted July 2, 2013; previously published online July 5, 2013

References

Akama, H., Kanemaki, M., Yoshimura, M., Tsukihara, T., Kashiwagi, T., Yoneyama, H., Narita, S., Nakagawa, A., and Nakae, T. (2004a). Crystal structure of the drug discharge outer membrane protein, OprM, of *Pseudomonas aeruginosa*: dual modes of membrane anchoring and occluded cavity end. J. Biol. Chem. *279*, 52816–52819.

Akama, H., Matsuura, T., Kashiwagi, S., Yoneyama, H., Narita, S., Tsukihara, T., Nakagawa, A., and Nakae, T. (2004b). Crystal structure of the membrane fusion protein, MexA, of the multidrug transporter in *Pseudomonas aeruginosa*. J. Biol. Chem. *279*, 25939–25942.

Ames, G.F., Mimura, C.S., Holbrook, S.R., and Shyamala, V. (1992). Traffic ATPases: a superfamily of transport proteins operating from *Escherichia coli* to humans. Adv. Enzymol. Relat. Areas. Mol. Biol. *65*, 1–47.

Andersen, C., Koronakis, E., Bokma, E., Eswaran, J., Humphreys, D., Hughes, C., and Koronakis, V. (2002). Transition to the open state of the TolC periplasmic tunnel entrance. Proc. Nat. Acad. Sci. USA *99*, 11103–11108.

Bakkes, P.J., Jenewein, S., Smits, S.H., Holland, I.B., and Schmitt, L. (2010). The rate of folding dictates substrate secretion by the *Escherichia coli* hemolysin type 1 secretion system. J. Biol. Chem. *285*, 40573–40580.

Balakrishnan, L., Hughes, C., and Koronakis, V. (2001). Substrate-triggered recruitment of the TolC channel-tunnel during type I export of hemolysin by *Escherichia coli*. J. Mol. Bol. *313*, 501–510.

Bavro, V.N., Pietras, Z., Furnham, N., Perez-Cano, L., Fernandez-Recio, J., Pei, X.Y., Misra, R., and Luisi, B. (2008). Assembly and channel opening in a bacterial drug efflux machine. Mol. Cell *30*, 114–121.

Benabdelhak, H., Kiontke, S., Horn, C., Ernst, R., Blight, M.A., Holland, I.B., and Schmitt, L. (2003). A specific interaction between the NBD of the ABC-transporter HlyB and a C-terminal fragment of its transport substrate haemolysin A. J. Mol. Biol. *327*, 1169–1179.

Binet, R. and Wandersman, C. (1995). Protein secretion by hybrid bacterial ABC-transporters: specific functions of the membrane ATPase and the membrane fusion protein. EMBO J. *14*, 2298–2306.

Blight, M.A. and Holland, I.B. (1994). Heterologous protein secretion and the versatile *Escherichia coli* haemolysin translocator. Trends. Biotechnol. *12*, 450–455.

Cescau, S., Debarbieux, L., and Wandersman, C. (2007). Probing the in vivo dynamics of type I protein secretion complex association through sensitivity to detergents. bacteriology Bacteriol. *189*, 1496–1504.

Chen, J., Lu, G., Lin, J., Davidson, A.L., and Quiocho, F.A. (2003). A tweezers-like motion of the ATP-binding cassette dimer in an ABC transport cycle. Mol. Cell *12*, 651–661.

Chen, M., Abele, R., and Tampe, R. (2004). Functional non-equivalence of ATP-binding cassette signature motifs in the transporter associated with antigen processing (TAP). J. Biol. Chem. *279*, 46073–46081.

Chervaux, C. and Holland, I.B. (1996). Random and directed mutagenesis to elucidate the functional importance of helix II and F-989 in the C-terminal secretion signal of *Escherichia coli* hemolysin. J. Bacteriol. *178*, 1232–1236.

Davidson, A.L., Dassa, E., Orelle, C., and Chen, J. (2008). Structure, function, and evolution of bacterial ATP-binding cassette systems. MMBR *72*, 317–364.

Dawson, R.J. and Locher, K.P. (2006). Structure of a bacterial multidrug ABC transporter. Nature *443*, 180–185.

Debarbieux, L. and Wandersman, C. (2001). Folded HasA inhibits its own secretion through its ABC exporter. EMBO J. *20*, 4657–4663.

Delepelaire, P. (1994). PrtD, the integral membrane ATP-binding cassette component of the *Erwinia chrysanthemi* metalloprotease secretion system, exhibits a secretion signal-regulated ATPase activity. J. Biol. Chem. *269*, 27952–27957.

Delepelaire, P. (2004). Type I secretion in gram-negative bacteria. Biochim. Biophys. Acta. *1694*, 149–161.

Delepelaire, P. and Wandersman, C. (1998). The SecB chaperone is involved in the secretion of the *Serratia marcescens* HasA protein through an ABC transporter. EMBO J. *17*, 936–944.

Delepelaire, P. and Wandersman, C. (2003). Protein export and secretion in Gram-negative bacteria. In: Microbial Transport Systems, G. Winkelmann, ed. (Weinheim: Wiley-VCH Verlag GmbH & Co. KGaA), pp. 165–208.

Eswaran, J., Hughes, C., and Koronakis, V. (2003). Locking TolC entrance helices to prevent protein translocation by the bacterial type I export apparatus. J. Mol. Biol. *327*, 309–315.

Finnie, C., Zorreguieta, A., Hartley, N.M., and Downie, J.A. (1998). Characterization of *Rhizobium leguminosarum* exopolysaccharide glycanases that are secreted via a type I exporter and have a novel heptapeptide repeat motif. J. Bacteriol. *180*, 1691–1699.

Gangola, P. and Rosen, B.P. (1987). Maintenance of intracellular calcium in *Escherichia coli*. J. Biol. Chem. *262*, 12570–12574.

Gentschev, I., Dietrich, G., and Goebel, W. (2002). The *E. coli* alpha-hemolysin secretion system and its use in vaccine development. Trends. Microbiol. *10*, 39–45.

Gentschev, I., Sokolovic, Z., Mollenkopf, H.J., Hess, J., Kaufmann, S.H., Kuhn, M., Krohne, G.F., and Goebel, W. (1995). *Salmonella* strain secreting active listeriolysin changes its intracellular localization. Infect. Immun. *63*, 4202–4205.

Gray, L., Mackman, N., Nicaud, J.M., and Holland, I.B. (1986). The carboxy-terminal region of haemolysin 2001 is required for secretion of the toxin from *Escherichia coli*. Mol. Gen. Genet. *205*, 127–133.

Higgins, C.F. (1992). ABC transporters: from microorganisms to man. Ann. Rev. Cell Biol. *8*, 67–113.

Higgins, M.K., Bokma, E., Koronakis, E., Hughes, C., and Koronakis, V. (2004). Structure of the periplasmic component of a bacterial drug efflux pump. Proc. Nat. Sci. USA *101*, 9994–9999.

Hinsa, S.M., Espinosa-Urgel, M., Ramos, J.L., and O'Toole, G.A. (2003). Transition from reversible to irreversible attachment during biofilm formation by *Pseudomonas fluorescens* WCS365 requires an ABC transporter and a large secreted protein. Mol. Microbiol. *49*, 905–918.

Holland, I.B., Schmitt, L., and Young, J. (2005). Type 1 protein secretion in bacteria, the ABC-transporter dependent pathway (review). Mol. Membr. Biol. *22*, 29–39.

Hollenstein, K., Frei, D.C., and Locher, K.P. (2007). Structure of an ABC transporter in complex with its binding protein. Nature *446*, 213–216.

Hui, D. and Ling, V. (2002). A combinatorial approach toward analyzing functional elements of the *Escherichia coli* hemolysin signal sequence. Biochem *41*, 5333–5339.

Hui, D., Morden, C., Zhang, F., and Ling, V. (2000). Combinatorial analysis of the structural requirements of the *Escherichia coli* hemolysin signal sequence. J. Biol. Chem. *275*, 2713–2720.

Hwang, J. and Tai, P.C. (1999). Mutational analysis of CvaA in the highly conserved domain of the membrane fusion protein family. Curr. Microbiol. *39*, 195–199.

Ishii, S., Yano, T., Ebihara, A., Okamoto, A., Manzoku, M., and Hayashi, H. (2010). Crystal structure of the peptidase domain of *Streptococcus* ComA, a bifunctional ATP-binding cassette transporter involved in the quorum-sensing pathway. J. Biol. Chem. *285*, 10777–10785.

Jarchau, T., Chakraborty, T., Garcia, F., and Goebel, W. (1994). Selection for transport competence of C-terminal polypeptides derived from *Escherichia coli* hemolysin: the shortest peptide capable of autonomous HlyB/HlyD-dependent secretion comprises the C-terminal 62 amino acids of HlyA. Mol. Gen. Genet. *245*, 53–60.

Johnson, J.M. and Church, G.M. (1999). Alignment and structure prediction of divergent protein families: periplasmic and outer membrane proteins of bacterial efflux pumps. J. Mol. Biol. *287*, 695–715.

Jones, H.E., Holland, I.B., Baker, H.L., and Campbell, A.K. (1999). Slow changes in cytosolic free Ca2+ in *Escherichia coli* highlight two putative influx mechanisms in response to changes in extracellular calcium. Cell Calcium *25*, 265–274.

Jones, P.M. and George, A.M. (1999). Subunit interactions in ABC transporters: towards a functional architecture. FEMS Micriobiol. Lett. *179*, 187–202.

Kadaba, N.S., Kaiser, J.T., Johnson, E., Lee, A., and Rees, D.C. (2008). The high-affinity *E. coli* methionine ABC transporter: structure and allosteric regulation. Science *321*, 250–253.

Kenny, B., Chervaux, C., and Holland, I.B. (1994). Evidence that residues -15 to -46 of the haemolysin secretion signal are involved in early steps in secretion, leading to recognition of the translocator. Mol. Microbiol. *11*, 99–109.

Kenny, B., Haigh, R., and Holland, I.B. (1991). Analysis of the haemolysin transport process through the secretion from *Escherichia coli* of PCM, CAT or beta-galactosidase fused to the Hly C-terminal signal domain. Mol. Microbiol. *5*, 2557–2568.

Kerr, I.D. (2002). Structure and association of ATP-binding cassette transporter nucleotide-binding domains. Biochim. Biophys. Acta *1561*, 47–64.

Kim, H.M., Xu, Y., Lee, M., Piao, S., Sim, S.H., Ha, N.C., and Lee, K. (2010). Functional relationships between the AcrA hairpin tip region and the TolC aperture tip region for the formation of the bacterial tripartite efflux pump AcrAB-TolC. J. Bacteriol. *192*, 4498–4503.

Koronakis, E., Hughes, C., Milisav, I., and Koronakis, V. (1995). Protein exporter function and in vitro ATPase activity are correlated in ABC-domain mutants of HlyB. Mol. Microbiol. *16*, 87–96.

Koronakis, V., Eswaran, J., and Hughes, C. (2004). Structure and function of TolC: the bacterial exit duct for proteins and drugs. Ann. Rev. Biochem. *73*, 467–489.

Koronakis, V., Hughes, C., and Koronakis, E. (1991). Energetically distinct early and late stages of HlyB/HlyD-dependent secretion across both *Escherichia coli* membranes. EMBO J. *10*, 3263–3272.

Koronakis, V., Hughes, C., and Koronakis, E. (1993). ATPase activity and ATP/ADP-induced conformational change in the soluble domain of the bacterial protein translocator HlyB. Mol. Microbiol. *8*, 1163–1175.

Koronakis, V., Sharff, A., Koronakis, E., Luisi, B., and Hughes, C. (2000). Crystal structure of the bacterial membrane protein TolC central to multidrug efflux and protein export. Nature *405*, 914–919.

Lecher, J., Schwarz, C.K., Stoldt, M., Smits, S.H., Willbold, D., and Schmitt, L. (2012). An RTX transporter tethers its unfolded substrate during secretion via a unique N-terminal domain. Structure *20*, 1778–1787.

Lecher, J., Stoldt, M., Schwarz, C.K., Smits, S.H., Schmitt, L., and Willbold, D. (2011). 1H, 15N and 13C resonance assignment of the N-terminal C39 peptidase-like domain of the ABC transporter Haemolysin B (HlyB). Biomol. NMR Assign. *5*, 199–201.

Lee, M., Jun, S.Y., Yoon, B.Y., Song, S., Lee, K., and Ha, N.C. (2012). Membrane fusion proteins of type I secretion system and tripartite efflux pumps share a binding motif for TolC in gram-negative bacteria. PloS One *7*, e40460.

Letoffe, S., Delepelaire, P., and Wandersman, C. (1996). Protein secretion in gram-negative bacteria: assembly of the three components of ABC protein-mediated exporters is ordered and promoted by substrate binding. EMBO J. *15*, 5804–5811.

Letoffe, S., Deniau, C., Wolff, N., Dassa, E., Delepelaire, P., Lecroisey, A., and Wandersman, C. (2001). Haemophore-mediated bacterial haem transport: evidence for a common or overlapping site for haem-free and haem-loaded haemophore on its specific outer membrane receptor. Mol. Microbiol. *41*, 439–450.

Letoffe, S., Ghigo, J.M., and Wandersman, C. (1994). Secretion of the *Serratia marcescens* HasA protein by an ABC transporter. J. Bacteriol. *176*, 5372–5377.

Linhartova, I., Bumba, L., Masin, J., Basler, M., Osicka, R., Kamanova, J., Prochazkova, K., Adkins, I., Hejnova-Holubova, J., Sadilkova, L., et al. (2010). RTX proteins: a highly diverse family secreted by a common mechanism. FEMS Microbiol. Rev. *34*, 1076–1112.

Lobedanz, S., Bokma, E., Symmons, M.F., Koronakis, E., Hughes, C., and Koronakis, V. (2007). A periplasmic coiled-coil interface underlying TolC recruitment and the assembly of bacterial drug efflux pumps. Proc. Nat. Acad. Sci. USA *104*, 4612–4617.

Locher, K.P., Lee, A.T., and Rees, D.C. (2002). The *E. coli* BtuCD structure: a framework for ABC transporter architecture and mechanism. Science *296*, 1091–1098.

Lu, S., and Zgurskaya, H.I. (2012). Role of ATP binding and hydrolysis in assembly of MacAB-TolC macrolide transporter. Mol. Microbiol. *86*, 1132–1143.

Ludwig, A. and Goebel, W. (1999). The family of the multigenic encoded RTX toxin. In: The Comprehensive Sourcebook of Bacterial Protein Toxins, J.E. Alouf, and J.H. Freer, eds. (Amsterdam: Academic Press), pp. 330–348.

Ludwig, A., Jarchau, T., Benz, R., and Goebel, W. (1988). The repeat domain of *Escherichia coli* haemolysin (HlyA) is responsible for its Ca2+-dependent binding to erythrocytes. Mol. Gen. Genet. *214*, 553–561.

Mackman, N., Baker, K., Gray, L., Haigh, R., Nicaud, J.M., and Holland, I.B. (1987). Release of a chimeric protein into the medium from *Escherichia coli* using the C-terminal secretion signal of haemolysin. EMBO J. *6*, 2835–2841.

Mackman, N. and Holland, I.B. (1984). Functional characterization of a cloned haemolysin determinant from *E. coli* of human origin, encoding information for the secretion of a 107K polypeptide. Mol. Gen. Genet. *196*, 129–134.

Martin, C., Higgins, C.F., and Callaghan, R. (2001). The vinblastine binding site adopts high- and low-affinity conformations during a transport cycle of P-glycoprotein. Biochem. *40*, 15733–15742.

Masi, M. and Wandersman, C. (2010). Multiple signals direct the assembly and function of a type 1 secretion system. J. Bacteriol. *192*, 3861–3869.

Mimmack, M.L., Gallagher, M.P., Pearce, S.R., Hyde, S.C., Booth, I.R., and Higgins, C.F. (1989). Energy coupling to periplasmic binding protein-dependent transport systems: stoichiometry of ATP hydrolysis during transport in vivo. Proc. Nat. Acad. Sci. USA *86*, 8257–8261.

Nehme, D. and Poole, K. (2007). Assembly of the MexAB-OprM multidrug pump of *Pseudomonas aeruginosa*: component interactions defined by the study of pump mutant suppressors. J. Bacteriol. *189*, 6118–6127.

Nicaud, J.M., Mackman, N., Gray, L., and Holland, I.B. (1986). The C-terminal, 23 kDa peptide of *E. coli* haemolysin 2001 contains all the information necessary for its secretion by the haemolysin (Hly) export machinery. FEBS Lett. *204*, 331–335.

Oldham, M.L., Khare, D., Quiocho, F.A., Davidson, A.L., and Chen, J. (2007). Crystal structure of a catalytic intermediate of the maltose transporter. Nature *450*, 515–521.

Oswald, C., Holland, I.B., and Schmitt, L. (2006). The motor domains of ABC-transporters. What can structures tell us? Naunyn-Schmiedeberg's archives of pharmacology *372*, 385–399.

Patzlaff, J.S., van der Heide, T., and Poolman, B. (2003). The ATP/substrate stoichiometry of the ATP-binding cassette (ABC) transporter OpuA. J. Biol. Chem. *278*, 29546–29551.

Pei, X.Y., Hinchliffe, P., Symmons, M.F., Koronakis, E., Benz, R., Hughes, C., and Koronakis, V. (2011). Structures of sequential open states in a symmetrical opening transition of the TolC exit duct. Proc. Nat. Sci. USA *108*, 2112–2117.

Pimenta, A.L., Racher, K., Jamieson, L., Blight, M.A., and Holland, I.B. (2005). Mutations in HlyD, part of the type 1 translocator for hemolysin secretion, affect the folding of the secreted toxin. J. Bacteriol. *187*, 7471–7480.

Pinkett, H.W., Lee, A.T., Lum, P., Locher, K.P., and Rees, D.C. (2007). An inward-facing conformation of a putative metal-chelate-type ABC transporter. Science *315*, 373–377.

Pugsley, A.P. and Schwartz, M. (1985). Export and secretion of proteins by bacteria. FEMS Microbiol. Lett. *32*, 3–38.

Rhodes, C.R., Gray, M.C., Watson, J.M., Muratore, T.L., Kim, S.B., Hewlett, E.L., and Grisham, C.M. (2001). Structural

consequences of divalent metal binding by the adenylyl cyclase toxin of *Bordetella pertussis*. Arch. Biochem. Biophys. *395*, 169–176.

Rose, T., Sebo, P., Bellalou, J., and Ladant, D. (1995). Interaction of calcium with *Bordetella pertussis* adenylate cyclase toxin. Characterization of multiple calcium-binding sites and calcium-induced conformational changes. J. Biol. Chem. *270*, 26370–26376.

Sapriel, G., Wandersman, C., and Delepelaire, P. (2003). The SecB chaperone is bifunctional in *Serratia marcescens*: SecB is involved in the Sec pathway and required for HasA secretion by the ABC transporter. J. Bacteriol. *185*, 80–88.

Satchell, K.J. (2011). Structure and function of MARTX toxins and other large repetitive RTX proteins. Ann. Rev. Microbiol. *65*, 71–90.

Schatz, P.J. and Beckwith, J. (1990). Genetic analysis of protein export in *Escherichia coli*. Ann. Rev. Genet. *24*, 215–248.

Schiebel, E., Driessen, A.J., Hartl, F.U., and Wickner, W. (1991). Delta mu H+ and ATP function at different steps of the catalytic cycle of preprotein translocase. Cell *64*, 927–939.

Schmitt, L., Benabdelhak, H., Blight, M.A., Holland, I.B., and Stubbs, M.T. (2003). Crystal structure of the nucleotide-binding domain of the ABC-transporter haemolysin B: identification of a variable region within ABC helical domains. J. Mol. Biol. *330*, 333–342.

Schulein, R., Gentschev, I., Schlor, S., Gross, R., and Goebel, W. (1994). Identification and characterization of two functional domains of the hemolysin translocator protein HlyD. Mol. Gen. Genet. *245*, 203–211.

Schwarz, C.K., Landsberg, C.D., Lenders, M.H., Smits, S.H., and Schmitt, L. (2012). Using an *E. coli* Type 1 secretion system to secrete the mammalian, intracellular protein IFABP in its active form. J. Biotechnol. *159*, 155–161.

Seeger, M.A. and van Veen, H.W. (2009). Molecular basis of multidrug transport by ABC transporters. Biochim Biophys Acta *1794*, 725–737.

Smith, P.C., Karpowich, N., Millen, L., Moody, J.E., Rosen, J., Thomas, P.J., and Hunt, J.F. (2002). ATP binding to the motor domain from an ABC transporter drives formation of a nucleotide sandwich dimer. Mol. Cell. *10*, 139–149.

Springer, W. and Goebel, W. (1980). Synthesis and secretion of hemolysin by *Escherichia coli*. J. Bacteriol. *144*, 53–59.

Stanley, P., Koronakis, V., and Hughes, C. (1991). Mutational analysis supports a role for multiple structural features in the C-terminal secretion signal of *Escherichia coli* haemolysin. Mol. Microbiol. *5*, 2391–2403.

Stegmeier, J.F., Polleichtner, G., Brandes, N., Hotz, C., and Andersen, C. (2006). Importance of the adaptor (membrane fusion) protein hairpin domain for the functionality of multidrug efflux pumps. Biochem. *45*, 10303–10312.

Strathdee, C.A. and Lo, R.Y. (1989). Cloning, nucleotide sequence, and characterization of genes encoding the secretion function of the *Pasteurella haemolytica* leukotoxin determinant. J. Bacteriol. *171*, 916–928.

Su, C.C., Yang, F., Long, F., Reyon, D., Routh, M.D., Kuo, D.W., Mokhtari, A.K., Van Ornam, J.D., Rabe, K.L., Hoy, J.A., et al. (2009). Crystal structure of the membrane fusion protein CusB from *Escherichia coli*. J. Mol. Biol. *393*, 342–355.

Tamura, N., Murakami, S., Oyama, Y., Ishiguro, M., and Yamaguchi, A. (2005). Direct interaction of multidrug efflux transporter AcrB and outer membrane channel TolC detected via site-directed disulfide cross-linking. Biochem. *44*, 11115–11121.

Thanabalu, T., Koronakis, E., Hughes, C., and Koronakis, V. (1998). Substrate-induced assembly of a contiguous channel for protein export from *E. coli*: reversible bridging of an inner-membrane translocase to an outer membrane exit pore. EMBO J. *17*, 6487–6496.

Tikhonova, E.B., Dastidar, V., Rybenkov, V.V., and Zgurskaya, H.I. (2009). Kinetic control of TolC recruitment by multidrug efflux complexes. Proc. Nat. Acad. Sci. USA *106*, 16416–16421.

Uchida, K., Mori, H., and Mizushima, S. (1995). Stepwise movement of preproteins in the process of translocation across the cytoplasmic membrane of *Escherichia coli*. J. Biol. Chem. *270*, 30862–30868.

Vaccaro, L., Scott, K.A., and Sansom, M.S. (2008). Gating at both ends and breathing in the middle: conformational dynamics of TolC. Biophys. J. *95*, 5681–5691.

Vakharia, H., German, G.J., and Misra, R. (2001). Isolation and characterization of *Escherichia coli* tolC mutants defective in secreting enzymatically active alpha-hemolysin. J. Bacteriol. *183*, 6908–6916.

Wandersman, C. and Delepelaire, P. (1990). TolC, an *Escherichia coli* outer membrane protein required for hemolysin secretion. Proc. Nat. Acad. Sci. USA *87*, 4776–4780.

Welch, R.A., Dellinger, E.P., Minshew, B., and Falkow, S. (1981). Haemolysin contributes to virulence of extra-intestinal *E. coli* infections. Nature *294*, 665–667.

Welch, R.A., Hull, R., and Falkow, S. (1983). Molecular cloning and physical characterization of a chromosomal hemolysin from *Escherichia coli*. Infect. Immun. *42*, 178–186.

Wolff, N., Ghigo, J.M., Delepelaire, P., Wandersman, C., and Delepierre, M. (1994). C-terminal secretion signal of an *Erwinia chrysanthemi* protease secreted by a signal peptide-independent pathway: proton NMR and CD conformational studies in membrane-mimetic environments. Biochem. *33*, 6792–6801.

Wolff, N., Sapriel, G., Bodenreider, C., Chaffotte, A., and Delepelaire, P. (2003). Antifolding activity of the SecB chaperone is essential for secretion of HasA, a quickly folding ABC pathway substrate. J. Biol. Chem. *278*, 38247–38253.

Xu, Y., Sim, S.H., Song, S., Piao, S., Kim, H.M., Jin, X.L., Lee, K., and Ha, N.C. (2010). The tip region of the MacA alpha-hairpin is important for the binding to TolC to the *Escherichia coli* MacAB-TolC pump. Biochem. Biophys. Res. Commun. *394*, 962–965.

Xu, Y., Lee, M., Moeller, A., Song, S., Yoon, B.Y., Kim, H.M., Jun, S.Y., Lee, K., and Ha, N.C. (2011a). Funnel-like hexameric assembly of the periplasmic adapter protein in the tripartite multidrug efflux pump in gram-negative bacteria. J. Biol. Chem. *286*, 17910–17920.

Xu, Y., Song, S., Moeller, A., Kim, N., Piao, S., Sim, S.H., Kang, M., Yu, W., Cho, H.S., Chang, I., et al. (2011b). Functional implications of an intermeshing cogwheel-like interaction between TolC and MacA in the action of macrolide-specific efflux pump MacAB-TolC. J. Biol. Chem. *286*, 13541–13549.

Yum, S., Xu, Y., Piao, S., Sim, S.H., Kim, H.M., Jo, W.S., Kim, K.J., Kweon, H.S., Jeong, M.H., Jeon, H., et al. (2009). Crystal structure of the periplasmic component of a tripartite macrolide-specific efflux pump. J. Mol. Biol. *387*, 1286–1297.

Zaitseva, J., Jenewein, S., Wiedenmann, A., Benabdelhak, H., Holland, I.B., and Schmitt, L. (2005). Functional characterization and ATP-induced dimerization of the isolated ABC-domain of the haemolysin B transporter. Biochem. *44*, 9680–9690.

Zaitseva, J., Oswald, C., Jumpertz, T., Jenewein, S., Wiedenmann, A., Holland, I.B., and Schmitt, L. (2006). A structural analysis of asymmetry required for catalytic activity of an ABC-ATPase domain dimer. EMBO J. *25*, 3432–3443.

Zgurskaya, H.I. and Nikaido, H. (2000). Cross-linked complex between oligomeric periplasmic lipoprotein AcrA and the inner-membrane-associated multidrug efflux pump AcrB from *Escherichia coli*. J. Bacteriol. *182*, 4264–4267.

Zgurskaya, H.I., Yamada, Y., Tikhonova, E.B., Ge, Q., and Krishnamoorthy, G. (2009). Structural and functional diversity of bacterial membrane fusion proteins. Biochim. Biophys. Acta. *1794*, 794–807.

Zhang, F., Sheps, J.A., and Ling, V. (1993). Complementation of transport-deficient mutants of *Escherichia coli* alpha-hemolysin by second-site mutations in the transporter hemolysin B. J. Biol. Chem. *268*, 19889–19895.

Zhang, F., Yin, Y., Arrowsmith, C.H., and Ling, V. (1995). Secretion and circular dichroism analysis of the C-terminal signal peptides of HlyA and LktA. Biochem. *34*, 4193–4201.

Zhou, Z., Wang, X., Liu, H.Y., Zou, X., Li, M., and Hwang, T.C. (2006). The two ATP binding sites of cystic fibrosis transmembrane conductance regulator (CFTR) play distinct roles in gating kinetics and energetics. J. Gen. Physiol. *128*, 413–422.

Zolnerciks, J.K., Andress, E.J., Nicolaou, M., and Linton, K.J. (2011). Structure of ABC transporters. Essays Biochem. *50*, 43–61.

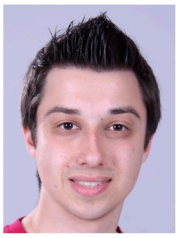

Michael Lenders studied Biochemistry at the Heinrich Heine University in Düsseldorf and graduated in 2012. His master thesis about the characterization of self-inserting membrane proteins by atomic force microscopy was prepared in cooperation with the Swiss Federal Institute of Technology Zürich. Since 2012, he is a PhD student focusing structural and functional characterization of the membrane fusion protein of the haemolysin A T1SS at the institute of Biochemistry, Heinrich Heine University Düsseldorf.

Sven Reimann studied Biochemistry at the Heinrich Heine University Düsseldorf. He did his Master's degree at the Forschungszentrum Jülich investigating a putative virulence factor of *Pseudomonas aeruginosa*. Since then he has been doing his PhD at the Institute of Biochemistry at a Heinrich Heine University Düsseldorf. His research field is the hemolysis A type 1 secretion system of *Escherichia coli* and particularly the ABC transporter HlyB.

Sander Smits obtained his PhD in Biochemistry at the Institute of Biochemistry, Heinrich Heine University Düsseldorf in 2008. Since then he has worked as a senior scientist with a special focus on membrane transporter, especially on the transporter of large unfolded proteins as well as peptides having an antimicrobial activity.

Lutz Schmitt studied Chemistry at the University of Freiburg and obtained his PhD from the Technical University Munich. After a Post Doc at Stanford University, he moved as a DFG-funded Emmy Noether Fellow to the Universities of Marburg and Frankfurt. In 2005 he was appointed as Professor of Biochemistry at the Heinrich Heine University Düsseldorf where he became full professor in 2008. His research interest are recognition processes at membranes and transport across membranes with an emphasis on ABC transporters.

3.2. Chapter II

Title: Interdomain regulation of the ATPase activity of the ABC transporter haemolysin B from *Escherichia coli*

Authors: Sven Reimann, Gereon Poschmann, Kerstin Kanonenberg, Kai Stühler, Sander H.J. Smits, Lutz Schmitt

Published in: *The Biochemical journal* (2016)
Impact factor: 3.562

Proportionate work on this publication: design and cloning of different mutants, expression and purification of proteins, ATPase assays, cross-linking studies, secretion analysis, data analysis, writing of the manuscript

Biochem. J. (2016) **473**, 2471–2483 doi:10.1042/BCJ20160154

Interdomain regulation of the ATPase activity of the ABC transporter haemolysin B from *Escherichia coli*

Sven Reimann*, Gereon Poschmann†, Kerstin Kanonenberg*, Kai Stühler†, Sander H.J. Smits* and Lutz Schmitt*‡[1]

*Institute of Biochemistry, Heinrich-Heine-University Düsseldorf, Universitätsstraße 1, 40225 Düsseldorf, Germany
†Molecular Proteomics Laboratory, Biomedizinisches Forschungszentrum (BMFZ), Heinrich-Heine-University Düsseldorf, Universitätsstraße 1, 40225 Düsseldorf, Germany
‡Center of Excellence on Plant Sciences (CEPLAS), Heinrich-Heine-University Düsseldorf, Universitätsstraße 1, 40225 Düsseldorf, Germany

Type 1 secretion systems (T1SS) transport a wide range of substrates across both membranes of Gram-negative bacteria and are composed of an outer membrane protein, a membrane fusion protein and an ABC (ATP-binding cassette) transporter. The ABC transporter HlyB (haemolysin B) is part of a T1SS catalysing the export of the toxin HlyA in *E. coli*. HlyB consists of the canonical transmembrane and nucleotide-binding domains. Additionally, HlyB contains an N-terminal CLD (C39-peptidase-like domain) that interacts with the transport substrate, but its functional relevance is still not precisely defined. In the present paper, we describe the purification and biochemical characterization of detergent-solubilized HlyB in the presence of its transport substrate. Our results exhibit a positive co-operativity in ATP hydrolysis. We characterized further the influence of the CLD on kinetic parameters by using an HlyB variant lacking the CLD (HlyBΔCLD). The biochemical parameters of HlyBΔCLD revealed an increased basal maximum velocity but no change in substrate-binding affinity in comparison with full-length HlyB. We also assigned a distinct interaction of the CLD and a transport substrate (HlyA1), leading to an inhibition of HlyB hydrolytic activity at low HlyA1 concentrations. At higher HlyA1 concentrations, we observed a stimulation of the hydrolytic activities of both HlyB and HlyBΔCLD, which was completely independent of the interaction of HlyA1 with the CLD. Notably, all observed effects on ATPase activity, which were also analysed in detail by mass spectrometry, were independent of the HlyA1 secretion signal. These results assign an interdomain regulatory role for the CLD modulating the hydrolytic activity of HlyB.

Key words: ABC transporter, ATPase inhibition, enzyme kinetics, haemolysin, protein translocation, RTX, type I secretion system.

INTRODUCTION

Type 1 secretion systems (T1SS) are membrane-embedded transport machineries involved in the secretion of a wide range of substrates in Gram-negative bacteria. Substrate transport occurs in one step from the cytosol directly into the exterior, passing both the inner and outer membrane [1]. Substrates of T1SS include lipases, proteases, toxins and S-layer proteins, as well as haem-binding proteins [2]. The paradigm of T1SS is the haemolysin transport system from *Escherichia coli*, which transports HlyA (haemolysin A), a 110 kDa toxin produced by several uropathogenic *E. coli* strains [3,4]. HlyA belongs to the large RTX (repeats in toxins) protein family [5]. RTX proteins contain nonapeptide repeats, so-called GG-repeats, with the consensus sequence GGxGxDxUx, where x can be any amino acid residue and U represents a large hydrophobic amino acid [6]. These repeats are able to bind Ca^{2+} ions with micromolar affinity, inducing protein folding to build up a so-called β-roll motif [6,7]. The number of GG-repeats varies within the transported substrates and correlates in general with the size of the protein [8,9].

In general, T1SS substrates contain a non-cleavable C-terminal secretion signal that initiates the assembly of the whole transport complex and are essential and sufficient for protein secretion [10–12]. In the case of HlyA, the secretion signal corresponds to the last 50–60 C-terminal amino acids [13–15].

The T1SS of HlyA in *E. coli* is composed of three components and spans the periplasm from the inner membrane to the outer membrane. Two proteins are located in the inner membrane, the ABC (ATP-binding cassette) transporter HlyB (haemolysin B) and the MFP (membrane-fusion protein) HlyD (haemolysin D) [10,11,16]. Upon substrate interaction, the MFP recruits the third component of the secretion machinery, the OMP (outer membrane protein) TolC [12]. The functional complex transports the substrate protein in an unfolded state in one step across both membranes [1,11].

The general ABC transporter blueprint includes two hydrophobic TMDs (transmembrane domains) and two hydrophilic NBDs (nucleotide-binding domains). In the case of HlyB, there is an additional 123-amino-acid large N-terminal domain (Figure 1), which possesses a striking sequence and structural homology with C39-peptidases. These C39-peptidases are part of ABC transporters that usually mediate the transport of class II microcins. The proteolytically active N-terminal domain cleaves the N-terminal signal sequence of the precursor peptide of the transport substrate and thereby evolves the mature and active bacteriocin [17]. In contrast, the N-terminal domain of HlyB contains a degenerated catalytic triad and shows no proteolytic activity. Therefore the N-terminal domain of HlyB was called a CLD (C39-peptidase-like domain). Despite the lack of proteolytic activity, the CLD interacts specifically with unfolded HlyA and

Abbreviations: ABC, ATP-binding cassette; $BS(PEG)_5$, bis-*N*-succinimidyl-penta(ethylene glycol) ester; CBB, Coomassie Brilliant Blue; CLD, C39-peptidase-like domain; CMC, critical micellar concentration; HCD, higher-energy collisional dissociation; HlyA, haemolysin A; HlyB, haemolysin B; HlyD, haemolysin D; IMAC, immobilized metal-ion-affinity chromatography; LMNG, lauryl maltose neopentyl glycol; MFP, membrane-fusion protein; NBD, nucleotide-binding domain; RTX, repeats in toxins; SEC, size-exclusion chromatography; T1SS, Type 1 secretion system; TBS-T, TBS with Tween 20; TEV, tobacco etch virus; TFA, trifluoroacetic acid; TMD, transmembrane domain.

[1] To whom correspondence should be addressed (email Lutz.Schmitt@hhu.de).

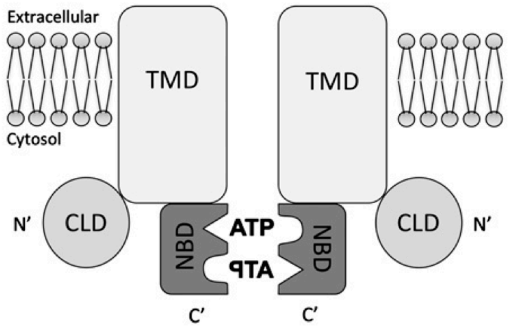

Figure 1 Schematic model of the spatial orientation of the HlyB domains

HlyB is schematically shown as a dimer with the suggested spatial orientation of the TMDs, the NBDs and the CLD.

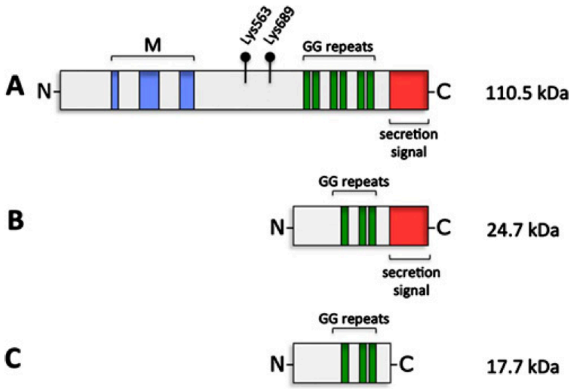

Figure 2 Schematic overview of the HlyA variants

(**A**) HlyA with the putative membrane insertion domain (M, blue), two lysine residues which are acylated by HlyC (haemolysin C), six RTX repeats of the consensus sequence GGxGxDxUx (x is any amino acid residue; U is a large hydrophobic amino acid residue) (green) and a C-terminal secretion signal (red). (**B**) HlyA1, the C-terminal fragment of HlyA with three RTX repeats. (**C**) HlyA2, the C-terminal fragment of HlyA without the last 57 amino acid residues harbouring the secretion signal.

is indispensable for protein secretion [18]. Furthermore, it was proposed that the CLD tethers the substrate in a secretion-competent state [18], but its precise molecular function during secretion remains elusive.

In a previous study, HlyA was replaced by a C-terminal fragment (amino acids 807–1024) called HlyA1 [19] (Figure 2). This truncated protein contains the C-terminal secretion signal and three GG-repeats. It was demonstrated that HlyA1 is secreted with an efficiency comparable with that of HlyA [20]. Additionally, such HlyA fragments also bind Ca^{2+} ions with the same affinity leading to folding into a stable conformation as observed for full-length HlyA [19,21].

In the present paper, we describe the purification of full-length HlyB and its co-operative ATPase activity and provide strong evidence that the N-terminal domain of HlyB, the CLD, exhibits a novel regulatory role by inhibiting the ATPase activity. Furthermore, we demonstrate stimulation of the ATPase activity of HlyB in the presence of its transport substrate, which we show to be independent of the CLD and its secretion signal. We also analysed different cross-linking patterns of HlyB and its substrate by mass spectrometry, which correlate to stimulation and inhibition of HlyB ATPase activity. On the basis of our results, we propose a negative intermolecular regulation of ATPase activity of HlyB by the CLD. These findings represent a further step to understand the molecular principles of the HlyA Type 1 secretion process.

EXPERIMENTAL

Cloning of HlyB, HlyBΔCLD, HlyB-H662A and HlyB-Y20A

For cloning of the HlyB expression plasmid primers P1 and P2 (Table 1) were used to amplify *hlyB* (2124 bp) from the template plasmid pLG814 [14,22]. The HlyB sequence was subcloned into vector pET401 by using compatible and cohesive ends (EcoRI, BamHI). An N-terminal decahistidine tag with a protease cleavage site (Factor Xa) was introduced by addition of an oligonucleotide pair at the 5′ end of *hlyB* (primers P3 and P4; Table 1). Subsequently, the tagged *hlyB* gene was cloned into the expression vector pBADHisB using the NcoI (5′) and the SacI (3′) restriction site. The latter was obtained from subcloning into vector pET401. The resulting expression vector was named pBADHisHlyB. For investigation of HlyB lacking the N-terminal CLD, we created an expression plasmid with *hlyB* lacking the N-terminal 123 amino acids and termed this construct HlyBΔCLD. The construct was obtained using the In-Fusion Advantage PCR Cloning kit (Clontech) as recommended by the manufacturer. The plasmid pBADHisHlyB was linearized with primers P5 and P6 (Table 1) and *hlyB* was amplified from pBADHisHlyB using primers P7 and P8 (Table 1). After successful cloning, we obtained the expression plasmid pBADHisHlyBΔCLD. All expression constructs were used to express and subsequently purify HlyB or HlyBΔCLD in *E. coli*. To evaluate our purification method, we used an HlyB-H662A mutant, which is deficient in ATP hydrolysis [23]. A H662A mutation was inserted into the plasmids pBADHisHlyB and pBADHisHlyBΔCLD using the QuikChange® site-directed mutagenesis kit (Stratagene) following the manufacturer's instructions. The Y20A mutation was also introduced by QuikChange® site-directed mutagenesis following the manufacturer's instructions [18]. The correctness of all constructs was verified by sequencing analysis.

Protein purification of HlyB, HlyBΔCLD, HlyB-H662A and HlyB-Y20A

E. coli BL21(DE3) cells were transformed with pBADHlyB and exposed on selective agar plates containing 100 μg/ml ampicillin. A selective overnight culture was inoculated with a single *E. coli* colony and incubated for 16 h at 37 °C and vigorously shaking at 200 rev./min. A main culture with selective 2YT medium [1.6 % (w/v) tryptone, 1 % (w/v) yeast extract and 0.5 % NaCl] was inoculated from the overnight culture and grown to a OD_{600} of 4.0 before expression was started by addition of 10 mM arabinose. After 2 h of incubation, cells were harvested by centrifugation and resuspended in buffer A (25 mM NaH_2PO_4, 100 mM KCl and 20 % glycerol, pH 8). Bacteria were disrupted by multiple passes through a cell disrupter (Constant Systems) at 2.5 kbar (1 bar = 100 kPa). The homogenate was centrifuged at 12000 ***g*** and the supernatant was centrifuged again at 120000 ***g***. The pellet containing cell membranes was resuspended in buffer A, solubilized with 1 % Fos-Choline-14 at 4 °C for 1 h and centrifuged again at 120000 ***g*** for 30 min. The supernatant was loaded on an IMAC (immobilized metal-ion-affinity chromatography) column [5 ml

Table 1 Overview of the primers used and their sequences

Name	Sequence (5′→3′)
P1	GCTATCCATGGCGAATTCTGATTCTTGTCATAAAATTGATTATGGG
P2	CGTGTCTAGATTACAGGATCCCGTCTGACTGTAACTGATATAAGTAACTG
P3	AATTCTCATCACCATCACCATCACCATCACCATCATAGCATCGAAGGGCGC
P4	AATTGCGCCCTTCGATGCTATGATGGTGATGGTGATGGTGATGGTGATGAG
P5	TCTAGAGCGGCCGCCACCG
P6	ATGGTGATGGTGATGGTGATGAGAATTCGCCATGGT
P7	CATCACCATCACCATCACCATCATGAGAATCTTTATTTTCAGGGCGCTTCCCGTTCTTCTGTTGC
P8	GGCGGCCGCTCTAGATTACAG
P9	CGCCTTGATGATGCGTTTTCACGGAATG
P10	CATTCCGTGAAAACGCATCATCAAGGCG
P11	CGCCTTGATGATTGGTTTTCACGGAATG
P12	CATTCCGTGAAAACCAATCATCAAGGCG

HiTrap Chelating HP column (GE Healthcare) loaded with $ZnSO_4$] and washed with buffer A including 0.02 % LMNG (lauryl maltose neopentyl glycol). Non-specifically bound protein was removed by washing with buffer A including 0.02 % LMNG and 40 mM histidine. HlyB was eluted with buffer A including 0.02 % LMNG and 150 mM histidine. Fractions containing HlyB were pooled and concentrated by ultrafiltration using an Amicon Ultra centrifugal filter unit (100 000 Da molecular-mass cut-off; Merck Millipore). To increase the protein purity and to change the buffer for long-term protein stability, SEC (size-exclusion chromatography) was performed using a Superdex 200 10/300 GL column (GE Healthcare) using buffer B (10 mM Caps and 20 % glycerol, pH 10.4) including 0.02 % LMNG [24]. HlyB-containing fractions were flash-frozen in liquid nitrogen and stored at −80 °C until further use. HlyBΔCLD, HlyB-H662A and HlyB-Y20A were purified accordingly.

Protein purification of HlyA1 and HlyA2

The HlyA derivatives HlyA1 (amino acids 807–1024; 24.9 kDa) and HlyA2 (amino acids 807–966; 17.7 kDa) were purified as described previously [19] with the following modifications. For overexpression of HlyA1, *E. coli* BL21(DE3) cells were transformed with pSOI-HlyA1 and exposed on selective 2YT agar plates containing 100 μg/ml ampicillin. A selective overnight culture was inoculated with a single *E. coli* colony and incubated for 16 h at 37 °C and vigorously shaken at 200 rev./min. A main culture with selective 2YT medium was inoculated from the overnight culture and grown to a OD_{600} of 1.0 and induced by the addition of 1 mM IPTG. After incubation for 3 h at 37 °C, cells were removed by centrifugation at 5800 ***g*** for 10 min. HlyA1 was purified from the medium supernatant. Supernatant from 200 ml of medium was concentrated to a final volume of 2 ml using an Amicon Ultra centrifugal filter unit (10 000 Da molecular-mass cut-off; Merck Millipore) and subjected to SEC using a HiLoad Superdex 75 16/600 prep grade column (GE Healthcare), equilibrated with 100 mM HEPES (pH 8) and 250 mM NaCl. Protein-containing fractions were pooled, concentrated to 4 mg/ml and stored at −20 °C.

For the purification of HlyA2, *E. coli* BL21(DE3) cells were transformed with pSOI-HlyA2 and expressed as described above for HlyA1. The main culture was grown to a OD_{600} of 1.0 and induced with 4 mM arabinose. After incubation for 90 min at 37 °C, cells were harvested by centrifugation at 5800 ***g*** for 10 min. The cell pellet was resuspended in buffer C (10 mM Tris/HCl, 100 mM KCl, 0.2 mM EGTA and 10 % glycerol, pH 8) and homogenized by three passages through a cell disruptor at 2.5 kbar (Constant Systems). The cell lysate was centrifuged at 120 000 ***g*** for 45 min at 4 °C and the supernatant was loaded on an IMAC column [5 ml HiTrap Chelating HP column (GE Healthcare) loaded with $NiSO_4$] equilibrated with buffer C containing 10 mM imidazole. Non-specifically bound protein was washed off the column with buffer C containing 25 mM imidazole and HlyA2 was eluted with buffer containing 500 mM imidazole. Fractions containing HlyA2 were pooled and diluted 15-fold in buffer D (10 mM Tris/HCl, 10 mM KCl, 0.2 mM EGTA and 10 % glycerol, pH 8). Further purification of HlyA2 was performed via anion-exchange chromatography using a HiTrap Q HP column (GE Healthcare) equilibrated with buffer D. HlyA2 was eluted with a KCl gradient from 10 mM to 500 mM over a volume of 200 ml. HlyA2-containing fractions were pooled and the buffer was exchanged with 10 mM CAPS (pH 10.4) via a PD-10 desalting column (GE Healthcare). The HlyA2 His tag was removed by TEV (tobacco etch virus) protease. The purification of the TEV protease was performed as described in [25]. HlyA2 was digested for 16 h in 100 mM HEPES with 150 mM NaCl (pH 8). The residual His tag and TEV protease were removed by an IMAC step and untagged HlyA2 was collected, concentrated using an Amicon Ultra centrifugal filter unit (10 000 Da molecular-mass cut-off; Merck Millipore) and stored at −80 °C.

Electrophoresis and immunological technique

SDS/PAGE and subsequent CBB (Coomassie Brilliant Blue) staining were used to analyse proteins. The immunodetection was performed with anti-HlyB antibody rabbit polyclonal serum at 1:8000 dilution in TBS-T (TBS with Tween 20: 20 mM Tris base, 300 mM NaCl and 0.05 % Tween 20, pH 8).

Solubilization screen via the dot-blot technique

Membranes were thawed on ice and the protein concentration was adjusted to 5 mg/ml. The solubilization was performed at 4 °C for 1 h with gentle mixing. The detergents were used at a concentration of 1 % (w/v) or higher, depending on their CMC (critical micellar concentration). After solubilization, the samples were centrifuged for 30 min at 100 000 ***g*** and 4 °C. The supernatant was supplemented with SDS sample buffer and heated to 65 °C for 10 min. Subsequently 3 μl of the probe was spotted on a nitrocellulose membrane and dried for 12 h. The membrane surface was blocked by incubation for 3 h in TBS-T supplemented with 5 % (w/v) non-fat dried skimmed milk powder. The target

protein was detected by immune detection using a polyclonal anti-HlyB antibody.

ATPase assays

The Malachite Green assay was used for quantification of hydrolytic activity as described in [26] with the following modifications. Reactions were performed in 100 mM HEPES (pH 7) containing 20-fold CMC of LMNG detergent and ATP concentrations ranging from 0 mM to 5 mM. HlyB and HlyBΔCLD were used at 1 μM concentration and diluted into assay buffer. Reactions were started by the addition of 10 mM $MgCl_2$, incubated at 25 °C and stopped after 30 min by transferring 25 μl of the reaction volume into 175 μl of 20 mM H_2SO_4. Free inorganic phosphate (P_i) was stained by adding 50 μl of dye solution [0.096 % Malachite Green, 1.48 % (w/v) ammonium molybdate and 0.173 % Tween 20 in 2.36 M H_2SO_4] to the quenched reaction volume. Quantification was performed spectroscopically 10 min after adding dye solution by measuring the absorbance at 595 nm. For data evaluation, all appropriate controls were subtracted. Data points were fitted using Prism software (GraphPad) to one of the following equations.

Eqn (1), the Hill equation, is:

$$v = \frac{V_{max}[S]^h}{K_{0.5}{}^h + [S]^h} \quad (1)$$

Here, v corresponds to the ATPase activity as a function of the substrate concentration [S], V_{max} is the maximum enzyme activity, h is the Hill coefficient, and $K_{0.5}$ is the substrate concentration at which 50 % enzyme binding sites are occupied.

Eqn (2), which assumes two independent binding sites, is:

$$v = \frac{K_1K_2v_0 + K_2v_1[S] + v_2[S]^2}{K_1K_2 + K_2[S] + [S]^2} \quad (2)$$

Here, v corresponds to the ATPase activity as a function of the substrate concentration [S]. K_1 represents the substrate concentration of half-maximum inhibition, K_2 represents the substrate concentration of half-maximum activation of ATPase activity, v_0 is the basal activity of HlyB in the absence of the substrate, v_1 is the minimal enzyme activity and v_2 is the maximum enzyme activity.

Eqn (3), the classic Michaelis–Menten equation, is:

$$v = \frac{V_{max}[S]}{K_m + [S]} \quad (3)$$

Here, v corresponds to the ATPase activity as a function of the substrate concentration [S], V_{max} is the maximum enzyme activity, and K_m is the Michaelis–Menten constant.

Substrate-modulated kinetics were performed as described above, but the reaction buffer contained additionally up to 20 μM HlyA1 or HlyA2. ATPase assays with folded substrate also included 4 mM $CaCl_2$ in the assay buffer. Appropriate controls confirmed that HlyB hydrolytic behaviour is not influenced by the assay buffer containing 4 mM $CaCl_2$.

In vitro cross-linking of HlyB and HlyA2

Reactions were performed in 100 mM HEPES (pH 7) containing 20-fold CMC of LMNG detergent and 2 mM ATP. HlyB was diluted in assay buffer to a final concentration of 1 μM. Additionally HlyA2 was added to a final concentration of 1 μM or 20 μM respectively. Reactions were started by the addition of 10 mM $MgCl_2$. After incubation at 25 °C for 30 min, proteins were cross-linked by employing $BS(PEG)_5$ [bis-*N*-succinimidyl-penta(ethylene glycol) ester] (Thermo Fisher Scientific), which is a homo-bifunctional lysine-specific cross-linker with a maximal arm length of 21.7 Å (1 Å = 0.1 nm). $BS(PEG)_5$ was used at a final concentrations of 0.8 mM (1 μM HlyA2) or 3.6 mM (20 μM HlyA2) respectively. The reaction mixture was incubated further at 25 °C for 1 h and finally quenched by adding 50 mM Tris/HCl (pH 7). Samples were analysed further by SDS/PAGE, LC and MS.

Liquid chromatography and mass spectrometry

Three independent preparations of cross-linked 'inhibition' (1 μM HlyA2) or 'stimulation' (20 μM HlyA2) samples were analysed by LC–MS.

Samples were separated by SDS/PAGE (10 % gel) and, after staining with CBB, protein-containing bands were excised and processed as described in [27]. Briefly, bands were washed, reduced, alkylated with iodoacetamide and digested overnight at 37 °C with 0.05 μg of trypsin (Serva) in 50 mM NH_4HCO_3. After peptide extraction with 1:1 (v/v) 0.1 % TFA (trifluoroacetic acid)/acetonitrile and vacuum concentration, peptides were resuspended in 0.1 % TFA.

First, peptides were separated by reverse-phase LC on an UltiMate 3000 RSLCnano system (Thermo Scientific). Here, peptides were initially pre-concentrated on a trap column (Acclaim PepMap100, 3 μm C_{18} particle size, 100 Å pore size, 75 μm inner diameter, 2 cm length, Thermo Scientific) for 10 min at a flow rate of 6 μl/min and subsequently separated at a flow rate of 300 nl/min on an analytical column (Acclaim PepMapRSLC, 2 μm C_{18} particle size, 100 Å pore size, 75 μm inner diameter, 25 cm length, Thermo Scientific) using 0.1 % TFA as the mobile phase and increasing concentrations of acetonitrile for 1 h.

In a second step, separated peptides were analysed with a Q Exactive hybrid quadrupole-Orbitrap mass spectrometer coupled to an LC system via a nanoelectrospray ionization source equipped with distal coated SilicaTip emitters (New Objective).

The mass spectrometer was operated in positive data-dependent mode, a spray voltage of 1400 V was applied and the capillary temperature set to 250 °C. First, full scans were recorded with a resolution of 70000 over a scan rage from 200 to 2000 *m/z* in the Orbitrap analyser in profile mode with a maximum ion time of 50 ms and the target value for the automatic gain control set to 3000000. Subsequently, up to 20 precursors (charge states 2–5) were isolated within a 2 *m/z* isolation window. Isolated precursors were individually fragmented by HCD (higher-energy collisional dissociation) in the HCD cell of the instrument and MS/MS spectra were recorded within the Orbitrap analyser with a maximal ion time of 50 ms and the target value for the automatic gain control set to 100000. MS/MS spectra were acquired over an available scan range of 200 to 2000 *m/z* at a resolution of 17500. Already fragmented precursors were excluded from further isolation for the next 10 s.

To initially identify HlyB and HlyA2 peptide sequences, Proteome Discoverer (version 1.1.1.14, Thermo Scientific) was used to trigger searches by MS Amanda in a database consisting of 787 *E. coli* K12 entries downloaded on 14 October 2015 and additional sequences of HlyB and HlyA2. Searches were conducted with tryptic cleavage specificity with a maximal number of two missed cleavages, a mass tolerance of 5 p.p.m. for precursor and 20 p.p.m. for fragment spectra. Carbamidomethyl at cysteine residues was set as fixed modification and methionine

oxidation, acetylation at protein N-termini and semihydrolysed $BS(PEG)_5$ linker attached to lysine residues (+320.1471 Da) were considered as dynamic modifications.

For the detection of cross-linked peptides, StavroX version 3.5.1 [28] was applied for mapping spectra against HlyB and HlyA2 sequences. Here, tryptic cleavage specificity was considered with a maximum of one missed cleavage after arginine residues and two missed cleavages after lysine residues. Carbamidomethyl at cysteine residues was set as fixed and oxidation of methionine as variable modification. A reaction of the cross-linker was considered between lysine residues as well as N-termini between peptides, within peptides and as dead-end linker after reaction with water. The precursor precision was set to 10 p.p.m., the fragment precision to 20 p.p.m. and a slow precise scoring was applied. For individual searches, the cut-off scores were 41–55 for detecting decoy hits at a 5 % false discovery rate and 52–67 at a 1 % false discovery rate.

Interesting candidate peptides and dipeptides were evaluated further using the Thermo Xcalibur 3.0.63 Qual Browser (Thermo Scientific) by manual inspection of spectra and quantification of peptide intensities by generating extracted ion chromatograms from precursor spectra within a mass window of 10 p.p.m.

Secretion analysis of HlyA in the presence of HlyB mutants

Plasmid pK184-HlyBD was mutated by site-directed mutagenesis to insert single point mutations in *hlyB*. Appropriate oligonucleotides (primers P9–P12; Table 1) were used to replace Lys^{322} of HlyB with alanine or tryptophan respectively. The correctness of all constructs was verified by sequencing analysis.

Chemically competent *E. coli* BL21(DE3) cells were transformed with pK184-HlyBD and pSU-HlyA and grown on selective 2YT agar plates containing 100 μg/ml ampicillin and 30 μg/ml kanamycin. A selective overnight culture was inoculated with a single *E. coli* colony and incubated for 16 h at 37 °C and vigorously shaken at 200 rev./min. A main culture with selective 2YT medium was inoculated from the overnight culture and grown to a OD_{600} of 1.0. The expression of HlyA, HlyB and HlyD was induced with 1 mM IPTG, and $CaCl_2$ was added to the medium at a final concentration of 5 mM. Cells were grown for 2 h at 200 rev./min at 37 °C. Subsequently a 1 ml aliquot was taken and centrifuged at 14 000 ***g*** for 5 min. Cells in the aliquot were adjusted with water to OD_{600} equivalents of 0.1. The expression level of HlyB was determined via Western blotting using a polyclonal anti-HlyB antibody. To determine the amount of secreted HlyA, aliquot supernatants were adjusted correlating to a OD_{600} of 3 and 15 μl were analysed via CBB-stained SDS/PAGE gels.

RESULTS

Cloning, expression and purification of the ABC transporter HlyB

We cloned *hlyB* (2124 bp) from the template plasmid pLG814 into the expression vector pBADHisB [14,22]. The construct encoded HlyB with a theoretical total mass of 82.2 kDa including an N-terminal decahistidine tag. For investigation of HlyB lacking the N-terminal CLD, we also created an expression plasmid encoding HlyB lacking the N-terminal 123 amino acids and termed this construct HlyBΔCLD (67.9 kDa). We also used the HlyB-H662A and HlyB-Y20A mutants, which display a deficiency in ATP hydrolysis [23] or strongly reduced substrate binding [18,23] respectively.

All HlyB derivatives described above were expressed and purified using the same protocol. To identify suitable detergents for the solubilization of HlyB, a dot-blot detergent screen [29] was used highlighting that Fos-Choline-14 was one of the few detergents appropriate for solubilizing HlyB from the membranes (Supplementary Figure S1 and Supplementary Table S1). On the basis of the results obtained from the dot-blot analysis, isolated *E. coli* membranes were adjusted to 50 mg/ml and solubilized by addition of 1 % (w/v) Fos-Choline-14 with gentle agitation at 4 °C for 1 h. To separate solubilized His-tagged HlyB from solubilized contaminants and to exchange the detergent, we used a IMAC column (loaded with $ZnSO_4$) equilibrated with buffer A containing 0.02 % LMNG. HlyB solubilized in Fos-Choline-14 showed no ATPase activity, therefore we exchanged the detergent to improve HlyB homogeneity as observed by SEC and to retain its ability to hydrolyse ATP. Fractions containing HlyB as judged from a CBB-stained SDS/PAGE gel were pooled, concentrated and subjected to SEC using buffer B containing 0.02 % LMNG (Figure 3). After this purification step, approximately 1.5 mg of homogeneous HlyB per litre of bacterial culture was obtained.

HlyB ATPase modulation by its transport substrate

ATPase activity of HlyB was monitored by the quantification of released P_i using a Malachite Green assay. ATP was applied at concentrations ranging from 0 to 5 mM while the HlyB concentration was kept constant at 1 μM. Results of the ATPase activity measurements are summarized in Figure 4(A) and followed a non-linear dependence on ATP concentration. The Hill equation (eqn 1) was used to analyse the results. According to this equation, the maximum velocity (V_{max}) of the reaction was calculated to be 8.1 ± 0.7 nmol of P_i/min per mg, the Hill coefficient h was 1.5 ± 0.4 and the kinetic constant $K_{0.5}$ was 0.3 ± 0.1 mM ATP (Table 2). The value for the Hill coefficient indicates positive co-operativity of ATP hydrolysis as observed previously for the isolated HlyB NBD [30]. An HlyB mutant defective in ATP hydrolysis (HlyB H662A) showed no hydrolytic activity under the experimental conditions demonstrating that the observed activity was derived from HlyB [23]. The co-operative nature of ATPase activity was also supported by data analysis using a double logarithmic evaluation {'Hill plot', $\log[v/(V_{max} - v)]$ against logATP (Figure 4B)}. Importantly, the value of the Hill coefficient was identical within experimental error for both evaluation procedures.

Next, we examined whether the transport substrate influences the hydrolytic activity of HlyB. Instead of HlyA we employed HlyA1 because of its higher stability and ease of purification [19] (Figure 2). ATPase activity was measured at a constant HlyB concentration of 1 μM and a constant ATP concentration of 2 mM, while the HlyA1 concentration varied from 0 μM to 20 μM. The applied concentration of ATP was approximately 6-fold above the determined $K_{0.5}$ value and ensured that HlyB was always saturated under these conditions. We observed both an inhibitory and a stimulatory effect of unfolded HlyA1 on HlyB ATPase activity (Figure 5). The two opposite effects depended on substrate concentration suggesting different modes of interaction between HlyA1 and HlyB, since no hydrolytic activity of HlyA1 was observed. The data were analysed according to eqn (2) assuming two independent binding sites [31]. The first binding site inhibits ATPase activity by 37 % and the second binding site stimulates hydrolytic activity of HlyB by 104 % (Table 2). However, higher concentrations of HlyA1 were not possible to measure due to aggregation of the protein. Therefore the K_2 value is only an estimation and represents a lower limit of the interaction (Table 2).

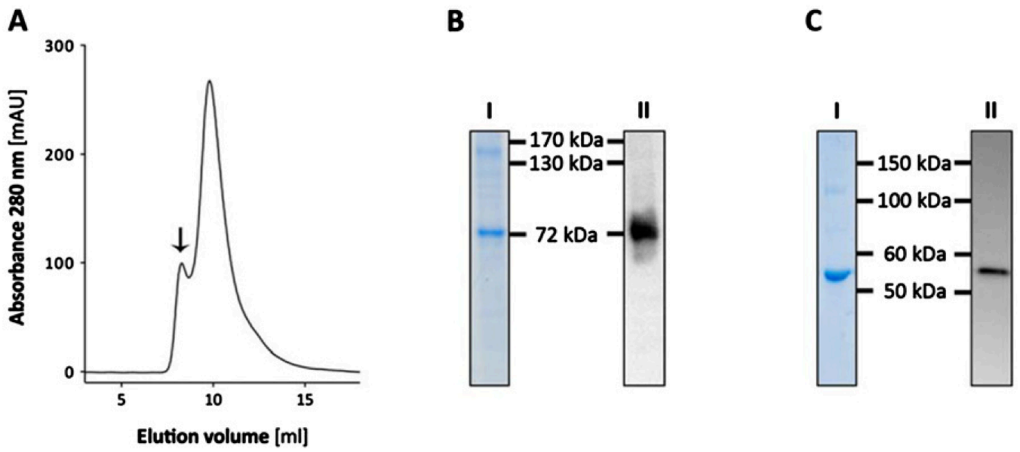

Figure 3 SEC profile, SDS/PAGE and Western blot analysis of purified HlyB and HlyBΔCLD

(**A**) HlyB protein was concentrated using an Amicon Ultra centrifugal filter unit and 500 μl (3 mg/ml) was loaded on to a Superdex 200 10/300 GL column. The buffer contained 10 mM Caps, 20 % glycerol and 0.02 % LMNG (pH 10.4). The arrow indicates the void volume of the column. mAU, milli-absorbance units. (**B**) Purified HlyB or (**C**) HlyBΔCLD was analysed by (I) SDS/PAGE and stained with CBB or detected by (II) Western blot analysis using polyclonal antisera. Including the decahistidine tag, HlyB has a theoretical mass of 82.2 kDa and HlyBΔCLD has a theoretical mass of 67.9 kDa.

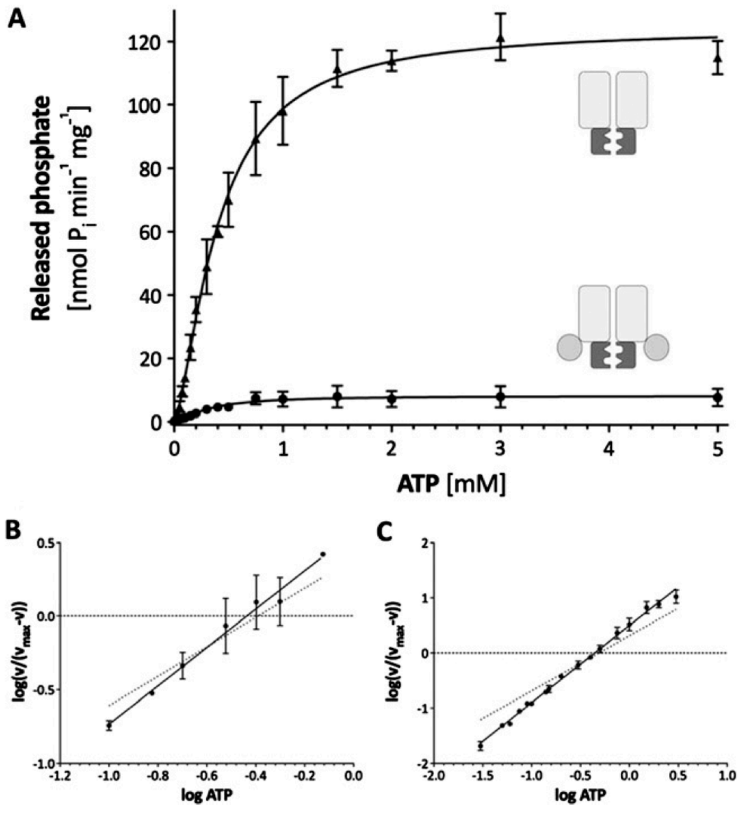

Figure 4 ATPase activity of purified HlyB and HlyBΔCLD

(**A**) ATPase activity of HlyB (circles) and HlyBΔCLD (triangle) in dependency of ATP concentration. Both datasets were analysed using the Hill equation (eqn 1). The plots are additionally labelled with schematic representations of HlyB and HlyBΔCLD. Hill plots of the data are shown for HlyB (**B**) and HlyBΔCLD (**C**). Data were also fitted according to the Michaelis–Menten equation (eqn 3), broken lines, or the Hill equation (eqn 1), unbroken lines. Results are means ± S.D. from at least two independent experiments.

Table 2 Kinetic parameters of HlyB, HlyBΔCLD and HlyB-Y20A

(HlyA1), kinetic parameters were determined in dependence of HlyA1 concentrations. (HlyA2), kinetic parameters were determined in dependence of HlyA2 concentrations. (HlyA1, folded), kinetic parameters were determined in the presence of HlyA1 and Ca^{2+} ions (see the Materials and methods section).

(a)

	$K_{0.5}$ (mM)	Vmax (nmol/min per mg)	h	Slope ('Hill plot')§	kcat (min^{-1})
HlyB*	0.3 ± 0.1	8.1 ± 0.7	1.5 ± 0.4	1.3 ± 0.1	0.7 ± 0.1
HlyBΔCLD*	0.40 ± 0.02	124.3 ± 3.1	1.5 ± 0.1	1.4 ± 0.1	8.4 ± 0.2

(b)

	$K_m/K_{0.5}$ (μM)	Vmax (nmol/min per mg)	h	Slope ('Hill plot')§
HlyBΔCLD (HlyA1)†	1.2 ± 0.3	151.6 ± 2.3 (+33%)	–	–
HlyBΔCLD (HlyA2)†	2.0 ± 0.3	154.4 ± 1.3 (+29%)	–	–
HlyB-Y20A (HlyA1)*	0.9 ± 0.2	9.1 ± 0.2 (+20%)	1.5 ± 0.4	1.4 ± 0.4
HlyB (HlyA1, folded)*	2.0 ± 0.3	9.5 ± 0.2 (+33%)	1.8 ± 0.4	1.6 ± 0.1

(c)

	K_1 (μM)	K_2 (μM)	v_0 (nmol/min per mg)	v_1 (nmol/min per mg)	v_2 (nmol/min per mg)
HlyB (HlyA1)‡	1.0 ± 0.5	19.4 ± 3.1	13.9 ± 0.4	8.8 ± 0.9 (–37%)	28.4 ± 0.1 (+104%)
HlyB (HlyA2)‡	0.4 ± 0.1	4.7 ± 0.3	17.9 ± 0.2	16.6 ± 0.2 (–7%)	21.7 ± 0.2 (+21%)

*Parameters were determined according to eqn (1), the Hill equation.
†Parameters were determined according to eqn (3), the Michaelis–Menten equation.
‡Parameters were determined according to eqn (2) which assumes two independent binding sites.
§Parameters were determined according to a double logarithmic evaluation ('Hill plot', $\log[v/(V_{max} - v)]$ against logATP.

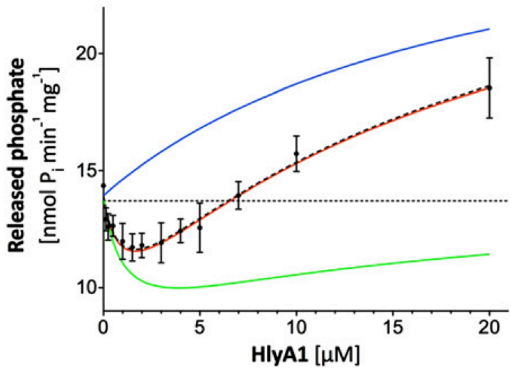

Figure 5 Modulation of ATPase activity of HlyB by unfolded HlyA1 and simulations of the inhibitory and stimulatory parts of ATPase activity

Experimental results of HlyB ATPase activity in the presence of unfolded substrate HlyA1 are shown in black (circles). Datasets were analysed according to eqn (2). Results are means ± S.D. from at least two independent experiments. A simulation of the inhibitory influence of HlyA1 on HlyB ATPase activity is shown in green, whereas a simulation of the stimulatory part is shown in blue. The red curve represents the summation of both effects.

We visualized the inhibitory as well as the stimulatory effect independently of each other by simulations (Figure 5). These simulations revealed a maximum inhibition of 28 % and a maximum stimulation of 52 %. A simple addition of both curves overlapped well with our experimental results and indicates that our assumption of inhibition at low substrate concentration, which is followed by stimulation at higher substrate concentrations, is valid.

The N-terminal CLD of HlyB inhibits ATPase activity

Next we investigated the role of the N-terminal CLD on the ATPase activity of HlyB. We used HlyBΔCLD lacking the N-terminal domain and measured its ATPase activity by quantifying released P_i by a Malachite Green assay as described above. The results of the ATPase activity measurements are summarized in Figure 4 and followed a non-linear dependence of activity on ATP concentration similar to HlyB. The Hill equation (eqn 1) was used to fit the data. The maximum velocity (V_{max}) of the reaction was calculated to be 124.3 ± 3.1 nmol of P_i/min per mg, the Hill coefficient h was 1.5 ± 0.1 and kinetic constant $K_{0.5}$ was 0.40 ± 0.02 mM (Table 2). Again, data analysis using a double logarithmic evaluation {'Hill plot', $\log[v/(V_{max} - v)]$ against logATP (Figure 4C)} supported the co-operative nature of ATP hydrolysis with the value of the Hill coefficient being identical within experimental error for both evaluation procedures. In comparison with HlyB, the lack of the CLD (HlyBΔCLD) resulted in a 15-fold increased V_{max} value, whereas the $K_{0.5}$ value and the Hill coefficient remained identical within experimental error for both. These results indicate an intermolecular regulatory role of the CLD, which reduces the NBDs' basal hydrolytic activity.

Furthermore, we also examined for HlyBΔCLD whether the transport substrate HlyA1 influences hydrolytic activity. The ATPase activity profile followed Michaelis–Menten kinetics and was fitted according to eqn (3) (Figure 6A, black circles). Remarkably, the co-operative nature of ATPase activity of HlyBΔCLD was abolished in the presence of unfolded HlyA1. The absence of co-operativity was supported by data analysis using a double-logarithmic evaluation {'Hill plot', $\log[v/(V_{max} - v)]$ against logATP (Figure 6B)}. Analysis of the data revealed an increase of 33 % in reaction velocity in comparison with HlyBΔCLD in the absence of the transport substrate (Table 2). For HlyBΔCLD, we observed only stimulation of ATPase activity, but an inhibition as in the case of HlyB (Figure 5) was not detected. Both sets of experiments were performed under identical conditions and differed only in the presence (HlyB) or absence (HlyBΔCLD) of the CLD. Therefore differences in the observed activity should originate from an

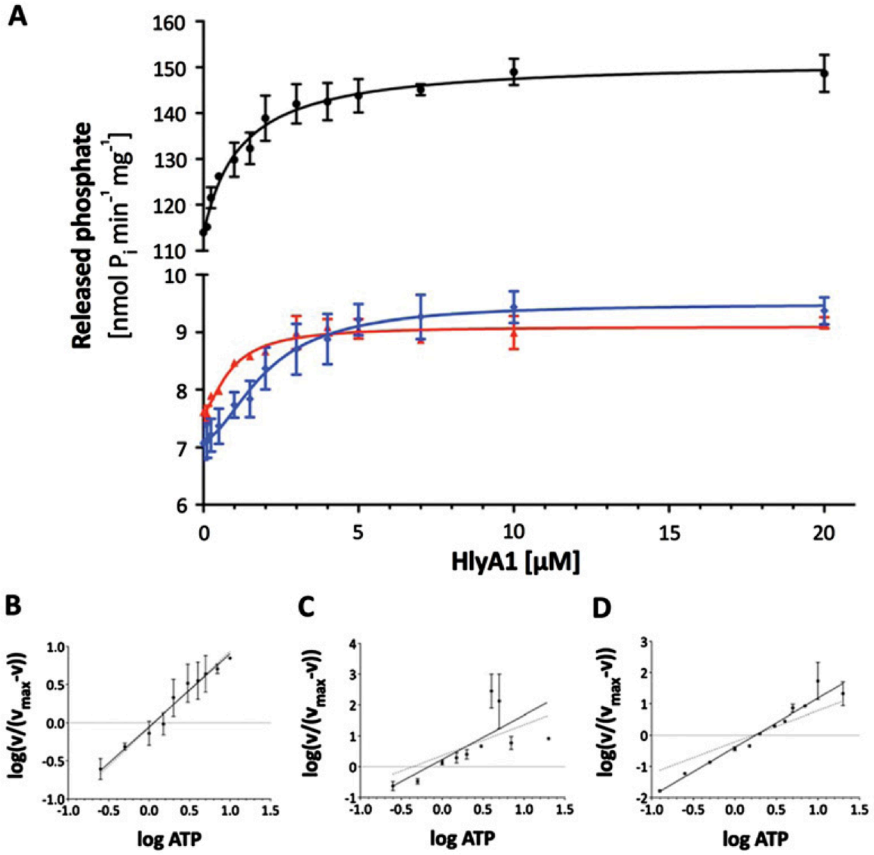

Figure 6 ATPase activity of HlyB, HlyBΔCLD and HlyB-Y20A in the presence of unfolded or folded HlyA1 respectively

(**A**) Datasets were analysed according to the Michaelis–Menten equation (eqn 3) for results of HlyBΔCLD in the presence of unfolded HlyA1 (black circles). The Hill equation (eqn 1) was used to analyse the results of HlyB-Y20A in the presence of unfolded HlyA1 (red triangles) and HlyB in the presence of folded HlyA1 (blue squares, folding induced by adding 4 mM $CaCl_2$). Hill plots of the data are shown for HlyBΔCLD (**B**), HlyB-Y20A (**C**) and HlyB (**D**) and were fitted according to the Michaelis–Menten equation (eqn 3), broken lines, or Hill equation (eqn 1), unbroken lines. Results are means ± S.D. from at least two independent experiments.

interaction of the unfolded transport substrate HlyA1 with the CLD. These results emphasize further the regulatory role of the CLD and demonstrate that the observed stimulatory effects are independent of the CLD.

To confirm a distinct interaction of the CLD with HlyA1 as the source of the observed negative regulation of the ATPase activity, we used the HlyB-Y20A mutant. It was already shown that the CLD interacts with unfolded HlyA1 and CSP (chemical shift perturbation) experiments suggested that Tyr^{20} is part of the HlyA-binding region [18]. *In vivo* secretion experiments with the HlyB-Y20A mutant confirmed this hypothesis as the mutation resulted in a significantly reduced secretion level when compared with HlyB. ATPase assays were performed with 1 μM HlyB-Y20A and 2 mM ATP, while the HlyA1 concentration varied from 0 μM to 20 μM. Results of the ATPase activity measurements are summarized in Figure 6(A) (red triangles) and the best fit of the data was obtained for the Hill equation (eqn 1). The value of the Hill coefficient was supported by data analysis using a double-logarithmic evaluation {'Hill plot', $\log[v/(V_{max} - v)]$ against logATP (Figure 6C)}. HlyB-Y20A showed only ATPase stimulation by 20 % in comparison with HlyB-Y20A in the absence of the unfolded substrate (Table 2). This general behaviour correlates with the results obtained from HlyBΔCLD. No ATPase inhibition was observed in the Y20A background, suggesting that the interaction of the mutated CLD and the substrate does not take place. This observation is in line with our previous results [18] and confirmed a CLD–HlyA1 interaction resulting in an inhibition of ATPase activity of HlyB.

Substrate folding prohibits HlyB ATPase inhibition

GG-repeats are characteristic features of RTX domains and folding experiments demonstrated that these GG-repeats trigger folding of the substrate by binding of Ca^{2+} [8]. Since HlyA is transported in an unfolded state, we assumed that a folded substrate is incompatible with an interaction with HlyB [1,32], as already demonstrated by pull-down experiments with the purified CLD [18]. In the present study, we examined whether folding of the substrate also induces an inhibition or stimulation of the ATPase activity of HlyB. Therefore substrate was folded by pre-incubating HlyA1 with 4 mM Ca^{2+} ions and ATPase assays of HlyB in the presence of folded HlyA1 were performed as described above. Data were analysed using the Hill equation

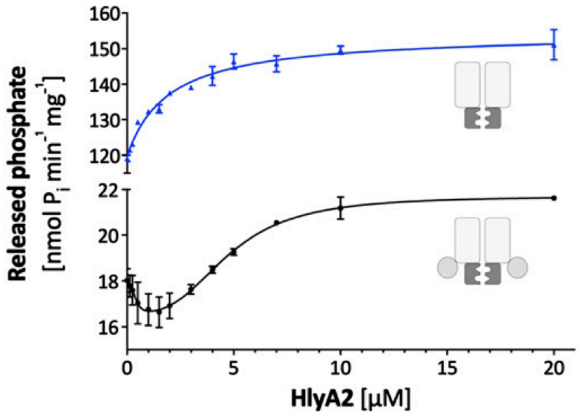

Figure 7 ATPase activity modulation of HlyB and HlyBΔCLD by unfolded HlyA2 (substrate without the secretion signal)

Datasets were analysed using eqn (2) in the case of HlyB (black circles) and the Michaelis–Menten equation (eqn 3) in the case of HlyBΔCLD (blue triangles). Results are means ± S.D. from at least two independent experiments. The plots are additionally labelled with schematic representations of HlyB and HlyBΔCLD.

(eqn 1) and the results are summarized in Figure 6(A) (blue squares). Again, data analysis using a double-logarithmic evaluation {'Hill plot', $\log[v/(V_{max} - v)]$ against logATP (Figure 6D)} supported the value of the Hill coefficient. We determined a stimulation of 33 % in comparison with the activity without the folded transported substrate (Table 2). In comparison with the ATPase assay in the presence of unfolded HlyA1 (Figure 5), no inhibition was observed (Figure 6A). Thus the CLD–HlyA1 interaction, the inhibition, does not take place if the transport substrate adopts a tertiary structure. However, the stimulation is independent of the folding state of HlyA1.

HlyB ATPase modulation occurs independently of the HlyA secretion signal

The observed stimulation of ATPase activity was independent of the CLD. We therefore examined whether the secretion signal of HlyA1 represents the interaction platform that modulates hydrolytic activity of HlyB in an inhibitory or stimulatory way. We used HlyA2 (Figure 2), which corresponds to HlyA1 but lacks the C-terminal 57 amino acid residues and therefore the secretion sequence. We abandoned measuring the influence of folded HlyA2 because of the missing extreme C-terminus of HlyA2. It has a major influence on protein folding [33] and it is suggested to stabilize the whole protein and especially the RTX domain [21]. The resulting data were analysed using eqns (2) and (3) for the data obtained for HlyB and HlyBΔCLD respectively (Figure 7). For HlyBΔCLD only, stimulation by 29 % was observed following Michaelis–Menten kinetics (Table 2). For HlyB in the presence of HlyA2, the velocity was inhibited by 7 % with 1.5 μM HlyA2 and stimulated by 21 % with 20 μM HlyA2 (Table 2). Taken together, the secretion signal of the transport substrate has no influence on the modulation of ATPase inhibition and stimulation in principal, either in the case of HlyB or in the case of HlyBΔCLD. However, we observed a variation of HlyB kinetic parameters depending on the presence of HlyA1 or HlyA2 (Table 2). In general, the substrate affinities in the presence of HlyA2 are higher ($K_1 = 0.4 \pm 0.1$ μM, $K_2 = 4.7 \pm 0.3$ μM) and the impact on ATPase inhibition (v_1) or ATPase stimulation (v_2) is lower in comparison with HlyA1.

Overall, both substrates showed the same general influence concerning inhibition and stimulation, whereas the absence of the CLD abolished ATPase inhibition. Therefore we conclude that the modulation of ATPase activity occurs independently of the secretion signal.

HlyB and its substrate interact concentration-dependently

Cross-linking studies were performed to analyse the interaction sites of HlyB and HlyA2 in the presence of ATP. We chose HlyA2 as the substrate for this experiment since the modulation of HlyB ATPase velocity occurs independently of the secretion signal. We compared the cross-linking pattern of both proteins at two distinct molar ratios according to the maximum inhibition and maximum stimulation of ATPase velocity. Therefore we used a 1:1 molar ratio of HlyB and HlyA2 (sample called 'inhibition') and a 1:20 molar ratio of HlyB and HlyA2 (sample called 'stimulation'). The concentration of ATP was kept constant at 2 mM. The new protein species obtained by cross-linking are shown in Figure 8(A). These species with higher molecular masses could only be detected by a CBB-stained SDS/PAGE gel or by Western blot analysis with an anti-HlyB antibody, but not with an anti-HlyA antibody. For further analysis of the cross-linked samples, we used LC–MS analysis and detected an intra-HlyB cross-link in the 'inhibition' sample linking the peptides SSVAGK and LAK (Figure 8B). The normalized signal intensity of this cross-linked dipeptide was at least 5-fold higher in comparison with the 'stimulation' sample. The cross-linked amino acids at positions 134 and 137 are located between the CLD and the TMD of HlyB.

To determine whether this observed intra-HlyB cross-link depends on the substrate, we repeated the experiment in the absence of the substrate. Here the cross-link fragments found previously were not observed, which is no final proof but suggests that the observed intra-HlyB cross-link depends on the substrate.

In comparison, the 'stimulation' sample contained a nearly exclusive cross-link between the HlyB peptide RRLDDKFSR (residues 317–325) and the HlyA2 peptide KAFEYQQSNNKVSYVYGHDA (corresponding to residues 944–963) (Figure 8C). The HlyA2 peptide identified is located at the C-terminal end of the protein, whereas the HlyB peptide is located in the TMD at position 322. The cross-linked peptides of HlyB detected are visualized schematically in Figure 8(D).

To verify *in vivo* the relevance of the identified HlyB–HlyA2 cross-link, we mutated Lys^{322} of HlyB to alanine and tryptophan respectively and examined the effect on HlyA secretion. Secretion supernatants were analysed by SDS/PAGE (Figure 8E). The secretion level of HlyB-K322A is similar to the secretion with wild-type HlyB. In contrast, the secretion level of HlyB-K322W is significantly reduced in comparison with wild-type HlyB. This difference is not due to a different expression level of HlyB as demonstrated by Western blot analysis (Figure 8F).

DISCUSSION

In the present paper, we report for the first time the purification and characterization of HlyB, the full-length ABC transporter of the HlyA T1SS of *E. coli*. Despite the large and diverse field of ABC transporters, proteins of this superfamily share a common organization consisting of at least two TMDs and two NBDs that can be arranged in any possible combination [34]. Many of these transporters possess positive co-operativity as has been observed in systems such as P-glycoprotein, BmrA, maltose or

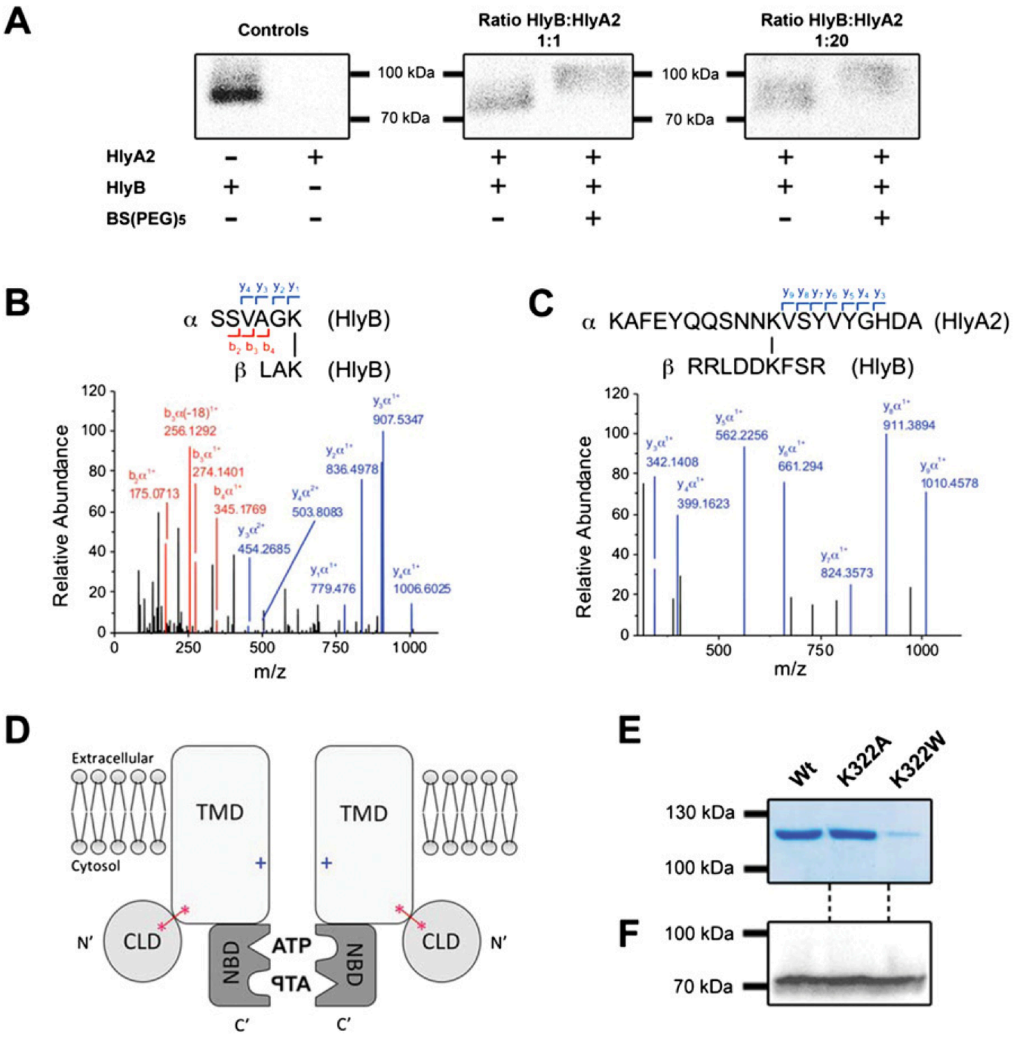

Figure 8 Analysis of cross-linked HlyB/HlyA2 products and influence of HlyB-K322 on HlyA secretion

(**A**) Analysis of cross-linked HlyB and HlyA2 products by Western blotting with a polyclonal anti-HlyB antibody. HlyB and HlyA2 were cross-linked by $BS(PEG)_5$ in the presence of ATP and $MgCl_2$. According to the maximum inhibition (1:1) and maximum stimulation (1:20) of ATPase velocity, we used two different molar ratios. We observed only in the presence of the cross-linking reagent a shift of the anti-HlyB antibody signal. (**B**) Representative fragment spectrum of the 2+ charged precursor mass *m/z* 590.8380 matching to an intra-HlyB cross-link linking the peptides SSVAGK and LAK (StavroX score 80, theoretical precursor mass 1180.667 Da, precursor mass deviation 1.39 p.p.m.). Fragment spectra have been identified from 'inhibition' samples of three independent replicates and two 'stimulation' samples. The signal intensity from extracted ion chromatograms (mass 590.8380, retention time 26 min) normalized with two non-cross-linked peptides of HlyB [YLIFDLEQR (residues 96–104), HLLALPISYFESR (residues 234–246)] is at least four times higher in 'inhibition' compared with 'stimulation' samples in three independent replicates. (**C**) Representative fragment spectrum of the 4+ charged precursor mass *m/z* 961.2247 which corresponds to the mass of the cross-linked peptides KAFEYQQSNNKVSYVYGHDA from HlyA2 (residues 944–963) and RRLDDKFSR from HlyB (residues 317–325) (StavroX score 65). The theoretical mass of the dipeptide is 3841.878 Da resulting in mass deviation of the measured precursor of −0.24 p.p.m. Thirteen fragment spectra generated from 3+ and 4+ charged precursor ions from three independent replicates of 'stimulation' samples could be mapped to this dipeptide (StavroX score between 52 and 284), whereas the dipeptide was not found in 'inhibition' samples. The extracted ion chromatogram signal from the corresponding peptides (retention time 56 min) is at least 69-fold higher in the 'stimulation' compared with the 'inhibition' sample in three independent replicates. (**D**) Schematic overview of a HlyB dimer and the cross-link results. The intra-HlyB cross-link between the CLD and the TMD of the 'inhibition' sample is marked with two red asterisks (*) connected by a straight line. The amino acid of HlyB, which cross-linked to the N-terminal part of HlyA2 in the 'stimulation' sample, is marked with a blue cross (+). (**E**) Secretion analysis of HlyA by SDS/PAGE in presence of wild-type (Wt) HlyB, HlyB-K322A and HlyB-K322W. Results are representative of three independent experiments. (**F**) Analysis of the expression level of wild-type (Wt) HlyB, HlyB-K322A and HlyB-K322W by Western blotting with a polyclonal anti-HlyB antibody. Results are representative of three independent experiments.

histidine importers [35–38]. Also the isolated soluble NBDs of HlyB displayed positive co-operativity, suggesting ATP-induced protein dimerization [30,39]. In the present study, solubilized full-length HlyB also exhibited positive co-operativity in ATP hydrolysis, which suggests that HlyB acts as a functional dimer. The range of our HlyB kinetic parameters is in line with those of, e.g., MacB, the ABC transporter of the macrolide-exporter system of *E. coli* [40].

The ABC transporter HlyB contains a CLD localized at its N-terminus [18]. To investigate the role of the CLD in the context

of its ABC transporter, we cloned, expressed and purified a HlyB derivative lacking this domain (HlyBΔCLD). Kinetic studies of HlyBΔCLD revealed a $K_{0.5}$ and a Hill coefficient almost identical with that of HlyB, but the maximal reaction velocity was increased approximately 15-fold. This comparison suggests a significant influence of the CLD on the hydrolytic velocity of the NBDs, whereas no influence on the substrate-binding affinity or co-operativity was detected.

For further investigation, we compared the activity of HlyB and HlyBΔCLD in the presence of a transport substrate. When increasing amounts of unfolded HlyA1 were added, HlyB ATPase activity showed a biphasic behaviour (Figure 5). By using the HlyB-Y20A mutation, we clearly assigned the distinct interaction of the CLD and HlyA1 being the reason for an inhibitory effect on HlyB ATPase activity. Lecher et al. [18] found that Tyr^{20} plays an important role, since the Y20A mutation resulted in a drastic reduction of substrate secretion, whereas the deletion of the CLD (HlyBΔCLD) abolished substrate secretion completely. Additionally, our results show that HlyBΔCLD possesses no co-operativity in the presence of HlyA1 or HlyA2, whereas an 'inactivated' CLD (e.g. Y20A mutant) shows co-operative interaction (Table 2). This points to a communication between the CLD and the NBD modulating hydrolytic activity (Figure 1). Overall, our results clearly confirm a distinct interaction of the substrate with the CLD leading to a reduction in HlyB hydrolytic velocity. This points to a regulatory role for the CLD as an autoinhibitory domain.

A regulatory role for the CLD by a hypothetical spatial reorientation within HlyB has also been supported by our cross-linking results (Figure 8). We suggest at least two different spatial conformations of HlyB with respect to the orientation of the CLD. Our findings imply a spatial reorientation of the CLD relative to the TMD as we observed a change in the cross-link pattern in the presence of low ('inhibiting') and high ('stimulating') substrate concentrations. As hydrolytic activity at the 'inhibiting' protein ratio is observed, we assume that the CLD position is also fixed during ATP binding and hydrolysis. This is in contrast with the structure of the PCAT (C39-peptidase-containing ABC transporter), in which the peptidase domain was not visible in the electron density of the ATP-bound state [41]. When we employed 'stimulating' HlyA2 concentrations, we observed a new cross-link product between the C-terminus of HlyA2 (residue 954) and the HlyB TMD (residue 322). Finally, the reduction of the HlyA secretion upon a K322W mutation supports the relevance of this position.

Terminal regulatory domains have already been described before for other ATPases and different systems such as the γ subunit of SpoIIIE, SecA, TrwK (type IV secretion system) and EccC (type VII protein secretion) [42–45]. For example, plant plasma membrane H^+- and Ca^{2+}-ATPases contain autoinhibitory domains, which are located C-terminally or N-terminally respectively [46,47]. In the case of P_{2B} Ca^{2+} pumps, calmodulin activates the pump upon binding [48]. In good agreement with the increased hydrolytic activity of HlyBΔCLD, it was also demonstrated that the removal of the autoinhibitory domain of the plant plasma H^+-ATPase results in an activated pump [49]. In principle, this regulatory mode is in line with our results. As it is generally accepted that exporters regulate ATPase activity upon substrate binding, we suggest that the CLD acts as an autoinhibitory and interdomain-regulating subunit. In this model, the CLD locks HlyB in an ATP-bound state with strongly reduced hydrolytic capability in the absence of the substrate. In the presence of the substrate, the lock (CLD) is removed, and the transporter operates with increased hydrolytic activity. This seems plausible as the intracellular ATP concentration is approximately 10-fold higher than the K_m of most ABC transporters, suggesting that NBDs are always present in the ATP-bound state *in vivo* [50]. A similar model has already been proposed for an ABC uptake system on the basis of the structures of MBP–$MalFGK_2$ and $ModB_2C_2A$ with the substrate-binding protein acting as a 'lock-release' [51]. Moreover, in the case of the ABC importer ModBC from *Methanosarcina acetivorans*, a molybdate ion inhibits the transporter by binding to a regulatory cytosolic domain, a mechanism termed 'transinhibition' [52]. Substrate-induced inhibition of the ATPase activity of HlyB variants or parts of HlyB has been described, probably caused by an interaction between HlyB-NBD and HlyA1 [19]. ATPase activities of GST–HlyB-NBD fusion protein as well as His-tagged HlyB-NBD were partially inhibited by HlyA or a C-terminal fragment of HlyA respectively [19,53]. Besides HlyB, the ABC transporter PrtD was also inhibited by its cognate C-terminal secretion signal of PrtG or PrtB metalloproteases [54]. However, the exact mechanistic details and amino acid residues involved in the interaction of the CLD and the NBD or TMD cannot be defined on the basis of the data from the present study.

Additionally, we investigated the role of the HlyA secretion signal in the context of substrate–CLD interaction. We observed that the absence of the secretion signal had only a minor impact on the kinetic parameters (Table 2). Variations of HlyB substrate affinities (K_1, K_2) and velocities (v_1, v_2) may be caused by different physical characteristics of HlyA1 and HlyA2. We found no impact on the general behaviour concerning ATPase stimulation or inhibition. Thus the interaction occurs independently of the secretion sequence. The N-terminal part of HlyA1 harbours the RTX domains that include the GG-repeats. The crystal structure of two members of the RTX toxin superfamily revealed that GG-repeats bind Ca^{2+} ions, and studies also showed that this binding induces substrate folding at the exterior of the cell [6,55–57]. The results of Lecher et al. [18] support our data and suggest an exclusive interaction of the unfolded substrate/RTX domain with the CLD. In turn, Ca^{2+}-induced folding of the substrate might be the reason that HlyA1 does not inhibit the HlyB ATPase activity in the presence of Ca^{2+}. Therefore participation of the GG-repeats in CLD interaction seems likely and results in a decrease in reaction velocity. The secretion of HlyA is dependent on the presence of its C-terminal secretion signal [20,58,59]. Thus our observed secretion-signal-independent interaction could only represent one step within a well-regulated and complex secretion mechanism. Although we have to take into account that solubilized HlyB shows a low uncoupled basal ATPase activity, which is not likely to be present *in* vivo, we demonstrated a distinct modulation of HlyB ATPase activity in the presence of its substrate.

Finally, we suggest that at least two different binding sites of HlyA exist within HlyB. We clearly identified a CLD–substrate interaction leading to a reduction in hydrolytic velocity. This underlines an interdomain and regulatory role of the CLD modulating the NBDs catalytic activity depending on the concentration of the substrate. Furthermore, we also observed stimulatory effects on the hydrolytic activity. Stimulatory effects were determined for HlyB as well as for HlyBΔCLD and HlyB-Y20A. This strongly suggests that the stimulation occurred independently of the CLD itself and the HlyA-binding ability to the CLD (Y20A mutant). The NBD of HlyB presumably can also be excluded to modulate stimulation, since at least the isolated domain interacts exclusively with the secretion signal of HlyA. In contrast, we observed a secretion-signal-independent stimulation of HlyB ATPase activity [19]. This subsequently leads to the assumption that a second binding site could be present within the TMD of HlyB stimulating the ATPase activity, which

is conceptually similar to the proposal for MsbA [60,61] and supported by our cross-linking data (Figure 8).

In summary, our data assign an interdomain regulatory role for the CLD, the N-terminal appendix of HlyB. Such an arrangement has not been identified for ABC export systems previously and suggests that the secretion of the substrate is a highly ordered and regulated process, in which the CLD possesses a key role.

AUTHOR CONTRIBUTION

Sven Reimann, Sander Smits, Lutz Schmitt, Gereon Poschmann and Kai Stühler conceived and designed the experiments and analysed the data. Sven Reimann and Gereon Poschmann performed the experiments. Kerstin Kanonenberg contributed HlyA1 protein. Sven Reimann, Sander Smits, Lutz Schmitt and Gereon Poschmann wrote the paper.

ACKNOWLEDGEMENTS

We thank Christian Schwarz and Michael Lenders for valuable discussions. We thank Diana Kleinschrodt and Iris Fey, Protein Production Facility of Heinrich-Heine-University, for their support. We gratefully acknowledge support (and training) from the International NRW Research School BioStruct, granted by the Ministry of Innovation, Science and Research of the State North Rhine-Westphalia, the Heinrich-Heine-University Düsseldorf and the Entrepreneur Foundation at the Heinrich-Heine-University of Düsseldorf.

FUNDING

This project was funded in part by the Deutsche Forschungsgemeinschaft (DFG) [CRC 1208, projects A01 to L.S. and Z01 to K.S.]

REFERENCES

1 Bakkes, P.J., Jenewein, S., Smits, S.H., Holland, I.B. and Schmitt, L. (2010) The rate of folding dictates substrate secretion by the *Escherichia coli* hemolysin type 1 secretion system. J. Biol. Chem. **285**, 40573–40580 CrossRef PubMed

2 Holland, I.B., Schmitt, L. and Young, J. (2005) Type 1 protein secretion in bacteria, the ABC-transporter dependent pathway. Mol. Membr. Biol. **22**, 29–39 CrossRef PubMed

3 Ludwig, A., Schmid, A., Benz, R. and Goebel, W. (1991) Mutations affecting pore formation by haemolysin from *Escherichia coli*. Mol. Gen. Genet. **226**, 198–208 CrossRef PubMed

4 Welch, R.A., Forestier, C., Lobo, A., Pellett, S., Thomas, Jr, W. and Rowe, G. (1992) The synthesis and function of the *Escherichia coli* hemolysin and related RTX exotoxins. FEMS Microbiol. Immunol. **5**, 29–36 CrossRef PubMed

5 Thomas, S., Holland, I.B. and Schmitt, L. (2014) The Type 1 secretion pathway: the hemolysin system and beyond. Biochim. Biophys. Acta **1843**, 1629–1641 CrossRef PubMed

6 Baumann, U., Wu, S., Flaherty, K.M. and McKay, D.B. (1993) Three-dimensional structure of the alkaline protease of *Pseudomonas aeruginosa*: a two-domain protein with a calcium binding parallel β roll motif. EMBO J. **12**, 3357–3364 PubMed

7 Ostolaza, H., Soloaga, A. and Goñi, F.M. (1995) The binding of divalent cations to *Escherichia coli* α-haemolysin. Eur. J. Biochem. **228**, 39–44 PubMed

8 Linhartová, I., Bumba, L., Mašín, J., Basler, M., Osička, R., Kamanová, J., Procházková, K., Adkins, I., Hejnová-Holubová, J., Sadílková, L. et al. (2010) RTX proteins: a highly diverse family secreted by a common mechanism. FEMS Microbiol Rev. **34**, 1076–1112 CrossRef PubMed

9 Delepelaire, P. (2004) Type I secretion in Gram-negative bacteria. Biochim. Biophys. Acta **1694**, 149–161 CrossRef PubMed

10 Letoffe, S., Delepelaire, P. and Wandersman, C. (1996) Protein secretion in Gram-negative bacteria: assembly of the three components of ABC protein-mediated exporters is ordered and promoted by substrate binding. EMBO J. **15**, 5804–5811 PubMed

11 Thanabalu, T., Koronakis, E., Hughes, C. and Koronakis, V. (1998) Substrate-induced assembly of a contiguous channel for protein export from *E.coli*: reversible bridging of an inner-membrane translocase to an outer membrane exit pore. EMBO J. **17**, 6487–6496 CrossRef PubMed

12 Balakrishnan, L., Hughes, C. and Koronakis, V. (2001) Substrate-triggered recruitment of the TolC channel-tunnel during type I export of hemolysin by *Escherichia coli*. J. Mol. Biol. **313**, 501–510 CrossRef PubMed

13 Ghigo, J.M. and Wandersman, C. (1994) A carboxyl-terminal four-amino acid motif is required for secretion of the metalloprotease PrtG through the *Erwinia chrysanthemi* protease secretion pathway. J. Biol. Chem. **269**, 8979–8985 PubMed

14 Kenny, B., Taylor, S. and Holland, I.B. (1992) Identification of individual amino acids required for secretion within the haemolysin (HlyA) C-terminal targeting region. Mol. Microbiol. **6**, 1477–1489 CrossRef PubMed

15 Kenny, B., Chervaux, C. and Holland, I.B. (1994) Evidence that residues − 15 to − 46 of the haemolysin secretion signal are involved in early steps in secretion, leading to recognition of the translocator. Mol. Microbiol. **11**, 99–109 CrossRef PubMed

16 Koronakis, V., Sharff, A., Koronakis, E., Luisi, B. and Hughes, C. (2000) Crystal structure of the bacterial membrane protein TolC central to multidrug efflux and protein export. Nature **405**, 914–919 CrossRef PubMed

17 Havarstein, L.S., Diep, D.B. and Nes, I.F. (1995) A family of bacteriocin ABC transporters carry out proteolytic processing of their substrates concomitant with export. Mol. Microbiol. **16**, 229–240 CrossRef PubMed

18 Lecher, J., Schwarz, C.K., Stoldt, M., Smits, S.H., Willbold, D. and Schmitt, L. (2012) An RTX transporter tethers its unfolded substrate during secretion via a unique N-terminal domain. Structure **20**, 1778–1787 CrossRef PubMed

19 Benabdelhak, H., Kiontke, S., Horn, C., Ernst, R., Blight, M.A., Holland, I.B. and Schmitt, L. (2003) A specific interaction between the NBD of the ABC-transporter HlyB and a C-terminal fragment of its transport substrate haemolysin A. J. Mol. Biol. **327**, 1169–1179 CrossRef PubMed

20 Nicaud, J.M., Mackman, N., Gray, L. and Holland, I.B. (1986) The C-terminal, 23 kDa peptide of *E. coli* haemolysin 2001 contains all the information necessary for its secretion by the haemolysin (Hly) export machinery. FEBS Lett. **204**, 331–335 CrossRef PubMed

21 Thomas, S., Bakkes, P.J., Smits, S.H. and Schmitt, L. (2014) Equilibrium folding of pro-HlyA from *Escherichia coli* reveals a stable calcium ion dependent folding intermediate. Biochim. Biophys. Acta **1844**, 1500–1510 CrossRef PubMed

22 Mackman, N. and Holland, I.B. (1984) Functional characterization of a cloned haemolysin determinant from *E. coli* of human origin, encoding information for the secretion of a 107K polypeptide. Mol. Gen. Genet. **196**, 129–134 CrossRef PubMed

23 Zaitseva, J., Jenewein, S., Jumpertz, T., Holland, I.B. and Schmitt, L. (2005) H662 is the linchpin of ATP hydrolysis in the nucleotide-binding domain of the ABC transporter HlyB. EMBO J. **24**, 1901–1910 CrossRef PubMed

24 Zaitseva, J., Holland, I.B. and Schmitt, L. (2004) The role of CAPS buffer in expanding the crystallization space of the nucleotide-binding domain of the ABC transporter haemolysin B from *Escherichia coli*. Acta Crystallogr. D Biol. Crystallogr. **60**, 1076–1084 CrossRef PubMed

25 Blommel, P.G. and Fox, B.G. (2007) A combined approach to improving large-scale production of tobacco etch virus protease. Protein Expr. Purif. **55**, 53–68 CrossRef PubMed

26 Baykov, A.A., Evtushenko, O.A. and Avaeva, S.M. (1988) A malachite green procedure for orthophosphate determination and its use in alkaline phosphatase-based enzyme immunoassay. Anal. Biochem. **171**, 266–270 CrossRef PubMed

27 Poschmann, G., Seyfarth, K., Besong Agbo, D., Klafki, H.W., Rozman, J., Wurst, W., Wiltfang, J., Meyer, H.E., Klingenspor, M. and Stühler, K. (2014) High-fat diet induced isoform changes of the Parkinson's disease protein DJ-1. J. Proteome Res. **13**, 2339–2351 CrossRef PubMed

28 Gotze, M., Pettelkau, J., Schaks, S., Bosse, K., Ihling, C.H., Krauth, F., Fritzsche, R., Kühn, U. and Sinz, A. (2012) StavroX: a software for analyzing crosslinked products in protein interaction studies. J. Am. Soc. Mass Spectrom. **23**, 76–87 CrossRef PubMed

29 Ellinger, P., Kluth, M., Stindt, J., Smits, S.H. and Schmitt, L. (2013) Detergent screening and purification of the human liver ABC transporters BSEP (ABCB11) and MDR3 (ABCB4) expressed in the yeast *Pichia pastoris*. PLoS One **8**, e60620 CrossRef PubMed

30 Zaitseva, J., Jenewein, S., Wiedenmann, A., Benabdelhak, H., Holland, I.B. and Schmitt, L. (2005) Functional characterization and ATP-induced dimerization of the isolated ABC-domain of the haemolysin B transporter. Biochemistry **44**, 9680–9690 CrossRef PubMed

31 Litman, T., Nielsen, D., Skovsgaard, T., Zeuthen, T. and Stein, W.D. (1997) ATPase activity of P-glycoprotein related to emergence of drug resistance in Ehrlich ascites tumor cell lines. Biochim. Biophys. Acta **1361**, 147–158 CrossRef PubMed

32 Jones, H.E., Holland, I.B., Baker, H.L. and Campbell, A.K. (1999) Slow changes in cytosolic free Ca^{2+} in *Escherichia coli* highlight two putative influx mechanisms in response to changes in extracellular calcium. Cell Calcium **25**, 265–274 CrossRef PubMed

33 Jumpertz, T., Chervaux, C., Racher, K., Zouhair, M., Blight, M.A., Holland, I.B. and Schmitt, L. (2010) Mutations affecting the extreme C terminus of *Escherichia coli* haemolysin A reduce haemolytic activity by altering the folding of the toxin. Microbiology **156**, 2495–2505 CrossRef PubMed

34 Biemans-Oldehinkel, E., Doeven, M.K. and Poolman, B. (2006) ABC transporter architecture and regulatory roles of accessory domains. FEBS Lett. **580**, 1023–1035 CrossRef PubMed

35 Senior, A.E. and Bhagat, S. (1998) P-glycoprotein shows strong catalytic cooperativity between the two nucleotide sites. Biochemistry **37**, 831–836 CrossRef PubMed

36 Liu, C.E., Liu, P.Q. and Ames, G.F. (1997) Characterization of the adenosine triphosphatase activity of the periplasmic histidine permease, a traffic ATPase (ABC transporter). J. Biol. Chem. **272**, 21883–21891 CrossRef PubMed

37 Davidson, A.L., Laghaeian, S.S. and Mannering, D.E. (1996) The maltose transport system of *Escherichia coli* displays positive cooperativity in ATP hydrolysis. J. Biol. Chem. **271**, 4858–4863 CrossRef PubMed

38 Steinfels, E., Orelle, C., Fantino, J.R., Dalmas, O., Rigaud, J.L., Denizot, F., Di Pietro, A. and Jault, J.M. (2004) Characterization of YvcC (BmrA), a multidrug ABC transporter constitutively expressed in *Bacillus subtilis*. Biochemistry **43**, 7491–7502 CrossRef PubMed

39 Benabdelhak, H., Schmitt, L., Horn, C., Jumel, K., Blight, M.A. and Holland, I.B. (2005) Positive co-operative activity and dimerization of the isolated ABC ATPase domain of HlyB from *Escherichia coli*. Biochem. J. **386**, 489–495 CrossRef PubMed

40 Lin, H.T., Bavro, V.N., Barrera, N.P., Frankish, H.M., Velamakanni, S., van Veen, H.W., Robinson, C.V., Borges-Walmsley, M.I. and Walmsley, A.R. (2009) MacB ABC transporter is a dimer whose ATPase activity and macrolide-binding capacity are regulated by the membrane fusion protein MacA. J. Biol. Chem. **284**, 1145–1154 CrossRef PubMed

41 Lin, D.Y., Huang, S. and Chen, J. (2015) Crystal structures of a polypeptide processing and secretion transporter. Nature **523**, 425–430 CrossRef PubMed

42 Besprozvannaya, M., Pivorunas, V.L., Feldman, Z. and Burton, B.M. (2013) SpoIIIE protein achieves directional DNA translocation through allosteric regulation of ATPase activity by an accessory domain. J. Biol. Chem. **288**, 28962–28974 CrossRef PubMed

43 Karamanou, S., Vrontou, E., Sianidis, G., Baud, C., Roos, T., Kuhn, A., Politou, A.S. and Economou, A. (1999) A molecular switch in SecA protein couples ATP hydrolysis to protein translocation. Mol. Microbiol. **34**, 1133–1145 CrossRef PubMed

44 Peña, A., Ripoll-Rozada, J., Zunzunegui, S., Cabezón, E., de la Cruz, F. and Arechaga, I. (2011) Autoinhibitory regulation of TrwK, an essential VirB4 ATPase in type IV secretion systems. J. Biol. Chem. **286**, 17376–17382 CrossRef PubMed

45 Rosenberg, O.S., Dovala, D., Li, X., Connolly, L., Bendebury, A., Finer-Moore, J., Holton, J., Cheng, Y., Stroud, R.M. and Cox, J.S. (2015) Substrates control multimerization and activation of the multi-domain ATPase motor of type VII secretion. Cell **161**, 501–512 CrossRef PubMed

46 Axelsen, K.B. and Palmgren, M.G. (2001) Inventory of the superfamily of P-type ion pumps in *Arabidopsis*. Plant Physiol. **126**, 696–706 CrossRef PubMed

47 Baekgaard, L., Fuglsang, A.T. and Palmgren, M.G. (2005) Regulation of plant plasma membrane H^+- and Ca^{2+}-ATPases by terminal domains. J. Bioenerg. Biomembr. **37**, 369–374 CrossRef PubMed

48 Harper, J.F., Hong, B., Hwang, I., Guo, H.Q., Stoddard, R., Huang, J.F., Palmgren, M.G. and Sze, H. (1998) A novel calmodulin-regulated Ca^{2+}-ATPase (ACA2) from *Arabidopsis* with an N-terminal autoinhibitory domain. J. Biol. Chem. **273**, 1099–1106 CrossRef PubMed

49 Palmgren, M.G., Sommarin, M., Serrano, R. and Larsson, C. (1991) Identification of an autoinhibitory domain in the C-terminal region of the plant plasma membrane H^+-ATPase. J. Biol. Chem. **266**, 20470–20475 PubMed

50 Neidhardt, F.C. et al (1987) *Escherichia coli* and *Salmonella typhimurium*: Cellular and Molecular Biology,. Vol. 1., American Society for Microbiology Publishers CrossRef

51 Oldham, M.L., Khare, D., Quiocho, F.A., Davidson, A.L. and Chen, J. (2007) Crystal structure of a catalytic intermediate of the maltose transporter. Nature **450**, 515–521 CrossRef PubMed

52 Gerber, S., Comellas-Bigler, M., Goetz, B.A. and Locher, K.P. (2008) Structural basis of trans-inhibition in a molybdate/tungstate ABC transporter. Science **321**, 246–250 CrossRef PubMed

53 Koronakis, V., Hughes, C. and Koronakis, E. (1993) ATPase activity and ATP/ADP-induced conformational change in the soluble domain of the bacterial protein translocator HlyB. Mol. Microbiol. **8**, 1163–1175 CrossRef PubMed

54 Delepelaire, P. (1994) PrtD, the integral membrane ATP-binding cassette component of the *Erwinia chrysanthemi* metalloprotease secretion system, exhibits a secretion signal-regulated ATPase activity. J. Biol. Chem. **269**, 27952–27957 PubMed

55 Hamada, K., Hata, Y., Katsuya, Y., Hiramatsu, H., Fujiwara, T. and Katsube, Y. (1996) Crystal structure of *Serratia* protease, a zinc-dependent proteinase from *Serratia* sp. E-15, containing a β-sheet coil motif at 2.0 Å resolution. J. Biochem. **119**, 844–851 CrossRef PubMed

56 Sánchez-Magraner, L., Viguera, A.R., García-Pacios, M., Garcillán, M.P., Arrondo, J.L., de la Cruz, F., Goñi, F.M. and Ostolaza, H. (2007) The calcium-binding C-terminal domain of *Escherichia coli* α-hemolysin is a major determinant in the surface-active properties of the protein. J. Biol. Chem. **282**, 11827–11835 CrossRef PubMed

57 Sánchez-Magraner, L., Cortajarena, A.L., García-Pacios, M., Arrondo, J.L., Agirre, J., Guérin, D.M., Goñi, F.M. and Ostolaza, H. (2010) Interdomain Ca^{2+} effects in *Escherichia coli* α-haemolysin: Ca^{2+} binding to the C-terminal domain stabilizes both C- and N-terminal domains. Biochim. Biophys. Acta **1798**, 1225–1233 CrossRef PubMed

58 Gray, L., Mackman, N., Nicaud, J.M. and Holland, I.B. (1986) The carboxy-terminal region of haemolysin 2001 is required for secretion of the toxin from *Escherichia coli*. Mol. Gen. Genet. **205**, 127–133 CrossRef PubMed

59 Felmlee, T., Pellett, S., Lee, E.Y. and Welch, R.A. (1985) *Escherichia coli* hemolysin is released extracellularly without cleavage of a signal peptide. J. Bacteriol. **163**, 88–93 PubMed

60 Aller, S.G., Yu, J., Ward, A., Weng, Y., Chittaboina, S., Zhuo, R., Harrell, P.M., Trinh, Y.T., Zhang, Q., Urbatsch, I.L. and Chang, G. (2009) Structure of P-glycoprotein reveals a molecular basis for poly-specific drug binding. Science **323**, 1718–1722 CrossRef PubMed

61 Smriti, Zou, P. and McHaourab, H.S. (2009) Mapping daunorubicin-binding Sites in the ATP-binding cassette transporter MsbA using site-specific quenching by spin labels. J. Biol. Chem. **284**, 13904–13913 CrossRef PubMed

Received 23 February 2016/23 May 2016; accepted 7 June 2016
Accepted Manuscript online 8 June 2016, doi:10.1042/BCJ20160154

Supplementary Information

Interdomain regulation of the ATPase activity of the ABC transporter hemolysin B from *E. coli*

Sven Reimann[a], Gereon Poschmann[b], Kerstin Kanonenberg[a], Kai Stühler[b], Sander H. J. Smits[a] and Lutz Schmitt[a,c,1]

[a]Institute of Biochemistry, Heinrich-Heine-University Düsseldorf, Universitätsstraße 1, 40225 Düsseldorf, Germany; [b]Molecular Proteomics Laboratory, Biomedizinisches Forschungszentrum (BMFZ); [c]Center of Excellence on Plant Sciences (CEPLAS), Heinrich-Heine-University Düsseldorf, Universitätsstraße 1, 40225 Düsseldorf, Germany

[1] To whom correspondence should be addressed: Institute of Biochemistry, Heinrich-Heine-University Düsseldorf, Universitätsstraße 1, 40225 Düsseldorf, Germany. Tel.: +49-211-81-10773; Fax: +49-211-81-15310; E-mail: Lutz.Schmitt@hhu.de

Supplementary Information comprises:

Supplementary Figure S1

Supplementary Table S1

Supplementary Figure. S1

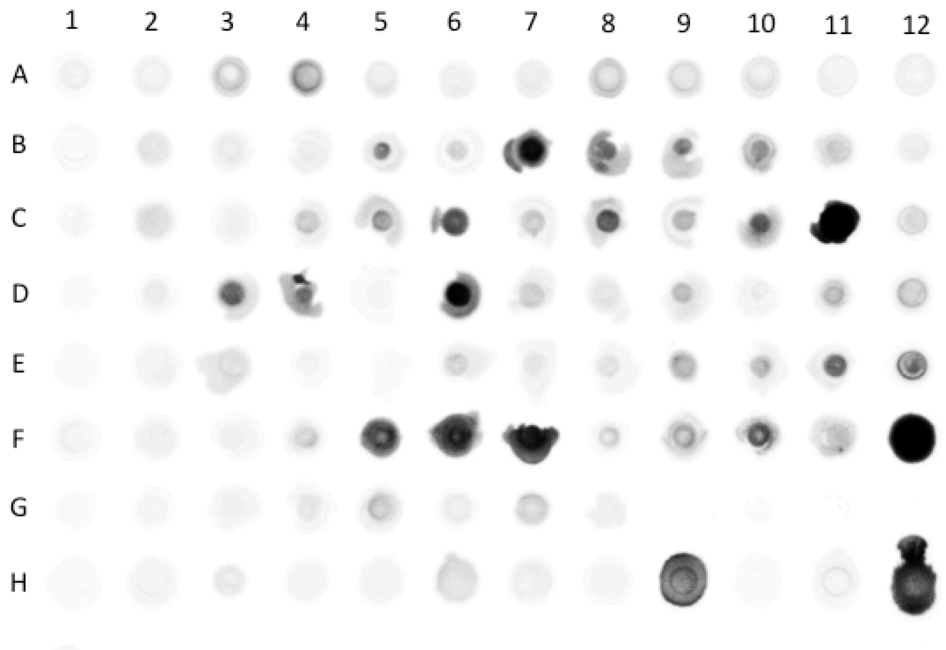

Supplementary Figure S1: Solubilization screen of HlyB using the Dot Blot technique. HlyB was overxpressed and the cell membranes treated as described in Material and Methods. The solubilized proteins were spotted onto a nitrocellulose membrane and examined via immune detection using a polyclonal anti-HlyB antibody. The used detergents and their concentrations are summarized in Table S1.

Supplementary Table S1

Supplementary Table S1: Overview of the detergents used for solubilization of HlyB by Dot Blot technique. N: Non-ionic detergents; Z: Zwitterionic detergents; A: Anionic detergents; C: Cationic detergents.

Position	Detergent	cmc [%]	used [%]	nature
A1	Anameg®-7	0,65	1%	N
A2	Anapoe®-20	0,0072	1%	N
A3	Anapoe®-35	0,001	1%	N
A4	Anapoe®-58	0,00045	1%	N
A5	Anapoe®-80	0,0016	1%	N
A6	Anapoe®-C10E6	0,025	1%	N
A7	Anapoe®-C10E9	0,053	1%	N
A8	Anapoe®-C12E8	0,0048	1%	N
A9	Anapoe®-C12E9	0,003	1%	N
A10	Anapoe®-C12E10	0,2	1%	N
A11	Anapoe®-C13E8	0,0055	1%	N
A12	Anapoe®-X-100	0,015	1%	N
B1	Anapoe®-X-114	0,011	1%	N
B2	Anapoe®-X-305	/	1%	N
B3	Anapoe®-X-405	0,16	1%	N
B4	Big CHAP	0,25	1%	N
B5	Big CHAP deoxy	0,12	1%	N
B6	CYGLU®-3	0,86	2%	N
B7	CYMAL®-1	15	2%	N
B8	CYMAL®-2	5,4	2%	N
B9	CYMAL®-3	0,37	1%	N
B10	2,6-Dimethyl-4-heptyl-β-D-maltose	1,2	2%	N
B11	2-propyl-1-pentyl maltose	1,9	2%	N
B12	MEGA-8	2,5	2%	N
C1	n-Octyl-β-D-glucoside	0,53	2%	N
C2	n-Nonyl-β-D-glucoside	0,2	1%	N
C3	n-Octyl-β-D-maltoside	0,89	2%	N
C4	n-Nonyl-β-D-maltoside	0,28	2%	N
C5	n-Decyl-α-D-maltoside	/	1%	N
C6	n-Tetradecyl-β-D-maltoside	0,00054	1%	N
C7	n-Undecyl-α-D-maltoside	0,029	1%	N
C8	n-Undecyl-β-D-maltoside	0,029	1%	N
C9	n-Dodecyl-α-D-maltoside	0,0076	1%	N
C10	n-Dodecyl-β-D-maltoside	0,0087	1%	N
C11	Fos-Choline®-16	0,00053	1%	N

C12	n-Heptyl-β-D-thioglucoside	0,85	2%	N
D1	n-Octyl-β-D-thiomaltoside	0,4	2%	N
D2	n-Nonyl-β-D-thiomaltoside	0,15	1%	N
D3	n-Undecyl-β-D-thiomaltoside	0,011	1%	N
D4	n-Dodecyl-β-D-thiomaltoside	0,0026	1%	N
D5	Pentaethylene glycol monodecylether(C10E5)	0,031	1%	N
D6	Lauryl maltose neopentyl glycol	0,001	1%	N
D7	Sucrose monododecanoate	0,016	1%	N
D8	Dimethyldecylphosphine oxide	0,1	1%	N
D9	n-Decyl-β-D-Maltopyranoside	0,087	1%	N
D10	n-Heptyl-β-D-glucoside	/	2%	N
D11	n-Hexyl-β-D-glucoside	/	2%	N
D12	n-Hexyl-β-D-maltoside	/	2%	N
E1	Anzergent® 3-10	1,2	2%	Z
E2	Anzergent®3-12	0,094	1%	Z
E3	Anzergent® 3-14	0,007	1%	Z
E4	CHAPS	0,49	2%	Z
E5	CHAPSO	0,5	2%	Z
E6	C-DODECAFOS™	0,77	2%	Z
E7	Cyclofos™-4	0,45	2%	Z
E8	Cyclofos™-5	0,15	1%	Z
E9	Cyclofos™-6	0,094	1%	Z
E10	Cyclofos™-2	7,5	1%	Z
E11	Fos-Choline®-9	1,2	2%	Z
E12	Cyclofos™-3	1,3	2%	Z
F1	Fos-Choline®-Iso-11	0,9	2%	Z
F2	Fos-Choline®-Iso-11-6U	0,87	2%	Z
F3	Fos-Choline®-Unisat-11-10	0,21	1%	Z
F4	Fos-Choline®-Iso-9	0,99	2%	Z
F5	Fos-Choline®-14	0,0046	1%	Z
F6	Fos-Choline®-15	0,0027	1%	Z
F7	Fos-Choline®-16	0,00053	1%	Z
F8	Fos-Choline®-8	3,4	2%	Z
F9	Fosfen™-9	0,014	1%	Z
F10	Nopol-Fos™	1,4	2%	Z
F11	PMAL™-8	/	1%	Z
F12	PMAL™-C10	/	1%	Z
G1	n-Decyl-N,N-dimethylglycine	0,46	2%	Z
G2	n-Dodecyl-N,N-dimethylglycine	0,041	1%	Z
G3	n-Tetradecyl-N,N-dimethylamine-N-oxide	0,0075	1%	Z
G4	n-Dodecyl-N,N-dimethylamine-N-oxide	0,023	1%	Z
G5	Cypfos-3	0,0075	1%	Z

G6	2-Carboxy-w-heptadecenamidopropyldimethylamine	/	1%	Z
G7	2-Carboxy-5-pentadecenamidopropyldimethylamine	/	1%	Z
G8	Anzergent 3-8	10,9	2%	Z
G9	Deoxycholic acid, sodium salt	0,24	1%	A
G10	Sodium cholate	0,41	2%	A
G11	Fosmea®-10	0,15	1%	A
G12	Sodium dodecanoyl sarcosine	0,42	2%	A
H1	Decyltrimethylammonium chloride	0,07	1%	C
H2	Dodecyltrimethylammonium chloride	0,0012	1%	C
H3	Hexadecyltrimethylammonium chloride	0,000102	1%	C
H4	Tetradecyltrimethylammonium chloride	0,0009	1%	C
H5	C12E8	0,11	1%	
H6	n-Dodecyl-beta-iminodipropionic acid, monosodium salt	/	2%	Z
H7	CYMAL®-5	0,12	2%	N
H8	ph-Tripglu	0,23	1%	N
H9	cy-Tripglu	0,11	1%	N
H10	Tripao	4,5	2%	Z
H11	LAPAO	0,052	2%	Z
H12	SDS		10%	

3.3. Chapter III

Title: Amber codon mutagenesis as a tool for analysing the haemolysin A type 1 secretion system from *Escherichia coli*

Authors: Sven Reimann, Julia Zaschke-Kriesche, Diana Kleinschrodt, Sander H.J. Smits, Lutz Schmitt

Published in: (*to be submitted*)

Proportionate work on this publication: design and cloning of different mutants, expression and purification of proteins with incorporated unnatural amino acids, secretion analysis of mutants, cross-linking experiments, data analysis, writing of the manuscript

Amber codon mutagenesis as a tool for analysing the haemolysin A type 1 secretion system from *Escherichia coli*

Sven Reimann, Julia Zaschke-Kriesche, Diana Kleinschrodt, Sander H.J. Smits and Lutz Schmitt [1]

Institute of Biochemistry, Heinrich-Heine-University Düsseldorf, Universitätsstraße 1, 40225 Düsseldorf, Germany

[1] To whom correspondence should be addressed: Institute of Biochemistry, Heinrich-Heine-University Düsseldorf, Universitätsstraße 1, 40225 Düsseldorf, Germany. Tel.: +49-211-81-10773; Fax: +49-211-81-15310; E-mail: Lutz.Schmitt@hhu.de

Abstract

The secretion of the toxin haemolysin A (HlyA) is mediated by a specific type 1 secretion system (T1SS) in *Escherichia coli*. The T1SS catalyses the transport across both membranes of Gram-negative bacteria and requires a C-terminal secretion sequence. The HlyA translocator complex is composed of the ABC transporter haemolysin B (HlyB) and the membrane fusion protein haemolysin D (HlyD), located in the inner membrane, and TolC, located in the outer membrane. HlyA is supposed to interact with the inner membrane proteins to initialize the translocation process. Subsequently, it is secreted without any periplasmic intermediate into the extracellular space. However, little is known about the translocation path and crucial amino acids within a putative translocation channel. Therefore, we used photoactivatable unnatural cross-linking amino acids as a tool to investigate the HlyA T1SS. We describe the incorporation of two different unnatural amino acids at several positions into HlyA. The incorporation of these amino acids has no influence on the amount of secreted HlyA *in vivo*. Furthermore, we successfully incorporated the unnatural amino acids into the fusion protein eGFP-HlyA at several positions. The fusion protein was used to stall the translocation process. Thereby, the unnatural amino acid is located within the putative translocation channel. A screening of UV exposure time, distance and varying cell treatments before and after UV irradiation, increased the amount of cross-link products detected by Western blot analysis. However, no cross-linked amino acids were identified by mass spectrometry. In addition, we purified HlyA with an incorporated unnatural amino acid and analysed cross-link products occurring during an ATPase assay together with purified HlyB. A subsequent Western blot analysis detected UV induced protein bands, however, a mass spectrometric analysis could not confirm cross-linked proteins.

Abbreviations

aaRS, aminoacyl-tRNA synthetase; ABC, ATP-binding cassette; Apa, *p*-azidophenylalanine; Bpa, *p*-benzoyl-L-phenylalanine; CBB, Coomassie Brilliant Blue; HlyA*, a HlyA amber variant; HlyA, haemolysin A; HlyB, haemolysin B; HlyD, haemolysin D; IMAC, immobilized metal-ion-affinity chromatography; LMNG, lauryl maltose neopentyl glycol; MFP, membrane-fusion protein; NBD, nucleotide-binding domain; RTX, repeats in toxin; SEC, size-exclusion chromatography; T1SS, Type 1 secretion system; TBS-T, TBS with Tween 20; TMD, transmembrane domain

Keywords

Cross-linking, type I secretion system, HlyA, unnatural amino acid, protein translocation, haemolysin, *Escherichia coli*

Introduction

The type I secretion system (T1SS) in Gram-negative bacteria mediates the transport of a wide range of substrates from the cytoplasm to the extracellular space (Delepelaire, 2004). The substrate transport occurs in an unfolded state in one step, passing both the inner and the outer bacterial membrane (Bakkes *et al.*, 2010). Translocated proteins include e.g. adenylate cyclases such as CyaA from *Bordetella pertussis*, lipases such as LipA from *Pseudomonas fluorescens*, proteases such as alkaline protease from *Pseudomonas aeruginosa*, toxins such as HlyA from *Escherichia coli* and surface layer proteins (Chabeaud *et al.*, 2001; Chenal *et al.*, 2010; Goebel *et al.*, 1982; Holland *et al.*, 2005; Lo *et al.*, 1987). They also vary greatly in size from small proteins such as the HasA from *Serratia marcescens* with a size of 19 kDa up to a molecular weight of 900 kDa for LapA from *P. fluorescens* (Gilson *et al.*, 1990; Hinsa *et al.*, 2003; Linhartova *et al.*, 2010). The secretion machinery is composed of three parts. Two proteins are located in the inner membrane (IM), an ATP-binding cassette (ABC) transporter and a membrane fusion protein (MFP). The third one is localized in the outer membrane (OM) and therefore called the outer membrane protein (OMP). In the case of the paradigm haemolysin A (HlyA) T1SS these three components are haemolysin B (HlyB) (ABC transporter), haemolysin D (HlyD) (MFP) and TolC (OMP). The information for secretion of HlyA is encoded within the most C-terminal 50-60 amino acids, forming the non-cleavable secretion signal (Balakrishnan *et al.*, 2001; Ghigo *et al.*, 1994; Kenny *et al.*, 1994; Kenny *et al.*, 1992; Letoffe *et al.*, 1996; Thanabalu *et al.*, 1998). Therefore, the common model implies that the HlyA secretion occurs posttranslational. The exact translocation mechanism, assembly and interactions are not understood in detail. Questions remain to be answered especially addressing the detailed translocation pathway of HlyA within the T1SS machinery, as well as the role of the N-terminal C39-peptidase like domain of HlyB. So far studies of Zhang *et al.* (1993) pointed to an interaction of the HlyB TMD and the HlyA secretion signal. Additionally an interaction of the purified NBD of HlyB and a purified fragment encoding the C-terminal secretion signal of HlyA was identified, that could be abolished by the addition of ATP (Benabdelhak *et al.*, 2003). These results may play a role in the initiation of the secretion process. Recently it was shown that a fusion protein of eGFP and HlyA stalled the T1SS and exposed the HlyA C-terminal part on the cell surface (Lenders *et al.*, 2015). Taking into account that HlyA is translocated in an unfolded state, the substrate must enter the translocation machinery with their C-terminus first.

Here, we established the incorporation of an unnatural amino acid into HlyA, to investigate the translocation processes in further detail (Figure 1). This approach allows us to manipulate the biological and chemical properties of HlyA *in vivo*. Unnatural amino acids have already been used in *E. coli, Saccharomyces cerevisiae, Pichia Pastoris* and mammalian cells (Chen *et al.*, 2007; Liu *et al.*, 2007; Sakamoto *et al.*, 2002; Simpson *et al.*, 2016; Wang *et al.*, 2007; Young *et al.*, 2009; Zhang *et al.*, 2003).

Therefore, an AMBER stop codon (TAG) was reassigned to encode the desired unnatural amino acid. Due to the lack of any cross reactivity between the host organism´s endogenous and the orthogonal tRNA and aminoacyl-tRNA synthetase (aaRS), the system ensures a high fidelity (Young *et al.*, 2010).

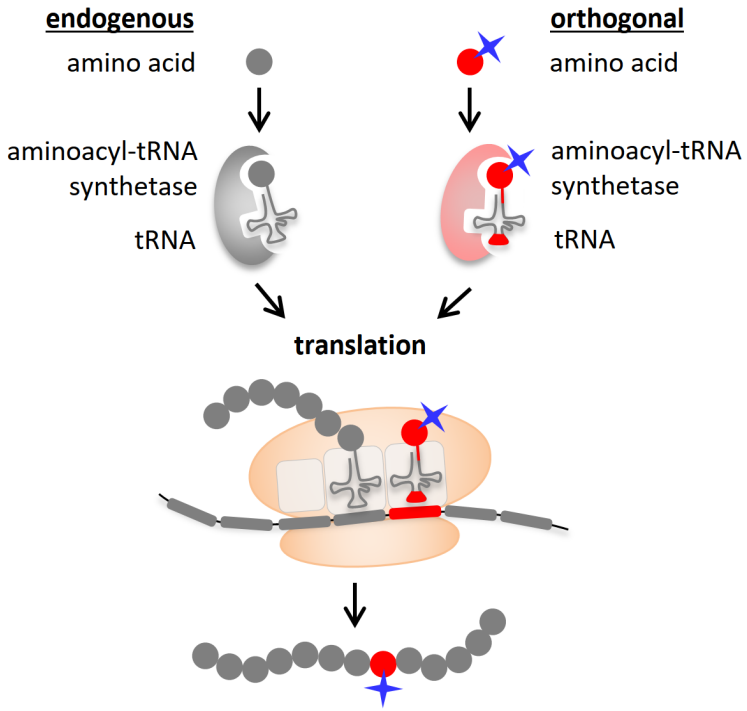

Figure 1. Principle method of the incorporation of photo-cross-linking amino acids. The residue specific introduction of an unnatural amino acid is mediated an exogenous and orthogonal system. The orthogonal aminoacyl-tRNA synthetase couples the orthogonal amber suppressor tRNA and a supplemented unnatural amino acid, which then is incorporated into proteins.

We used an orthogonal aaRS/suppressor $tRNA_{CUA}$ pair from *Methanocaldococcus jannaschii* to selectively incorporate the unnatural photoactivatable amino acids *p*-benzoyl-L-phenylalanine (Bpa) or *p*-azidophenylalanine (Apa), respectively into HlyA at ten different positions. We showed that the incorporation did not affect the amount of secreted HlyA *in vivo*. The unnatural amino acids were also incorporated into the fusion protein eGFP-HlyA at ten positions. Lenders *et al.* (2015) already used the fusion protein to stall the substrate translocation process. Therefore, we suggest that an unnatural amino acid in HlyA is exposed to the interior of the putative T1SS translocation channel. We optimised the experimental conditions by screening the UV exposure time, distance and cell treatment before and after irradiation to increase the total amount of cross-linked products *in vivo*. Additionally, we used the photoactivatable amino acid in HlyA to analyse its interaction with HlyB *in vitro*. Therefore, we purified both proteins and activated the cross-linker during an ATPase assay. In both experiments we observed protein mass shifts upon UV irradiation by Western blot analysis, however, no cross-link products were identified with subsequent mass spectrometry.

Experimental procedures

Plasmid constructions

The vector pEVOL-pBpa (gift from Peter Schultz (Addgene plasmid #31190), (Chin *et al.*, 2002)) encodes a suppressor tRNA/aminoacyl-tRNA synthetase pair and has been further described in Young *et al.* (2010). To provide compatibility with other plasmids we exchanged the origin of replication in this vector from p15A to ColA. Therefore, we isolated a ColA containing fragment from pCOLADuet-1 using the restriction endonucleases XbaI and NheI, and ligated it into the same restriction sites in pEVOL-Bpa (Zverev *et al.*, 1985). To obtain pEVOL-Apa-ColA we isolated a ColA containing fragment from pEVOL-Bpa-ColA using the restriction endonucleases AfeI and ClaI, and ligated it into the same restriction sites. For the production of HlyB and HlyD the plasmid pSU-HlyBD (pK184) was used and protein expression was under the control of a *lacZ* promotor, inducible with IPTG (isopropyl β-D-1-thiogalactopyranoside) (Bakkes *et al.*, 2010). To evaluate the secretion competency of pro-HlyA and to purify the AMBER mutants we used the plasmid pSU2726-HlyA (Bakkes *et al.*, 2010; Jumpertz *et al.*, 2010). The plasmid pSOI-eGFP-HlyA was used for the expression of eGFP-HlyA and has been described (Lenders *et al.*, 2015). AMBER mutants were introduced into pSU2726-HlyA or pSOI-eGFP-HlyA by site-directed mutagenesis using the QuikChange mutagenesis kit (Stratagene) following manufacturer´s instructions. A list of all mutated positions in HlyA or eGFP-HlyA, and of the corresponding primers can be found in supplementary Table S1. A list of all used plasmids can be found in supplementary Table S2. All constructs were verified by sequencing analysis.

Bacterial strains and growth conditions

E. coli BL21 (DE3) cells were transformed with pK184 and pEVOL-Bpa or pEVOL-Apa, respectively. The cells were also transformed with either pSU2726-HlyA variants to test the secretion competency, or with pSOI-eGFP-HlyA variants for photo-cross-linking experiments. Cells were exposed on selective agar plates containing 100 µg/ml ampicillin, 30 µg/ml kanamycin and 30 µg/ml chloramphenicol. A selective overnight culture with 2YT medium [1.6% (w/v) tryptone, 1% (w/v) yeast extract and 0.5% NaCl] was inoculated and grown for 16 h at 37 °C and vigorously shaking at 200 rev./min. The main culture with selective 2YT medium was inoculated from the overnight culture and grown to an OD_{600} of 1.0 before expression was induced with 6.6 mM arabinose and 1 mM IPTG. Simultaneously to induce the folding of secreted pro-HlyA and thereby to stabilise the protein 4 mM $CaCl_2$ was added. Additionally 1 mM of the unnatural amino acids Bpa or Apa was added, respectively. After four hours of incubation, cell cultures were used for photo-cross-linking experiments or analysed to detect secreted pro-HlyA.

Expression and purification of HlyB, HlyA-K823*and HlyA-K945*

HlyB was purified as described (Reimann *et al.*, 2016). The proteins HlyA-K823*and HlyA-K945* were expressed and isolated as described previously (Thomas *et al.*, 2014c) with the following modifications. *E. coli* BL21 (DE3) cells were transformed with pK184 and pEVOL-Bpa or pEVOL-Apa, respectively and pSU2726-HlyA-K823 or pSU2726-K945, respectively. Cells were treated and incubated as described above, using a 50 ml main culture with selective 2YT medium. Cells were harvested after fours hours of incubation by centrifugation (100,000 g, 30 min) and the supernatant was filtered (0.45 µm) and concentrated to 5 ml using an Amicon Ultra centrifugal filter unit (100 kDa molecular mass cut-off; Merck Milipore). To increase the sample purity, a SEC (size-exclusion chromatography) was performed using a 'HiLoad 16/600 Superdex 200 pg' (GE Healthcare Life Sciences) column and a buffer containing 100 mM HEPES, pH 8. The purity of eluted protein was determined by SDS/PAGE and subsequent CBB (Coomassie Brilliant Blue) staining.

Unfolding of purified HlyA-K823*and HlyA-K945*

Purified HlyA-K823*and HlyA-K945* protein containing Bpa or Apa, respectively, was secreted in the presence of calcium ions that bound to the protein and induced its folding. Protein with a final concentration of 1.5 mg/ml was unfolded with 4 M urea and 50 mM EGTA and incubated for 10 minutes at 25 °C. To change the buffer subsequently the protein sample was applied on a 'PD MidiTrap G-10' (GE Healthcare Life Sciences) column and eluted with 100 mM HEPES, pH 8, into an ice cooled reaction tube. Residual urea was removed by washing the protein in excess (10-times) of elution buffer using an Amicon Ultra centrifugal filter unit (100 kDa molecular mass cut-off; Merck Milipore).

Electrophoresis and immunological technique

To analyse proteins SDS/PAGE and subsequent CBB staining was used. To estimate protein molecular weight the PageRuler Prestained Protein Ladder (#26616, Thermo Fisher Scientific, Waltham, MA, USA) was used. The immunodetection was done with anti-HlyB or anti-HlyA antibody rabbit polyclonal serum at 1:8000 dilutions in TBS-T (TBS with Tween 20: 20 mM Tris base, 300 mM NaCl and 0.05% Tween 20, pH 8).

In vivo photo-cross-linking

For *in vivo* photo-cross-linking experiments *E. coli* BL21 (DE3) cells encoding for one eGFP-HlyA* variants were treated and cultivated as described above. Four hours after induction along with the unnatural amino acid, duplicate 1 ml aliquots were pipetted over ice into a reaction tube (untreated sample) or a six-well plate and were UV irradiated with a distance of 4 cm by a Spectroline E-Series UV

lamp (Sigma-Aldrich). The exposure time varied in each experiment and is described in the results chapter accordingly.

In vitro photo-cross-linking

For *in vitro* photo-cross-linking experiments purified proteins were used in an ATPase assay together with the ABC transporter. Reactions were performed in 100 mM HEPES (pH 7) containing 20-fold CMC of LMNG detergent and an ATP concentration of 1 mM. Purified HlyB was used at a concentration of 1 µM and HlyA-K823* or HlyA-K945* were used at a concentration of 1 µM or 15 µM, respectively. Reactions were started by the addition of 10 mM $MgCl_2$ and incubated at 25 °C. After 30 min incubation the samples were irradiated in reaction tubes with a distance of 4 cm by Spectroline E-Series UV lamp (Sigma-Aldrich). The exposure time varied to each experiment and is described in the results chapter.

Results

p-benzoyl-L-phenylalanine incorporation to HlyA does not influence its secretion competency

The purpose of this project is to identify crucial amino acids within the translocation pathway of HlyA through its T1SS. For this purpose, a site-specific photo-cross-link method was used that employs the coexpression of an amber suppressor tRNA and an amino acyl-tRNA synthetase from *M. jannaschii* (Wang *et al.*, 2000; Wang *et al.*, 2001; Young *et al.*, 2010). This system is orthogonal to the *E. coli* translation machinery and enables the incorporation of a photoactivatable amino acid at amber codons. It was previously successfully used to e.g. investigate the twin-arginine translocation (Tat) machinery of *E. coli* (Maurer *et al.*, 2010). Our approach used the photoactivatable amino acid analog *p*-benzoyl-L-phenylalanine (Bpa), which is capable of inserting into most C-H bonds that are within a range of about 3 Å of the polypeptide backbone (Dorman *et al.*, 1994; Sato *et al.*, 2011). The activation of the cross-link reaction is started by an irradiation with UV light at a wavelength of 365 nm. We introduced an amber codon at one of ten positions in HlyA evenly distributed from the very N-terminus to the C-terminus, except the secretion signal: L13, F110, L209, G308, M417, P517, I610, K708, L810 and W914. The secretion signal remained unaffected on purpose because it is known to be mandatory for the translocation process (Lenders *et al.*, 2015). The secretion process of HlyA is not completely understood and potentially crucial amino acids still have to be identified. HlyA is secreted in an unfolded state across both *E. coli* membranes and first we investigated whether the incorporation of Bpa in HlyA influences its secretion competency.

E. coli BL21 (DE3) cells were transformed with three plasmids that encode (i) the amber suppression system (pEVOL-Bpa), (ii) the T1SS (pSU-HlyBD) and (iii) a HlyA amber mutant (pSU-HlyA*) or the wild-type protein, respectively. Protein expression was induced with IPTG and arabinose, furthermore, calcium was added to stabilise secreted HlyA containing an unnatural amino acid (HlyA*). We incubated two equal cultures in parallel and only one was supplemented with the unnatural amino acid. After four hours of protein expression the culture supernatant was separated from the cells and OD_{600} equivalents were analysed on a SDS/PAGE (Figure 2). We found that all of our ten tested HlyA* (Bpa) variants were secreted to the supernatant of the culture, represented by a band correlating to a molecular mass of HlyA (110.1 kDa). In comparison high amounts of HlyA* (Bpa) were secreted in the presence of Bpa and in contrast very small amounts of HlyA* were secreted in the absence of Bpa. Latter may occur due to a ‘read-through’ of the amber codon by the translation machinery. The sample of the variant HlyA-I610* also contained a protein with a size of about 70 kDa, which was secreted in absence of Bpa.

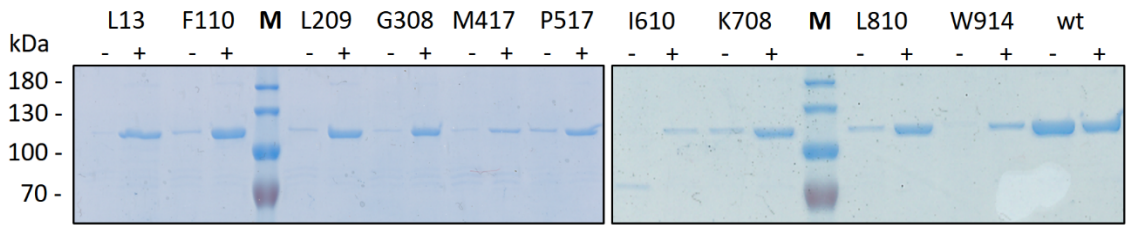

Figure 2. SDS/PAGE analysis of secreted HlyA* variants expressed in presence (+) or absence (-) of the unnatural amino acid Bpa. In two equal bacterial cultures the protein expression of the T1SS and the HlyA* variants were induced and only one culture was supplemented with the unnatural amino acid Bpa. After four hours of protein expression the culture supernatant was analysed for secreted HlyA* via an SDS/PAGE and stained with CBB. The variants of HlyA* have a theoretical mass of 110.1 kDa. M, protein weight standard.

We also found that the position of the amber codon and/or the substituted amino acid influenced the amount of secreted HlyA* strikingly with a reduced amount for the variants M417 and I610. Overall this result confirms the successful incorporation of Bpa to HlyA.

eGFP-HlyA* (Bpa) fusion proteins are located in the cell membrane

HlyA is translocated across both membranes of *E. coli* without any periplasmic intermediate (Mackman *et al.*, 1987; Mackman *et al.*, 1986; Thanabalu *et al.*, 1998). Therefore, a photoactivatable amino acid incorporated in the transport substrate would be exposed to continuously changing potential interaction partners, due to the proceeding translocation process. The activation of this photoactivatable unnatural amino acid during the transport process suggests to result in a broad spectrum of cross-linked products. To address this problem we stalled the T1SS with an eGFP-HlyA* fusion protein. This technique has already been used to show that the HlyA C-terminus is secreted first (Lenders *et al.*, 2015). It is expected that the C-terminal part of the fusion protein containing HlyA* threads into the T1SS and subsequently the N-terminal fast folding eGFP stalls the secretion process. However, the mechanism that keeps HlyA in a secretion competent and unfolded state in the cytoplasm is unknown so far. We expect that Bpa is located within the translocation pathway and exposed to adjacent amino acids of the translocation machinery. Due to the stalled translocation process we expect that every HlyA amber mutant interacts with a distinct part of the T1SS upon UV activation of the cross-linker.

First, we have shown the correct localisation of the fusion eGFP-HlyA* variants within the bacterial membrane. *E. coli* BL21 (DE3) cells were transformed with three plasmids that encode (i) the amber suppression system (pEVOL-Bpa), (ii) the T1SS (pSU-HlyBD) and (iii) one eGFP-HlyA* amber mutant (pSU-eGFP-HlyA*) or the wild-type protein, respectively. Protein expression was induced with Bpa, IPTG and arabinose, furthermore, calcium was added to stabilise exposed eGFP-HlyA on the cell surface. After four hours of protein expression cells were harvested, membranes isolated and OD_{600}

equivalents were analysed by Western blot and an anti-HlyA antibody. The fusion protein eGFP-HlyA* has a calculated molecular mass of 140.0 kDa correlating to the most prominent signal of each analysed sample apart from eGFP-HlyA-I610* (Figure 3).

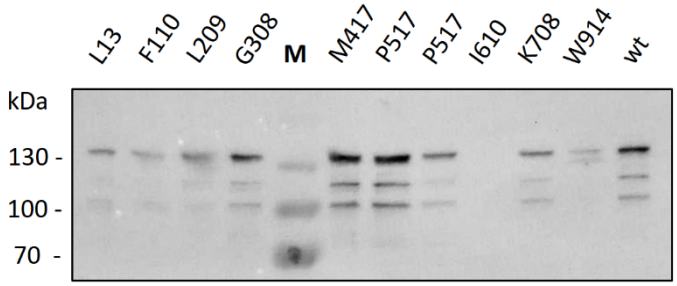

Figure 3. Western blot analysis (anti-HlyA) of *E. coli* membranes after expression of eGFP-HlyA* variants containing the unnatural amino acid Bpa. *E. coli* cells expressed the T1SS and variants of eGFP-HlyA* in presence of Bpa. The isolated membranes of the *E. coli* cells were analysed by Western blot using polyclonal antisera (anti-HlyA). eGFP-HlyA* has a theoretical mass of 140.0 kDa. M, protein weight standard.

An additional band below correlates to HlyA* without eGFP fused to the N-terminus (110.1 kDa). A third band correlates to HlyA without eGFP and the secretion signal (103.1 kDa). The reason for the formation of these fragments is not clear. We also analysed the supernatants of the bacterial cultures by Western blot and an anti-HlyA antibody and we detected no secreted eGFP-HlyA* (data not shown). The eGFP-HlyA fusion protein has already been established as a tool to stall the T1SS (Lenders *et al.*, 2015). Our study confirmed that also significant amounts of most eGFP-HlyA* (Bpa) variants can be found within the bacterial membrane. Therefore, we suggest the unnatural amino acid does not prohibit the fusion proteins to stall the T1SS in principal. However, the signal intensities on the Western blot varied.

Varying UV exposure time to enhance the cross-link of eGFP-HlyA* (Bpa) and the T1SS *in vivo*

As an initial experimental setup to activate the cross-linker, we first used the same *E. coli* cultivation conditions for eGFP-HlyA* fusion proteins as described before. After four hours of protein expression the bacterial culture was cooled on ice and irradiated for seven minutes. In parallel another aliquot of the sample remained untreated to allow us to assign any effect to the UV irradiation treatment. OD_{600} equivalents containing whole cells were diluted in SDS sample buffer and analysed by Western blot and anti-HlyA antibody (Figure 4). We observed no distinct signal shifts correlating to cross-link induced molecular mass shifts on the Western blot by comparing the samples with and without UV irradiation. Slight differences in the signal intensity were noticeable for the mutations HlyA-F110*, HlyA-G308* and HlyA-M417* especially a signal band correlating to a high protein molecular mass.

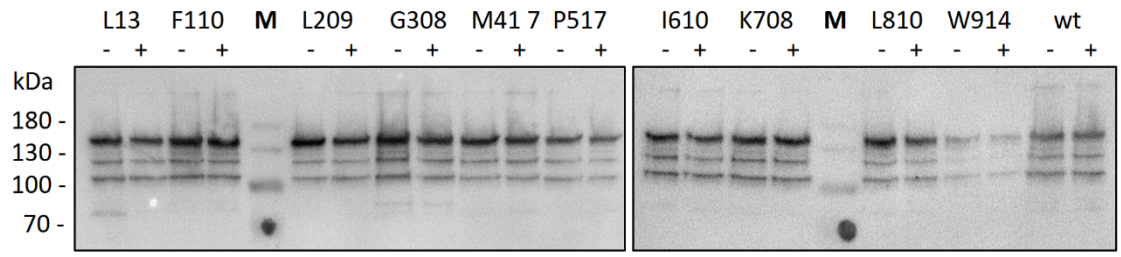

Figure 4. Detection of eGFP-HlyA* (Bpa) *in vivo* photo-cross-linking products by Western blot analysis (anti-HlyA). *E. coli* cells containing variants of the fusion protein eGFP-HlyA* (Bpa), stalling the T1SS, were irradiated for seven minutes with UV light (+) or remained untreated (-). Cells were analysed by Western blot using polyclonal antisera (anti-HlyA). eGFP-HlyA* has a theoretical mass of 140.0 kDa. M, protein weight standard.

Due to the lack of an appropriate molecular weight standard we cannot determine the protein size. Subsequently, we screened for further experimental conditions and chose only four HlyA* mutants due to an easier handling. We used the HlyA* variants HlyA-F110*, HlyA-M417*, HlyA-L810* and HlyA-W914* to investigate the effect of increasing irradiation times of 15 minutes, 30 minutes and 45 minutes while other experimental conditions remained as described before. OD_{600} equivalents containing whole cells were diluted in SDS sample buffer and analysed by Western blot and anti-HlyA antibody. We found no differences in the signal pattern of the Western blot with an increased irradiation time of 15 minutes (Figure 5 A).

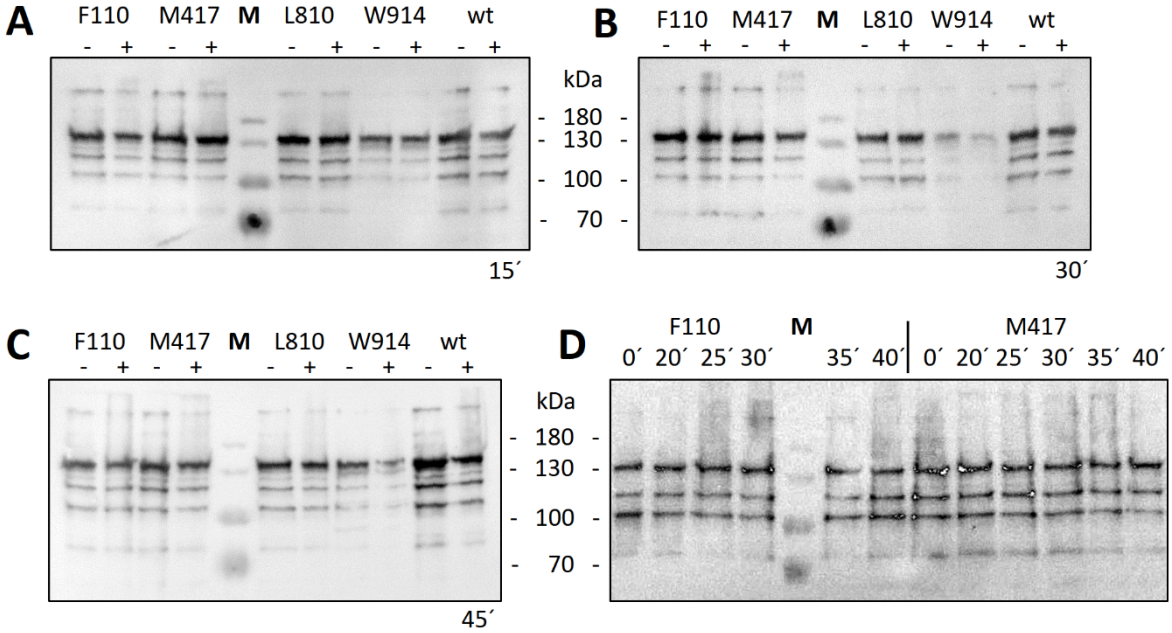

Figure 5. Detection of UV exposure time dependent eGFP-HlyA* (Bpa) *in vivo* photo-cross-linking products by Western blot analysis (anti-HlyA). *E. coli* cells containing variants of the fusion protein eGFP-HlyA* (Bpa), stalling the T1SS, were UV irradiated (+) for (A) 15 minutes, (B) 30 minutes, (C) 45 minutes or remained untreated (-). (D) UV exposure time fine-screen of the fusion proteins eGFP-HlyA-F110* (Bpa) and eGFP-HlyA-M417* (Bpa). Cells were analysed by Western blot using polyclonal antisera (anti-HlyA). eGFP-HlyA* has a theoretical mass of 140.0 kDa. M, protein weight standard.

However, a further increase to 30 minutes and 45 minutes resulted in the occurrence of an additional signal on the Western blot (Figure 5 B, C). This signal occurred only upon UV irradiation of the protein variants eGFP-HlyA-F110* and eGFP-HlyA-M417* and represents an increased protein molecular mass. The specific protein weight was not detectable due to the lack of correlating marker signals. The UV induced, additional protein bands were isolated and analysed by mass spectrometry. Both samples contained HlyA protein with incorporated Bpa, however, no cross-linking product was detected. The proteins HlyA-L810* and HlyA-W914* did not show any changes in the signal pattern upon increased UV exposure times. The preceding experiments confirmed the formation of protein species with shifted molecular masses upon UV irradiation. However, we were not able to detect cross-linked products. Nevertheless, these experiments identified a sufficient irradiation time between 15 minutes and 30 minutes. As a proof of principle we repeated the experimental setup with a more detailed time screen to determine the optimal experimental conditions. Therefore, separate bacterial cultures containing eGFP-HlyA-F110* and eGFP-HlyA-M417* were irradiated from 20 minutes up to 40 minutes with increments of five minutes, while other experimental conditions remained as described before (Figure 5 D). OD_{600} equivalents containing whole cells were diluted in SDS sample buffer and analysed by Western blot and anti-HlyA antibody. The analysis confirmed a correlation of duration of irradiation time and intensity of an occurring protein band with a molecular mass of about 250 kDa. The signal intensity of this band increases to the maximum if the sample was irradiated up to 30 minutes (HlyA-F110*) or 35 minutes (HlyA-M417*), respectively. Longer exposures to UV light resulted in a decrease of the signal intensity for both variants. This effect was more pronounced in the case of HlyA-F110*. Based on these findings we rated the exposure of 30 minutes as the optimal length for the activation of the cross-linker Bpa.

Varying cell treatments to enhance the cross-link of eGFP-HlyA* (Bpa) with the T1SS *in vivo*

Multiple factors have an influence on the cross-linking reaction. Besides the exposure time of the sample by UV light we also changed bacterial culture growth conditions to prevent an unintentional and premature activation of the cross-link reaction by spare UV light. In this study we protected the cultivation flask from any contaminating light using aluminium foil and induced protein expression as described before. After four hours of protein expression the bacterial culture was cooled on ice and irradiated for a duration of 30 minutes. In parallel another aliquot of the sample remained untreated to allow us to assign any effect to the UV irradiation treatment. OD_{600} equivalents containing whole cells were diluted in SDS sample buffer and analysed by Western blot and anti-HlyA antibody (Figure 6 A). Samples of the variants eGFP-HlyA-L13*, eGFP-HlyA-F110*, eGFP-HlyA-L209*, eGFP-HlyA-G308*, eGFP-HlyA-M417* and eGFP-HlyA-P517* showed an additional signal band with an increased

size of about 250 kDa after treatment with UV light (Figure 6 A). Samples of the variants eGFP-HlyA-F110* and eGFP-HlyA-G308* also showed signal bands correlating to proteins with an even higher molecular mass.

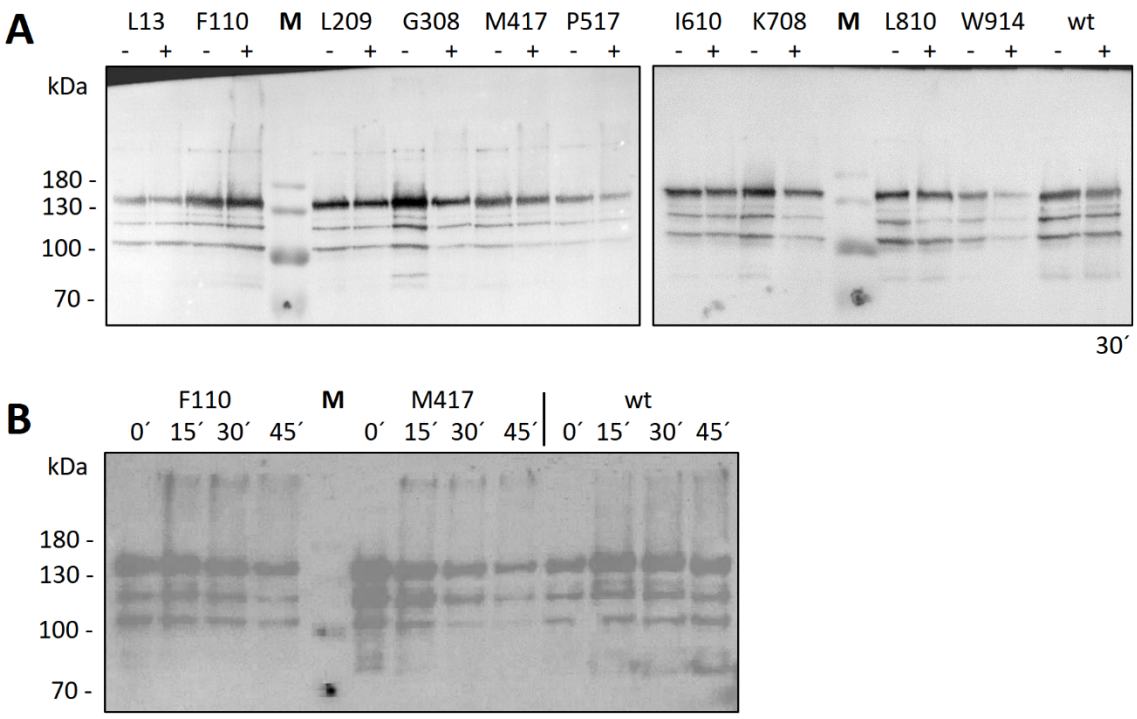

Figure 6. Detection of eGFP-HlyA* (Bpa) *in vivo* photo-cross-linking products by Western blot analysis (anti HlyA) depending on cell treatment. (A) *E. coli* cells expressing variants of the fusion protein eGFP-HlyA* (Bpa) were incubated in a light protected environment and subsequently UV irradiated for 30 minutes (+) or remained untreated (-). (B) Unprotected *E. coli* cells were lysed prior to varying UV exposure times. Afterwards the cell membranes were isolated from the cell debris. Samples containing (A) *E. coli* cells or (B) cell membranes were analysed by Western blot using polyclonal antisera (anti-HlyA). eGFP-HlyA* has a theoretical mass of 140.0 kDa. M, protein weight standard.

The distinct weight could not be determined due to an insufficient protein size standard. In parallel to the light protection described above, we changed the treatment of the cells before and after UV irradiation. To increase the UV accessibility of the unnatural amino acids we lysed cells prior to the UV treatment. Moreover, in order to increase the concentration of potentially cross-linked T1SS we separated the cell membranes from cell debris after UV irradiation. These experimental setup modifications were investigated together with an increasing exposure by UV light ranging from 15 minutes to 45 minutes. The isolated cell membranes were diluted in SDS sample buffer and analysed by Western blot and anti-HlyA antibody (Figure 6 B). The Western blot showed additional signals for every sample correlating to the irradiation by UV light, so the same for wild-type eGFP-HlyA. The increasing amount of UV exposure did not change the intensity of these signals. In comparison to a treatment without cell disruption no improvements were observed.

p-azidophenylalanine incorporation to HlyA does not influence its secretion competency

Aside from Bpa, our approach also used the photoactivatable unnatural amino acid *p*-azidophenylalanine (Apa). When a phenyl azide is exposed to UV light with 254 nm, it forms a nitrene group. This can undergo an insertion into C-H and N-H sites or initiate addition reactions with double bonds. The incorporation of the unnatural amino acid to HlyA was done with the same orthogonal system and the same amber mutants of HlyA as described for Bpa. However, deviating from Bpa experiments another amino acyl-tRNA synthetase was needed. First we investigated whether the incorporation of Apa influences HlyA secretion competency.

E. coli BL21 (DE3) cells were transformed with three plasmids that encode (i) the amber suppression system (pEVOL-Apa), (ii) the T1SS (pSU-HlyBD) and (iii) a HlyA amber mutant (pSU-HlyA*) or the wild -type protein, respectively. Protein expression was induced with IPTG and arabinose, furthermore, calcium was added to stabilise secreted HlyA in the cell supernatant. We incubated two equal cultures at the same time and only one was also supplemented with the unnatural amino acid Apa. After four hours of protein expression OD_{600} equivalents of cell-free culture supernatant were analysed on a SDS/PAGE (Figure 7). We found that all of our tested HlyA* (Apa) variants were secreted into the cell supernatant if the unnatural amino acid was added to the media. The intensity of the signal bands correlating to the molecular mass of secreted HlyA* (110.1 kDa) containing Apa were affected by the mutated amino acid and/or position of the substitution. The variant HlyA-I610* was secreted to the least extent. Furthermore, this result confirms the successful incorporation of Apa to HlyA.

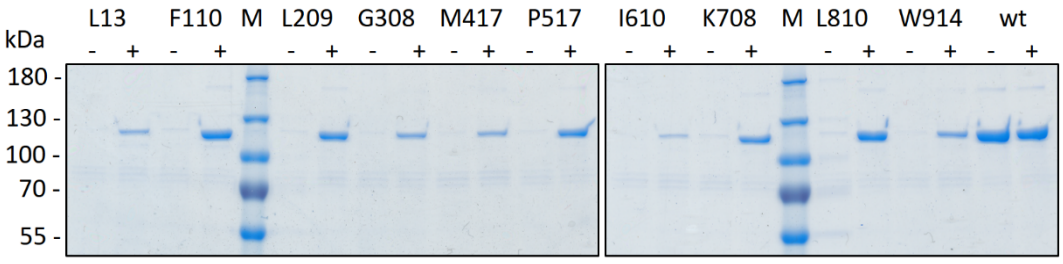

Figure 7. SDS/PAGE analysis of secreted HlyA* variants expressed in presence (+) or absence (-) of the unnatural amino acid Apa. In two equal bacterial cultures the protein expression of the T1SS and the HlyA* variants were induced and only one culture was supplemented with the unnatural amino acid Apa. After four hours of protein expression the culture supernatant was analysed for secreted HlyA* via an SDS/PAGE and stained with CBB. The variants of HlyA* have a theoretical mass of 110.1 kDa. M, protein weight standard.

eGFP-HlyA* (Apa) mutants are located in the cell membrane

As already tested for Bpa, we also proved the correct localisation of the eGFP-HlyA* fusion protein variants containing Apa. *E. coli* BL21 (DE3) cells were transformed and treated as described before.

Protein expression was induced with Apa, IPTG and arabinose, in addition, calcium was added to stabilise exposed eGFP-HlyA on the cell surface. After four hours of protein expression cells were harvested, membranes isolated and OD_{600} equivalents were analysed by Western blot and an anti-HlyA antibody (Figure 8).

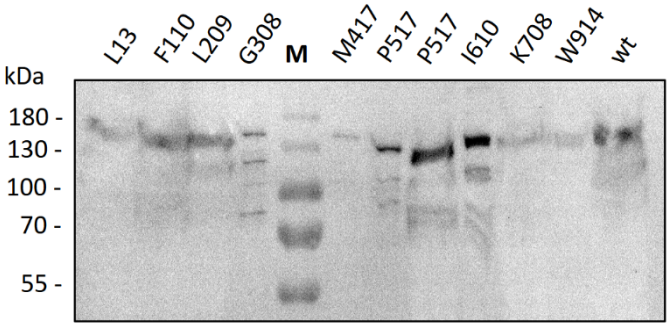

Figure 8. Western blot analysis (anti-HlyA) of *E. coli* membranes after expression of eGFP-HlyA* variants containing the unnatural amino acid Apa. *E. coli* cells expressed the T1SS and variants of eGFP-HlyA* (140.0 kDa) in presence of Apa. The isolated membranes of the *E. coli* cells were analysed by Western blot using polyclonal antisera (anti-HlyA). eGFP-HlyA* has a theoretical mass of 140.0 kDa. M, protein weight standard.

The fusion protein eGFP-HlyA* has a calculated molecular mass of 140.0 kDa correlating to the most prominent signals of each analysed sample. For HlyA-L209*, HlyA-P517* and HlyA-I610* an additional band correlates to HlyA* without eGFP fused to the N-terminus with a molecular mass of 110.1 kDa. For HlyA-G308*, HlyA*-P517*, HlyA-I610* and HlyA-K708* a third band correlates to HlyA without the secretion signal (103.1 kDa). In the case of HlyA-G308* a fourth band occurred with a size of about 80 kDa. The reason for this protein fragmentation is not clear. We also analysed the supernatants of the bacterial cultures by Western blot and an anti-HlyA antibody and we detected no secreted eGFP-HlyA* (data not shown). The eGFP-HlyA fusion protein has already been established as a tool to stall the T1SS (Lenders *et al.*, 2015). Our Western blot confirmed that also significant amounts of eGFP-HlyA* (Apa) can be found within the bacterial membrane. Therefore, we suggest that the unnatural amino acid does not prohibit the fusion proteins to stall the T1SS. However, the signal intensities on the Western blot varied with the mutated position.

Varying conditions to enhance the cross-link of eGFP-HlyA*Apa with the T1SS in vivo

For the initial experimental setup to activate the cross-linker Apa, we used the same cultivation conditions of *E. coli* as described before. After four hours of protein expression the bacterial culture was cooled on ice and irradiated for 60 minutes with UV light. In parallel another aliquot of the sample remained untreated to allow us to assign any effect to the UV irradiation treatment. OD_{600} equivalents

of whole cells were diluted in SDS sample buffer and analysed by Western blot and anti-HlyA antibody (Figure 9 A).

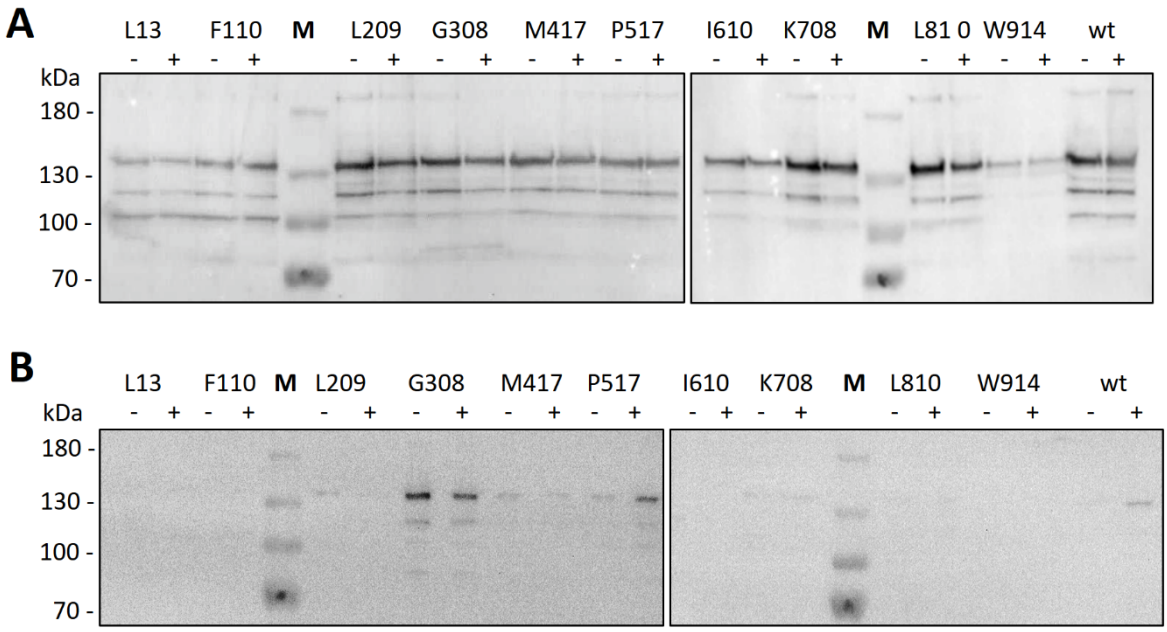

Figure 9. Detection of eGFP-HlyA* (Apa) *in vivo* photo-cross-linking products by Western blot analysis (anti-HlyA). (A) *E. coli* cells containing variants of the fusion protein eGFP-HlyA* (Apa), stalling the T1SS, were irradiated for 60 minutes with UV light (+) or remained untreated (-). (B) *E. coli* cells were irradiated as described before (+) or remained untreated (-). Afterwards the cell membranes were isolated from the cell debris. Samples containing (A) *E. coli* cells or (B) cell membranes were analysed by Western blot using polyclonal antisera (anti-HlyA). eGFP-HlyA* has a theoretical mass of 140.0 kDa. M, protein weight standard.

The observed protein band pattern was according to Figure 8. The fusion protein eGFP-HlyA* has a calculated molecular mass of 140.0 kDa correlating to the most prominent signals of most analysed samples. An additional band correlates to HlyA* without eGFP fused to the N-terminus (110.1 kDa). A third band correlates to HlyA without the secretion signal (103.1 kDa). Furthermore, we observed signals correlating to proteins with a higher molecular mass than eGFP-HlyA* but these species occurred independent of the UV irradiation. We suggested that the abundance of any visible effects upon UV light occurs due to a very low population of cross-linked protein species. Therefore, we repeated the same experiment and in order to increase the concentration of cross-linked proteins we isolated the cell membranes afterwards. The subsequent analysis via Western blot revealed the absence of HlyA in most samples (Figure 9B). The samples of the fusion proteins eGFP-HlyA-L209*, eGFP-HlyA-G308*, eGFP-HlyA-M417*, eGFP-HlyA-P517*, eGFP-HlyA-K708* and eGFP-HlyA contained a most prominent band correlating to a protein size of about 140 kDa. The variants eGFP-HlyA-G308* and eGFP-HlyA-P517* also showed three additional bands correlating to smaller proteins and were described above.

In vitro cross-linking of isolated HlyA* and the solubilised ABC transporter HlyB

Here, we also investigated an *in vitro* approach to cross-link purified HlyA* and solubilised HlyB. Elsewhere we already demonstrated distinct interactions of a shorter HlyA variant (HlyA2) with HlyB by cross-linking experiments *in vitro* and subsequent mass spectrometric analysis (Reimann *et al.*, 2016). Thereby we found that position K945 of HlyA is closely located to the HlyB transmembrane domain. An additional one-time cross-link experiment also pointed to position K823 of HlyA to somehow interact with HlyB (not published).

Both, HlyA-K823* and HlyA-K945* were incorporated with one of the unnatural amino acids Apa or Bpa, respectively. First, we investigated whether the incorporation of these unnatural amino acids influenced the HlyA secretion competency. *E. coli* BL21 (DE3) cells were transformed with three plasmids that encode (i) the amber suppression system (pEVOL-Bpa/Apa), (ii) the T1SS (pSU-HlyBD) and (iii) a HlyA* amber mutant (pSU-HlyA*) encoding for the mutants HlyA-K823* and HlyA-K945*. Each mutant was incubated in parallel in presence or absence of the unnatural amino acids Bpa or Apa, respectively, and the supernatants (OD_{600} equivalents) of the samples were analysed after 4 hours of expression with an SDS/PAGE (Figure 10).

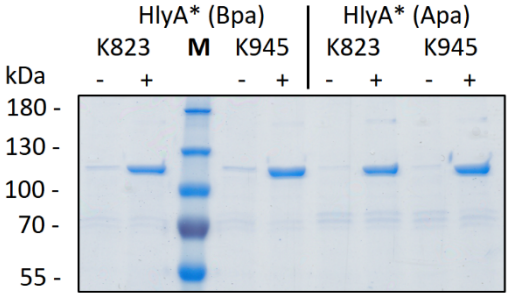

Figure 10. SDS/PAGE analysis of secreted HlyA-K823* and HlyA-K945* expressed in presence (+) or absence (-) of the unnatural amino acids Apa or Bpa, respectively. In two equal bacterial cultures the protein expression of the T1SS and the HlyA* variants were induced and only one culture was supplemented with the unnatural amino acid Apa. After four hours of protein expression the culture supernatant was analysed for secreted HlyA* via an SDS/PAGE and stained with CBB. The variants of HlyA* have a theoretical mass of 110.1 kDa. M, protein weight standard.

We found that both tested HlyA* amber variants (110.1 kDa) were secreted into the cell supernatant, if the corresponding unnatural amino acids were added to the media. However, low amounts of HlyA-K823* and HlyA-K945* were also secreted in the absence of Bpa and Apa. Minor concentrations of non-identified proteins occurred correlating to protein molecular masses of about 70 kDa and 150 kDa.

Expression and purification of HlyA* variants

To obtain purified HlyA* for *in vitro* cross-linking experiments the variants HlyA-K823* and HlyA-K945* were expressed and secreted to the *E. coli* supernatant as described before. Secreted HlyA* protein accumulated in the media supernatant and was subsequently separated from bacterial cells by centrifugation. Protein contaminants were separated from the target protein by size exclusion chromatography (SEC) (Figure 11 A) and subsequently analysed by SDS/PAGE (Figure 11 B).

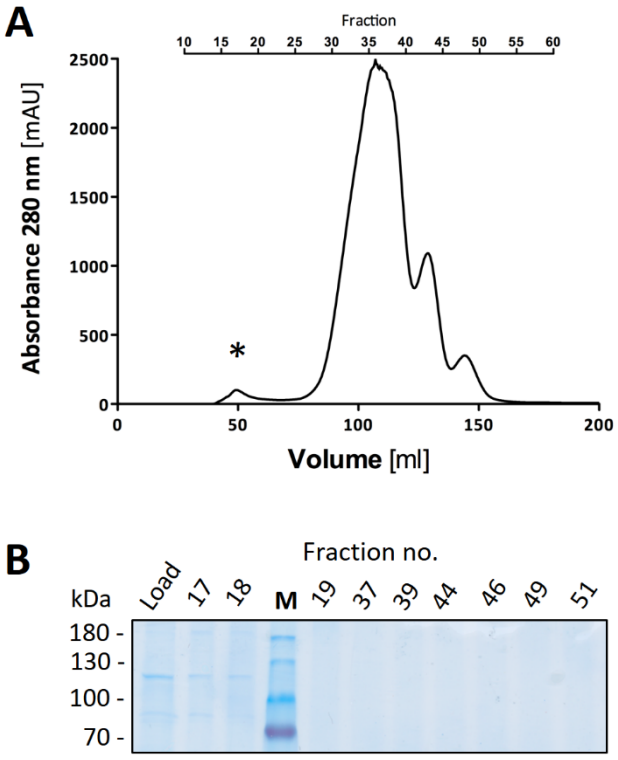

Figure 11. SEC profile and SDS/PAGE analysis of HlyA-K823*Bpa. (A) *E. coli* culture supernatant containing HlyA-K823* was concentrated using an Amicon Ultra centrifugal filter unit and 2 ml was loaded onto a HiLoad 16/600 Superdex 200 pg column. (*) HlyA-K823*Bpa was eluted from the column at about 50 ml. mAU, mili-absorbance units. (B) Samples of HlyA-K823* were analysed by SDS/PAGE and stained with CBB. HlyA-K823* has a theoretical mass of 110.1 kDa. Load, concentrated protein loaded onto the column. M, protein weight standard.

The purification protocol did neither vary depending on the mutated position of HlyA nor on the used unnatural amino acid. Figure 11 is representative for the purification of both HlyA* variants with both unnatural amino acids. The target protein has a molecular mass of 110.1 kDa and eluted from the column in the range of 50 ml. The purification via a SEC separated high amounts of contaminants that were detectable in the UV chromatogram but not by the SDS/PAGE. We suggest that these UV sensitive species are peptides in media supernatant (e.g. yeast extract). Obtained HlyA* protein was concentrated and subsequently unfolded with high concentrations of Urea. The buffer was exchanged to HEPES and stored at 4 °C.

In vitro cross-linking of HlyB and HlyA-K823* / HlyA-K945*

It was already demonstrated elsewhere that HlyB ATPase activity varies depending on the concentration of unfolded HlyA1 *in vitro*, a 24.7 kDa C-terminal part of HlyA (Reimann *et al.*, 2016). Here, a 1:1 molar ratio of HlyB and HlyA1 resulted in maximal inhibition of HlyB ATPase velocity, while a 1:15 molar ratio stimulated HlyB ATPase velocity maximally. We expect crucial protein-protein interactions at these molar ratios that shall be investigated with photoactivatable cross-linker and mass spectrometry. We reproduced these experimental conditions and the ATPase assay was started by the addition of Mg^{2+}. After 30 minutes of incubation the reaction was stopped by an UV irradiation for up to 30 minutes (Bpa) or up to 90 minutes (Apa), respectively. The resulting samples were analysed with by SDS/PAGE and Western blot using anti-HlyA antibodies. Figure 12 summarises the results of both HlyA* mutants and both used unnatural amino acid. We found an UV induced signal in the case of HlyA-K823* (Bpa) and HlyB with a molar ratio of 1:1 (Figure 12 A). The signal occurred upon 10 minutes UV irradiation but disappeared at longer exposures. The experimental setups with both, HlyA-K823* (Apa) and HlyA-K823* (Bpa) in presence of HlyB revealed no further UV induced Western blot signals (Figure 12 A). The analysed cross-linking studies of HlyA-K945* (Bpa) in presence of HlyB also showed no additional bands (Figure 12 B). HlyA-K945* (Apa) and HlyB with a molar ratio of 1:15 resulted in the formation of a UV induced protein species detectable by the Western blot (Figure 12 B). The additional signal corresponds to a protein size of about 190 kDa and correlates to the theoretical molecular mass of a HlyB / HlyA* cross-link product. The sample was analysed again by Western blot and an anti-HlyB antibody. Clear signals corresponding to a molecular mass of 70 kDa were visible, however, no signals could be detected belonging to the latter found protein species with a shifted weight of about 190 kDa (supplementary Figure S1). In parallel we used mass spectrometry to analyse the HlyA*-K945 (Apa) sample protein band correlating to a size of 190 kDa, after 90 minutes of UV irradiation. The proteins HlyA and HlyB were detectable in the sample, however, the unnatural amino acid Apa or a cross-link product were abundant.

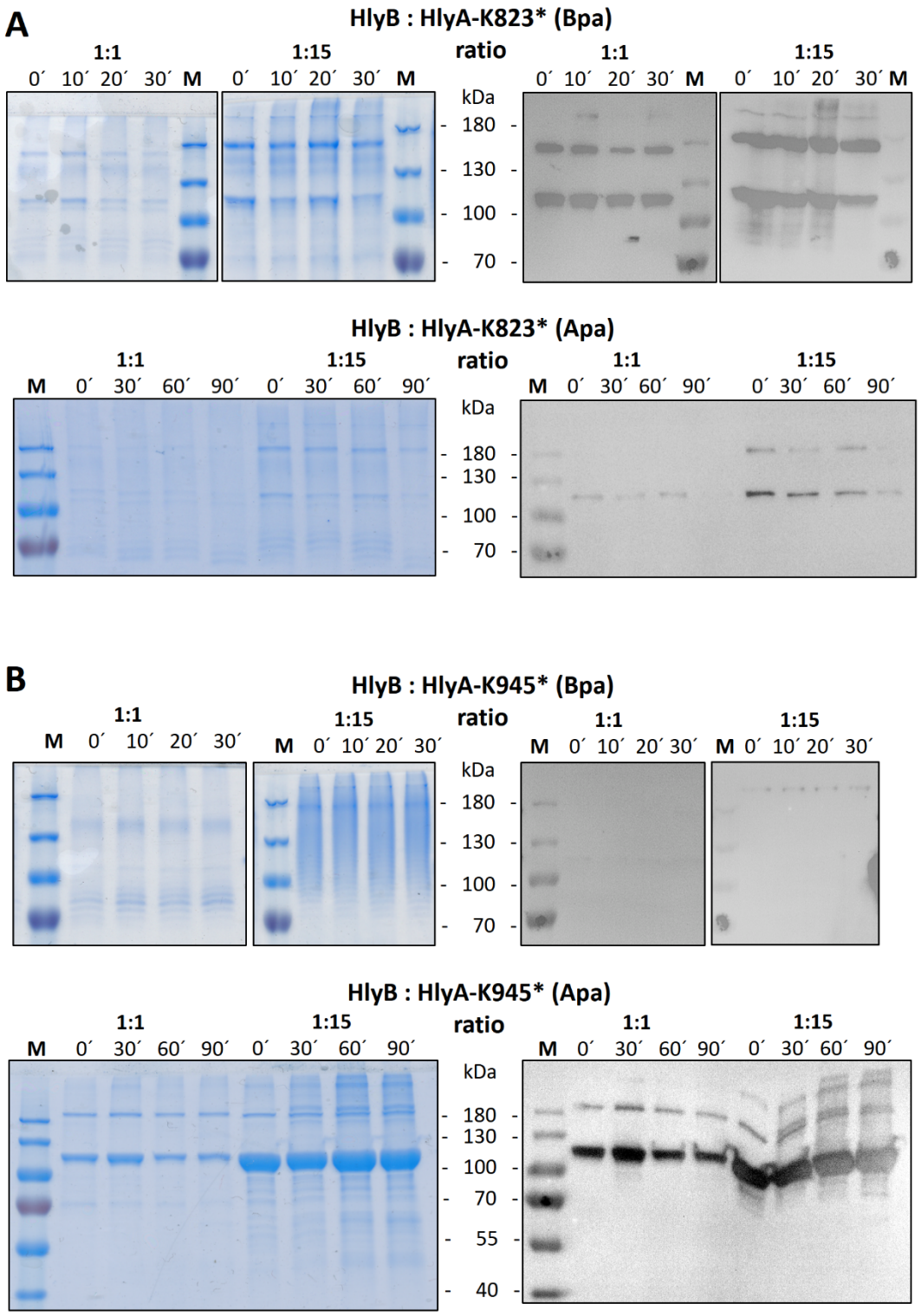

Figure 12. Detection of purified HlyA* (Bpa/Apa) in vitro photo-cross-linking products depending on the molar ratio of HlyB and HlyA*. (A) Purified HlyA-K823* or (B) HlyA-K945* with incorporated Apa or Bpa, respectively, were added to an ATPase assay with the purified T1SS ABC transporter HlyB. The protein molar concentration ratios of HlyB and HlyA* varied from 1:1 or 1:15 µM. After 30 minutes of incubation the reaction was stopped by UV irradiation for up 90 minutes (Apa) or 30 minute (Bpa), respectively. Samples were analysed by SDS/PAGE and stained with CBB or by Western blot using polyclonal antisera (anti-HlyA). eGFP-HlyA* has a theoretical mass of 140.0 kDa and HlyB has a theoretical mass of 82.2 kDa including the decahistidine tag. M, protein weight standard.

Discussion

Here we describe *in vivo* and *in vitro* cross-linking studies of HlyA and its cognate T1SS. Cellular processes are regulated by protein-protein interactions and cross-linking has already been used to prove even weak and transient contacts (Ieva *et al.*, 2009; Panahandeh *et al.*, 2008). We found that the secretion process of the transport substrate HlyA is not affected by the incorporation of an unnatural amino acid. This means that also in the presence of the unnatural amino acid the translation process fully proceeds until the C-terminal secretion signal is synthesized. Only then, the transport substrate is secreted, as the secretion signal is necessary and sufficient for the translocation of the unfolded HlyA (Jarchau *et al.*, 1994; Zhang *et al.*, 1995). These results thereby confirm the successful incorporation of the unnatural amino acid and the substrate remains its secretion competency. Interestingly we also noticed a variation of the amount of secreted protein in presence of the unnatural amino acids. This effect was independent on the cross-linker, therefore, we suppose either the substituted position or the substituted amino acid to be responsible for this behaviour. The substitution of position I610 to an unnatural amino acid decreased the secretion relatively to the lowest amount. However, this part of HlyA contains no elements that are crucial for secretion competency as known so far. Nevertheless, the protein has to remain in an unfolded state, which may be influenced by this point mutation. Apart from the HlyA* secretion in presence of the unnatural amino acids we also found that the substrate was secreted in relatively low amounts even in the absence of the unnatural amino acids. We suppose the translocation machinery at least in some amounts ‘skips’ the codon or the ‘wrong’ tRNA binds. Anyway the C-terminal secretion signal is synthesized and the peptide is secreted.

We used the fusion protein eGFP-HlyA for cross-linking experiments and successfully incorporated the unnatural amino acids Bpa and Apa at ten different positions. Recently it was shown the fusion protein eGFP-HlyA stalls the T1SS and the HlyA C-terminus is secreted first while the N-terminal eGFP remains in the cytoplasm (Lenders *et al.*, 2015). We confirmed that this fusion protein is located in the bacterial membrane, also with incorporated unnatural amino acids. However, the subsequent irradiation of bacterial cells did not result in any detectable cross-link products, whilst the exposure time did not extend 30 minutes. In comparable experiments, Bpa containing samples were already sufficiently irradiated by 7 minutes (Bpa) (Ieva *et al.*, 2009), or 20 minutes (Bpa) (Panahandeh *et al.*, 2008). Deviant from our protocol Ieva *et al.* collected proteins by trichloroacetic acid (TCA) precipitation or Alami *et al.* used immunoprecipitation to concentrate and purify cross-linked products subsequently (Alami *et al.*, 2003; Ieva *et al.*, 2011). In contrast we increased the sample concentration of cross-linked products by isolating the bacterial cell membranes. This step seems not sufficient to detect any cross-linked proteins by Western blot analysis. Furthermore, the usage of an aryl azide and an irradiation for

60 minutes at 254 nm resulted in the absence of most Western blot signals. This may occur due to subsequent protein damage. The dominant chromophores at 254 nm are tryptophan and tyrosine as well as with small contribution the peptide bond itself. Here, a significant decrease of irradiation time could improve the overall yield (Shao *et al.*, 2015). In general, our attempts to prevent the bacterial culture from an unintentional and premature activation of the cross-link reaction by spare UV light did not improve the subsequent detection by Western blot analysis. A preceding cell lysis to the UV irradiation did also not improve the signal intensity of UV induced signals.

We also studied cross-linking experiments *in vitro* and in contrast to our *in vivo* assays we obtained UV induced protein species with Bpa as well as Apa. Noticeable the signals intensities of UV induced signals correlated with the irradiation time and did not decrease with extending exposures. However, the detection of HlyB within the cross-linked bands was not possible. Taken together additional work is required to increase the yield of protein-protein cross-link products and their purity, so that the system can be used in interaction studies.

This study based upon the aaRS/tRNA pair encoded on the vector pEVOL, as described in Young *et al.* (2010). Notably the same system did also not result in cross-linked products in the laboratories of Prof. Samuel Wagner (University of Tübingen, personal communication).

Overall we showed the successful incorporation of Bpa and Apa to HlyA and the fusion protein eGFP-HlyA. The presence of these unnatural amino acids does not influence the secretion competency of transport substrate and it can be purified from bacterial supernatant for further *in vitro* assays. A comparison of *in vitro* and *in vivo* cross-linking trials demonstrate the obstacles of this technique but we also revealed possible improvements.

Acknowledgement

We thank all members of the Institute of Biochemistry and Samuel Wagner for valuable discussions. We thank Diana Kleinschrodt and Iris Fey, Protein Production Facility, for technical support. We gratefully acknowledge support (and training) from the International NRW Research School BioStruct, granted by the Ministry of Innovation, Science and Research of the State North Rhine-Westphalia, the Heinrich-Heine-University Düsseldorf and the Entrepreneur Foundation at the Heinrich-Heine-University of Düsseldorf. This work was supported in part by the DFG (CRC 1208, project A01 to L.S.).

Literature

Alami, M., Luke, I., Deitermann, S., Eisner, G., Koch, H.G., Brunner, J., and Muller, M. (2003). Differential interactions between a twin-arginine signal peptide and its translocase in *Escherichia coli*. Mol Cell *12*, 937-946.

Bakkes, P.J., Jenewein, S., Smits, S.H., Holland, I.B., and Schmitt, L. (2010). The rate of folding dictates substrate secretion by the *Escherichia coli* hemolysin type 1 secretion system. J Biol Chem *285*, 40573-40580.

Balakrishnan, L., Hughes, C., and Koronakis, V. (2001). Substrate-triggered recruitment of the TolC channel-tunnel during type I export of hemolysin by *Escherichia coli*. J Mol Biol *313*, 501-510.

Benabdelhak, H., Kiontke, S., Horn, C., Ernst, R., Blight, M.A., Holland, I.B., and Schmitt, L. (2003). A Specific Interaction Between the NBD of the ABC-transporter HlyB and a C-Terminal Fragment of its Transport Substrate Haemolysin A. Journal of Molecular Biology *327*, 1169-1179.

Chabeaud, P., de Groot, A., Bitter, W., Tommassen, J., Heulin, T., and Achouak, W. (2001). Phase-variable expression of an operon encoding extracellular alkaline protease, a serine protease homolog, and lipase in *Pseudomonas brassicacearum*. J Bacteriol *183*, 2117-2120.

Chen, S., Schultz, P.G., and Brock, A. (2007). An improved system for the generation and analysis of mutant proteins containing unnatural amino acids in *Saccharomyces cerevisiae*. J Mol Biol *371*, 112-122.

Chenal, A., Karst, J.C., Sotomayor Perez, A.C., Wozniak, A.K., Baron, B., England, P., and Ladant, D. (2010). Calcium-induced folding and stabilization of the intrinsically disordered RTX domain of the CyaA toxin. Biophys J *99*, 3744-3753.

Chin, J.W., Martin, A.B., King, D.S., Wang, L., and Schultz, P.G. (2002). Addition of a photocrosslinking amino acid to the genetic code of *Escherichia coli*. Proc Natl Acad Sci U S A *99*, 11020-11024.

Delepelaire, P. (2004). Type I secretion in gram-negative bacteria. Biochim Biophys Acta *1694*, 149-161.

Dorman, G., and Prestwich, G.D. (1994). Benzophenone photophores in biochemistry. Biochemistry *33*, 5661-5673.

Ghigo, J.M., and Wandersman, C. (1994). A carboxyl-terminal four-amino acid motif is required for secretion of the metalloprotease PrtG through the *Erwinia chrysanthemi* protease secretion pathway. J Biol Chem *269*, 8979-8985.

Gilson, L., Mahanty, H.K., and Kolter, R. (1990). Genetic analysis of an MDR-like export system: the secretion of colicin V. EMBO J *9*, 3875-3884.

Goebel, W., and Hedgpeth, J. (1982). Cloning and functional characterization of the plasmid-encoded hemolysin determinant of *Escherichia coli*. J Bacteriol *151*, 1290-1298.

Hinsa, S.M., Espinosa-Urgel, M., Ramos, J.L., and O'Toole, G.A. (2003). Transition from reversible to irreversible attachment during biofilm formation by *Pseudomonas fluorescens* WCS365 requires an ABC transporter and a large secreted protein. Mol Microbiol *49*, 905-918.

Holland, I.B., Schmitt, L., and Young, J. (2005). Type 1 protein secretion in bacteria, the ABC-transporter dependent pathway (review). Mol Membr Biol *22*, 29-39.

Ieva, R., and Bernstein, H.D. (2009). Interaction of an autotransporter passenger domain with BamA during its translocation across the bacterial outer membrane. Proc Natl Acad Sci U S A *106*, 19120-19125.

Ieva, R., Tian, P., Peterson, J.H., and Bernstein, H.D. (2011). Sequential and spatially restricted interactions of assembly factors with an autotransporter beta domain. Proc Natl Acad Sci U S A *108*, E383-391.

Jarchau, T., Chakraborty, T., Garcia, F., and Goebel, W. (1994). Selection for transport competence of C-terminal polypeptides derived from *Escherichia coli* hemolysin: the shortest peptide capable of autonomous HlyB/HlyD-dependent secretion comprises the C-terminal 62 amino acids of HlyA. Mol Gen Genet *245*, 53-60.

Jumpertz, T., Chervaux, C., Racher, K., Zouhair, M., Blight, M.A., Holland, I.B., and Schmitt, L. (2010). Mutations affecting the extreme C terminus of *Escherichia coli* haemolysin A reduce haemolytic activity by altering the folding of the toxin. Microbiology *156*, 2495-2505.

Kenny, B., Chervaux, C., and Holland, I.B. (1994). Evidence that residues -15 to -46 of the haemolysin secretion signal are involved in early steps in secretion, leading to recognition of the translocator. Mol Microbiol *11*, 99-109.

Kenny, B., Taylor, S., and Holland, I.B. (1992). Identification of individual amino acids required for secretion within the haemolysin (HlyA) C-terminal targeting region. Mol Microbiol *6*, 1477-1489.

Lenders, M.H., Weidtkamp-Peters, S., Kleinschrodt, D., Jaeger, K.E., Smits, S.H., and Schmitt, L. (2015). Directionality of substrate translocation of the hemolysin A Type I secretion system. Sci Rep *5*, 12470.

Letoffe, S., Delepelaire, P., and Wandersman, C. (1996). Protein secretion in Gram-negative bacteria: assembly of the three components of ABC protein-mediated exporters is ordered and promoted by substrate binding. EMBO J *15*, 5804-5811.

Linhartova, I., Bumba, L., Masin, J., Basler, M., Osicka, R., Kamanova, J., Prochazkova, K., Adkins, I., Hejnova-Holubova, J., Sadilkova, L.*, et al.* (2010). RTX proteins: a highly diverse family secreted by a common mechanism. FEMS Microbiol Rev *34*, 1076-1112.

Liu, W., Brock, A., Chen, S., Chen, S., and Schultz, P.G. (2007). Genetic incorporation of unnatural amino acids into proteins in mammalian cells. Nat Methods *4*, 239-244.

Lo, R.Y., Strathdee, C.A., and Shewen, P.E. (1987). Nucleotide sequence of the leukotoxin genes of *Pasteurella haemolytica* A1. Infect Immun *55*, 1987-1996.

Mackman, N., Baker, K., Gray, L., Haigh, R., Nicaud, J.M., and Holland, I.B. (1987). Release of a chimeric protein into the medium from *Escherichia coli* using the C-terminal secretion signal of haemolysin. EMBO J *6*, 2835-2841.

Mackman, N., Nicaud, J.M., Gray, L., and Holland, I.B. (1986). Secretion of haemolysin by *Escherichia coli*. Curr Top Microbiol Immunol *125*, 159-181.

Maurer, C., Panahandeh, S., Jungkamp, A.C., Moser, M., and Muller, M. (2010). TatB functions as an oligomeric binding site for folded Tat precursor proteins. Mol Biol Cell *21*, 4151-4161.

Panahandeh, S., Maurer, C., Moser, M., DeLisa, M.P., and Muller, M. (2008). Following the path of a twin-arginine precursor along the TatABC translocase of *Escherichia coli*. J Biol Chem *283*, 33267-33275.

Reimann, S., Poschmann, G., Kanonenberg, K., Stuhler, K., Smits, S.H., and Schmitt, L. (2016). Interdomain regulation of the ATPase activity of the ABC transporter haemolysin B from *Escherichia coli*. Biochem J *473*, 2471-2483.

Sakamoto, K., Hayashi, A., Sakamoto, A., Kiga, D., Nakayama, H., Soma, A., Kobayashi, T., Kitabatake, M., Takio, K., Saito, K.*, et al.* (2002). Site-specific incorporation of an unnatural amino acid into proteins in mammalian cells. Nucleic Acids Res *30*, 4692-4699.

Sato, S., Mimasu, S., Sato, A., Hino, N., Sakamoto, K., Umehara, T., and Yokoyama, S. (2011). Crystallographic study of a site-specifically cross-linked protein complex with a genetically incorporated photoreactive amino acid. Biochemistry *50*, 250-257.

Shao, N., Singh, N.S., Slade, S.E., Jones, A.M., and Balasubramanian, M.K. (2015). Site Specific Genetic Incorporation of Azidophenylalanine in *Schizosaccharomyces pombe*. Sci Rep *5*, 17196.

Simpson, B.W., Owens, T.W., Orabella, M.J., Davis, R.M., May, J.M., Trauger, S.A., Kahne, D., and Ruiz, N. (2016). Identification of Residues in the Lipopolysaccharide ABC Transporter That Coordinate ATPase Activity with Extractor Function. MBio *7*.

Thanabalu, T., Koronakis, E., Hughes, C., and Koronakis, V. (1998). Substrate-induced assembly of a contiguous channel for protein export from *E.coli*: reversible bridging of an inner-membrane translocase to an outer membrane exit pore. EMBO J *17*, 6487-6496.

Thomas, S., Smits, S.H., and Schmitt, L. (2014). A simple in vitro acylation assay based on optimized HlyA and HlyC purification. Anal Biochem *464*, 17-23.

Wang, L., J., M.T., Liu, D.R., and Schultz, P.G. (2000). A new functional suppressor tRNA/aminoacyl-tRNA synthetase pair for the in vivo incorporation of unnatural amino acids into proteins. Journal of the American Chemical Society *122*, 5010-5011.

Wang, L., and Schultz, P.G. (2001). A general approach for the generation of orthogonal tRNAs. Chem Biol *8*, 883-890.

Wang, W., Takimoto, J.K., Louie, G.V., Baiga, T.J., Noel, J.P., Lee, K.F., Slesinger, P.A., and Wang, L. (2007). Genetically encoding unnatural amino acids for cellular and neuronal studies. Nat Neurosci *10*, 1063-1072.

Young, T.S., Ahmad, I., Brock, A., and Schultz, P.G. (2009). Expanding the genetic repertoire of the methylotrophic yeast *Pichia pastoris*. Biochemistry *48*, 2643-2653.

Young, T.S., Ahmad, I., Yin, J.A., and Schultz, P.G. (2010). An enhanced system for unnatural amino acid mutagenesis in *E. coli*. J Mol Biol *395*, 361-374.

Zhang, F., Sheps, J.A., and Ling, V. (1993). Complementation of transport-deficient mutants of *Escherichia coli* alpha-hemolysin by second-site mutations in the transporter hemolysin B. J Biol Chem *268*, 19889-19895.

Zhang, F., Yin, Y., Arrowsmith, C.H., and Ling, V. (1995). Secretion and circular dichroism analysis of the C-terminal signal peptides of HlyA and LktA. Biochemistry *34*, 4193-4201.

Zhang, Z., Smith, B.A., Wang, L., Brock, A., Cho, C., and Schultz, P.G. (2003). A new strategy for the site-specific modification of proteins in vivo. Biochemistry *42*, 6735-6746.

Zverev, V.V., and Khmel, I.A. (1985). The nucleotide sequences of the replication origins of plasmids ColA and ColD. Plasmid *14*, 192-199.

Supplementary information

Amber codon mutagenesis as a tool for analysing the haemolysin A type 1 secretion system from *Escherichia coli*

Sven Reimann, Julia Zaschke-Kriesche, Diana Kleinschrodt, Sander H.J. Smits and Lutz Schmitt [1]

Institute of Biochemistry, Heinrich-Heine-University Düsseldorf, Universitätsstraße 1, 40225 Düsseldorf, Germany

[1] To whom correspondence should be addressed: Institute of Biochemistry, Heinrich-Heine-University Düsseldorf, Universitätsstraße 1, 40225 Düsseldorf, Germany. Tel.: +49-211-81-10773; Fax: +49-211-81-15310; E-mail: Lutz.Schmitt@hhu.de

Supplementary information comprises:

Supplementary Figure S1

Supplementary Table S1

Supplementary Table S2

Literature (supplementary)

Supplementary Figure S1

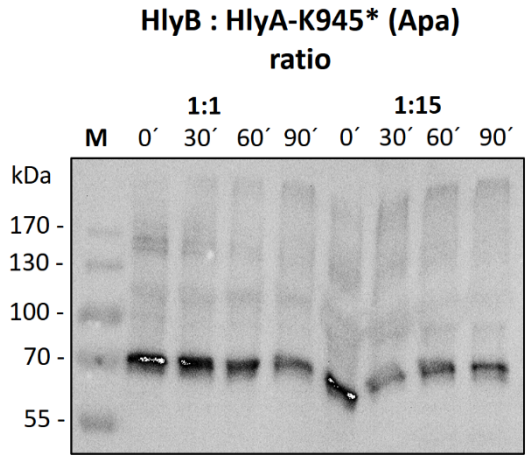

Supplementary Figure S1. Detection of purified HlyA* (Bpa/Apa) *in vitro* photo-cross-linking products depending on the molar ratio of HlyB and HlyA*. Purified HlyA-K945* with incorporated Apa was added to an ATPase assay with the purified T1SS ABC transporter HlyB. The protein molar concentration ratios of HlyB and HlyA* varied from 1:1 or 1:15 µM. After 30 minutes of incubation the reaction was stopped by UV irradiation for up 90 minutes (Apa). Samples were analysed by Western blot using polyclonal antisera (anti-HlyB). eGFP-HlyA* has a theoretical mass of 140.0 kDa and HlyB has a theoretical mass of 82.2 kDa including the decahistidine tag.

Supplementary Table S1

Supplementary Table S1. **Primer for AMBER insertion with QuikChange PCR.**

Mutated position in HlyA	Primer sequences (5'→3')
L13	CAA ATT AAA AGC ACA TAG CAG TCT GCA AAG CAA TC
	GA TTG CTT TGC AGA CTG CTA TGT GCT TTT AAT TTG
F110	GGG GAG TGA CTA TCT AGG CAC CAC AAT TAG AC
	GT CTA ATT GTG GTG CCT AGA TAG TCA CTC CCC
L209	GTT AAC TCA TTT TCT CAA CAA TAG AAT ACT CTG GGA AGT GTA TTA
	TAA TAC ACT TCC CAG AGT ATT CTA TTG TTG AGA AAA TGA GTT AAC
G308	CTG CTG CTG CTG CCT AGT TAA TTGCTT CTG C
	G CAG AAG CAA TTA ACT AGG CAG CAG CAG CAG
M417	GCA ACA TGT TCA AAC TAT GCC TGC TTT GAA G
	C TTC AAA GCA GGC ATA GTT TGA ACA TGT TGC
P517	CGT CTG GAG AAA AAA TAG GAT GAA TTC CAG AAG
	CTT CTG GAA TTC ATC CTA TTT TTT CTC CAG ACG
I610	CCA GTA TCG GGA ATA GCG TAT TGA GTC ACA CC
	GG TGT GAC TCA ATA CGC TAT TCC CGA TAC TGG
K708	GTT ATG AAT TCA CTC ATA TCA ATG GTT AGA ATT TAA CAG AGA CTG
	CAG TCT CTG TTA AAT TCT AAC CAT TGA TAT GAG TGA ATT CAT AAC
L810	GGT TCA GGG AAA TTC TTA GGC AAA AAA TGT ATT ATT CGG
	CCG AAT AAT ACA TTT TTT GCC TAA GAA TTT CCC TGA ACC
W914	GTA TTA CAT TCA GGA ACT AGT TTG AAA AAG AGT CAG
	CTG ACT CTT TTT CAA ACT AGT TCC TGA ATG TAA TAC
K823	GGA AAA GGT AAT GAC TAG CTG TAC GGC
	GCC GTA CAG CTA GTC ATT ACC TTT TCC
K945	CCT GAT TCC CTT AAA TAG GCA CTT GAG TAT C
	G ATA CTC AAG TGC CTA TTT AAG GGA ATC AGG

Supplementary Table S2

Supplementary Table S2. Plasmids used in this study.

Name	Description	Reference
pK184	Plasmid encoding *hlyB* and *hlyD*	(Bakkes *et al.*, 2010)
pCOLADuet-1	Plasmid used to obtain the origin of replication ColA	(Zverev *et al.*, 1985)
pEVOL-Apa	Plasmid encoding the orthogonal suppressor tRNA/aminoacyl-tRNA synthetase pair for the unnatural amino acid *p*-azidophenylalanine	(Young *et al.*, 2010)
pEVOL-Bpa	Plasmid encoding the orthogonal suppressor tRNA/aminoacyl-tRNA synthetase pair for the unnatural amino acid *p*-benzoyl-L-phenylalanine	(Young *et al.*, 2010)
pEVOL-Apa-ColA	Plasmid encoding the orthogonal suppressor tRNA/aminoacyl-tRNA synthetase pair for the unnatural amino acid *p*-azidophenylalanine with ColA	This study
pEVOL-Bpa-ColA	Plasmid encoding the orthogonal suppressor tRNA/aminoacyl-tRNA synthetase pair for the unnatural amino acid *p*-benzoyl-L-phenylalanine with ColA	This study
pSU2726-HlyA	Plasmid encoding *hlyA*	(Bakkes *et al.*, 2010)
pSU2726-HlyA-L13	Plasmid encoding *hlyA-L13X*	This study
pSU2726-HlyA-F110	Plasmid encoding *hlyA-L110X*	This study
pSU2726-HlyA-L209	Plasmid encoding *hlyA-L209X*	This study
pSU2726-HlyA-G308	Plasmid encoding *hlyA-L308X*	This study
pSU2726-HlyA-M417	Plasmid encoding *hlyA-L417X*	This study
pSU2726-HlyA-P517	Plasmid encoding *hlyA-L517X*	This study
pSU2726-HlyA-I610	Plasmid encoding *hlyA-L610X*	This study

pSU2726-HlyA-K708	Plasmid encoding *hlyA-L708X*	This study
pSU2726-HlyA-L810	Plasmid encoding *hlyA-L810X*	This study
pSU2726-HlyA-K823	Plasmid encoding *hlyA-K823X*	This study
pSU2726-HlyA-W914	Plasmid encoding *hlyA-L914X*	This study
pSU2726-HlyA-K945	Plasmid encoding *hlyA-K945X*	This study
pSOI-eGFP-HlyA	Plasmid encoding *eGFP-HlyA*	(Lenders *et al.*, 2015)
pSOI-eGFP-HlyA-L13	Plasmid encoding *eGFP-HlyA-L13X*	This study
pSOI-eGFP-HlyA-F110	Plasmid encoding *eGFP-HlyA-L110X*	This study
pSOI-eGFP-HlyA-L209	Plasmid encoding *eGFP-HlyA-L209X*	This study
pSOI-eGFP-HlyA-G308	Plasmid encoding *eGFP-HlyA-L308X*	This study
pSOI-eGFP-HlyA-M417	Plasmid encoding *eGFP-HlyA-L417X*	This study
pSOI-eGFP-HlyA-P517	Plasmid encoding *eGFP-HlyA-L517X*	This study
pSOI-eGFP-HlyA-I610	Plasmid encoding *eGFP-HlyA-L610X*	This study
pSOI-eGFP-HlyA-K708	Plasmid encoding *eGFP-HlyA-L708X*	This study
pSOI-eGFP-HlyA-L810	Plasmid encoding *eGFP-HlyA-L810X*	This study
pSOI-eGFP-HlyA-K823	Plasmid encoding *eGFP-HlyA-K823X*	This study
pSOI-eGFP-HlyA-W914	Plasmid encoding *eGFP-HlyA-L914X*	This study
pSOI-eGFP-HlyA-K945	Plasmid encoding *eGFP-HlyA-K945X*	This study

Literature (supplementary)

Bakkes, P.J., Jenewein, S., Smits, S.H., Holland, I.B., and Schmitt, L. (2010). The rate of folding dictates substrate secretion by the *Escherichia coli* hemolysin type 1 secretion system. J Biol Chem *285*, 40573-40580.

Lenders, M.H., Weidtkamp-Peters, S., Kleinschrodt, D., Jaeger, K.E., Smits, S.H., and Schmitt, L. (2015). Directionality of substrate translocation of the hemolysin A Type I secretion system. Sci Rep *5*, 12470.

Young, T.S., Ahmad, I., Yin, J.A., and Schultz, P.G. (2010). An enhanced system for unnatural amino acid mutagenesis in *E. coli*. J Mol Biol *395*, 361-374.

Zverev, V.V., and Khmel, I.A. (1985). The nucleotide sequences of the replication origins of plasmids ColA and ColD. Plasmid *14*, 192-199.

3.4. Chapter IV

Title: The RTX Repeats of HlyA interact with the N-terminal Domain of HlyB

Authors: Sven Reimann, Michael H.H. Lenders, Sander H.J. Smits and Lutz Schmitt

Published in: (*to be submitted*)

Proportionate work on this publication: design of different mutants, expression and purification of proteins, ATPase assays, pull-down assays, data analysis, computational analysis, writing of the manuscript

The RTX repeats of HlyA interact with the N-terminal domain of HlyB

Sven Reimann, Michael H.H. Lenders, Sander H.J. Smits and Lutz Schmitt [1]

Institute of Biochemistry, Heinrich-Heine-University Düsseldorf, Universitätsstraße 1, 40225 Düsseldorf, Germany

[1] To whom correspondence should be addressed: Institute of Biochemistry, Heinrich-Heine-University Düsseldorf, Universitätsstraße 1, 40225 Düsseldorf, Germany. Tel.: +49-211-81-10773; Fax: +49-211-81-15310; E-mail: Lutz.Schmitt@hhu.de

Abstract

Type 1 secretion systems (T1SS) mediate the transport of a broad range of substrates across both membranes of Gram-negative bacteria. The haemolysin A T1SS from *Escherichia coli* is well-studied and it is composed of three membrane proteins. The inner membrane proteins are the ABC transporter haemolysin B (HlyB) and the membrane fusion protein haemolysin D (HlyD), while the outer membrane contains the membrane channel TolC. The transported substrate HlyA is a toxin that harbours a RTX domain with canonical nonapeptide, glycine- and aspartate-rich repeats (RTX repeats). These repeats are the hallmark of T1SS substrates and are supposed to bind Ca^{2+} ions with high affinity after being secreted into the exterior, which induces folding of the protein. Studies by Lecher *et al.* (2012) also showed an interaction of the HlyA RTX domain with the C39-peptidase like domain (CLD) of the ABC transporter. This finding suggests a specific interaction of the RTX domain with the ABC transporter prior to the secretion process. Nevertheless, the specific intrinsic function of these RTX repeats remain unknown. Here, we describe the effects of mutations within the RTX repeats of HlyA1, a truncated version of HlyA, on the ATPase modulation of HlyB and HlyBΔCLD *in vitro*. Our results suggest that mutations within the RTX repeats abolish the interaction to the CLD of HlyB. These findings are supported by the loss of HlyB ATPase inhibition in presence of HlyA1 variants that harbour single or multiple mutations within the RTX repeats. Additionally, we found indications for a helical domain close to the most C-terminal RTX repeat that might play a crucial role in the regulation of HlyB ATPase activity. Furthermore, the secretion rate of HlyA1 was quantified *in vivo* and mutations of the RTX domain revealed no significant impact.

Abbreviations

ABC, ATP-binding cassette; CBB, Coomassie Brilliant Blue; CLD; C39-peptidase like domain; HlyA, haemolysin A; HlyB, haemolysin B; HlyD, haemolysin D; IMAC, immobilized metal-ion-affinity chromatography; LMNG, lauryl maltose neopentyl glycol; MFP, membrane-fusion protein; NBD, nucleotide-binding domain; RTX, repeats in toxin; SEC, size-exclusion chromatography; T1SS, Type 1 secretion system; TBS-T, TBS with Tween 20; TMD, transmembrane domain

Keywords

ABC transporter, enzyme kinetics, protein translocation, type I secretion system, HlyA, RTX repeats

Introduction

Gram-negative bacteria transport a broad range of compounds varying in size and function into the extracellular space. Thereby the transport process of proteins is mediated by secretion systems differing greatly in composition. The type 1 secretion system (T1SS) adapts a rather simple architecture of three proteins and the secretion process is independent of the Sec pathway. T1SS substrates include e.g. adenylate cyclases, lipases, surface layer proteins, proteases and toxins (Chabeaud *et al.*, 2001; Chenal *et al.*, 2010; Goebel *et al.*, 1982; Holland *et al.*, 2005; Lo *et al.*, 1987). Despite the vast differences in function they also vary in size from small proteins such as the hemophore HasA (19 kDa) from *Serratia marcescens* up to large proteins such as the adhesion factor LapA (900 kDa) from *Pseudomonas fluorescens* (Gilson *et al.*, 1990; Hinsa *et al.*, 2003; Linhartova *et al.*, 2010). The translocation substrates contain a C-terminal, 50-60 amino acids long and non-cleavable secretion signal that is essential for secretion and initiates the assembly of the translocon (Balakrishnan *et al.*, 2001; Ghigo *et al.*, 1994; Kenny *et al.*, 1994; Kenny *et al.*, 1992; Letoffe *et al.*, 1996; Thanabalu *et al.*, 1998).

One of the best-studied translocation machineries from *Escherichia coli* is the haemolysin A (HlyA) T1SS. It is composed of three proteins spanning both the inner and the outer membrane. The ATP-binding cassette (ABC) transporter haemolysin B (HlyB) and the membrane fusion protein (MFP) haemolysin D (HlyD) are located in the inner membrane. The third protein is localized in the outer membrane and it is called the outer membrane protein (OMP) TolC. The translocation substrate HlyA belongs to the family of repeats in toxins (RTX) proteins, which build the vast majority of T1SS substrates. RTX proteins contain repetitions of glycine- and aspartate-rich sequences, which are located mostly within the carboxy-terminal part of the protein but upstream of the secretion signal. The consensus sequence of these repeats is GGxGxDxUx, where x can be any amino acid and U is a large, hydrophobic amino acid (Linhartova *et al.*, 2010; Welch, 2001). These repeats bind calcium ions with an approximately K_D of 100 µM as demonstrated by folding experiments *in vitro* (Blenner *et al.*, 2010; Chenal *et al.*, 2009; Ostolaza *et al.*, 1991; Thomas *et al.*, 2014a). The average cytosolic concentration of calcium ions in *E. coli* bacteria is approximately 300 nM, while it can reach up to 10 mM in the extracellular space (Jones *et al.*, 1999a). This suggests that proteins bind calcium ions at the outside of the cell to the nonapeptide repeats in a 1:1 stoichiometry and this appears to promote the folding in the extracellular environment (Felmlee *et al.*, 1988; Ludwig *et al.*, 1988; Rhodes *et al.*, 2001; Rose *et al.*, 1995). One calcium ion is bound by a pair of loops, built by the RTX repeat sequences and thereby a β-roll conformation is induced (Baumann *et al.*, 1993). The backbone carbonyl groups of the glycine residues and the side chains of aspartate residues of two different RTX repeats coordinate one calcium ion (Baumann *et al.*, 1993).

The intrinsic function of the RTX repeats of the majority of RTX toxins remain ambiguous. Nevertheless, the hallmark of the substrates of the T1SS are the RTX repeats and thereby indicating that these nonapeptide motifs are somehow involved in the secretion process (Jumpertz *et al.*, 2010; Sotomayor Perez *et al.*, 2010). This effect is also suggested by experiments showing increased yields of secreted proteins containing RTX repeats, when compared to the secretion signal alone or further truncation variants and fusion proteins (Felmlee *et al.*, 1988; Kenny *et al.*, 1991). The interaction of the transport substrate and HlyB has already been demonstrated by e.g. SPR and cross-linking experiments (Benabdelhak *et al.*, 2003; Lecher *et al.*, 2012; Thanabalu *et al.*, 1998). Furthermore, pull-down experiments with HlyA1, lacking the secretion signal, suggested an interaction of the C-terminal part, upstream of the secretion signal and the isolated C39-peptidase like domain (CLD) of HlyB (Lecher *et al.*, 2012). This interaction occurred exclusively with unfolded HlyA variants, suggesting a participation of the RTX repeats. The binding of calcium ions to the RTX repeats would induce a conformational change and thereby preclude any interaction.

Here, we used HlyA1, an N-terminally truncated construct of HlyA and inserted substitutions within the RTX repeats (Figure 1). We substituted the aspartate of each nonapeptide repeat to an alanine and investigated the influence of single and multiple substitutions on HlyB and HlyBΔCLD ATPase activity, as well as their specific interaction with the CLD *in vitro*. Our results demonstrate that the introduced mutations reduce the specific interaction of the transport substrate with the CLD of HlyB.

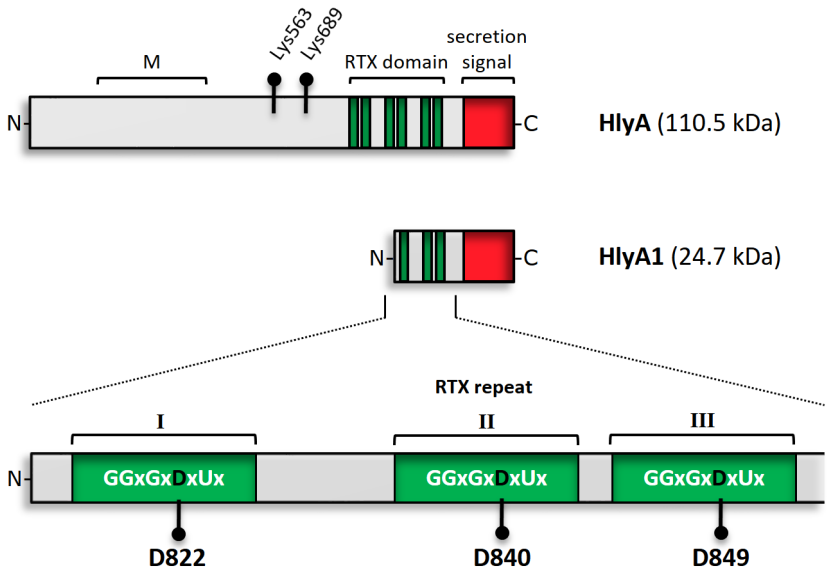

Figure 1: Schematic overview if the HlyA variants and positions of mutations within the RTX repeats. HlyA consists of the putative membrane insertion domain (M), two lysine residues, which are acylated prior to the secretion by haemolysin C (HlyC), six RTX repeats and the C-terminal secretion signal. HlyA1 is an N-terminally truncated version of HlyA, harbouring three RTX repeats and the C-terminal secretion signal. The three RTX repeats of HlyA1 were mutated at position D822, D840 and D849.

Furthermore, the mutations change the effect on HlyB ATPase modulation *in vitro*. The former reported decrease of HlyB ATPase velocity in presence of low HlyA1 concentrations was abolished (Reimann *et al.*, 2016). A software based analysis of the secondary structure of HlyA1 predicted a helical domain close to RTX repeat III, which was found to correlate to a specific modulation of HlyB maximum velocity. In contrast to the significant effects *in vitro*, the mutations of the RTX repeats did not affect the HlyA1 secretion rate *in vivo*.

Experimental procedures

Cloning of HlyA1 RTX repeat mutant variants

To obtain amino acid substitutions within the RTX repeats of HlyA1 we used the plasmid pSU2726-HlyA1 and site-directed mutagenesis using the QuikChange mutagenesis kit (Stratagene) following manufacturer´s instructions (Bakkes *et al.*, 2010; Jumpertz *et al.*, 2010). We obtained seven variants of pSU2726-HlyA1: pSU2726-HlyA1-D822A, pSU2726-HlyA1-D840A, pSU2726-HlyA1-D849A, pSU2726-HlyA1-D822A-D849A, pSU2726-HlyA1-D840A-D849A, pSU2726-HlyA1-D822A-D840A and pSU2726-HlyA1-D822A-D840A-D849A. A list of all mutated positions in HlyA1 and the corresponding primers can be found in supplementary Table S1. A list of all used plasmids can be found in supplementary Table S2. All constructs were verified by sequencing analysis.

Expression and purification of HlyA1 variants, HlyB and HlyBΔCLD

The mutations of HlyA1 were expressed and isolated as described previously with the following modifications (Thomas *et al.*, 2014c). For the secretion and purification of HlyA1 variants *E. coli* BL21 (DE3) cells were transformed with pK184-HlyBD encoding for HlyB and HlyD, and pSU2726-HlyA1 encoding for each HlyA1 variant. Cells were grown on selective agar plates containing 100 µg/ml ampicillin and 30 µg/ml kanamycin. For a selective overnight culture 2YT medium [1.6% (w/v) tryptone, 1% (w/v) yeast extract and 0.5% NaCl] was inoculated and grown for 16 h at 37 °C and vigorously shaking at 200 rev./min. The main culture with selective 2YT medium was inoculated from the overnight culture and grown to an OD_{600} of 0.8 in presence of 5 $CaCl_2$. Then expression was induced with 1 mM isopropyl β-D-1-thiogalactopyranoside (IPTG). Cells were harvested after three hours of incubation by centrifugation (44,000 g, 15 min) and the supernatant was filtered (0.2 µM) and concentrated to 2 ml using an Amicon Ultra centrifugal filter unit (10 kDa molecular mass cut-off; Merck Milipore). To increase the sample purity, a size-exclusion chromatography (SEC) was performed using a HiLoad 16/60 Superdex 75 pg (GE Healthcare Life Sciences) column and a buffer containing 100 mM HEPES, pH 8.

HlyB and HlyBΔCLD were expressed and purified as described previously in Reimann *et al.* (2016). The purity of eluted protein was determined by SDS/PAGE and subsequent CBB (Coomassie Brilliant Blue) staining.

Pull-down assays of His_{10}-CLD and HlyA

For pull-down assays Ni-NTA magnetic beads (Qiagen, Hilden) were used at room temperature. Fifty microliter of magnetic Ni-NTA magnetic beads were equilibrated three times with 100 µl 'washing' buffer (100 mM HEPES, 150 mM NaCl, 20 mM Imidazole, pH 8) and the supernatant was removed.

30 µg of His_{10}-CLD protein was added to the beads and incubated for 3 minutes. The beads were washed three times with 'washing' buffer and the supernatant was removed. 60 µg of interaction protein (HlyA1 variants) were added and incubated for 15 minutes. Each 3 minutes the reaction tube was mildly mixed. The beads were washed seven times with 100 µl 'washing' buffer and the supernatant was removed. For the elution 'washing' buffer supplemented with 300 mM imidazole and 30 µl were added to the beads and incubated for three minutes. The same protocol was used in the absence of His_{10}-CLD protein to investigate non-specific binding of HlyA1 variants.

ATPase assays

To quantify the hydrolytic activity of HlyB and HlyBΔCLD the Malachite Green assay was used as described previously in Baykov *et al.* (1988) with the following modifications. All reactions were done at room temperature in 100 mM HEPES (pH 7) containing 20-fold CMC of LMNG detergent (0.02 % w/v) (Anatrace, Maumee, OH, USA). HlyB or HlyBΔCLD, respectively, were used at 1 µM concentration and ATP at 1 mM concentration. The concentration of a HlyA1 variant varied up to 20 µM. Reactions were started by the addition of 10 mM $MgCl_2$ and stopped by pipetting 25 µl of the reaction volume into 175 µL of 20 mM H_2SO_4 after 30 minutes. The staining of free inorganic phosphate (P_i) was done with by adding 50 µl of dye solution [0.096 % Malachite Green, 1.48 % (w/v) ammonium molybdate and 0.173 %Tween 20 in 2.36 M H_2SO_4] to the stopped reaction. Parallel dilutions of P_i were stained to calculate the absolute amount of released inorganic phosphate. A spectroscopic analysis was performed 10 minutes after adding the dye solution by measuring the absorbance at a wavelength of 595 nm. For data evaluation, all appropriate controls were subtracted. Data points were fitted using Prism software (GraphPad) to one of the following equations.

(i) The Hill equation:

$$v = \frac{V_{\max}\,[\mathrm{S}]^h}{{K_{0.5}}^h + \,[\mathrm{S}]^h} \qquad (1)$$

Here, the ATPase activity corresponds to *v*, which is described as a function of the substrate concentration [S]. The maximum enzyme activity is V_{max}, the Hill coefficient is *h* and $K_{0.5}$ is the substrate concentration at which 50 % enzyme binding sites are occupied.

(ii) The Michaelis-Menten equation:

$$v = \frac{V_{\max}\,[\mathrm{S}]}{K_{\mathrm{m}} + \,[\mathrm{S}]} \qquad (2)$$

Here, the ATPase activity corresponds to *v*, which is described as a function of the substrate concentration [S]. The maximum enzyme activity is V_{max} and K_m is the substrate concentration at which 50 % enzyme binding sites are occupied.

(iii) An equation assuming two independent binding sites:

$$v = \frac{K_1 K_2 v_0 \ + K_2 v_1 [\mathrm{S}] \ + \ v_2 [\mathrm{S}]^2}{K_1 K_2 \ + \ K_2 [\mathrm{S}] \ + \ [\mathrm{S}]^2} \quad (3)$$

Here, the ATPase activity *v* is described as a function of the substrate concentration [S], K_1 represents the substrate concentration of half-maximum inhibition, K_2 represents the substrate concentration of half-maximum stimulation, v_0 is the basal activity of HlyB in the absence of the substrate, v_1 is the minimal enzyme activity and v_2 the maximum enzyme activity at infinite substrate concentration. This equation bases on enzyme kinetics algebra described in Stein (1986) and was first described in Litman *et al.* (1997a). Group comparisons were made using Student's t test for unpaired data (Prism software, GraphPad). P values < 0.05 were considered statistically significant.

Electrophoresis and immunological technique

To analyse proteins SDS/PAGE and subsequent CBB staining was used. To estimate protein molecular weight the PageRuler Prestained Protein Ladder (Thermo Fisher Scientific, Waltham, MA, USA) was used. The immunodetection was done with anti-HlyB or anti-HlyA antibody rabbit polyclonal serum at 1:8000 dilutions in TBS-T (TBS with Tween 20: 20 mM Tris base, 300 mM NaCl and 0.05% Tween 20, pH 8).

Quantification of the secretion of HlyA1 variants

The quantification of the secretion rate of HlyA1 variants by cell expression and data processing were performed as described previously with the following modifications (Lenders *et al.*, 2016). *E. coli* Bl21 (DE3) cells were transformed with pK184-HlyBD encoding for HlyB and HlyD, and pSU2726-HlyA1 encoding for one of the HlyA1 mutations variants, described above. The calculation of the amount of secreted HlyA1 was done first of all as described in Lenders *et al*. (2016). Additionally, an alternative calculation of the secretion rate was performed (stated in the text), which is based on Lenders *et al.* (2016) and includes the following modifications: The amount of secreted HlyA1 in the cell supernatant was calculated by the integrated signal intensity of HlyA1 protein on a SDS/PAGE. Here, we selectively chose two values for each variant after 60 minutes and 120 minutes of secretion, respectively, deviating from the original protocol. We evaluated the lowest values for the variants HlyA1-D849A, HlyA1-D822A-D849A, HlyA1-D840A-D849A and HlyA1-D822A-D840A-D849A, and the highest values for the variants HlyA1-D822A, HlyA1-D840A and HlyA1-D822A-D840A. Subsequently, we calculated the distinct secretion rate for each variant after 60 minutes and 120 minutes, separately and thereby we obtained four individually calculated secretion rates for each HlyA1 variant. This subjective and selective processing was calculating for assumption only whether the error propagation and

methodical difficulties could be minimized. For the analysis 4532 ± 966 T1SS cell^{-1} were estimated (Lenders *et al.*, 2016).

Secondary structure analysis

For the analysis of the secondary structure prediction the software SOPMA (self-optimized prediction method with alignment) was used (Geourjon *et al.*, 1995).

(http://npsa-pbil.ibcp.fr/cgi-bin/npsa_automat.pl?page=npsa_sopma.html)

Visualisation of the predicted secondary structures was done by POLYVIEW-2D (Porollo *et al.*, 2004).

Results

Expression and purification of HlyA1 RTX repeat mutants

Previous studies demonstrated that an N-terminally shortened variant of HlyA (HlyA1), modulated the ATPase activity of HlyB in a concentration dependent manner *in vitro* (Reimann *et al.*, 2016) (Chapter 4). This effect occurred in the presence as well as in the absence of the C-terminal secretion signal. These findings suggested that the truncated substrate still contains a sequence that modulates the ATPase activity of HlyB. This N-terminal part of HlyA1 only contains the RTX repeats, glycine- and aspartate-rich nonapeptide repeats with the consensus sequence GGxGxDxUx (x, any amino acid; U, large and hydrophobic amino acid). These RTX repeats bind calcium ions at the outside of the cell, which triggers the folding of the protein. Despite this already known function we chose to mutate the RTX repeats of HlyA1 to investigate their influence on HlyB ATPase modulation. In our study we employed HlyA1 instead of HlyA because of its higher stability and ease of purification. We used site-directed mutagenesis to replace the aspartate of each RTX repeat motif into alanine (Figure 1). Every combination of these three substitutions delivered in total seven different HlyA1 RTX repeat variants, each encoded on one plasmid. The variants are HlyA1-D822A, HlyA1-D840A, HlyA1-D849A, HlyA1-D822A-D849A, HlyA1-D840A-D849A, HlyA1-D822A-D840A and HlyA1-D822A-D840A-D849A.

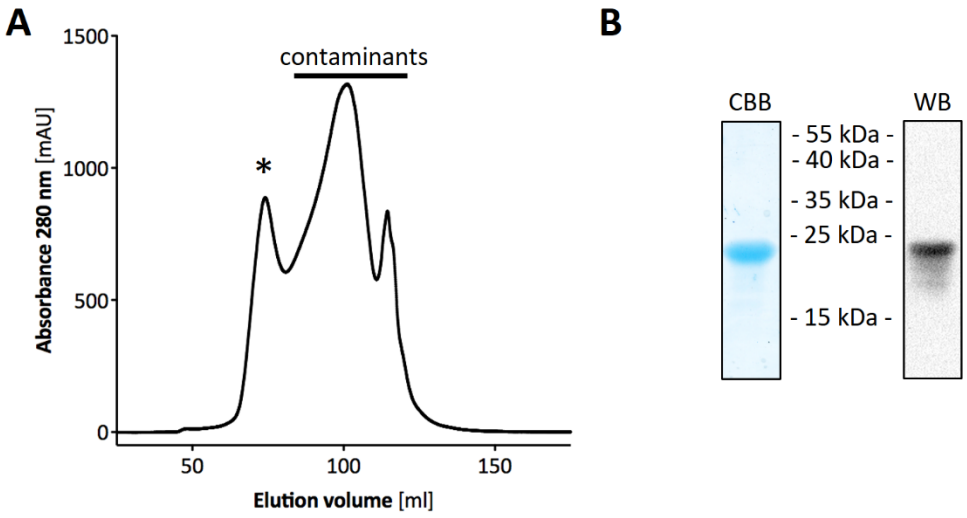

Figure 2. SEC profile and analysis of HlyA1-D822A-D840. (A) *E. coli* culture supernatant containing HlyA1-D822A-D840A was concentrated using an Amicon Ultra centrifugal filter unit and 5 ml was loaded onto a HiLoad 16/600 Superdex 200 pg column. (*) HlyA1 was eluted from the column at about 72 ml. The elution of contaminating proteins is marked with a black bar. mAU, mili-absorbance units. (B) HlyA1 containing fractions were pooled and concentrated again as described above. The sample was analysed by (CBB) SDS/PAGE and stained with CBB or detected by (WB) Western blot analysis using polyclonal antisera anti-HlyA. HlyA1-D822A-D840A has a theoretical mass of 24.7 kDa.

We chose the conserved aspartate of each RTX repeat to be modified because it is the only amino acids within the conserved motif, which side chain is involved in the coordination of calcium ions. The first

residues of each motif form a turn and the remaining part builds up a short β-strand. The backbone carbonyl groups of the glycine residues and the side chains of aspartate residues of two subsequent RTX repeats coordinate one Ca^{2+} ion (Baumann *et al.*, 1993). The repetitive arrangement of this structure then forms the β-roll (Baumann *et al.*, 1993). For the expression of proteins in *E. coli* BL21 (DE3) cells were transformed with two plasmids that encode (i) the T1SS (pK184-HlyBD) and (ii) one of the HlyA1 mutant variants (pSU2726-HlyA1) or the wild-type protein, respectively. Protein expression was induced with IPTG and furthermore, calcium was added to stabilise secreted HlyA in the supernatant. After four hours of protein expression the culture supernatant was separated from the cells by centrifugation. Protein contaminants were separated from the target protein by a SEC and analysed by SDS/PAGE and Western blot analysis (Figure 2 A, B). The purification protocol did not vary depending on the mutated position of HlyA1 and every HlyA1 RTX repeat variant was secreted to the supernatant and subsequently isolated. The SEC chromatogram shown in Figure 2 A is representative for all purified HlyA1 variants (Figure 2A). HlyA1 has a theoretical molar mass of 24.7 kDa and it was eluted from the column at about 72 ml. The HlyA1 variant protein was analysed by SDS/PAGE and Western blot analysis (Figure 2 B). Furthermore, the SEC chromatogram revealed proteins with an intense absorbance of 280 nm and the elution volume correlated to a smaller protein size in comparison to HlyA1 (Figure 2 A). The analysis of the correlating SEC fractions by SDS/PAGE showed no signals. This finding suggests that small peptides of the yeast extract media component may cause these signals. Due to their small size, these peptides are not detectable by SDS/PAGE. For further experiments HlyA1 was unfolded with high concentrations of urea and subsequently the buffer was exchanged to HEPES (pH 8) and the protein was finally stored at 4 °C.

Pull-Down assays of the isolated CLD with HlyA1 RTX repeat mutants

In vitro assays showed that the CLD in involved in the regulation of HlyB ATPase velocity (Reimann *et al.*, 2016). Previous studies also showed with pull-down assays that isolated and solely unfolded HlyA1 protein interacts with the isolated CLD of HlyB (Lecher *et al.*, 2012). This interaction was independent of the C-terminal secretion signal, further it could be abolished whether HlyA1 was folded by the addition of Ca^{2+} ions. Therefore, Lecher *et al.* (2012) suggested the RTX repeats being the binding partner of the CLD.

We investigated the interaction of HlyA1 RTX repeat mutants with purified CLD by pull-down assays. His_{10}-CLD protein was immobilized on magnetic Ni-NTA resin and incubated with purified unfolded HlyA1 mutant variants. The preparation was washed extensively and afterwards bound His_{10}-CLD protein was eluted. The elution fractions were analysed by SDS/PAGE and stained with CBB. Figure 3 shows the result of His_{10}-CLD and HlyA1-D849A or HlyA1, respectively.

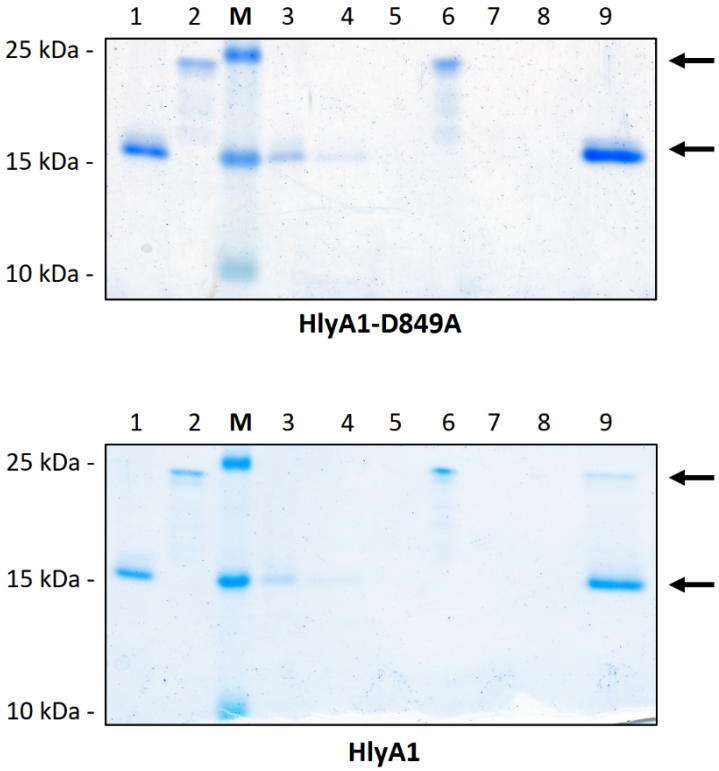

Figure 3. Detection of pull-down experiments with Ni-NTA Beads of His_{10}-CLD and HlyA1-D849A or HlyA1, respectively. The eluted sample fractions were analysed by SDS/PAGE and stained with CBB. The first two lanes contain the positive controls of (1) His_{10}-CLD and (2) HlyA1-D849A (top) or HlyA1 (bottom). Additional lanes contain: (3) supernatant after incubation with His_{10}-CLD; (4) and (5) supernatant after first and second washing step with buffer; (6) supernatant after incubation with HlyA1-D849A or HlyA1; (7) and (8) supernatant after third and 7th washing step with buffer, (9) eluted fraction after incubation with buffer supplemented with 300 mM imidazole. The elution sample (9) shows a protein band correlating to His_{10}-CLD and no co-elution in the case of HlyA1-D849A (top). The elution sample (9) in the case of HlyA1 shows a co-elution and indicates an interaction of His10-CLD and HlyA1. His_{10}-CLD has a theoretical mass of 18.5 kDa and HlyA1-D849A has a theoretical mass of 24.7 kDa. M, protein weight standard.

We observed no unspecific binding of the HlyA1 RTX repeat mutants and we confirmed a coelution of wild-type HlyA1 together with His_{10}-CLD in our control experiments. None of the HlyA1 RTX repeat mutants coeluted with the His_{10}-CLD (Supplementary Figure S1). These data demonstrate that all mutated positions within the RTX repeats of HlyA1 are involved in the interaction with the CLD of HlyB.

Mutations of the HlyA1 RTX repeats affect the ATPase modulation of HlyB

Previous studies demonstrated that a HlyA1 - CLD interaction leads to an inhibition of the hydrolytic activity of HlyB at low HlyA1 concentration, pointing to regulatory role of the CLD (Reimann *et al.*, 2016). Since we showed that mutations within the RTX repeats of HlyA1 affect the interaction to the isolated CLD of HlyB, we investigated this lack of interaction in the context of an ATPase assay in

presence of HlyB *in vitro*. We used a constant concentration of HlyB (1 µM) and ATP (1 mM) in this assay while the concentration of the HlyA1 variants varied from 0 µM to 20 µM. The ATPase activity of HlyB was monitored by the quantification of released P_i using a Malachite Green assay. The results of the measurements are summarized in Figure 4 and followed a non-linear dependence on substrate concentration. Due to variations of the basal activity of each experiment we show the modulation of ATPase activity relative to the basal HlyB ATPase activity (Figure 4 A).

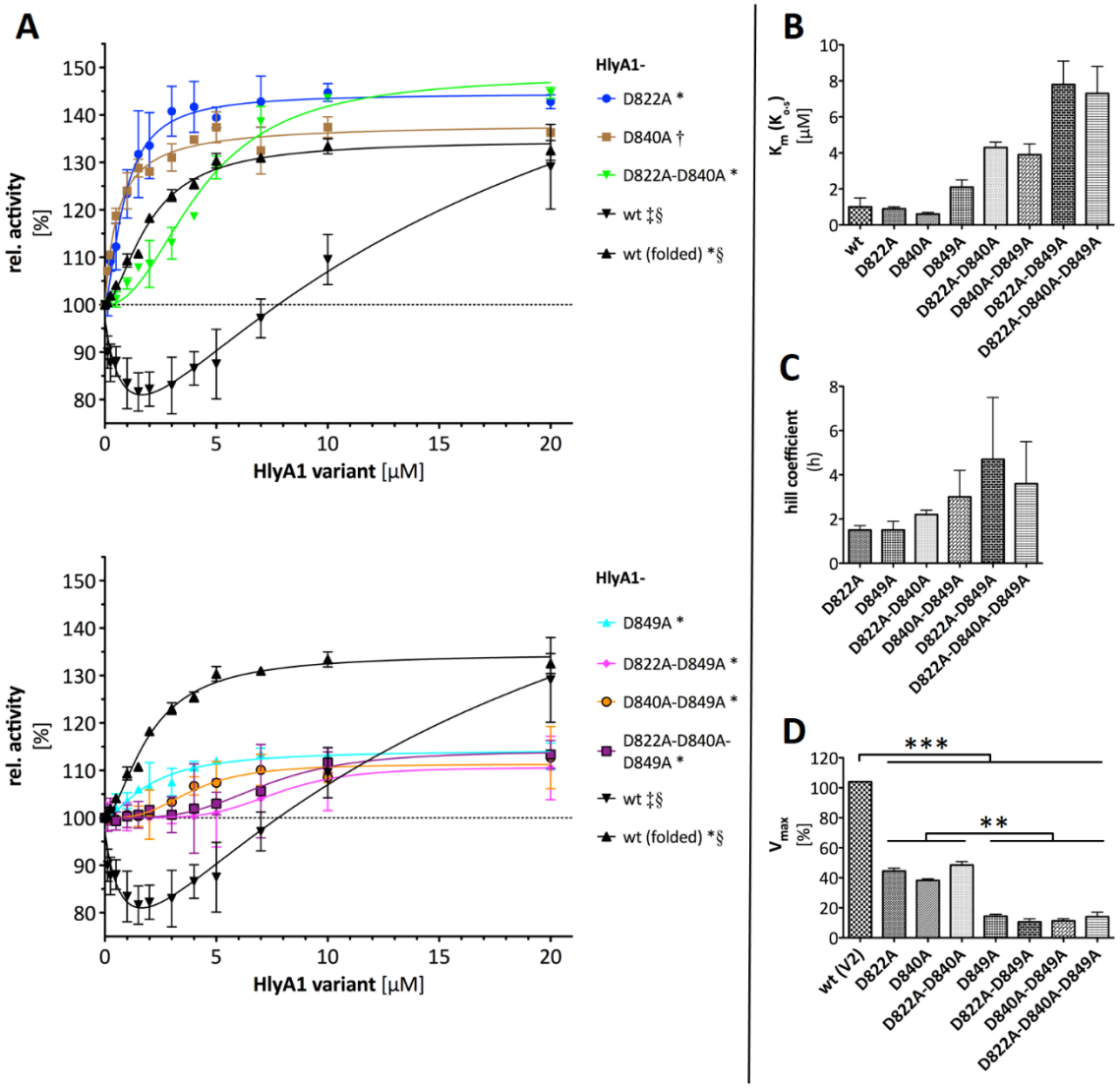

Figure 4. ATPase activity of HlyB in the presence of HlyA1 variants and related kinetic parameters. (A) Experimental results of HlyB ATPase activity in the presence of HlyA1 variants containing mutations within the RTX repeats. The results are grouped in two graphs for an improved visualisation of the data. * Datasets were analysed according to eqn (1), Hill equation; † Datasets were analysed according to eqn (2), Michaelis–Menten equation; ‡ Datasets were analysed according to eqn (3), which assumes two independent binding sites. § Data published in Reimann *et al.* (2016). Results are means ± S.D. (B) Overview of the calculated K_m or $K_{0.5}$ values, respectively. (C) Overview of calculated Hill coefficients of data that were analysed according to eqn (1), Hill equation. (D) Overview of calculated V_{max} values or calculated v_2 value, respectively. Results are means ± S.D, statistical differences are indicated with **P<0.01 and ***P<0.001 by t test.

All substrates but HlyA1-D840A induced a positive cooperativity in HlyB ATP hydrolysis and were analysed using the Hill equation (eqn 1). Noticeable the best fit of HlyB ATPase activity in presence of HlyA1-D840A was obtained with the Michaelis-Menten equation (eqn 2), deviating from any other variant, and thereby indicating the loss of positive cooperative behaviour (Table 1). Furthermore, this variant also shows the lowest K_m value (0.6 ± 0.1 µM) compared to other $K_{0.5}$ value. In general, the increasing number of introduced mutations within one HlyA1 variant protein correlates to an increasing Hill coefficient and $K_{0.5}$, respectively (Figure 4B and Figure 4C). The Hill coefficient of HlyB varies from 1.5 ± 0.2 in presence of HlyA-D822A up to 4.7 ± 2.8 in presence of HlyA1-D822A-D849A (Table 1).

Table 1. Kinetic parameters of HlyB in dependence of HlyA1 RTX repeat variants. (folded), kinetic parameters were determined in presence of HlyA1 and Ca^{2+} ions (see experimental procedures section)

(a)

	$K_{0.5}$ (K_m) [µM]	rel. V_{max} [%]	h
HlyA1-D822A *	0.9 ± 0.1	44.5 ± 1.9	1.5 ± 0.2
HlyA1-D840A †	0.6 ± 0.1	38.3 ± 1.0	-
HlyA1-D849A *	2.1 ± 0.4	14.4 ± 1.3	1.5 ± 0.4
HlyA1-D822A-D840A *	4.3 ± 0.3	48.5 ± 2.3	2.2 ± 0.2
HlyA1-D822A-D849A *	7.8 ± 1.3	10.6 ± 2.1	4.7 ± 2.8
HlyA1-D840A-D849A *	3.9 ± 0.6	11.3 ± 1.5	3.0 ± 1.2
HlyA1-D822A-D840A-D849A *	7.3 ± 1.5	14.1 ± 3.0	3.6 ± 1.9
HlyA1 (folded) *§	2.0 ± 0.3	33.6 ± 1.3	1.8 ± 0.4

(b)

	K_1 [µM]	K_2 [µM]	v_1 [%]	v_2 [%]
HlyA1 ‡§	1.0 ± 0.5	19.4 ± 3.1	-37 ± 0.1	+104 ± 0.1

* Parameters were determined according to eqn (1), Hill equation.
† Parameters were determined according to eqn (2), Michaelis–Menten equation
‡ Parameters were determined according to eqn (3), which assumes two independent binding sites.
§ Data published in Reimann *et al.* (2016)

None of the HlyA1 mutants inhibited the ATPase activity of HlyB, however, all HlyA1 mutants stimulated HlyB ATPase activity. We observed two groups of HlyA1 variants that affected HlyB ATPase maximum velocity (V_{max}) in different ways. The first group comprises the variants, which do not contain a D849A substitution and were stimulated by an average of 41.2 % (Figure 4 A, top). The second group was stimulated by an average of 12.6 % and comprises all HlyA1 variants that contain a D849A substitution (Figure 4 A, bottom). The stimulatory effects of the substrates on HlyB ATPase activity are summarized in Figure 4 D and visualise the statistical difference of both groups and in addition to the wild-type substrate. The obtained kinetic parameters are summarized in Table 1.

Secondary structure predictions of the RTX domain

The previously shown correlation of the V_{max} and the D849A substitution point to a crucial role of the most C-terminal RTX repeat of HlyA1. Therefore, we suggest the third RTX repeat has to vary from its C-terminal homologues. All three investigated motifs are composed of the same signature motif GGxGxDxUx and only differing in the sequence position within the HlyA1 protein.

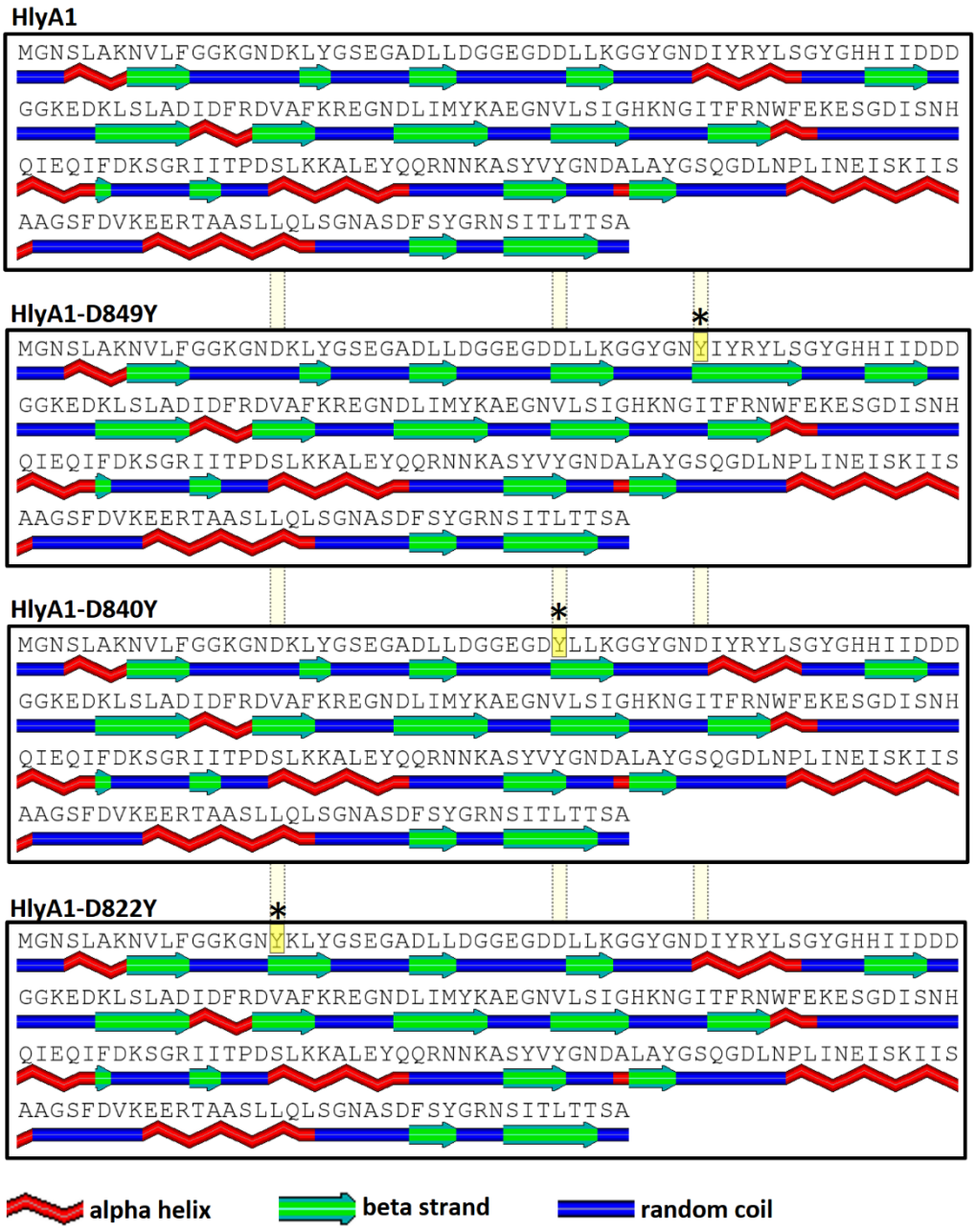

Figure 5. Computational prediction of the secondary structure of HlyA1 variants. Predicted secondary structure of HlyA1 and of the hypothetical mutations D849Y, D840Y and D822Y by SOPMA (Geourjon *et al.*, 1995). Each mutated residue is highlighted with an asterisk (*) and a vertical yellow bar. The secondary structure predictions are visualised by the software POLYVIEW-2D (Porollo *et al.*, 2004). The predicted secondary structure starting at position D849 changes depending on the mutations D849Y and D840Y. red zig-zag-pattern, alpha helix; green arrow, beta strand; blue bar, random coil.

As we are investigating the sequence of HlyA1, which modulates HlyB ATPase velocity and not the RTX repeats themselves, we used a software tool to predict a potential secondary structure of HlyA1 (Combet *et al.*, 2000). Representative for our point mutations we introduced a tyrosine at the mutated positions instead of an alanine to underline a significant impact on the secondary structure of the peptide (Figure 5).

The wild-type protein contains a predicted α-helix ranging from D849 to S855, representing theoretically 1.9 turns with a length of 10.3 Å. The D849Y mutation abolishes this predicted helix completely while the substitutions D840Y and D822Y do not affect the formation of at all or with a minor impact, respectively. Additionally, the substitution D822Y affects the N-terminal part concerning the formation of beta turns, random coils and extended strands. Overall the predicted presence of a helical structure close to RTX repeat III and the impact of a point mutation at position D849 would support the ATPase velocity results shown above. Therefore, we suggest this helix being a hypothetical factor regulating HlyB ATPase velocity.

Modulation of HlyBΔCLD ATPase activity by mutations within the RTX repeats of HlyA1

Recent studies suggested that the RTX repeats of HlyA1 interact with the CLD of HlyB and thereby decrease the ATPase velocity of HlyB (Reimann *et al.*, 2016). Hence HlyBΔCLD does not show any ATPase velocity inhibition in presence of the substrate due to the lack of the CLD and thereby the interaction partner of the regulating sequence.

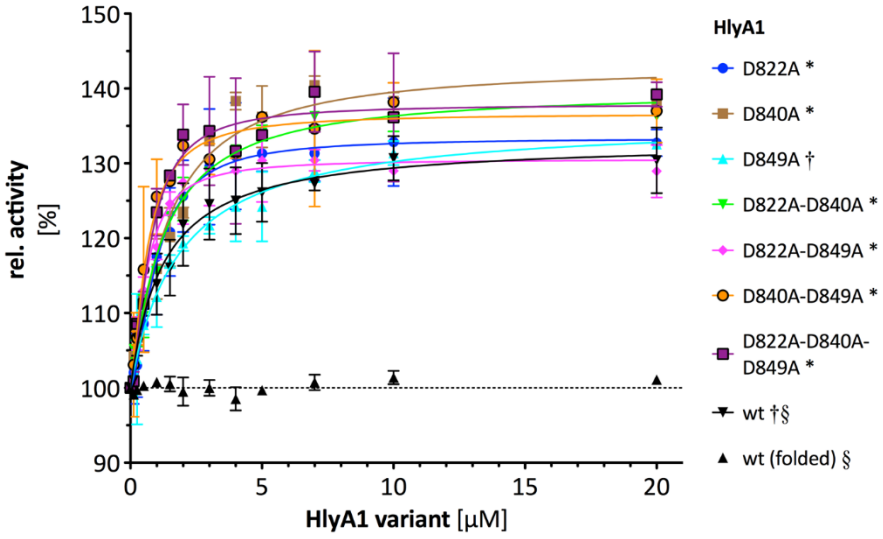

Figure 6. ATPase activity of HlyBΔCLD in the presence of HlyA1 variants. Experimental results of HlyBΔCLD ATPase activity in the presence of HlyA1 variants containing mutations within the RTX repeats. * Datasets were analysed according to eqn (1), Hill equation; † Datasets were analysed according to eqn (2), Michaelis–Menten equation. § Data published in Reimann *et al.* (2016). Results are means ± S.D.

Nevertheless both, HlyB as well as HlyBΔCLD share the ability to be stimulated with low and high substrate concentrations. Here, we investigate the influence of mutations within the RTX repeats of HlyA1 on the ATPase activity of HlyBΔCLD. Therefore, we quantified the ATPase activity of HlyBΔCLD in presence of each HlyA1 variant as described above. We used a constant concentration of HlyBΔCLD (1 µM) and ATP (1 mM) in this assay while the concentration of the HlyA1 variants varied from 0 µM to 20 µM. The ATPase activity of HlyB was monitored by the quantification of released P_i using a Malachite Green assay. The results of the measurements are summarized in Figure 6 and followed a non-linear dependence on substrate concentration. Due to variations of the basal activity of each experiment we show the modulation of ATPase activity relative to the basal HlyB ATPase activity (Figure 6).

All substrates but HlyA1-D849A induced a positive cooperativity in HlyB ATP hydrolysis and were analysed using the Hill equation (eqn 1). The best fit of HlyB ATPase activity in presence of HlyA1-D840A was obtained with the Michaelis-Menten equation (eqn 2), deviating from other substrate RTX variants, however, being in line with the result of HlyA1 wild-type protein (Table 2). The detected $K_m/K_{0.5}$ values varied from 0.6 ± 0.1 µM (HlyA1-D822A-D849A, HlyA1-D840A-D849A) up to 1.8 ± 0.3 µM (HlyA1-D849A). The HlyA1 variants stimulated ATPase velocity ranging from 30.6 ± 1.0 % (HlyA1-D822A-D849A) up to 43.1 ± 2.3 % (HlyA1-D840A). Furthermore, the analysis delivered a Hill coefficient ranging from 1.1 ± 0.1 (HlyA1-D822A-D840A) up to 1.6 ± 0.3 (HlyA1-D822A), pointing to a positive cooperative ATP hydrolysis. The obtained kinetic parameters are summarized in Table 2.

Table 2. Kinetic parameters of HlyBΔCLD in dependence of HlyA1 RTX repeat variants.

	K_m / $K_{0.5}$ [µM]	rel. V_{max} [%]	*h*
HlyA1-D822A *	1.0 ± 0.1	33.4 ± 1.8	1.6 ± 0.3
HlyA1-D840A *	1.3 ± 0.2	43.1 ± 2.3	1.2 ± 0.2
HlyA1-D849A †	1.8 ± 0.3	35.8 ± 1.7	-
HlyA1-D822A-D840A *	1.2 ± 0.1	39.8 ± 1.4	1.1 ± 0.1
HlyA1-D822A-D849A *	0.6 ± 0.1	30.6 ± 1.0	1.5 ± 0.2
HlyA1-D840A-D849A *	0.6 ± 0.1	36.7 ± 1.9	1.4 ± 0.3
HlyA1-D822A-D840A-D849A *	0.7 ± 0.1	38.0 ± 1.8	1.5 ± 0.3
HlyA1 †§	1.2 ± 0.3	33.0 ± 1.5	-

* Parameters were determined according to eqn (1), Hill equation.
† Parameters were determined according to eqn (2), Michaelis–Menten equation
§ Data published in Reimann *et al.* (2016)

Quantification of the secretion rate of HlyA1 RTX repeat variants by the T1SS

Since we observed major differences in the kind of modulation of HlyA1 variants on HlyB or HlyBΔCLD ATPase activity, the question raised about the influence on the HlyA T1SS. Lenders *et al*. described a method to quantify the substrate secretion rate of HlyA that enabled us to investigate the effect of mutations within the RTX repeats on the T1SS translocon *in vivo*. *E. coli* BL21 (DE3) cells were transformed with plasmids that encode one HlyA1 variant and the T1SS simultaneously. After protein expression we quantified the amount of secreted HlyA1 in the supernatant and T1SS per cell via SDS/PAGE analysis and evaluated the results as described in Lenders *et al.* (2016) (Figure 7 A).

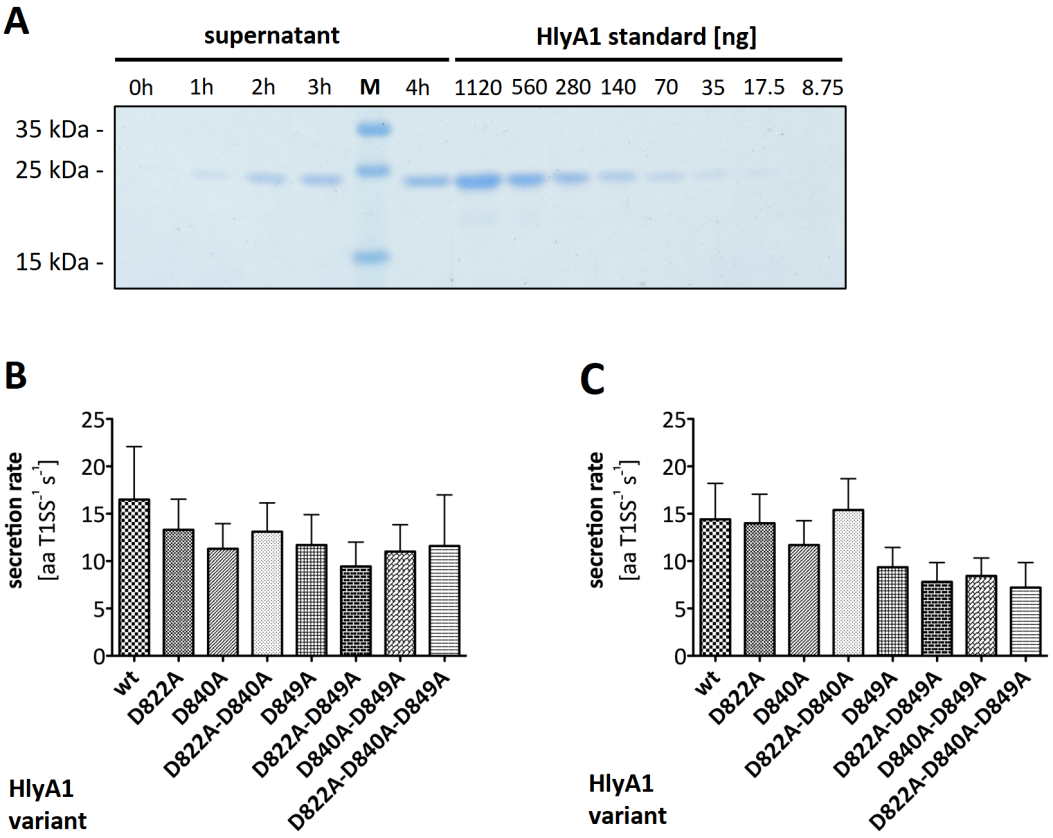

Figure 7. HlyA1 secretion rate with parallel expression of the T1SS in *E. coli* BL21 (DE3) cells. (A) Example of a CBB stained SDS/PAGE that was used to calculate the amount of secreted HlyA1-D840A. Here, samples of culture supernatant were analysed 1h, 2h, 3h and 4h after induction of the expression of HlyB, HlyD and HlyA1-D840A. The amount of secreted protein was quantified with a dilution series of purified HlyA1 (HlyA1 standard). (B) Results based on the amount of secreted HlyA1 variants. Values are averaged 120 minutes after induction of protein expression. Error bars represent the S.D. of three biological replicates. (C) Results after the selective removal of datasets and with an alternative calculation as described below. The amounts of secreted HlyA1 variants were determined separately 60 minutes and 120 minutes after induction of protein expression and were subsequently averaged. Therefore, every time point was rated as a separate measurement, resulting in error bar representing the S.D. of four replicates. (Experiments carried out by Dr. Michael H.H. Lenders).

Our results demonstrate that all investigated HlyA1 variants and the HlyA1 wild-type protein were secreted with similar secretion rates (Figure 7 B). We have to take into account that during the incubation of the bacterial cultures slight amounts of white aggregate was observed at the inner glass wall of the incubating flasks. Increased amounts were visible for variants containing the mutation D849A. These aggregates were not observed in the case of wild-type protein. Additionally, we obtained increased deviations of the calculated amounts of secreted HlyA1. This has led us to a second and different evaluation of the measured values. The amount of secreted HlyA1 in the cell supernatant was calculated by the integrated signal intensity of HlyA1 protein on a SDS/PAGE. Here, we chose only two values for each variant after 60 minutes and 120 minutes of secretion, respectively, deviating from the original protocol. We evaluated the lowest values for the variants HlyA1-D849A, HlyA1-D822A-D849A, HlyA1-D840A-D849A and HlyA1-D822A-D840A-D849A, and the highest values for the variants HlyA1-D822A, HlyA1-D840A and HlyA1-D822A-D840A. Subsequently we calculated the distinct secretion rate for each variant after 60 minutes and 120 minutes, separately and thereby we obtained four individually calculated secretion rates for each HlyA1 variant. These final result are shown in Figure 7 C and indicate a decreased secretion rate, if the most C-terminal RTX repeat is mutated, correlating to a decreased V_{max} value as already shown *in vitro*. However, these results were selectively modified and demonstrate a possible result whether the error propagation and methodical difficulties could be minimized.

A model of HlyB ATPase inhibition by its transport substrate

The results of this study demonstrate that a single point mutation within at least one of three known RTX repeats of HlyA1 results in the loss of HlyB ATPase velocity inhibition *in vitro*. The inhibitory effect could be assigned to a distinct HlyA1 - CLD interaction, independent of the C-terminal secretion signal. Therefore, our results suggest that the RTX repeats are at least one part of a sequence within HlyA1 that interacts with the CLD of HlyB. Interestingly, we only observed an ATPase inhibition if all three RTX repeats are present. From a structural point of view our results appear unusual, because the mutations are spread within a sequence of 27 amino acids. Keeping in mind that HlyA is assumed to be translocated in an unfolded state, this stretch spans a distance of about 90 Å and according to our results this stretch would interact multiple times with the CLD. Taking these findings into account we developed a model of the HlyA1 and CLD interaction based on the findings of Lecher *et al.* (2012). They used chemical shift perturbation experiments with (^{1}H-^{15}N)-HSQC spectra to map the substrate-binding region of HlyA2 within the CLD and identified two stretches, which could be interpreted as binding regions. For our model, we assume each identified region of the CLD binding to one RTX repeat. With this assumption a single HlyA1 molecule, that contains three RTX repeats, could interact with both CLDs of a potential HlyB dimer. A crucial part of this interaction model would be the ability of the

substrate to span the distance between the CLDs of a HlyB dimer. However, no three-dimensional structure of HlyB is available, only the sequence between RTX repeat I and II can be considered to span this distance (Figure 1). This 'linker'-sequence spanning from residue 826 to residue 834 (GSEGADLLD) has to be long enough to reach both CLDs at the same time.

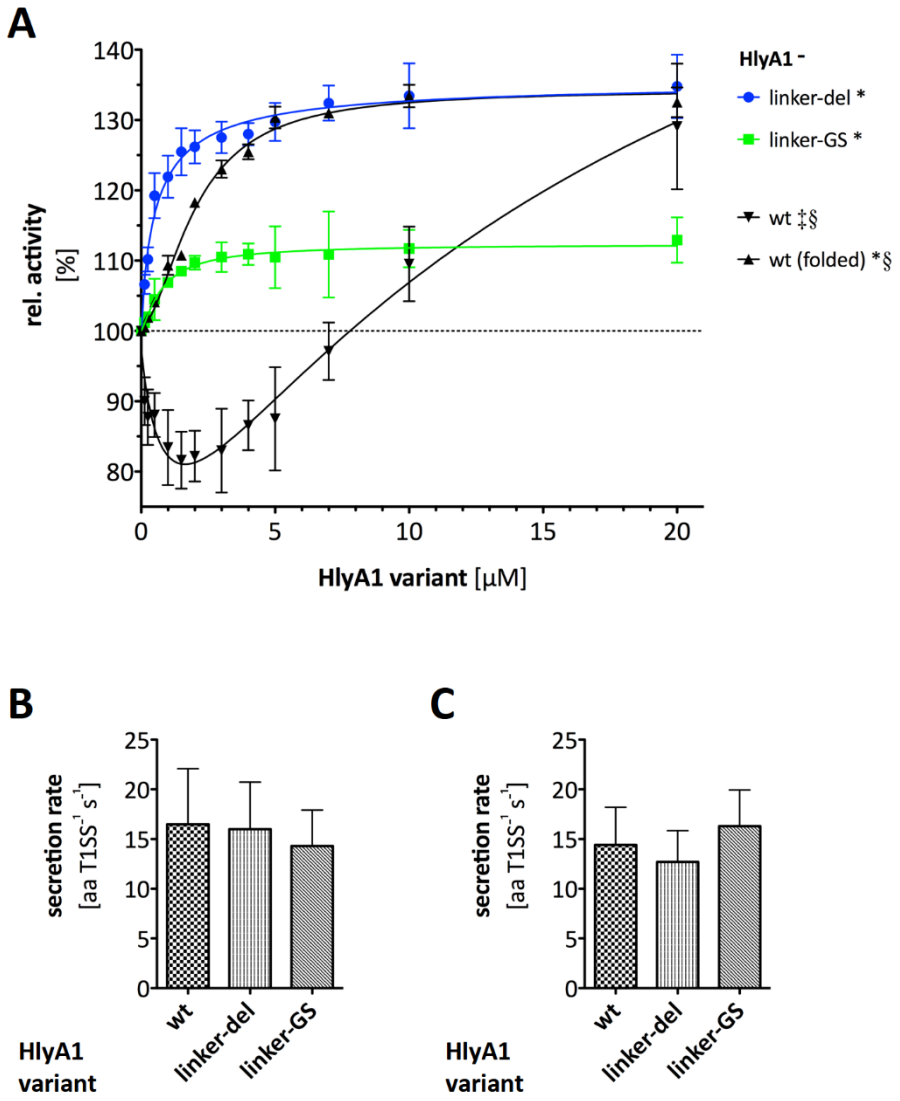

Figure 8. ATPase activity of HlyB in the presence of HlyA1 linker variants. (A) Experimental results of HlyB ATPase activity in the presence of HlyA1 variants containing mutations of the 'linker'-sequence between the RTX repeats I and II. * Datasets were analysed according to eqn (1), Hill equation; ‡ Datasets were analysed according to eqn (3), which assumes two independent binding sites. § Data published in Reimann *et al.* (2016). Results are means ± S.D. (B) Results based on the amount of secreted HlyA1 variants and the values were averaged 120 minutes after induction of protein expression. Error bars represent the S.D. of two replicates. (C) Results after the removal of selective datasets and with an alternative calculation as described below. The amounts of secreted HlyA1 variants were determined separately 60 minutes and 120 minutes after induction of protein expression and were subsequently averaged. Therefore, every time point was rated as a separate measurement and resulting in error bars representing the S.D. of four biological replicates.

We cloned two mutants of HlyA1 that contain modified linker-sequences, one mutant contains a deleted linker-sequence (HlyA1-linker-del) and the linker-sequence of the other mutant was substituted by a "GS" linker (GSGSGSGSG) (HlyA1-linker-GS) (Argos, 1990). Subsequently, we purified these variants to investigate the influence of the proteins on HlyB ATPase activity *in vitro* and we quantified the secretion rate *in vivo* as described above (Figure 8). The results were analysed using the Hill equation (eqn 1). We found that the deletion of the linker-sequence (HlyA-linker-del) abolished an inhibition of HlyB with low substrate concentrations, while a stimulation of the ABC transporter still occurs, supporting our model. However, the substitution of the linker (HlyA-linker-GS), still providing the length of the sequence, showed the same result and thereby disagrees with our model. The kinetic parameters are summarized in Table 3. Furthermore, both HlyA1 variants showed the same secretion rate as the wild-type protein *in vivo* (Figure 8B). We obtained the same result with the modified evaluation of the data as described above to demonstrate a possible result if the error propagation and methodical difficulties could be minimized (Figure 8C).

Additionally, we also cloned a third variant of the linker-sequence that contains a duplication of the original sequence and thereby extending the stretch by nine amino acids. This variant was not detectable in the supernatant nor in the cytoplasm. A software analysis of the mRNA sequence predicted a secondary structures (hairpin) that may have prohibited the transcription (Gruber *et al.*, 2008) (Supplementary Figure S2).

Table 3. Kinetic parameters of HlyB in dependence of HlyA1 RTX repeat variants. (folded), kinetic parameters were determined in presence of HlyA1 and Ca^{2+} ions (see experimental procedures section).

(a)

	$K_{0.5}$ [µM]	rel. V_{max} [%]	h
HlyA1-linker-del *	0.6 ± 0.1	35.6 ± 2.1	0.9 ± 0.1
HlyA1-linker-GS *	0.8 ± 0.2	12.3 ± 1.2	1.2 ± 0.4
HlyA1 (folded) *§	2.0 ± 0.3	33.6 ± 1.3	1.8 ± 0.4

(b)

	K_1 [µM]	K_2 [µM]	v_1 [%]	v_2 [%]
HlyA1 ‡§	1.0 ± 0.5	19.4 ± 3.1	-37 ± 0.1	+104 ± 0.1

* Parameters were determined according to eqn (1), Hill equation.
‡ Parameters were determined according to eqn (3), which assumes two independent binding sites.
§ Data published in Reimann *et al.* (2016)

Discussion

In this study we investigate the ATPase activity of HlyB in presence of HlyA1 variants, harbouring distinct mutations within the RTX repeats. The RTX motif of HlyA1 contains nonapeptide sequence repeats, which bind calcium ions at the outside of the cell and induce the folding of the protein. So far it is not known if these repeats also obtain a functional role prior to the secretion process, in the cytoplasm. We found that shortened variants of HlyA (HlyA1) have a regulatory effect on the ATPase activity of HlyB *in vitro*, by decreasing or increasing the ATPase velocity depending on the concentration of the substrate (Reimann *et al.*, 2016). The interacting sequence of HlyA1 could be assigned to an amino acid sequence within the RTX domain, while the CLD of HlyB is supposed to be the interaction partner (Lecher *et al.*, 2012). Lecher *et al.* (2012) provided evidence for an interaction of isolated HlyA2 and His-CLD via pull-down experiments with Ni-NTA beads. Our control experiments confirmed this finding and single substitutions of amino acids within the RTX repeats abolished this interaction completely. Although we could not detect a co-elution of His-CLD and any other HlyA1 variant, we do not exclude any residual weak interactions that may still be present. Nevertheless, these pull-down experiments and *in vitro* ATPase assays confirm a crucial impact of the HlyA RTX repeats concerning the regulation of HlyB ATPase activity. Our former studies revealed that the inhibition of HlyB by its transport substrate is also most likely directed by an interaction of the transport substrate and the CLD. Therefore, this supports our observations about the loss of inhibitory effects in presence of mutated RTX repeats, by permitting an interaction with the CLD.

Furthermore, we detected a potential secondary structure that may be related to the modulation of HlyB *in vitro*. This predicted helix is closely located to the most C-terminal RTX repeat III (Figure 1). Its presence or absence depends on the mutated position and suggests to affect HlyB ATPase maximal velocity. The predicted helix starts at D849 and spans the amino acids 'DIYRYLS'. Noticeable it was already reported that the C-terminal HlyA secretion signal also contains helices that may be required for an interaction with the membrane associated transporter complex (Yin *et al.*, 1995). For comparison the predicted helices of the HlyA secretion signal start at L976 'LINEISKIIS' and continue at A998 'AASLLQLSGNA' (Yin *et al.*, 1995; Zhang *et al.*, 1995). Despite Yin *et al.* detected the helices of HlyA in the presence of triflourethanol, the strongest helix-promoting agent know, the data correlate to our software based predictions of the secondary structure (Thomas *et al.*, 2014b) (Figure 5). The helix commonality of the secretion signal and the distinct RTX repeat III are mentionable, however, both subunits seem to act independently as the modulation of HlyB ATPase activity also occurred in the absence of the secretion signal (Reimann *et al.*, 2016).

On the one hand residue D849 affected HlyB V_{max} in two clearly separated ways (Figure 4 A), while on the other hand the same residue affected $K_{0.5}$ and the Hill coefficient less significant with a vague

tendency. Both parameters seem to rise depending on the amount of mutated position within HlyA1 but we have no evidence for further interpretations. Anyway and in clear contrast, the same HlyA1 variants affected the parameters of HlyBΔCLD ATPase activity less intense. This observation points to the CLD being the only interaction partner of the mutated HlyA1 variants since the CLD is absent in HlyBΔCLD. Furthermore, stimulation was observed independent of the CLD and independent of HlyA1 concentrations. This shows that HlyB ATPase stimulation is mediated separately of ATPase inhibition, however, the responsible mechanism remains ambiguous.

So far, it is not understood in every detail, how the RTX domain is involved in the translocation process. For CyaA it has already been shown that a deletion of these repeats affect the translocation effectivity with a considerable impact (Bumba *et al.*, 2016). Also the deletions of several RTX repeats of HlyA did reduce the transport level, at least to a certain degree (Felmlee *et al.*, 1988; Kenny *et al.*, 1991; Ludwig *et al.*, 1988). Latter results are in contrast to our quantification of the secretion rate, which showed a non-significant reduction in the case of all HlyA1 variants in comparison to the wild type HlyA1 protein. On one side this would mean in mechanistic terms that *in vitro* observed kinetic changes do not affect the rate of the translocation process itself. Therefore, the inhibitory effect could represent (a) a process prior to the translocation, e.g. the recruitment of TolC or (b) the secretion rate is independent of the ATP hydrolysis velocity of HlyB. The latter could be explained by the hypothetical mechanism of an ATP binding and hydrolysis 'gated' opening and closing 'channel' as described in Bumba *et al.* (2016). Such a model would propose ATP hydrolysis for early stages of the translocation process while the substrate is pulled by a calcium-driven folding of the RTX domain. The folding occurs outside of the cell and ratchets the translocation through the T1SS.

On the other side we have to take into account that the error propagation of the secretion rate quantification of HlyA1 mutants resulted in high standard deviations (Figure 7). Supposing that mutations within the RTX repeats of HlyA1 reduce the secretion rate, this would be in line with results of former RTX studies (Felmlee *et al.*, 1988; Kenny *et al.*, 1991; Ludwig *et al.*, 1988). Furthermore, this assumption would support the putative function of the CLD as a chaperone (Lecher *et al.*, 2012).

Our findings point to a complex regulation mechanism that has to be investigated by further experiments and alternative methods. Since the isolation of HlyA1 is accompanied by high amounts of supernatant contaminants, the complete absence of interfering components cannot be excluded even after intensive purification steps. Furthermore, the secreted protein has to be exposed to calcium ions, which stabilise the protein in the supernatant but induce its folding. Therefore, the protein has to be unfolded again prior to experimental usage. These steps could be replaced by a purification of HlyA1 from inclusion bodies within the expressing cell and a subsequent refolding step of the protein in the absence of calcium ions. First attempts of this technique resulted in unstable protein, which was unsuitable for further experiments.

Acknowledgement

We thank all members of the Institute of Biochemistry for valuable discussions and especially Iris Fey, Protein Production Facility, for technical support. We would like to thank Jan Stindt for help with statistical analysis. This work was supported in part by the DFG (CRC 1208, project A01 to L.S.).

Literature

Argos, P. (1990). An investigation of oligopeptides linking domains in protein tertiary structures and possible candidates for general gene fusion. J Mol Biol *211*, 943-958.

Bakkes, P.J., Jenewein, S., Smits, S.H., Holland, I.B., and Schmitt, L. (2010). The rate of folding dictates substrate secretion by the *Escherichia coli* hemolysin type 1 secretion system. J Biol Chem *285*, 40573-40580.

Balakrishnan, L., Hughes, C., and Koronakis, V. (2001). Substrate-triggered recruitment of the TolC channel-tunnel during type I export of hemolysin by *Escherichia coli*. J Mol Biol *313*, 501-510.

Baumann, U., Wu, S., Flaherty, K.M., and McKay, D.B. (1993). Three-dimensional structure of the alkaline protease of *Pseudomonas aeruginosa*: a two-domain protein with a calcium binding parallel beta roll motif. EMBO J *12*, 3357-3364.

Baykov, A.A., Evtushenko, O.A., and Avaeva, S.M. (1988). A malachite green procedure for orthophosphate determination and its use in alkaline phosphatase-based enzyme immunoassay. Anal Biochem *171*, 266-270.

Benabdelhak, H., Kiontke, S., Horn, C., Ernst, R., Blight, M.A., Holland, I.B., and Schmitt, L. (2003). A Specific Interaction Between the NBD of the ABC-transporter HlyB and a C-Terminal Fragment of its Transport Substrate Haemolysin A. Journal of Molecular Biology *327*, 1169-1179.

Blenner, M.A., Shur, O., Szilvay, G.R., Cropek, D.M., and Banta, S. (2010). Calcium-induced folding of a beta roll motif requires C-terminal entropic stabilization. J Mol Biol *400*, 244-256.

Bumba, L., Masin, J., Macek, P., Wald, T., Motlova, L., Bibova, I., Klimova, N., Bednarova, L., Veverka, V., Kachala, M.*, et al.* (2016). Calcium-Driven Folding of RTX Domain beta-Rolls Ratchets Translocation of RTX Proteins through Type I Secretion Ducts. Mol Cell *62*, 47-62.

Chabeaud, P., de Groot, A., Bitter, W., Tommassen, J., Heulin, T., and Achouak, W. (2001). Phase-variable expression of an operon encoding extracellular alkaline protease, a serine protease homolog, and lipase in *Pseudomonas brassicacearum*. J Bacteriol *183*, 2117-2120.

Chenal, A., Guijarro, J.I., Raynal, B., Delepierre, M., and Ladant, D. (2009). RTX calcium binding motifs are intrinsically disordered in the absence of calcium: implication for protein secretion. J Biol Chem *284*, 1781-1789.

Chenal, A., Karst, J.C., Sotomayor Perez, A.C., Wozniak, A.K., Baron, B., England, P., and Ladant, D. (2010). Calcium-induced folding and stabilization of the intrinsically disordered RTX domain of the CyaA toxin. Biophys J *99*, 3744-3753.

Combet, C., Blanchet, C., Geourjon, C., and Deleage, G. (2000). NPS@: network protein sequence analysis. Trends Biochem Sci *25*, 147-150.

Felmlee, T., and Welch, R.A. (1988). Alterations of amino acid repeats in the *Escherichia coli* hemolysin affect cytolytic activity and secretion. Proc Natl Acad Sci U S A *85*, 5269-5273.

Geourjon, C., and Deleage, G. (1995). SOPMA: significant improvements in protein secondary structure prediction by consensus prediction from multiple alignments. Comput Appl Biosci *11*, 681-684.

Ghigo, J.M., and Wandersman, C. (1994). A carboxyl-terminal four-amino acid motif is required for secretion of the metalloprotease PrtG through the *Erwinia chrysanthemi* protease secretion pathway. J Biol Chem *269*, 8979-8985.

Gilson, L., Mahanty, H.K., and Kolter, R. (1990). Genetic analysis of an MDR-like export system: the secretion of colicin V. EMBO J *9*, 3875-3884.

Goebel, W., and Hedgpeth, J. (1982). Cloning and functional characterization of the plasmid-encoded hemolysin determinant of *Escherichia coli*. J Bacteriol *151*, 1290-1298.

Gruber, A.R., Lorenz, R., Bernhart, S.H., Neubock, R., and Hofacker, I.L. (2008). The Vienna RNA websuite. Nucleic Acids Res *36*, W70-74.

Hinsa, S.M., Espinosa-Urgel, M., Ramos, J.L., and O'Toole, G.A. (2003). Transition from reversible to irreversible attachment during biofilm formation by *Pseudomonas fluorescens* WCS365 requires an ABC transporter and a large secreted protein. Mol Microbiol *49*, 905-918.

Holland, I.B., Schmitt, L., and Young, J. (2005). Type 1 protein secretion in bacteria, the ABC-transporter dependent pathway (review). Mol Membr Biol *22*, 29-39.

Jones, H.E., Holland, I.B., Baker, H.L., and Campbell, A.K. (1999). Slow changes in cytosolic free Ca2+ in *Escherichia coli* highlight two putative influx mechanisms in response to changes in extracellular calcium. Cell Calcium *25*, 265-274.

Jumpertz, T., Chervaux, C., Racher, K., Zouhair, M., Blight, M.A., Holland, I.B., and Schmitt, L. (2010). Mutations affecting the extreme C terminus of *Escherichia coli* haemolysin A reduce haemolytic activity by altering the folding of the toxin. Microbiology *156*, 2495-2505.

Kenny, B., Chervaux, C., and Holland, I.B. (1994). Evidence that residues -15 to -46 of the haemolysin secretion signal are involved in early steps in secretion, leading to recognition of the translocator. Mol Microbiol *11*, 99-109.

Kenny, B., Haigh, R., and Holland, I.B. (1991). Analysis of the haemolysin transport process through the secretion from *Escherichia coli* of PCM, CAT or beta-galactosidase fused to the Hly C-terminal signal domain. Mol Microbiol *5*, 2557-2568.

Kenny, B., Taylor, S., and Holland, I.B. (1992). Identification of individual amino acids required for secretion within the haemolysin (HlyA) C-terminal targeting region. Mol Microbiol *6*, 1477-1489.

Lecher, J., Schwarz, C.K., Stoldt, M., Smits, S.H., Willbold, D., and Schmitt, L. (2012). An RTX transporter tethers its unfolded substrate during secretion via a unique N-terminal domain. Structure *20*, 1778-1787.

Lenders, M.H., Beer, T., Smits, S.H., and Schmitt, L. (2016). In vivo quantification of the secretion rates of the hemolysin A Type I secretion system. Sci Rep *6*, 33275.

Letoffe, S., Delepelaire, P., and Wandersman, C. (1996). Protein secretion in Gram-negative bacteria: assembly of the three components of ABC protein-mediated exporters is ordered and promoted by substrate binding. EMBO J *15*, 5804-5811.

Linhartova, I., Bumba, L., Masin, J., Basler, M., Osicka, R., Kamanova, J., Prochazkova, K., Adkins, I., Hejnova-Holubova, J., Sadilkova, L.*, et al.* (2010). RTX proteins: a highly diverse family secreted by a common mechanism. FEMS Microbiol Rev *34*, 1076-1112.

Litman, T., Nielsen, D., Skovsgaard, T., Zeuthen, T., and Stein, W.D. (1997). ATPase activity of P-glycoprotein related to emergence of drug resistance in Ehrlich ascites tumor cell lines. Biochim Biophys Acta *1361*, 147-158.

Lo, R.Y., Strathdee, C.A., and Shewen, P.E. (1987). Nucleotide sequence of the leukotoxin genes of *Pasteurella haemolytica* A1. Infect Immun *55*, 1987-1996.

Ludwig, A., Jarchau, T., Benz, R., and Goebel, W. (1988). The repeat domain of *Escherichia coli* haemolysin (HlyA) is responsible for its Ca2+-dependent binding to erythrocytes. Mol Gen Genet *214*, 553-561.

Ostolaza, H., Bartolome, B., Serra, J.L., de la Cruz, F., and Goni, F.M. (1991). Alpha-haemolysin from *E. coli*. Purification and self-aggregation properties. FEBS Lett *280*, 195-198.

Porollo, A.A., Adamczak, R., and Meller, J. (2004). POLYVIEW: a flexible visualization tool for structural and functional annotations of proteins. Bioinformatics *20*, 2460-2462.

Reimann, S., Poschmann, G., Kanonenberg, K., Stuhler, K., Smits, S.H., and Schmitt, L. (2016). Interdomain regulation of the ATPase activity of the ABC transporter haemolysin B from *Escherichia coli*. Biochem J *473*, 2471-2483.

Rhodes, C.R., Gray, M.C., Watson, J.M., Muratore, T.L., Kim, S.B., Hewlett, E.L., and Grisham, C.M. (2001). Structural consequences of divalent metal binding by the adenylyl cyclase toxin of *Bordetella pertussis*. Arch Biochem Biophys *395*, 169-176.

Rose, T., Sebo, P., Bellalou, J., and Ladant, D. (1995). Interaction of calcium with *Bordetella pertussis* adenylate cyclase toxin. Characterization of multiple calcium-binding sites and calcium-induced conformational changes. J Biol Chem *270*, 26370-26376.

Sotomayor Perez, A.C., Karst, J.C., Davi, M., Guijarro, J.I., Ladant, D., and Chenal, A. (2010). Characterization of the regions involved in the calcium-induced folding of the intrinsically disordered RTX motifs from the *Bordetella pertussis* adenylate cyclase toxin. J Mol Biol *397*, 534-549.

Stein, W.D. (1986). Transport and Diffusion Across Cell Membranes (Academic Press, San Diego).

Thanabalu, T., Koronakis, E., Hughes, C., and Koronakis, V. (1998). Substrate-induced assembly of a contiguous channel for protein export from *E.coli*: reversible bridging of an inner-membrane translocase to an outer membrane exit pore. EMBO J *17*, 6487-6496.

Thomas, S., Bakkes, P.J., Smits, S.H., and Schmitt, L. (2014a). Equilibrium folding of pro-HlyA from *Escherichia coli* reveals a stable calcium ion dependent folding intermediate. Biochim Biophys Acta *1844*, 1500-1510.

Thomas, S., Holland, I.B., and Schmitt, L. (2014b). The Type 1 secretion pathway - the hemolysin system and beyond. Biochim Biophys Acta *1843*, 1629-1641.

Thomas, S., Smits, S.H., and Schmitt, L. (2014c). A simple in vitro acylation assay based on optimized HlyA and HlyC purification. Anal Biochem *464*, 17-23.

Welch, R.A. (2001). RTX toxin structure and function: a story of numerous anomalies and few analogies in toxin biology. Curr Top Microbiol Immunol *257*, 85-111.

Yin, Y., Zhang, F., Ling, V., and Arrowsmith, C.H. (1995). Structural analysis and comparison of the C-terminal transport signal domains of hemolysin A and leukotoxin A. FEBS Lett *366*, 1-5.

Zhang, F., Sheps, J.A., and Ling, V. (1993). Complementation of transport-deficient mutants of *Escherichia coli* alpha-hemolysin by second-site mutations in the transporter hemolysin B. J Biol Chem *268*, 19889-19895.

Zhang, F., Yin, Y., Arrowsmith, C.H., and Ling, V. (1995). Secretion and circular dichroism analysis of the C-terminal signal peptides of HlyA and LktA. Biochemistry *34*, 4193-4201.

Supplementary information

The RTX Repeats of HlyA Interact with the N-terminal Domain of HlyB

Sven Reimann, Michael H.H. Lenders, Sander H.J. Smits and Lutz Schmitt [1]

Institute of Biochemistry, Heinrich-Heine-University Düsseldorf, Universitätsstraße 1, 40225 Düsseldorf, Germany

[1] To whom correspondence should be addressed: Institute of Biochemistry, Heinrich-Heine-University Düsseldorf, Universitätsstraße 1, 40225 Düsseldorf, Germany. Tel.: +49-211-81-10773; Fax: +49-211-81-15310; E-mail: Lutz.Schmitt@hhu.de

Supplementary information comprises:

Supplementary Figure S1

Supplementary Figure S2

Supplementary Table S1

Supplementary Table S2

Literature (supplementary)

Supplementary Figure S1

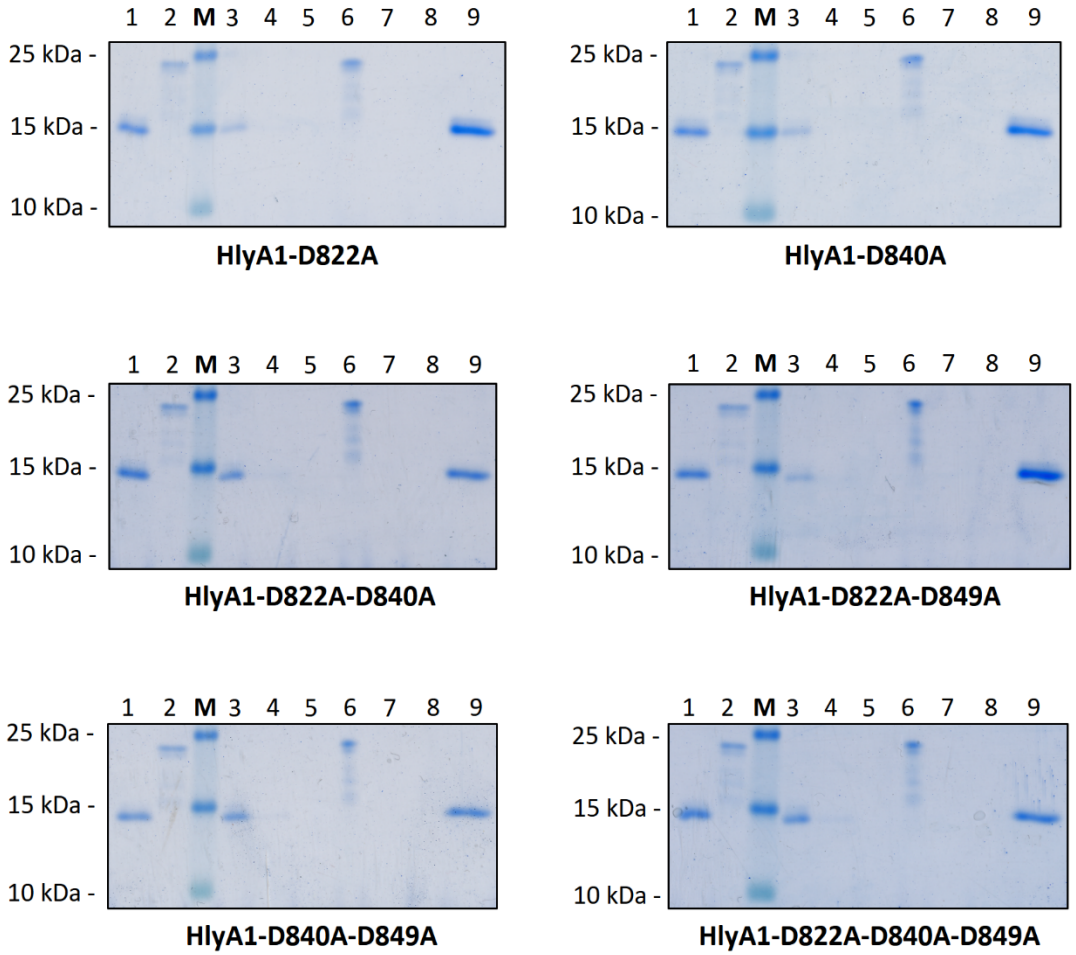

Supplementary Figure S1. Detection of pull-down experiments with Ni-NTA Beads of His_{10}-CLD and HlyA1 variants. (1) His_{10}-CLD; (2) HlyA1-D849A; (3) supernatant after incubation with His_{10}-CLD; (4) and (5) supernatant after first and second washing step with buffer; (6) supernatant after incubation with each HlyA1 variant; (7) and (8) supernatant after third and 7th washing step with buffer, (9) eluted fraction after incubation with buffer supplemented with 300 mM imidazole. His_{10}-CLD has a theoretical mass of 18.5 kDa and HlyA1 variants have a theoretical mass of 24.7 kDa. M, protein weight standard.

Supplementary Figure S2

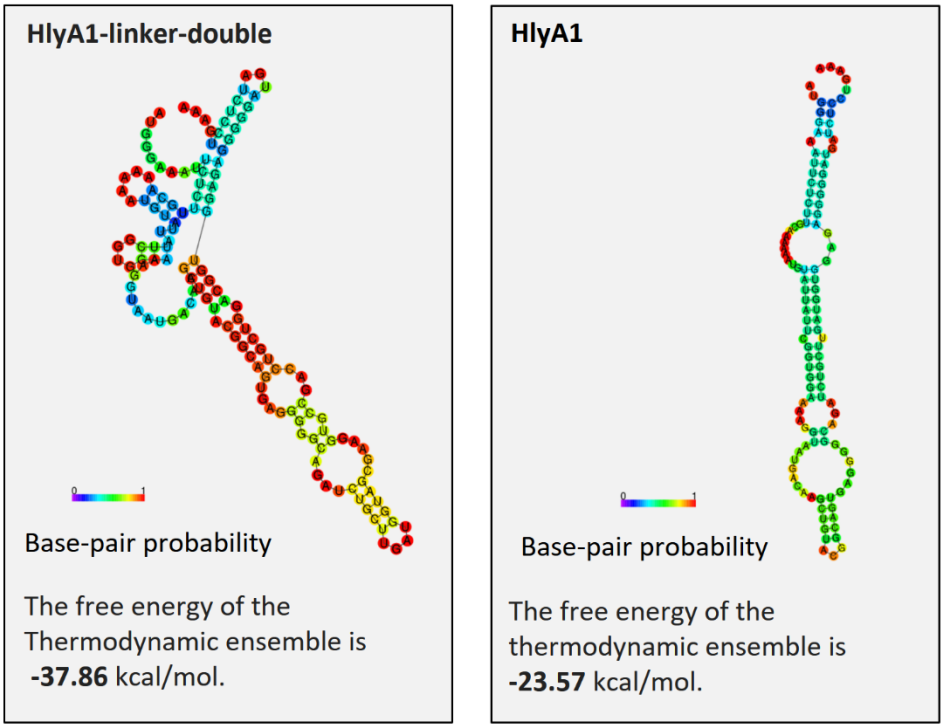

Supplementary Figure S2. Prediction of the secondary structure and free energy of the mRNA of HlyA1 (right) and HlyA1-linker-double (left). The mRNA secondary structure was computational predicted by the RNAfold WebServer (http://rna.tbi.univie.ac.at/cgi-bin/RNAWebSuite/RNAfold.cgi) (Gruber *et al.*, 2008).

Supplementary Table S1

Supplementary Table S1. **Primer for substitutions in HlyA1 with QuikChange PCR.**

Mutated position in HlyA	Sequence (5'→3')
D822A	GGA AAA GGT AAT GCC AAG CTG TAC GG CC GTA CAG CTT GGC ATT ACC TTT TCC
D840A	GAG AGG GGG ATG CTC TCC TGA AAG CTT TCA GGA GAG CAT CCC CCT CTC
D849A	GGC GGA TAT GGT AAT GCT ATT TAT CGT TAT C G ATA ACG ATA AAT AGC ATT ACC ATA TCC GCC

Supplementary Table S2

Supplementary Table S2. Plasmids used in this study.

Name	Description	Reference
pK184-HlyBD	Plasmid encoding *hlyB* and *hlyD*	(Bakkes *et al.*, 2010)
pBADHisHlyB	Plasmid encoding *hlyB*	
pBADHisHlyBΔCLD	Plasmid encoding *hlyBΔCLD*	(Reimann *et al.*, 2016)
pSU2726-HlyA1	Plasmid encoding *hlyA*	(Bakkes *et al.*, 2010)
pSU2726-HlyA1-D822A	Plasmid encoding *hlyA* with the mutation D822A	This study
pSU2726-HlyA1-D840A	Plasmid encoding *hlyA* with the mutation D840A	This study
pSU2726-HlyA1-D849A	Plasmid encoding *hlyA* with the mutation D849A	This study
pSU2726-HlyA1-D822A-D840A	Plasmid encoding *hlyA* with the mutations D822A and-D840A	This study
pSU2726-HlyA1-D822A-D849A	Plasmid encoding *hlyA* with the mutations D822A and-D849A	This study
pSU2726-HlyA1-D840A-D849A	Plasmid encoding *hlyA* with the mutations D840A and D849A	This study
pSU2726-HlyA1-D822A-D840A-D849A	Plasmid encoding *hlyA* with the mutations D822A, D840A and D849A	This study
pSU2726-HlyA1-HlyA1-linker-del	Plasmid encoding *hlyA* with a deletion of residues 826 to 834	This study
pSU2726-HlyA1-HlyA1-linker-GS	Plasmid encoding *hlyA* with a substitution of residues 826 to 834 to GSGSGSGSG	This study

Literature (supplementary)

Bakkes, P.J., Jenewein, S., Smits, S.H., Holland, I.B., and Schmitt, L. (2010). The rate of folding dictates substrate secretion by the *Escherichia coli* hemolysin type 1 secretion system. J Biol Chem *285*, 40573-40580.

Gruber, A.R., Lorenz, R., Bernhart, S.H., Neubock, R., and Hofacker, I.L. (2008). The Vienna RNA websuite. Nucleic Acids Res *36*, W70-74.

Reimann, S., Poschmann, G., Kanonenberg, K., Stuhler, K., Smits, S.H., and Schmitt, L. (2016). Interdomain regulation of the ATPase activity of the ABC transporter haemolysin B from *Escherichia coli*. Biochem J *473*, 2471-2483.

4. Discussion

Uropathogenic *Escherichia coli* (UPEC) strains are one of the frequent causes of urinary tract infections. The toxin haemolysin A (HlyA) is usually produced by UPEC strains and promotes the death of urothelial cells (Nagamatsu *et al.*, 2015). The translocation system of this toxin was discovered in the 1980s and it was the first described example of bacterial protein secretion. The *hly* operon was sequenced first by Felmlee *et al.* (1985b) identifying the putative toxin gene *hlyA*. Later the products of the genes *hlyB* and *hlyD* were located in the bacterial inner membrane and shown to be essential for the translocation (Felmlee *et al.*, 1985a; Felmlee *et al.*, 1985b; Mackman *et al.*, 1985a, b, 1986). Finally in 1990 Wandersman and Delepelaire identified TolC being the third and last piece of the HlyA T1SS (Wandersman *et al.*, 1990).

The topic of this thesis deals with haemolysin B (HlyB), the ATP-binding cassette (ABC) transporter of the HlyA translocation machinery. The major focus points are (i) the establishment of a purification protocol and kinetic analysis of the membrane protein HlyB, (ii) the investigation of the role of the N-terminal C39-peptidase like domain (CLD) of HlyB and (iii) the characterisation of the interactions and regulation of HlyB by the transport substrate HlyA.

4.1. The biphasic modulation of HlyB ATPase activity

In order to investigate HlyB protein *in vitro*, the initial aim of this thesis was the establishment of a protein isolation and purification protocol (Chapter 1). Therefore, overexpressed N-terminally His-tagged HlyB was solubilised from *E. coli* membranes with the detergent Fos-Choline-14. The identification of an appropriate detergent for the solubilisation of the membrane protein is a crucial process and was determined via a dot-blot screening assay (Ellinger *et al.*, 2013; Infed *et al.*, 2011). Since it was shown that harsh detergents such as FC-14 tend to unfold the protein (Kiefer, 2003), the detergent was changed during an immobilized metal-ion-affinity chromatography (IMAC). Here, the protein was exposed to the washing buffer containing the second detergent lauryl maltose neopentyl glycol (LMNG). Thereby LMNG replaced FC-14 and increased the purity as well as the stability of purified HlyB. Lauryl maltoside derivatives were already used to purify the ABC transporter PrtD of the metalloproteases secretion system of *Erwinia chrysanthemi* (Delepelaire, 1994) or TatC of the Tat pathway of *Aquifex aelicus* (Rollauer *et al.*, 2012). The stability of HlyB was also strikingly dependent on the pH-value of the buffer as investigated by several assays during this thesis. It is supposed that the pH-value mediates structural modifications of the protein that changes protein stability and activity, as already suggested for the HlyB nucleotide-binding domain (NBD) (Zaitseva *et al.*, 2004). Also

precise control of the salt concentration was crucial for the subsequent characterisation of HlyB activity *in vitro*. On one side the addition of even low millimolar NaCl concentrations improved the stability of the protein, but on the other side the activity of the protein was reduced simultaneously. This effect was also observed for the isolated HlyB NBD (Benabdelhak *et al.*, 2005). Taken together, a relatively high pH-value and the presence of salt are suggested to trigger the protein to adopt an inactive but stable conformation, while a neutral pH value and the absence of salt activates the protein while decreasing its stability in parallel. Hence, a protocol was established that enables to purify, isolate and store inactive HlyB for several months. The activity can be restored, if necessary, while the protein still retains a moderate and sufficient stability (Reimann *et al.*, 2016) (Chapter 1).

HlyB was characterised *in vitro* and displayed a positive cooperativity in dependence of ATP concentration (Reimann *et al.*, 2016). This behaviour is comparable to systems such as P-glycoprotein, BmrA, maltose and histidine importers (Davidson *et al.*, 1996; Liu *et al.*, 1997; Senior *et al.*, 1998; Steinfels *et al.*, 2004). Additionally, HlyB ATPase activity was quantified in the presence of the transport substrate HlyA. Therefore, HlyA1 was used, which is a shorter, more stable and easier to handle derivative of HlyA. The substrate was unfolded prior to the assays, in order to simulate the cytoplasmic *in vivo* situation as close as possible and as good as we understand it so far. Interestingly, HlyB ATPase activity was decreased by a HlyA1 concentration close to a protein molar ratio of 1:1. Higher substrate amounts increased ATPase activity and further stimulates HlyB velocity to a maximum, at a molar ratio of 1:15 (monomeric HlyB : HlyA1). A biphasic modulation of an ABC transporter was also observed for P-glycoprotein from Chinese Hamster Ovary cell line (CHO CR1R12) or Ehrlich ascites tumour cell lines in the presence of different drugs, however, the ATPase activity was first stimulated and then inhibited with higher drug concentration (Litman *et al.*, 1997a; Litman *et al.*, 1997b). Whether this effect occurred due to an inhibitory site or nonspecific membrane-altering effects was not clear (Litman *et al.*, 1997b). Even for the HlyB NBD an inhibition of ATPase activity was detected previously (Benabdelhak *et al.*, 2003; Koronakis *et al.*, 1993). Here, a fusion protein composed of the NBD-containing C-terminal HlyB fragment and GST was cloned and purified. The fusion protein was exposed to HlyA derivatives and thereby its activity was reduced up to 25 % (Koronakis *et al.*, 1993). The ABC transporter PrtD shares 37 % identity to HlyB and was also investigated concerning ATPase modulation (Delepelaire, 1994). The C-terminal secretion signal of the substrate PrtG inhibited the purified PrtD almost completely even at submicromolar amounts (Delepelaire, 1994). The authors of the study assume an abortive reaction of the *in vitro* system or an early stage of the translocation mechanism (Delepelaire, 1994). The present study and others, which deal with an incomplete secretion system have to take into account, that missing compartments might induce artificial effects. Nevertheless, these results still deliver valuable information in the context of possible protein interactions.

4.2. HlyB obtains multiple substrate binding sites

The activity of the HlyB ABC transporter can be inhibited and stimulated by the transport substrate HlyA, while a CLD-deficient HlyB mutant can be only stimulated (Chapter 1). These findings suggest multiple HlyA binding sites within HlyB, which mediate ATPase inhibition and stimulation independently.

One HlyA binding site was located within the HlyB CLD (Lecher *et al.*, 2012). The studies described in this thesis, showed that a specific interaction of HlyA repeats in toxins (RTX) repeats and the HlyB CLD mediates ATPase inhibition *in vitro* (Reimann *et al.*, 2016) (Chapter 4) (Figure 11 a). This finding was supported by the observation that ATPase inhibition was not inducible in the absence of the CLD. In this context, it was also observed that the most C-terminal HlyA RTX repeat differed concerning HlyB modulation upon interacting with the CLD (Chapter 4). A computational analysis predicted a short α-helix exclusively close to this RTX motif (Chapter 4). So far secondary structure elements of the RTX domain are suggested to be induced only upon calcium ion binding at the outside of the cell (Baumann *et al.*, 1993). Furthermore, the presence of a α-helix was also predicted for the C-terminal secretion signal of HlyA. Here, a potential helix was speculated to be a possible export signal of T1SS substrates (Hess *et al.*, 1990; Holland *et al.*, 1990; Koronakis *et al.*, 1989; Mackman *et al.*, 1987; Stanley *et al.*, 1991).

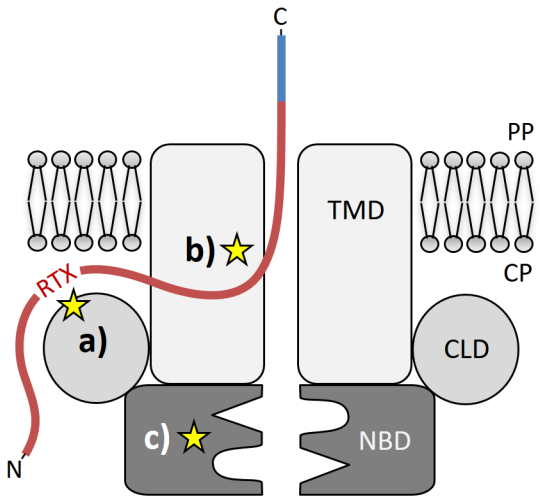

Figure 11. Overview of investigated HlyA and HlyB interactions. A schematic model of a membrane-embedded HlyB dimer (grey). Each monomer contains a transmembrane domain (TMD), a C39-peptidase like domain (CLD) and a nucleotide-binding domain (NBD). The transport substrate (red) harbours the C-terminal secretion signal (blue) and the RTX domain (RTX). Investigated interactions of HlyA and HlyB are marked with a yellow star. a) Interaction of the HlyA RTX domain with the HlyB CLD (Lecher *et al.*, 2012; Reimann *et al.*, 2016) (Chapter 4). b) Interaction of a HlyA sequence region located between the RTX domain and the C-terminal secretion signal and the HlyB TMD (Reimann *et al.*, 2016). c) Interaction of the HlyA secretion signal and the HlyB NBD (Benabdelhak *et al.*, 2003). PP, periplasm; CP, cytoplasm.

Since these show low sequence conservation, it has been suggested that secondary structure elements play a crucial role for the transport process. In summary, the substrate was shown to modulate HlyB ATPase activity in two different ways upon an interaction to the CLD (Chapter 4). First, the interaction of the RTX domains is suggested to induce an ATPase inhibition (Lecher *et al.*, 2012; Reimann *et al.*, 2016). Second, the most C-terminal RTX repeat additionally effects ATPase stimulation, however, this interaction is not sufficient for stimulation (Chapter 4). These findings suggest a differentiation of the RTX repeats by the CLD. The most C-terminal RTX repeat might be recognized due to its terminal position, by a second binding sites within the CLD and/or due to potential secondary structure close this motif. Anyway, these suggestions are fragile and need further investigation. Cross-linking experiments of HlyA and the CLD followed by a subsequent mass spectrometry analysis revealed the distinct interaction pattern of both proteins. The incorporation of unnatural photoactivatable amino acids into HlyA has been established during this thesis (Chapter 3).

Stimulation of HlyB ATPase activity upon interaction with the transport substrate, was shown to be independent of the CLD and thereby suggesting a further binding site. Cross-linking experiments of HlyB and a HlyA1 derivative that lacks the C-terminal secretion signal (HlyA2) point to a distinct substrate to HlyB transmembrane domain (TMD) interaction, which might mediate ATPase stimulation (Figure 11 b). The cross-linked peptides included on one side a fragment of the HlyB TMD (discussed later, Figure 13, blue residue) and on the other side a HlyA fragment between the RTX domain and the secretion signal (Reimann *et al.*, 2016). Interestingly, the cross-linked amino acid of the TMD faces into the putative translocation path of the HlyB model (Figure 13). These residues may harbour crucial parts of a substrate recognition pattern, but this was not investigated in further detail during this thesis. The cross-linked fragment was detected with a 1:20 molar ratio of HlyB and HlyA2, corresponding to the maximum HlyB ATPase stimulation. In contrast, this cross-link product was not detected with a 1:1 molar ratio, corresponding to the maximum HlyB ATPase inhibition. The presence of a second binding site is also probable, since ATPase stimulation still occurs in the absence of the first binding site located at the CLD (HlyBΔCLD) (Reimann *et al.*, 2016). Taken together, these data suggest an interaction of HlyA2 and the TMD. However, an interaction of HlyA2 and the NBD that mediates stimulation cannot be excluded by these results. To shed further light on this question, the cross-linked residues within the TMD, which represent the putative interacting amino acids, could be substituted and investigated for ATPase stimulation by the substrate *in vitro*. A suitable mutation would be HlyB-K322W, which was already shown to mediate a reduced secretion rate of HlyA *in vivo* (Reimann *et al.*, 2016). Here, it is not clear whether the secretion rate was reduced due to sterically effects within the translocation path or due to a reduced interaction that mediates e.g. transport stimulation. Also the stimulatory sequence motif of the substrate could be identified by a set of HlyA1 mutations. A substrate variant with deleted

residues between the RTX domain and the secretion signal could be investigated also for its stimulatory competence on HlyB *in vitro* and the secretion rate *in vivo*.

The described interactions so far were observed in the absence the C-terminal secretion signal, however, it is necessary for translocation as a matter of course (Thanabalu *et al.*, 1998). An additional interaction was observed, which occurred exclusively with the secretion signal of HlyA and the isolated HlyB NBD (Benabdelhak *et al.*, 2003) (Figure 11 c). This can be assumed at least as the third binding site of the substrate, however, ATPase inhibition and stimulation of HlyB were observed in the absence of the secretion signal. Taking together all evidence, HlyB is suggested to harbour multiple binding sites for its transport substrate.

4.3. The multifunctional N-terminal domain of HlyB

The N-terminal CLD of HlyB constitutes an inactive C39 cysteine protease, which is essential for the secretion of HlyA (Lecher *et al.*, 2012). It was shown to interact exclusively with the unfolded and not with the folded HlyA1, a truncated derivative of the transport substrate HlyA. Even HlyA2, a variant of HlyA1 that lacks the C-terminal secretion signal binds to the CLD.

4.3.1. The CLD as a chaperone

RTX proteins such as HlyA are translocated across both membranes in an unfolded state by their cognate T1SS (Bakkes *et al.*, 2010). These proteins vary greatly in size and extend frequently the size of 100 kDa. In most cases the peptide sequence obtains a C-terminal secretion signal, which arises the question how these proteins are kept in a secretion competent state during protein translation.

The ABC transporters of T1SSs were divided into three groups regarding their N-terminal domains (Kanonenberg *et al.*, 2013). The first group harbours C39-peptidase containing ABC transporters (PCATs) and translocates e.g. bacteriocins (mostly Gram-positive bacteria) and microcins (Gram-negative bacteria) (substrates < 10 kDa) (Gebhard, 2012; Lin *et al.*, 2015). The transport substrates contain an N-terminal leader peptide with a double glycine (GG) motif (Havarstein *et al.*, 1994; Holo *et al.*, 1991; Klaenhammer, 1993; Muriana *et al.*, 1991). The ABC transporter, containing a C39-peptidase domain, recognizes this motif and cleaves it at the C-terminal site of the GG motif (Havarstein *et al.*, 1995). So far no chaperone has yet been identified for this group and it seems likely that the interaction of the leader peptide and the C39 peptidase are involved in this function. However, the N-terminal leader peptide does not exclude a co-translational secretion process.

The HasA secretion system is one of the best-characterised T1SS and belongs to the second group of ABC transporters, which contain no additional regulatory domain. The relatively small iron scavenger

protein HasA has a weight of 19 kDa and is not a member of the RTX proteins. It obtains primary recognition sites that are shown to be required for the interaction with the cognate ABC transporter HasD (Masi *et al.*, 2010). Furthermore, HasA was shown to be kept in an unfolded state by SecB prior to the secretion process (Delepelaire *et al.*, 1998). However, HasA is a small protein, it tends to fold in the cytoplasm and it depends on the "anti-folding" activity of SecB (Debarbieux *et al.*, 2001). In contrast, so far no chaperone was identified in the case of the transport substrates of other ABC transporters belonging to this group. Nevertheless, it has to be taken into account that these substrates are in general relatively small in comparison to RTX proteins. The assumption that HasA dependency on SecB is an exception in this group, rises the question whether these proteins do need a chaperone to remain unfolded within the cell.

The ABC transporter of the HlyA T1SS belongs to the third group in this comparison and contains an N-terminal CLD. Since the HlyA T1SS was shown to be independent of the chaperone SecB it was very likely that another cytoplasmic protein or domain has to fulfil this function (Bakkes *et al.*, 2010). So far no chaperone could be identified, however, strong indications were provided by a proven interaction of exclusively unfolded HlyA and the CLD (Lecher *et al.*, 2012). Here, it was suggested that the RTX repeats of HlyA interact with the CLD and thereby tethering the substrate and preventing it from aggregation. During the studies of this PhD thesis mutations within each RTX repeat of HlyA1 and diverse mutational combination were cloned, purified and analysed concerning this question. It was shown that mutations of the RTX repeats decreased the interaction to the CLD (Chapter 4). Interestingly, the *in vivo* secretion rate of these proteins was not affected by the mutations and was comparable to the secretion rate of the wild-type protein (Chapter 4). These proteins may not tend to fold in the cytoplasm due to their relatively small size in comparison to other RTX proteins and this possibly explains the optimal secretion rate even independent of the chaperone-like function of the CLD. In contrast, the high standard deviation of the secretion assay may hide differences of the secretion rate and thereby changing the conclusion.

Here, further investigations are necessary. The described mutations could be also introduced in HlyA wild-type protein and investigated concerning their affect on the secretion rate *in vivo*. Preventing a protein of this increased size from its interaction to the potential CLD chaperone-like function could magnify secretion rate differences. Furthermore, instead of single residue substitutions within the RTX repeats, substitutions or deletions of complete RTX motifs could be investigated concerning *in vitro* HlyB ATPase modulation and *in vivo* secretion. Further experiments that investigate the actual folding process of HlyA would enlighten the role of the CLD as a chaperone. An appropriate technique to analyse the time-resolved folding of HlyA could be H/D exchange in the presence and the absence of the CLD coupled to a subsequent mass spectrometry analysis. Hereby CLD-shielded amino acid regions of HlyA could be identified and also the effect of point mutations within the CLD could be analysed.

This technique was widely used for soluble proteins and emerges also for membrane-embedded proteins such as BmrA, HIV-1 Nef (Mehmood *et al.*, 2012; Pirrone *et al.*, 2015) and others (Duc *et al.*, 2015; Hebling *et al.*, 2010; Koshy *et al.*, 2013; Orban *et al.*, 2015) [reviewed in (Vadas *et al.*, 2017)].

4.3.2. The CLD acts as an autoinhibitor and beyond

The deletion of the N-terminal CLD of HlyB increased the maximum basal ATPase activity by about 15 fold and thereby highlights at least one of its functions (Reimann *et al.*, 2016). A kind of regulatory inhibiting function of terminal domains was already observed and described for a large variety of proteins such as SpoIIIE, TrwK or EccC (Besprozvannaya *et al.*, 2013; Pena *et al.*, 2011; Rosenberg *et al.*, 2015). For these proteins the affecting domains are located N-terminally or C-terminally as in the case of Ca^{2+}-ATPases or H^{+}-ATPases, respectively (Harper *et al.*, 1998; Palmgren *et al.*, 1990; Palmgren *et al.*, 1991). For these ATPases the removal of the regulatory autoinhibitory domain increased the hydrolytic activity, which is according to the increased basal activity of HlyBΔCLD described in this thesis (Reimann *et al.*, 2016). The results about the C-terminal domain of TrwK, a member of the VirB4 family, are also in good agreement to the results shown in this thesis. Pena *et al.* (2011) removed three α-helices of a C-terminal autoinhibitory domain of TrwK and measured a 10 fold increased ATP hydrolysis while the remaining kinetic parameters were not affected. Also HlyB and HlyBΔCLD kinetic values only differ in the V_{max} value, indicating that the CLD deletion did not induce conformational changes in the NBD (Reimann *et al.*, 2016). Taken together, these results indicate that even the CLD acts as an autoinhibitory domain and prevents futile ATP hydrolysis.

The autoinhibitory domains of H^{+}-ATPase and P_{2B} Ca^{2+}-ATPase are suggested to be relieved following binding of a small protein, inducing a conformational change that results in increased ATPase activity (Baekgaard *et al.*, 2005; Pena *et al.*, 2011). Since HlyB is a functional dimer the binding of two substrate molecules to one HlyB dimer seems plausible. This hypothesis is supported by the experimental results of this PhD thesis. The maximum inhibition of HlyB ATPase activity by HlyA1 was observed with a molar ratio of about 1:1 (monomeric HlyB : HlyA2) and higher concentrations of the substrate increased hydrolytic activity (Reimann *et al.*, 2016) (Figure 12). Interestingly, although all necessary signals to stimulate ATPase hydrolysis are present, a molar symmetry (1:1) seems to be mandatory to relieve inhibition. It appears plausible that the relieve of one autoinhibitory domain and thereby the "activation" of only one NBD is not sufficient to hydrolyse ATP, since both NBDs are essential for hydrolysis (Jones *et al.*, 2002; Smith *et al.*, 2002; Zaitseva *et al.*, 2005b). The mutant HlyBΔCLD does not contain the autoinhibitor and it can be stimulated by transport substrate concentrations below a 1:1 molar ratio. This clearly shows stimulation and inhibition are two separately controlled mode of action of HlyB.

Assuming that an equimolar substrate to autoinhibitor (CLD) interaction relieves any HlyB ATPase inhibitory effects, how is it possible that HlyA RTX repeat mutants stimulated ATPase activity even below equimolar concentrations (Figure 12) (Chapter 4)? These mutants were shown to be unable to interact with the CLD anymore and thereby they should not be able to relieve the autoinhibitor at any concentration. These findings seem to be in contrast to the model of the CLD as a solely autoinhibitory domain. One explanation would be that even inhibition is also the result of a substrate to CLD binding. Therefore, inhibition only takes place if the substrate is able to bind to the CLD in the first place and thereby somehow leading to a molar dependency to relieve inhibition subsequently. Substrates that are not even able to bind to the CLD would avoid an inhibition and thereby a molar ratio dependency for ATPase stimulation. The reason why all three investigated RTX repeats have to remain unaltered to mediate this HlyB ATPase inhibition is not understood so far.

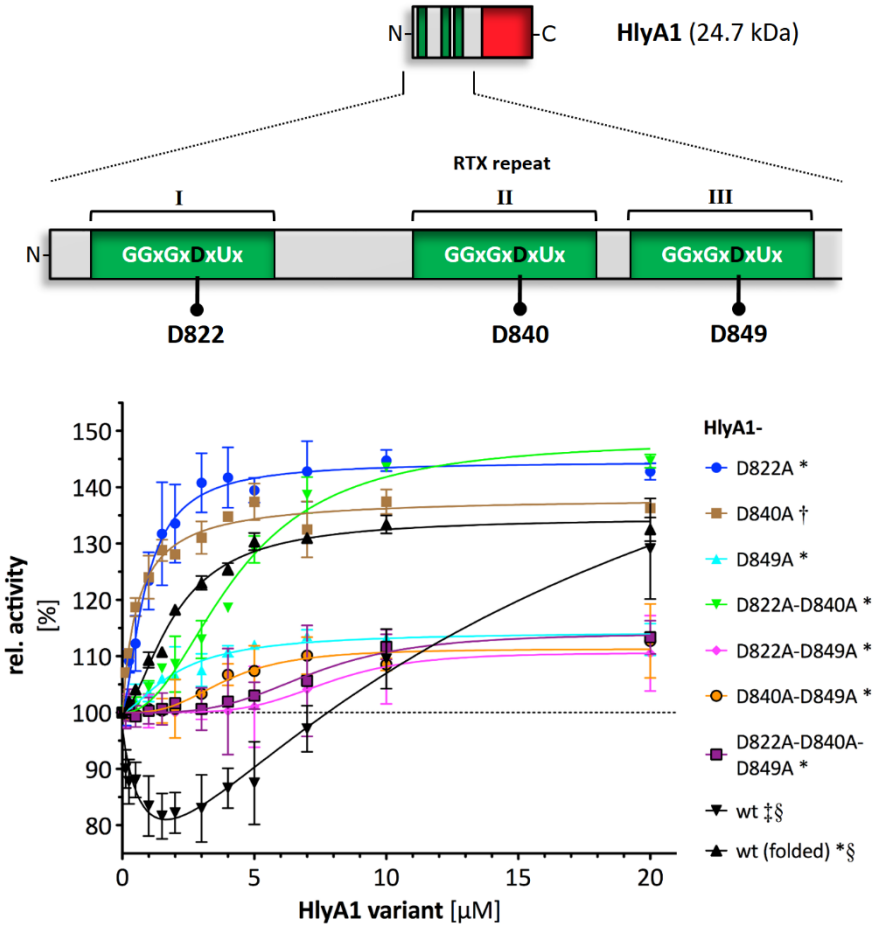

Figure 12. ATPase activity of HlyB in the presence of HlyA1 variants. Experimental results of HlyB ATPase activity in the presence of HlyA1 variants containing mutations within the RTX repeats. * Datasets were analysed according to eqn (1), Hill equation; † Datasets were analysed according to eqn (2), Michaelis–Menten equation; ‡ Datasets were analysed according to eqn (3), which assumes two independent binding sites. For the equations see Chapter 4. § Data published and adapted from Reimann *et al.* (2016). Results are means ± S.D.

Interestingly, the results showed that as long as the most C-terminal RTX repeat of HlyA1 is not mutated, the maximum stimulation of HlyB was less affected, while a mutation of this RTX repeat decreased the maximum velocity significantly (Figure 12). ATPase assays with HlyBΔCLD and these mutants revealed no negative impact on the stimulatory properties of the substrate (Chapter 4). This also indicates that this C-terminal RTX repeat solely interacts with the CLD and thereby affecting the stimulatory process, however, this interaction is not sufficient for stimulation. A computational analysis predicted a α-helix exclusively close to this RTX repeat, which may also stress out its distinguished function. One explanation bases on the structural information of PCAT1 (Lin *et al.*, 2015) and the homology model of HlyB (see Chapter 1.5.3. The ABC transporter – HlyB). The PCAT1 peptidase domain was shown to dock onto the lateral openings of the two TMDs and the HlyB CLD engages an analogous position within the HlyB model (Lin *et al.*, 2015) (Figure 13). The hydrolytic domain of PCAT1 is supposed to cleave the leader peptide and matches perfectly to position the substrate into the translocation pathway (Lin *et al.*, 2015). The degenerated catalytic centre of the HlyB CLD may also recruit the substrate into the translocation pathway, however, it does not hydrolyse the peptide (Figure 13, cyan). This function could be investigated by distinct mutations and subsequent ATPase assays.

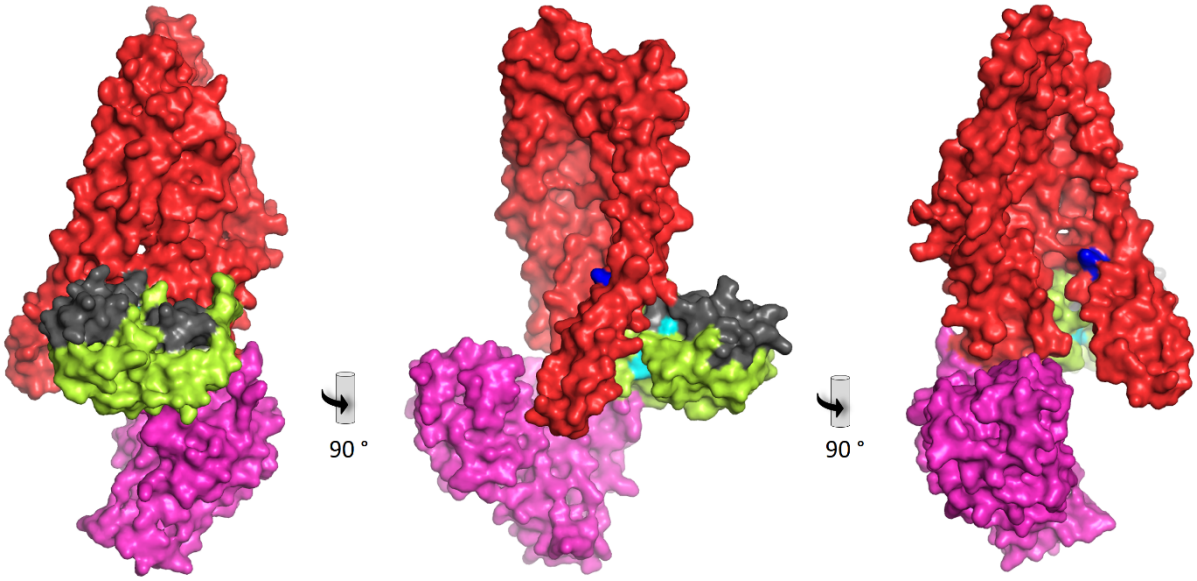

Figure 13. Schematic model of the HlyB monomer and putative substrate interaction sites. The model of HlyB was predicted using Phyre2 and bases on PCAT1 (see Chapter 1.5.3) (Kelley *et al.*, 2015; Lin *et al.*, 2015). The images show the same model from different perspectives. The peptide is shown in a surface representation and colored in green (CLD), red (TMD) and magenta (NBD). The CLD amino acids, which were shown to interact with HlyA1 are highlighted in black (Lecher *et al.*, 2012). The degenerated active centre is located close to the lateral openings and highlighted in cyan. The TMD residue, which was shown by cross-linking experiments to be in close distance to HlyA2, is marked in blue (Reimann *et al.*, 2016).

HlyB ATPase assays with the mutated substrate and a quantification of the *in vivo* secretion rate could answer this question. Furthermore, surface plasmon resonance spectroscopy of these mutants and the substrate could determine the dissociation constants.

Taken together, the general RTX repeats of HlyA are supposed to be tethered by the CLD and benefit from the chaperone-like function (Lecher *et al.*, 2012; Reimann *et al.*, 2016). The binding region of the RTX repeats was located within the CLD on the opposite site of the degenerated catalytic centre (Figure 13) (Lecher *et al.*, 2012). In addition, the most C-terminal RTX repeat, which encodes the predicted α-helix, may hypothetically bind to the degenerated catalytic centre of the CLD. This interaction would be located close to the lateral opening of the TMDs and threading the substrate into the translocation pathway, where ATPase stimulation would be mediated. In this model, an abolished interaction of the C-terminal RTX repeat and the CLD, e.g. by a mutation, would thereby hinder the threading of the substrate and impair the stimulatory process.

Additional experiments are necessary to identify the substrate translocation path entrance within HlyB and further the translocation pathway within the TMDs of HlyB. Cross-linking experiments of the stalled transport substrate within the T1SS could covalently attach HlyA to its most proximate amino acids within HlyB. A subsequent mass spectrometry analysis of cross-linked peptides could reveal a map of the translocation pathway. The incorporation of unnatural amino acids into HlyA and also the purification of this modified protein are described in this thesis (Chapter 3). In addition, first *in vitro* and *in vivo* cross-linking experiments were performed and provide a basis to establish this technique for the HlyA T1SS (Chapter 3).

4.4. A model of the HlyA T1SS

Cross-linking studies of Thanabalu *et al.* (1998) demonstrated that the ABC transporter HlyB and the membrane fusion protein haemolysin D (HlyD) assemble as a stable complex in the absence of HlyA and TolC. This conformation of the IM complex in the absence of the transport substrate may represent the resting state of HlyB *in vivo*. Upon translation of the HlyA peptide it is most likely that the N-terminal amino acids reach the IM complex first. Depending on the stringency of the criterion of the RTX consensus motif, HlyA is supposed to obtain up to 17 RTX repeats (Linhartova *et al.*, 2010), however, only six RTX repeats contain the strict consensus motif (Uniprot: P08715). In order to keep the transport substrate in an unfolded and translocation competent state, the putative RTX repeats could interact with the HlyB CLD and benefit from the chaperone-like function (Lecher *et al.*, 2012; Reimann *et al.*, 2016). Furthermore, it was shown that the cytosolic domain of HlyD interacts with HlyA (Balakrishnan *et al.*, 2001). The distinct interaction sites were not described so far, nonetheless it is crucial for the assembly of the translocon (Thanabalu *et al.*, 1998). Upon this interaction HlyD recruits

the outer membrane factor TolC by its periplasmic domain, while a direct interaction of HlyB and TolC was excluded (Lee *et al.*, 2012; Thanabalu *et al.*, 1998). These steps seem to be independent of ATP hydrolysis, since substrate interaction and TolC recruitment were also shown with a HlyB mutant that binds, but did not hydrolyse ATP (Thanabalu *et al.*, 1998).

So far it is not clear whether HlyA translocation occurs co- or posttranslational. For the sake of discussion a posttranslational translocation is assumed to simplify the model. The completed translation of the HlyA peptide will finally enable C-terminal sequence regions to reach the assembled translocon, so does the most C-terminal RTX repeat. As discussed above, this RTX repeats encodes a predicted α-helix, which may bind to the degenerated catalytic centre of the CLD (Chapter 4). This binding site of the CLD is assumed to be located close to the lateral openings of the TMDs and maybe threading the substrate into the translocation pathway. As shown by cross-linking experiments in this thesis, amino acids located downstream of this predicted α-helix and around 80 residues upstream of the secretion signal were already located within the TMDs interface (Reimann *et al.*, 2016). This interaction was only found with ATPase stimulatory substrate concentrations and thereby indicating the putative entrance of the translocation pathway. Subsequently, another HlyA molecule or even the N-terminus of the same, could bind to the opposite CLD of the HlyB dimer, thereby negating its autoinhibitory function and initiating the translocation.

The detailed path of the secretion signal during the threading process remains ambiguous. In general, the HlyA secretion signal is supposed to initiate the translocation and it is known to be essential for secretion itself (Gray *et al.*, 1989; Gray *et al.*, 1986; Kenny *et al.*, 1991). Lenders *et al.* (2015) demonstrated that the C-terminus of HlyA leads the transport substrate through the translocation pathway and it is exposed first at the outside of the cell (Lenders *et al.*, 2015). Therefore, the secretion signal can also be assumed to thread into the translocation pathway first. Simultaneously, the CLD could support this step at the entrance of the TMD dimer interface, upon an interaction with the upstream RTX repeat as described above. One has to take into account, that the secretion signal was also shown to bind to the HlyB NBD (Benabdelhak *et al.*, 2003). So far, the effect and the relevance of this interaction is not clear in a mechanistic context. Anyway, the interaction was measured with the isolated NBD and therefore, this result does not exclude an interaction of the TMD and the secretion signal, as described above. Additionally, this thesis demonstrated a secretion signal independent stimulation of HlyB ATPase activity *in vitro* (Reimann *et al.*, 2016). In combination, this raises the question for the role of the secretion signal, however, it is assumed to be essential for initiation and recognition, although detailed evidence is missing.

Substrate interactions are supposed to mediate conformational changes and / or ATP hydrolysis, which go along with the translocation process. Jones *et al.* (2002) suggested that ATP hydrolysis is connected to a rotational flexibility of the NBD α-subdomain, which is controlled by the TMDs (Jones *et al.*, 2002).

In response to substrate binding, the TMDs traverse a structural reorganisation and mediate this signal to the NBDs (Jones *et al.*, 2002). To investigate this assumption for the HlyA T1SS, the Pro-loop could be mutated and this would disturb and interdomain communication, as it was shown for HisP (Hung *et al.*, 1998). This mutation (P624) was already investigated *in vivo* by Koronakis *et al.* and it was shown to result in a reduced HlyA secretion rate (Koronakis *et al.*, 1995). The additional investigation of its influence on HlyB ATPase activity modulation *in vitro* would shed further light on the role of ATP hydrolysis.

4.4.1. Energization of the translocation process

The observed stimulation of HlyB ATP hydrolysis leads to the question of its role during the translocation process. Studies already showed that complex assembly is independent of ATP hydrolysis while the translocation process relies on it (Lenders *et al.*, 2015; Thanabalu *et al.*, 1998). In general, two modes of action can be assumed: (a) an iterative, sequential mode where ATP hydrolysis energises the translocation process and the length of the translocated peptide/protein correlates directly to the amount of consumed ATP. Hereby the translocation machinery recognises every single polypeptide by the peptide bond or it recognises units of a certain length. This mode of action was described for the translocation by SecA (Schiebel *et al.*, 1991; Uchida *et al.*, 1995). Here, about 30 amino acids are translocated by the consumption of one ATP molecule (Uchida *et al.*, 1995). (b) ATP hydrolysis only starts the translocation process of the whole polypeptide in a one-step mode.

Experiments in this thesis suggest that ATP velocity is not coupled to the secretion rate of the transport substrate (Chapter 4). Different mutants of HlyA showed first comparable substrate translocation rates *in vivo* and second varying effects on HlyB ATPase modulation *in vitro*. For example, a mutation within the most C-terminal RTX repeat of HlyA1 stimulated HlyB ATPase activity *in vitro* by about 10 %, while wild-type HlyA1 stimulated ATPase activity by about 30 %. In contrast, both substrates were translocated with comparable secretion rates *in vivo* (Chapter 4). These results indicate that the intensity of HlyB ATPase stimulation is not relevant for the substrate secretion rate, otherwise a correlation of *in vitro* ATPase velocity and *in vivo* secretion rate would be present. Thereby, these results suggest that the substrate molecule once triggers a switch-like mechanism, initiating the translocation process, rather than keeping ATP hydrolysis on a constant level. This is also supported by the observation that ATP binding or hydrolysis diminishes the interaction of the HlyA secretion signal and the NBD (Benabdelhak *et al.*, 2003). Taken together, an image occurs, which suggests HlyB to open a translocation path upon ATP binding.

Further open questions are first, the driving force that triggers the substrate out of the translocation channel and second, the signal that releases the translocon. Bumba *et al.* (2016) showed with a detailed study of the adenylate cyclase toxin-haemolysin (CyaA) the “push-ratchet” mechanism, which

could represent a general folding pathway of T1SS RTX substrates. The proposed mechanism involves an initial folding of the substrate C-terminus upon Ca^{2+} binding at the outside of the cell and thereby the substrate is prevented from backsliding. This results in Brownian ratchets and accelerates the forward movement of the substrate (Bumba *et al.*, 2016). Presumably, this mechanism is not relevant for the HlyA T1SS, since it was shown to be independent of the extracellular Ca^{2+} concentration (Lenders *et al.*, 2016). The final signal, which releases the translocon was not determined yet. Potentially the simple absence of the transport substrate could initiate the disassembly of the translocon. The discussion in this thesis also proposes the simultaneous binding of two substrate molecules to the HlyB dimer, one interacting with each CLD. This raises the possibility of an iterative substrate threading into the transporter, alternating from both sides. Thereby the next translocation process would be ready to start.

5. Literature

Al-Shawi, M.K. (2011). Catalytic and transport cycles of ABC exporters. Essays Biochem *50*, 63-83.

Alami, M., Luke, I., Deitermann, S., Eisner, G., Koch, H.G., Brunner, J., and Muller, M. (2003). Differential interactions between a twin-arginine signal peptide and its translocase in *Escherichia coli*. Mol Cell *12*, 937-946.

Alvarez-Martinez, C.E., and Christie, P.J. (2009). Biological diversity of prokaryotic type IV secretion systems. Microbiol Mol Biol Rev *73*, 775-808.

Ambudkar, S.V., Kim, I.W., Xia, D., and Sauna, Z.E. (2006). The A-loop, a novel conserved aromatic acid subdomain upstream of the Walker A motif in ABC transporters, is critical for ATP binding. FEBS Lett *580*, 1049-1055.

Ames, G.F., Mimura, C.S., and Shyamala, V. (1990). Bacterial periplasmic permeases belong to a family of transport proteins operating from *Escherichia coli* to human: Traffic ATPases. FEMS Microbiol Rev *6*, 429-446.

Andersen, C., Hughes, C., and Koronakis, V. (2001). Protein export and drug efflux through bacterial channel-tunnels. Curr Opin Cell Biol *13*, 412-416.

Anderson, M., Chen, Y.H., Butler, E.K., and Missiakas, D.M. (2011). EsaD, a secretion factor for the Ess pathway in *Staphylococcus aureus*. J Bacteriol *193*, 1583-1589.

Anes, J., McCusker, M.P., Fanning, S., and Martins, M. (2015). The ins and outs of RND efflux pumps in *Escherichia coli*. Front Microbiol *6*, 587.

Angot, A., Vergunst, A., Genin, S., and Peeters, N. (2007). Exploitation of eukaryotic ubiquitin signaling pathways by effectors translocated by bacterial type III and type IV secretion systems. PLoS Pathog *3*, e3.

Argos, P. (1990). An investigation of oligopeptides linking domains in protein tertiary structures and possible candidates for general gene fusion. J Mol Biol *211*, 943-958.

Atmakuri, K., Cascales, E., and Christie, P.J. (2004). Energetic components VirD4, VirB11 and VirB4 mediate early DNA transfer reactions required for bacterial type IV secretion. Mol Microbiol *54*, 1199-1211.

Badtke, M.P., Hammer, N.D., and Chapman, M.R. (2009). Functional amyloids signal their arrival. Sci Signal *2*, pe43.

Baekgaard, L., Fuglsang, A.T., and Palmgren, M.G. (2005). Regulation of plant plasma membrane H+- and Ca2+-ATPases by terminal domains. J Bioenerg Biomembr *37*, 369-374.

Bakas, L., Ostolaza, H., Vaz, W.L., and Goni, F.M. (1996). Reversible adsorption and nonreversible insertion of *Escherichia coli* alpha-hemolysin into lipid bilayers. Biophys J *71*, 1869-1876.

Bakkes, P.J., Jenewein, S., Smits, S.H., Holland, I.B., and Schmitt, L. (2010). The rate of folding dictates substrate secretion by the *Escherichia coli* hemolysin type 1 secretion system. J Biol Chem *285*, 40573-40580.

Balakrishnan, L., Hughes, C., and Koronakis, V. (2001). Substrate-triggered recruitment of the TolC channel-tunnel during type I export of hemolysin by *Escherichia coli*. J Mol Biol *313*, 501-510.

Ball, G., Durand, E., Lazdunski, A., and Filloux, A. (2002). A novel type II secretion system in *Pseudomonas aeruginosa*. Mol Microbiol *43*, 475-485.

Bangia, N., Lehner, P.J., Hughes, E.A., Surman, M., and Cresswell, P. (1999). The N-terminal region of tapasin is required to stabilize the MHC class I loading complex. Eur J Immunol *29*, 1858-1870.

Baptista, C., Barreto, H.C., and Sao-Jose, C. (2013). High levels of DegU-P activate an Esat-6-like secretion system in *Bacillus subtilis*. PLoS One *8*, e67840.

Basler, M., Pilhofer, M., Henderson, G.P., Jensen, G.J., and Mekalanos, J.J. (2012). Type VI secretion requires a dynamic contractile phage tail-like structure. Nature *483*, 182-186.

Baumann, U., Wu, S., Flaherty, K.M., and McKay, D.B. (1993). Three-dimensional structure of the alkaline protease of *Pseudomonas aeruginosa*: a two-domain protein with a calcium binding parallel beta roll motif. EMBO J *12*, 3357-3364.

Bavro, V.N., Pietras, Z., Furnham, N., Perez-Cano, L., Fernandez-Recio, J., Pei, X.Y., Misra, R., and Luisi, B. (2008). Assembly and channel opening in a bacterial drug efflux machine. Mol Cell *30*, 114-121.

Baykov, A.A., Evtushenko, O.A., and Avaeva, S.M. (1988). A malachite green procedure for orthophosphate determination and its use in alkaline phosphatase-based enzyme immunoassay. Anal Biochem *171*, 266-270.

Beck, K., Eisner, G., Trescher, D., Dalbey, R.E., Brunner, J., and Muller, M. (2001). YidC, an assembly site for polytopic *Escherichia coli* membrane proteins located in immediate proximity to the SecYE translocon and lipids. EMBO Rep *2*, 709-714.

Beck, K., Wu, L.F., Brunner, J., and Muller, M. (2000). Discrimination between SRP- and SecA/SecB-dependent substrates involves selective recognition of nascent chains by SRP and trigger factor. EMBO J *19*, 134-143.

Becker, J.P., Van Bambeke, F., Tulkens, P.M., and Prevost, M. (2010). Dynamics and structural changes induced by ATP binding in SAV1866, a bacterial ABC exporter. J Phys Chem B *114*, 15948-15957.

Benabdelhak, H., Kiontke, S., Horn, C., Ernst, R., Blight, M.A., Holland, I.B., and Schmitt, L. (2003). A Specific Interaction Between the NBD of the ABC-transporter HlyB and a C-Terminal Fragment of its Transport Substrate Haemolysin A. Journal of Molecular Biology *327*, 1169-1179.

Benabdelhak, H., Schmitt, L., Horn, C., Jumel, K., Blight, M.A., and Holland, I.B. (2005). Positive co-operative activity and dimerization of the isolated ABC ATPase domain of HlyB from *Escherichia coli*. Biochem J *386*, 489-495.

Berg, J., Tymoczko, J., and Stryer, L. (2002). Biochemistry (New York: W.H. Freeman).

Berks, B.C., Palmer, T., and Sargent, F. (2005). Protein targeting by the bacterial twin-arginine translocation (Tat) pathway. Curr Opin Microbiol *8*, 174-181.

Berntsson, R.P., Smits, S.H., Schmitt, L., Slotboom, D.J., and Poolman, B. (2010). A structural classification of substrate-binding proteins. FEBS Lett *584*, 2606-2617.

Besprozvannaya, M., Pivorunas, V.L., Feldman, Z., and Burton, B.M. (2013). SpoIIIE protein achieves directional DNA translocation through allosteric regulation of ATPase activity by an accessory domain. J Biol Chem *288*, 28962-28974.

Biemans-Oldehinkel, E., Doeven, M.K., and Poolman, B. (2006a). ABC transporter architecture and regulatory roles of accessory domains. FEBS Lett *580*, 1023-1035.

Biemans-Oldehinkel, E., Mahmood, N.A., and Poolman, B. (2006b). A sensor for intracellular ionic strength. Proc Natl Acad Sci U S A *103*, 10624-10629.

Blanco, L.P., Evans, M.L., Smith, D.R., Badtke, M.P., and Chapman, M.R. (2012). Diversity, biogenesis and function of microbial amyloids. Trends Microbiol *20*, 66-73.

Blenner, M.A., Shur, O., Szilvay, G.R., Cropek, D.M., and Banta, S. (2010). Calcium-induced folding of a beta roll motif requires C-terminal entropic stabilization. J Mol Biol *400*, 244-256.

Bohm, A., Diez, J., Diederichs, K., Welte, W., and Boos, W. (2002). Structural model of MalK, the ABC subunit of the maltose transporter of *Escherichia coli*: implications for mal gene regulation, inducer exclusion, and subunit assembly. J Biol Chem *277*, 3708-3717.

Boyer, P.D. (1997). The ATP synthase - a splendid molecular machine. Annu Rev Biochem *66*, 717-749.

Bradley, D.E. (1980). Morphological and serological relationships of conjugative pili. Plasmid *4*, 155-169.

Breydo, L., Wu, J.W., and Uversky, V.N. (2012). Alpha-synuclein misfolding and Parkinson's disease. Biochim Biophys Acta *1822*, 261-285.

Brooks, H.J., O'Grady, F., McSherry, M.A., and Cattell, W.R. (1980). Uropathogenic properties of *Escherichia coli* in recurrent urinary-tract infection. J Med Microbiol *13*, 57-68.

Bumba, L., Masin, J., Macek, P., Wald, T., Motlova, L., Bibova, I., Klimova, N., Bednarova, L., Veverka, V., Kachala, M.*, et al.* (2016). Calcium-Driven Folding of RTX Domain beta-Rolls Ratchets Translocation of RTX Proteins through Type I Secretion Ducts. Mol Cell *62*, 47-62.

Bungert, S., Molday, L.L., and Molday, R.S. (2001). Membrane topology of the ATP binding cassette transporter ABCR and its relationship to ABC1 and related ABCA transporters: identification of N-linked glycosylation sites. J Biol Chem *276*, 23539-23546.

Burts, M.L., DeDent, A.C., and Missiakas, D.M. (2008). EsaC substrate for the ESAT-6 secretion pathway and its role in persistent infections of *Staphylococcus aureus*. Mol Microbiol *69*, 736-746.

Burts, M.L., Williams, W.A., DeBord, K., and Missiakas, D.M. (2005). EsxA and EsxB are secreted by an ESAT-6-like system that is required for the pathogenesis of *Staphylococcus aureus* infections. Proc Natl Acad Sci U S A *102*, 1169-1174.

Buttner, D. (2012). Protein export according to schedule: architecture, assembly, and regulation of type III secretion systems from plant- and animal-pathogenic bacteria. Microbiol Mol Biol Rev *76*, 262-310.

Cao, T.B., and Saier, M.H., Jr. (2003). The general protein secretory pathway: phylogenetic analyses leading to evolutionary conclusions. Biochim Biophys Acta *1609*, 115-125.

Cascales, E. (2008). The type VI secretion toolkit. EMBO Rep *9*, 735-741.

Cascales, E., and Christie, P.J. (2004a). *Agrobacterium* VirB10, an ATP energy sensor required for type IV secretion. Proc Natl Acad Sci U S A *101*, 17228-17233.

Cascales, E., and Christie, P.J. (2004b). Definition of a bacterial type IV secretion pathway for a DNA substrate. Science *304*, 1170-1173.

Chabeaud, P., de Groot, A., Bitter, W., Tommassen, J., Heulin, T., and Achouak, W. (2001). Phase-variable expression of an operon encoding extracellular alkaline protease, a serine protease homolog, and lipase in *Pseudomonas brassicacearum*. J Bacteriol *183*, 2117-2120.

Chapman, M.R., Robinson, L.S., Pinkner, J.S., Roth, R., Heuser, J., Hammar, M., Normark, S., and Hultgren, S.J. (2002). Role of *Escherichia coli* curli operons in directing amyloid fiber formation. Science *295*, 851-855.

Charlson, E.S., Werner, J.N., and Misra, R. (2006). Differential effects of yfgL mutation on *Escherichia coli* outer membrane proteins and lipopolysaccharide. J Bacteriol *188*, 7186-7194.

Chen, J., Lu, G., Lin, J., Davidson, A.L., and Quiocho, F.A. (2003). A tweezers-like motion of the ATP-binding cassette dimer in an ABC transport cycle. Mol Cell *12*, 651-661.

Chen, J.Y., Chang, W.C., Chang, T., Chang, W.C., Liu, M.Y., Payne, W.J., and LeGall, J. (1996). Cloning, characterization, and expression of the nitric oxide-generating nitrite reductase and of the blue copper protein genes of *Achromobacter* cycloclastes. Biochem Biophys Res Commun *219*, 423-428.

Chen, S., Schultz, P.G., and Brock, A. (2007). An improved system for the generation and analysis of mutant proteins containing unnatural amino acids in *Saccharomyces cerevisiae*. J Mol Biol *371*, 112-122.

Chenal, A., Guijarro, J.I., Raynal, B., Delepierre, M., and Ladant, D. (2009). RTX calcium binding motifs are intrinsically disordered in the absence of calcium: implication for protein secretion. J Biol Chem *284*, 1781-1789.

Chenal, A., Karst, J.C., Sotomayor Perez, A.C., Wozniak, A.K., Baron, B., England, P., and Ladant, D. (2010). Calcium-induced folding and stabilization of the intrinsically disordered RTX domain of the CyaA toxin. Biophys J *99*, 3744-3753.

Chin, J.W., Martin, A.B., King, D.S., Wang, L., and Schultz, P.G. (2002). Addition of a photocrosslinking amino acid to the genetic code of *Escherichia coli*. Proc Natl Acad Sci U S A *99*, 11020-11024.

Cianciotto, N.P. (2005). Type II secretion: a protein secretion system for all seasons. Trends Microbiol *13*, 581-588.

Combet, C., Blanchet, C., Geourjon, C., and Deleage, G. (2000). NPS@: network protein sequence analysis. Trends Biochem Sci *25*, 147-150.

Cornelis, G.R. (2006). The type III secretion injectisome. Nat Rev Microbiol *4*, 811-825.

Costa, T.R., Felisberto-Rodrigues, C., Meir, A., Prevost, M.S., Redzej, A., Trokter, M., and Waksman, G. (2015). Secretion systems in Gram-negative bacteria: structural and mechanistic insights. Nat Rev Microbiol *13*, 343-359.

da Silva, A.C., Ferro, J.A., Reinach, F.C., Farah, C.S., Furlan, L.R., Quaggio, R.B., Monteiro-Vitorello, C.B., Van Sluys, M.A., Almeida, N.F., Alves, L.M.*, et al.* (2002). Comparison of the genomes of two *Xanthomonas* pathogens with differing host specificities. Nature *417*, 459-463.

Dahan, D., Evagelidis, A., Hanrahan, J.W., Hinkson, D.A., Jia, Y., Luo, J., and Zhu, T. (2001). Regulation of the CFTR channel by phosphorylation. Pflugers Arch *443 Suppl 1*, S92-96.

Danese, P.N., and Silhavy, T.J. (1998). Targeting and assembly of periplasmic and outer-membrane proteins in *Escherichia coli*. Annu Rev Genet *32*, 59-94.

Davidson, A.L., Laghaeian, S.S., and Mannering, D.E. (1996). The maltose transport system of *Escherichia coli* displays positive cooperativity in ATP hydrolysis. J Biol Chem *271*, 4858-4863.

Dawson, R.J., and Locher, K.P. (2006). Structure of a bacterial multidrug ABC transporter. Nature *443*, 180-185.

Dawson, R.J., and Locher, K.P. (2007). Structure of the multidrug ABC transporter Sav1866 from *Staphylococcus aureus* in complex with AMP-PNP. FEBS Lett *581*, 935-938.

De Vrind, J., De Groot, A., Brouwers, G.J., Tommassen, J., and De Vrind-De Jong, E. (2003). Identification of a novel Gsp-related pathway required for secretion of the manganese-oxidizing factor of *Pseudomonas putida* strain GB-1. Mol Microbiol *47*, 993-1006.

Dean, D.A., Reizer, J., Nikaido, H., and Saier, M.H., Jr. (1990). Regulation of the maltose transport system of *Escherichia coli* by the glucose-specific enzyme III of the phosphoenolpyruvate-sugar phosphotransferase system. Characterization of inducer exclusion-resistant mutants and reconstitution of inducer exclusion in proteoliposomes. J Biol Chem *265*, 21005-21010.

Deane, J.E., Cordes, F.S., Roversi, P., Johnson, S., Kenjale, R., Picking, W.D., Picking, W.L., Lea, S.M., and Blocker, A. (2006). Expression, purification, crystallization and preliminary crystallographic analysis of MxiH, a subunit of the *Shigella flexneri* type III secretion system needle. Acta Crystallogr Sect F Struct Biol Cryst Commun *62*, 302-305.

Debarbieux, L., and Wandersman, C. (2001). Folded HasA inhibits its own secretion through its ABC exporter. EMBO J *20*, 4657-4663.

Delepelaire, P. (1994). PrtD, the integral membrane ATP-binding cassette component of the *Erwinia chrysanthemi* metalloprotease secretion system, exhibits a secretion signal-regulated ATPase activity. J Biol Chem *269*, 27952-27957.

Delepelaire, P. (2004). Type I secretion in gram-negative bacteria. Biochim Biophys Acta *1694*, 149-161.

Delepelaire, P., and Wandersman, C. (1998). The SecB chaperone is involved in the secretion of the *Serratia marcescens* HasA protein through an ABC transporter. EMBO J *17*, 936-944.

Demers, J.P., Habenstein, B., Loquet, A., Kumar Vasa, S., Giller, K., Becker, S., Baker, D., Lange, A., and Sgourakis, N.G. (2014). High-resolution structure of the *Shigella* type-III secretion needle by solid-state NMR and cryo-electron microscopy. Nat Commun *5*, 4976.

Deuerling, E., Patzelt, H., Vorderwulbecke, S., Rauch, T., Kramer, G., Schaffitzel, E., Mogk, A., Schulze-Specking, A., Langen, H., and Bukau, B. (2003). Trigger Factor and DnaK possess overlapping substrate pools and binding specificities. Mol Microbiol *47*, 1317-1328.

Dong, J., Yang, G., and McHaourab, H.S. (2005). Structural basis of energy transduction in the transport cycle of MsbA. Science *308*, 1023-1028.

Dorman, G., and Prestwich, G.D. (1994). Benzophenone photophores in biochemistry. Biochemistry *33*, 5661-5673.

Doshi, R., and van Veen, H.W. (2013). Substrate binding stabilizes a pre-translocation intermediate in the ATP-binding cassette transport protein MsbA. J Biol Chem *288*, 21638-21647.

Driessen, A.J. (2001). SecB, a molecular chaperone with two faces. Trends Microbiol *9*, 193-196.

Duc, N.M., Du, Y., Thorsen, T.S., Lee, S.Y., Zhang, C., Kato, H., Kobilka, B.K., and Chung, K.Y. (2015). Effective application of bicelles for conformational analysis of G protein-coupled receptors by hydrogen/deuterium exchange mass spectrometry. J Am Soc Mass Spectrom *26*, 808-817.

Durrenberger, M.B., Villiger, W., and Bachi, T. (1991). Conjugational junctions: morphology of specific contacts in conjugating *Escherichia coli* bacteria. J Struct Biol *107*, 146-156.

Ellinger, P., Kluth, M., Stindt, J., Smits, S.H., and Schmitt, L. (2013). Detergent screening and purification of the human liver ABC transporters BSEP (ABCB11) and MDR3 (ABCB4) expressed in the yeast *Pichia pastoris*. PLoS One *8*, e60620.

Eswaran, J., Hughes, C., and Koronakis, V. (2003). Locking TolC entrance helices to prevent protein translocation by the bacterial type I export apparatus. J Mol Biol *327*, 309-315.

Fekkes, P., de Wit, J.G., Boorsma, A., Friesen, R.H., and Driessen, A.J. (1999). Zinc stabilizes the SecB binding site of SecA. Biochemistry *38*, 5111-5116.

Felmlee, T., Pellett, S., Lee, E.Y., and Welch, R.A. (1985a). *Escherichia coli* hemolysin is released extracellularly without cleavage of a signal peptide. J Bacteriol *163*, 88-93.

Felmlee, T., Pellett, S., and Welch, R.A. (1985b). Nucleotide sequence of an *Escherichia coli* chromosomal hemolysin. J Bacteriol *163*, 94-105.

Felmlee, T., and Welch, R.A. (1988). Alterations of amino acid repeats in the *Escherichia coli* hemolysin affect cytolytic activity and secretion. Proc Natl Acad Sci U S A *85*, 5269-5273.

Fowler, D.M., Koulov, A.V., Balch, W.E., and Kelly, J.W. (2007). Functional amyloid - from bacteria to humans. Trends Biochem Sci *32*, 217-224.

Foxman, B. (2002). Epidemiology of urinary tract infections: incidence, morbidity, and economic costs. Am J Med *113 Suppl 1A*, 5S-13S.

Gadsby, D.C., and Nairn, A.C. (1999). Control of CFTR channel gating by phosphorylation and nucleotide hydrolysis. Physiol Rev *79*, S77-S107.

Galan, J.E., Lara-Tejero, M., Marlovits, T.C., and Wagner, S. (2014). Bacterial type III secretion systems: specialized nanomachines for protein delivery into target cells. Annu Rev Microbiol *68*, 415-438.

Galan, J.E., and Wolf-Watz, H. (2006). Protein delivery into eukaryotic cells by type III secretion machines. Nature *444*, 567-573.

Garufi, G., Butler, E., and Missiakas, D. (2008). ESAT-6-like protein secretion in *Bacillus anthracis*. J Bacteriol *190*, 7004-7011.

Gebhard, S. (2012). ABC transporters of antimicrobial peptides in *Firmicutes* bacteria - phylogeny, function and regulation. Mol Microbiol *86*, 1295-1317.

Geiger, O., Rohrs, V., Weissenmayer, B., Finan, T.M., and Thomas-Oates, J.E. (1999). The regulator gene phoB mediates phosphate stress-controlled synthesis of the membrane lipid diacylglyceryl-N,N,N-trimethylhomoserine in *Rhizobium* (*Sinorhizobium*) *meliloti*. Mol Microbiol *32*, 63-73.

Geourjon, C., and Deleage, G. (1995). SOPMA: significant improvements in protein secondary structure prediction by consensus prediction from multiple alignments. Comput Appl Biosci *11*, 681-684.

Gerber, S., Comellas-Bigler, M., Goetz, B.A., and Locher, K.P. (2008). Structural basis of trans-inhibition in a molybdate/tungstate ABC transporter. Science *321*, 246-250.

Gerlach, R.G., and Hensel, M. (2007). Protein secretion systems and adhesins: the molecular armory of Gram-negative pathogens. Int J Med Microbiol *297*, 401-415.

Ghigo, J.M., and Wandersman, C. (1994). A carboxyl-terminal four-amino acid motif is required for secretion of the metalloprotease PrtG through the *Erwinia chrysanthemi* protease secretion pathway. J Biol Chem *269*, 8979-8985.

Gilson, L., Mahanty, H.K., and Kolter, R. (1990). Genetic analysis of an MDR-like export system: the secretion of colicin V. EMBO J *9*, 3875-3884.

Glauert, A.M., and Thornley, M.J. (1969). The topography of the bacterial cell wall. Annu Rev Microbiol *23*, 159-198.

Goebel, W., and Hedgpeth, J. (1982). Cloning and functional characterization of the plasmid-encoded hemolysin determinant of *Escherichia coli*. J Bacteriol *151*, 1290-1298.

Goodfellow, M., and Jones, A.L. (2015). *Corynebacteriales ord. nov.* In Bergey's Manual of Systematics of Archaea and Bacteria (John Wiley & Sons, Ltd).

Gouaux, E., and Mackinnon, R. (2005). Principles of selective ion transport in channels and pumps. Science *310*, 1461-1465.

Gram, H.C. (1884). Über die isolierte Färbung der *Schizomyceten* in Schnitt- und Trockenpräparaten. Fortschritte der Medizin *2*, 185-189.

Gray, L., Baker, K., Kenny, B., Mackman, N., Haigh, R., and Holland, I.B. (1989). A novel C-terminal signal sequence targets *Escherichia coli* haemolysin directly to the medium. J Cell Sci Suppl *11*, 45-57.

Gray, L., Mackman, N., Nicaud, J.M., and Holland, I.B. (1986). The carboxy-terminal region of haemolysin 2001 is required for secretion of the toxin from *Escherichia coli*. Mol Gen Genet *205*, 127-133.

Green, E.R., and Mecsas, J. (2016). Bacterial Secretion Systems: An Overview. Microbiol Spectr *4*.

Gruber, A.R., Lorenz, R., Bernhart, S.H., Neubock, R., and Hofacker, I.L. (2008). The Vienna RNA websuite. Nucleic Acids Res *36*, W70-74.

Guo, X., Chen, X., Weber, I.T., Harrison, R.W., and Tai, P.C. (2006). Molecular basis for differential nucleotide binding of the nucleotide-binding domain of ABC-transporter CvaB. Biochemistry *45*, 14473-14480.

Hagan, C.L., Kim, S., and Kahne, D. (2010). Reconstitution of outer membrane protein assembly from purified components. Science *328*, 890-892.

Ham, H., Sreelatha, A., and Orth, K. (2011). Manipulation of host membranes by bacterial effectors. Nat Rev Microbiol *9*, 635-646.

Hammar, M., Arnqvist, A., Bian, Z., Olsen, A., and Normark, S. (1995). Expression of two csg operons is required for production of fibronectin- and congo red-binding curli polymers in *Escherichia coli* K-12. Mol Microbiol *18*, 661-670.

Harper, J.F., Hong, B., Hwang, I., Guo, H.Q., Stoddard, R., Huang, J.F., Palmgren, M.G., and Sze, H. (1998). A novel calmodulin-regulated Ca2+-ATPase (ACA2) from *Arabidopsis* with an N-terminal autoinhibitory domain. J Biol Chem *273*, 1099-1106.

Harris, R.L., Prudencio, M., Hasnain, S.S., Eady, R.R., and Sawers, R.G. (2005). Heterologous metalloprotein biosynthesis in *Escherichia coli*: conditions for the overproduction of functional copper-containing nitrite reductase and azurin from *Alcaligenes xylosoxidans*. J Synchrotron Radiat *12*, 13-18.

Havarstein, L.S., Diep, D.B., and Nes, I.F. (1995). A family of bacteriocin ABC transporters carry out proteolytic processing of their substrates concomitant with export. Mol Microbiol *16*, 229-240.

Havarstein, L.S., Holo, H., and Nes, I.F. (1994). The leader peptide of colicin V shares consensus sequences with leader peptides that are common among peptide bacteriocins produced by Gram-positive bacteria. Microbiology *140 (Pt 9)*, 2383-2389.

Hebling, C.M., Morgan, C.R., Stafford, D.W., Jorgenson, J.W., Rand, K.D., and Engen, J.R. (2010). Conformational analysis of membrane proteins in phospholipid bilayer nanodiscs by hydrogen exchange mass spectrometry. Anal Chem *82*, 5415-5419.

Hess, J., Gentschev, I., Goebel, W., and Jarchau, T. (1990). Analysis of the haemolysin secretion system by PhoA-HlyA fusion proteins. Mol Gen Genet *224*, 201-208.

Higgins, C.F. (1992). ABC transporters: from microorganisms to man. Annu Rev Cell Biol *8*, 67-113.

Higgins, C.F., and Linton, K.J. (2004a). The ATP switch model for ABC transporters. Nat Struct Mol Biol *11*, 918-926.

Higgins, M.K., Bokma, E., Koronakis, E., Hughes, C., and Koronakis, V. (2004b). Structure of the periplasmic component of a bacterial drug efflux pump. Proc Natl Acad Sci U S A *101*, 9994-9999.

Hinsa, S.M., Espinosa-Urgel, M., Ramos, J.L., and O'Toole, G.A. (2003). Transition from reversible to irreversible attachment during biofilm formation by *Pseudomonas fluorescens* WCS365 requires an ABC transporter and a large secreted protein. Mol Microbiol *49*, 905-918.

Hobbs, M., and Mattick, J.S. (1993). Common components in the assembly of type 4 fimbriae, DNA transfer systems, filamentous phage and protein-secretion apparatus: a general system for the formation of surface-associated protein complexes. Mol Microbiol *10*, 233-243.

Holland, I.B., Benabdelhak, H., Young, J., De Lima Pimenta, A., Schmitt, L., and Blight, M.A. (2003). Chapter 11 - Bacterial ABC Transporters Involved in Protein Translocation. In ABC Proteins (London: Academic Press), pp. 209-241.

Holland, I.B., Kenny, B., and Blight, M. (1990). Haemolysin secretion from *E. coli*. Biochimie *72*, 131-141.

Holland, I.B., Peherstorfer, S., Kanonenberg, K., Lenders, M., Reimann, S., and Schmitt, L. (2016). Type I Protein Secretion-Deceptively Simple yet with a Wide Range of Mechanistic Variability across the Family. EcoSal Plus *7*.

Holland, I.B., Schmitt, L., and Young, J. (2005). Type 1 protein secretion in bacteria, the ABC-transporter dependent pathway (review). Mol Membr Biol *22*, 29-39.

Hollenstein, K., Frei, D.C., and Locher, K.P. (2007). Structure of an ABC transporter in complex with its binding protein. Nature *446*, 213-216.

Holo, H., Nilssen, O., and Nes, I.F. (1991). Lactococcin A, a new bacteriocin from *Lactococcus lactis* subsp. *cremoris*: isolation and characterization of the protein and its gene. J Bacteriol *173*, 3879-3887.

Hood, R.D., Singh, P., Hsu, F., Guvener, T., Carl, M.A., Trinidad, R.R., Silverman, J.M., Ohlson, B.B., Hicks, K.G., Plemel, R.L.*, et al.* (2010). A type VI secretion system of *Pseudomonas aeruginosa* targets a toxin to bacteria. Cell Host Microbe *7*, 25-37.

Hopfner, K.P., and Tainer, J.A. (2003). Rad50/SMC proteins and ABC transporters: unifying concepts from high-resolution structures. Curr Opin Struct Biol *13*, 249-255.

Houben, E.N., Korotkov, K.V., and Bitter, W. (2014). Take five - Type VII secretion systems of *Mycobacteria*. Biochim Biophys Acta *1843*, 1707-1716.

Hu, B., Morado, D.R., Margolin, W., Rohde, J.R., Arizmendi, O., Picking, W.L., Picking, W.D., and Liu, J. (2015). Visualization of the type III secretion sorting platform of *Shigella flexneri*. Proc Natl Acad Sci U S A *112*, 1047-1052.

Hung, L.W., Wang, I.X., Nikaido, K., Liu, P.Q., Ames, G.F., and Kim, S.H. (1998). Crystal structure of the ATP-binding subunit of an ABC transporter. Nature *396*, 703-707.

Hyland, C., Vuillard, L., Hughes, C., and Koronakis, V. (2001). Membrane interaction of *Escherichia coli* hemolysin: flotation and insertion-dependent labeling by phospholipid vesicles. J Bacteriol *183*, 5364-5370.

Ieva, R., and Bernstein, H.D. (2009). Interaction of an autotransporter passenger domain with BamA during its translocation across the bacterial outer membrane. Proc Natl Acad Sci U S A *106*, 19120-19125.

Ieva, R., Skillman, K.M., and Bernstein, H.D. (2008). Incorporation of a polypeptide segment into the beta-domain pore during the assembly of a bacterial autotransporter. Mol Microbiol *67*, 188-201.

Ieva, R., Tian, P., Peterson, J.H., and Bernstein, H.D. (2011). Sequential and spatially restricted interactions of assembly factors with an autotransporter beta domain. Proc Natl Acad Sci U S A *108*, E383-391.

Infed, N., Hanekop, N., Driessen, A.J., Smits, S.H., and Schmitt, L. (2011). Influence of detergents on the activity of the ABC transporter LmrA. Biochim Biophys Acta *1808*, 2313-2321.

Irvine, G.B., El-Agnaf, O.M., Shankar, G.M., and Walsh, D.M. (2008). Protein aggregation in the brain: the molecular basis for Alzheimer's and Parkinson's diseases. Mol Med *14*, 451-464.

Issartel, J.P., Koronakis, V., and Hughes, C. (1991). Activation of *Escherichia coli* prohaemolysin to the mature toxin by acyl carrier protein-dependent fatty acylation. Nature *351*, 759-761.

Izore, T., Job, V., and Dessen, A. (2011). Biogenesis, regulation, and targeting of the type III secretion system. Structure *19*, 603-612.

Jain, S., and Goldberg, M.B. (2007). Requirement for YaeT in the outer membrane assembly of autotransporter proteins. J Bacteriol *189*, 5393-5398.

Janas, E., Hofacker, M., Chen, M., Gompf, S., van der Does, C., and Tampe, R. (2003). The ATP hydrolysis cycle of the nucleotide-binding domain of the mitochondrial ATP-binding cassette transporter Mdl1p. J Biol Chem *278*, 26862-26869.

Janganan, T.K., Bavro, V.N., Zhang, L., Matak-Vinkovic, D., Barrera, N.P., Venien-Bryan, C., Robinson, C.V., Borges-Walmsley, M.I., and Walmsley, A.R. (2011). Evidence for the assembly of a bacterial tripartite multidrug pump with a stoichiometry of 3:6:3. J Biol Chem *286*, 26900-26912.

Jarchau, T., Chakraborty, T., Garcia, F., and Goebel, W. (1994). Selection for transport competence of C-terminal polypeptides derived from *Escherichia coli* hemolysin: the shortest peptide capable of autonomous HlyB/HlyD-dependent secretion comprises the C-terminal 62 amino acids of HlyA. Mol Gen Genet *245*, 53-60.

Jones, C.H., Danese, P.N., Pinkner, J.S., Silhavy, T.J., and Hultgren, S.J. (1997). The chaperone-assisted membrane release and folding pathway is sensed by two signal transduction systems. EMBO J *16*, 6394-6406.

Jones, H.E., Holland, I.B., Baker, H.L., and Campbell, A.K. (1999a). Slow changes in cytosolic free Ca2+ in *Escherichia coli* highlight two putative influx mechanisms in response to changes in extracellular calcium. Cell Calcium *25*, 265-274.

Jones, P.M., and George, A.M. (1999b). Subunit interactions in ABC transporters: towards a functional architecture. FEMS Microbiol Lett *179*, 187-202.

Jones, P.M., and George, A.M. (2002). Mechanism of ABC transporters: a molecular dynamics simulation of a well characterized nucleotide-binding subunit. Proc Natl Acad Sci U S A *99*, 12639-12644.

Jones, P.M., and George, A.M. (2007). Nucleotide-dependent allostery within the ABC transporter ATP-binding cassette: a computational study of the MJ0796 dimer. J Biol Chem *282*, 22793-22803.

Jones, P.M., and George, A.M. (2009). Opening of the ADP-bound active site in the ABC transporter ATPase dimer: evidence for a constant contact, alternating sites model for the catalytic cycle. Proteins *75*, 387-396.

Jones, P.M., and George, A.M. (2011). Molecular-dynamics simulations of the ATP/apo state of a multidrug ATP-binding cassette transporter provide a structural and mechanistic basis for the asymmetric occluded state. Biophys J *100*, 3025-3034.

Jones, P.M., and George, A.M. (2013). Mechanism of the ABC transporter ATPase domains: catalytic models and the biochemical and biophysical record. Crit Rev Biochem Mol Biol *48*, 39-50.

Jumpertz, T., Chervaux, C., Racher, K., Zouhair, M., Blight, M.A., Holland, I.B., and Schmitt, L. (2010). Mutations affecting the extreme C terminus of *Escherichia coli* haemolysin A reduce haemolytic activity by altering the folding of the toxin. Microbiology *156*, 2495-2505.

Junker, M., Besingi, R.N., and Clark, P.L. (2009). Vectorial transport and folding of an autotransporter virulence protein during outer membrane secretion. Mol Microbiol *71*, 1323-1332.

Kanonenberg, K., Schwarz, C.K., and Schmitt, L. (2013). Type I secretion systems - a story of appendices. Res Microbiol *164*, 596-604.

Karpowich, N., Martsinkevich, O., Millen, L., Yuan, Y.R., Dai, P.L., MacVey, K., Thomas, P.J., and Hunt, J.F. (2001). Crystal structures of the MJ1267 ATP binding cassette reveal an induced-fit effect at the ATPase active site of an ABC transporter. Structure *9*, 571-586.

Kelley, L.A., Mezulis, S., Yates, C.M., Wass, M.N., and Sternberg, M.J. (2015). The Phyre2 web portal for protein modeling, prediction and analysis. Nat Protoc *10*, 845-858.

Kenny, B., Chervaux, C., and Holland, I.B. (1994). Evidence that residues -15 to -46 of the haemolysin secretion signal are involved in early steps in secretion, leading to recognition of the translocator. Mol Microbiol *11*, 99-109.

Kenny, B., Haigh, R., and Holland, I.B. (1991). Analysis of the haemolysin transport process through the secretion from *Escherichia coli* of PCM, CAT or beta-galactosidase fused to the Hly C-terminal signal domain. Mol Microbiol *5*, 2557-2568.

Kenny, B., Taylor, S., and Holland, I.B. (1992). Identification of individual amino acids required for secretion within the haemolysin (HlyA) C-terminal targeting region. Mol Microbiol *6*, 1477-1489.

Khare, D., Oldham, M.L., Orelle, C., Davidson, A.L., and Chen, J. (2009). Alternating access in maltose transporter mediated by rigid-body rotations. Mol Cell *33*, 528-536.

Kiefer, H. (2003). In vitro folding of alpha-helical membrane proteins. Biochim Biophys Acta *1610*, 57-62.

Kim, H.M., Xu, Y., Lee, M., Piao, S., Sim, S.H., Ha, N.C., and Lee, K. (2010). Functional relationships between the AcrA hairpin tip region and the TolC aperture tip region for the formation of the bacterial tripartite efflux pump AcrAB-TolC. J Bacteriol *192*, 4498-4503.

Kim, J.S., Song, S., Lee, M., Lee, S., Lee, K., and Ha, N.C. (2016). Crystal Structure of a Soluble Fragment of the Membrane Fusion Protein HlyD in a Type I Secretion System of Gram-Negative Bacteria. Structure *24*, 477-485.

Kimbrough, T.G., and Miller, S.I. (2000). Contribution of *Salmonella typhimurium* type III secretion components to needle complex formation. Proc Natl Acad Sci U S A *97*, 11008-11013.

Klaenhammer, T.R. (1993). Genetics of bacteriocins produced by lactic acid bacteria. FEMS Microbiol Rev *12*, 39-85.

Korkhov, V.M., Mireku, S.A., Hvorup, R.N., and Locher, K.P. (2012). Asymmetric states of vitamin B(1)(2) transporter BtuCD are not discriminated by its cognate substrate binding protein BtuF. FEBS Lett *586*, 972-976.

Koronakis, E., Hughes, C., Milisav, I., and Koronakis, V. (1995). Protein exporter function and in vitro ATPase activity are correlated in ABC-domain mutants of HlyB. Mol Microbiol *16*, 87-96.

Koronakis, V. (2003). TolC - the bacterial exit duct for proteins and drugs. FEBS Lett *555*, 66-71.

Koronakis, V., Eswaran, J., and Hughes, C. (2004). Structure and function of TolC: the bacterial exit duct for proteins and drugs. Annu Rev Biochem *73*, 467-489.

Koronakis, V., Hughes, C., and Koronakis, E. (1993). ATPase activity and ATP/ADP-induced conformational change in the soluble domain of the bacterial protein translocator HlyB. Mol Microbiol *8*, 1163-1175.

Koronakis, V., Koronakis, E., and Hughes, C. (1989). Isolation and analysis of the C-terminal signal directing export of *Escherichia coli* hemolysin protein across both bacterial membranes. EMBO J *8*, 595-605.

Koronakis, V., Sharff, A., Koronakis, E., Luisi, B., and Hughes, C. (2000). Crystal structure of the bacterial membrane protein TolC central to multidrug efflux and protein export. Nature *405*, 914-919.

Korotkov, K.V., Gonen, T., and Hol, W.G. (2011). Secretins: dynamic channels for protein transport across membranes. Trends Biochem Sci *36*, 433-443.

Korotkov, K.V., Sandkvist, M., and Hol, W.G. (2012). The type II secretion system: biogenesis, molecular architecture and mechanism. Nat Rev Microbiol *10*, 336-351.

Korotkova, N., Freire, D., Phan, T.H., Ummels, R., Creekmore, C.C., Evans, T.J., Wilmanns, M., Bitter, W., Parret, A.H., Houben, E.N.*, et al.* (2014). Structure of the *Mycobacterium tuberculosis*

type VII secretion system chaperone EspG5 in complex with PE25-PPE41 dimer. Mol Microbiol *94*, 367-382.

Koshy, S.S., Eyles, S.J., Weis, R.M., and Thompson, L.K. (2013). Hydrogen exchange mass spectrometry of functional membrane-bound chemotaxis receptor complexes. Biochemistry *52*, 8833-8842.

Kotake, Y., Ishii, S., Yano, T., Katsuoka, Y., and Hayashi, H. (2008). Substrate recognition mechanism of the peptidase domain of the quorum-sensing-signal-producing ABC transporter ComA from *Streptococcus*. Biochemistry *47*, 2531-2538.

Kubori, T., Sukhan, A., Aizawa, S.I., and Galan, J.E. (2000). Molecular characterization and assembly of the needle complex of the *Salmonella typhimurium* type III protein secretion system. Proc Natl Acad Sci U S A *97*, 10225-10230.

Kudryashev, M., Wang, R.Y., Brackmann, M., Scherer, S., Maier, T., Baker, D., DiMaio, F., Stahlberg, H., Egelman, E.H., and Basler, M. (2015). Structure of the type VI secretion system contractile sheath. Cell *160*, 952-962.

Kudva, R., Denks, K., Kuhn, P., Vogt, A., Muller, M., and Koch, H.G. (2013). Protein translocation across the inner membrane of Gram-negative bacteria: the Sec and Tat dependent protein transport pathways. Res Microbiol *164*, 505-534.

Lally, E.T., Kieba, I.R., Sato, A., Green, C.L., Rosenbloom, J., Korostoff, J., Wang, J.F., Shenker, B.J., Ortlepp, S., Robinson, M.K.*, et al.* (1997). RTX toxins recognize a beta2 integrin on the surface of human target cells. J Biol Chem *272*, 30463-30469.

Lanyi, J.K. (2004). Bacteriorhodopsin. Annu Rev Physiol *66*, 665-688.

Lecher, J., Schwarz, C.K., Stoldt, M., Smits, S.H., Willbold, D., and Schmitt, L. (2012). An RTX transporter tethers its unfolded substrate during secretion via a unique N-terminal domain. Structure *20*, 1778-1787.

Lecher, J., Stoldt, M., Schwarz, C.K., Smits, S.H., Schmitt, L., and Willbold, D. (2011). 1H, 15N and 13C resonance assignment of the N-terminal C39 peptidase-like domain of the ABC transporter Haemolysin B (HlyB). Biomol NMR Assign *5*, 199-201.

Lee, M., Jun, S.Y., Yoon, B.Y., Song, S., Lee, K., and Ha, N.C. (2012). Membrane fusion proteins of type I secretion system and tripartite efflux pumps share a binding motif for TolC in Gram-negative bacteria. PLoS One *7*, e40460.

Lehnert, E., Mao, J., Mehdipour, A.R., Hummer, G., Abele, R., Glaubitz, C., and Tampe, R. (2016). Antigenic Peptide Recognition on the Human ABC Transporter TAP Resolved by DNP-Enhanced Solid-State NMR Spectroscopy. J Am Chem Soc.

Lenders, M.H., Beer, T., Smits, S.H., and Schmitt, L. (2016). In vivo quantification of the secretion rates of the hemolysin A Type I secretion system. Sci Rep *6*, 33275.

Lenders, M.H., Reimann, S., Smits, S.H., and Schmitt, L. (2013). Molecular insights into type I secretion systems. Biol Chem *394*, 1371-1384.

Lenders, M.H., Weidtkamp-Peters, S., Kleinschrodt, D., Jaeger, K.E., Smits, S.H., and Schmitt, L. (2015). Directionality of substrate translocation of the hemolysin A Type I secretion system. Sci Rep *5*, 12470.

Leo, J.C., Grin, I., and Linke, D. (2012). Type V secretion: mechanism(s) of autotransport through the bacterial outer membrane. Philos Trans R Soc Lond B Biol Sci *367*, 1088-1101.

Leonhardt, R.M., Keusekotten, K., Bekpen, C., and Knittler, M.R. (2005). Critical role for the tapasin-docking site of TAP2 in the functional integrity of the MHC class I-peptide-loading complex. J Immunol *175*, 5104-5114.

Letoffe, S., Delepelaire, P., and Wandersman, C. (1996). Protein secretion in Gram-negative bacteria: assembly of the three components of ABC protein-mediated exporters is ordered and promoted by substrate binding. EMBO J *15*, 5804-5811.

Letoffe, S., Ghigo, J.M., and Wandersman, C. (1994). Secretion of the *Serratia marcescens* HasA protein by an ABC transporter. J Bacteriol *176*, 5372-5377.

Lillington, J., Geibel, S., and Waksman, G. (2015). Reprint of "Biogenesis and adhesion of type 1 and P pili". Biochim Biophys Acta *1850*, 554-564.

Lim, K.B., Walker, C.R., Guo, L., Pellett, S., Shabanowitz, J., Hunt, D.F., Hewlett, E.L., Ludwig, A., Goebel, W., Welch, R.A.*, et al.* (2000). *Escherichia coli* alpha-hemolysin (HlyA) is heterogeneously acylated in vivo with 14-, 15-, and 17-carbon fatty acids. J Biol Chem *275*, 36698-36702.

Lin, D.Y., Huang, S., and Chen, J. (2015). Crystal structures of a polypeptide processing and secretion transporter. Nature *523*, 425-430.

Linhartova, I., Bumba, L., Masin, J., Basler, M., Osicka, R., Kamanova, J., Prochazkova, K., Adkins, I., Hejnova-Holubova, J., Sadilkova, L.*, et al.* (2010). RTX proteins: a highly diverse family secreted by a common mechanism. FEMS Microbiol Rev *34*, 1076-1112.

Litman, T., Nielsen, D., Skovsgaard, T., Zeuthen, T., and Stein, W.D. (1997a). ATPase activity of P-glycoprotein related to emergence of drug resistance in Ehrlich ascites tumor cell lines. Biochim Biophys Acta *1361*, 147-158.

Litman, T., Zeuthen, T., Skovsgaard, T., and Stein, W.D. (1997b). Structure-activity relationships of P-glycoprotein interacting drugs: kinetic characterization of their effects on ATPase activity. Biochim Biophys Acta *1361*, 159-168.

Liu, C.E., Liu, P.Q., and Ames, G.F. (1997). Characterization of the adenosine triphosphatase activity of the periplasmic histidine permease, a traffic ATPase (ABC transporter). J Biol Chem *272*, 21883-21891.

Liu, F., Zhang, Z., Csanady, L., Gadsby, D.C., and Chen, J. (2017). Molecular Structure of the Human CFTR Ion Channel. Cell *169*, 85-95 e88.

Liu, W., Brock, A., Chen, S., Chen, S., and Schultz, P.G. (2007). Genetic incorporation of unnatural amino acids into proteins in mammalian cells. Nat Methods *4*, 239-244.

Lo, R.Y., Strathdee, C.A., and Shewen, P.E. (1987). Nucleotide sequence of the leukotoxin genes of *Pasteurella haemolytica* A1. Infect Immun *55*, 1987-1996.

Locher, K.P. (2009). Structure and mechanism of ATP-binding cassette transporters (review). Philos Trans R Soc Lond B Biol Sci *364*, 239-245.

Locher, K.P., Lee, A.T., and Rees, D.C. (2002). The *E. coli* BtuCD structure: a framework for ABC transporter architecture and mechanism. Science *296*, 1091-1098.

Loo, T.W., Bartlett, M.C., and Clarke, D.M. (2010). Human P-glycoprotein is active when the two halves are clamped together in the closed conformation. Biochem Biophys Res Commun *395*, 436-440.

Lu, H.M., and Lory, S. (1996). A specific targeting domain in mature exotoxin A is required for its extracellular secretion from *Pseudomonas aeruginosa*. EMBO J *15*, 429-436.

Ludwig, A., Jarchau, T., Benz, R., and Goebel, W. (1988). The repeat domain of *Escherichia coli* haemolysin (HlyA) is responsible for its Ca2+-dependent binding to erythrocytes. Mol Gen Genet *214*, 553-561.

Ludwig, A., Schmid, A., Benz, R., and Goebel, W. (1991). Mutations affecting pore formation by haemolysin from *Escherichia coli*. Mol Gen Genet *226*, 198-208.

Luirink, J., von Heijne, G., Houben, E., and de Gier, J.W. (2005). Biogenesis of inner membrane proteins in *Escherichia coli*. Annu Rev Microbiol *59*, 329-355.

Mackman, N., Baker, K., Gray, L., Haigh, R., Nicaud, J.M., and Holland, I.B. (1987). Release of a chimeric protein into the medium from *Escherichia coli* using the C-terminal secretion signal of haemolysin. EMBO J *6*, 2835-2841.

Mackman, N., Nicaud, J.M., Gray, L., and Holland, I.B. (1985a). Genetical and functional organisation of the *Escherichia coli* haemolysin determinant 2001. Mol Gen Genet *201*, 282-288.

Mackman, N., Nicaud, J.M., Gray, L., and Holland, I.B. (1985b). Identification of polypeptides required for the export of haemolysin 2001 from *E. coli*. Mol Gen Genet *201*, 529-536.

Mackman, N., Nicaud, J.M., Gray, L., and Holland, I.B. (1986). Secretion of haemolysin by *Escherichia coli*. Curr Top Microbiol Immunol *125*, 159-181.

Malinverni, J.C., Werner, J., Kim, S., Sklar, J.G., Kahne, D., Misra, R., and Silhavy, T.J. (2006). YfiO stabilizes the YaeT complex and is essential for outer membrane protein assembly in *Escherichia coli*. Mol Microbiol *61*, 151-164.

Marlovits, T.C., Kubori, T., Lara-Tejero, M., Thomas, D., Unger, V.M., and Galan, J.E. (2006). Assembly of the inner rod determines needle length in the type III secretion injectisome. Nature *441*, 637-640.

Masi, M., and Wandersman, C. (2010). Multiple signals direct the assembly and function of a type 1 secretion system. J Bacteriol *192*, 3861-3869.

Maurer, C., Panahandeh, S., Jungkamp, A.C., Moser, M., and Muller, M. (2010). TatB functions as an oligomeric binding site for folded Tat precursor proteins. Mol Biol Cell *21*, 4151-4161.

Mehmood, S., Domene, C., Forest, E., and Jault, J.M. (2012). Dynamics of a bacterial multidrug ABC transporter in the inward- and outward-facing conformations. Proc Natl Acad Sci U S A *109*, 10832-10836.

Mimmack, M.L., Gallagher, M.P., Pearce, S.R., Hyde, S.C., Booth, I.R., and Higgins, C.F. (1989). Energy coupling to periplasmic binding protein-dependent transport systems: stoichiometry of ATP hydrolysis during transport in vivo. Proc Natl Acad Sci U S A *86*, 8257-8261.

Muller, M. (2005). Twin-arginine-specific protein export in *Escherichia coli*. Res Microbiol *156*, 131-136.

Muller, M., and Klosgen, R.B. (2005). The Tat pathway in bacteria and chloroplasts (review). Mol Membr Biol *22*, 113-121.

Murdoch, S.L., Trunk, K., English, G., Fritsch, M.J., Pourkarimi, E., and Coulthurst, S.J. (2011). The opportunistic pathogen *Serratia marcescens* utilizes type VI secretion to target bacterial competitors. J Bacteriol *193*, 6057-6069.

Muriana, P.M., and Klaenhammer, T.R. (1991). Purification and partial characterization of lactacin F, a bacteriocin produced by *Lactobacillus acidophilus* 11088. Appl Environ Microbiol *57*, 114-121.

Nagamatsu, K., Hannan, T.J., Guest, R.L., Kostakioti, M., Hadjifrangiskou, M., Binkley, J., Dodson, K., Raivio, T.L., and Hultgren, S.J. (2015). Dysregulation of *Escherichia coli* alpha-hemolysin expression alters the course of acute and persistent urinary tract infection. Proc Natl Acad Sci U S A *112*, E871-880.

Nagamori, S., Smirnova, I.N., and Kaback, H.R. (2004). Role of YidC in folding of polytopic membrane proteins. J Cell Biol *165*, 53-62.

Natale, P., Bruser, T., and Driessen, A.J. (2008). Sec- and Tat-mediated protein secretion across the bacterial cytoplasmic membrane - distinct translocases and mechanisms. Biochim Biophys Acta *1778*, 1735-1756.

Nelson, S.O., and Postma, P.W. (1984). Interactions in vivo between IIIGlc of the phosphoenolpyruvate:sugar phosphotransferase system and the glycerol and maltose uptake systems of *Salmonella typhimurium*. Eur J Biochem *139*, 29-34.

Nenninger, A.A., Robinson, L.S., and Hultgren, S.J. (2009). Localized and efficient curli nucleation requires the chaperone-like amyloid assembly protein CsgF. Proc Natl Acad Sci U S A *106*, 900-905.

Neu, H.C., and Heppel, L.A. (1965). The release of enzymes from *Escherichia coli* by osmotic shock and during the formation of spheroplasts. J Biol Chem *240*, 3685-3692.

Noll, A., Thomas, C., Herbring, V., Zollmann, T., Barth, K., Mehdipour, A.R., Tomasiak, T.M., Bruchert, S., Joseph, B., Abele, R.*, et al.* (2017). Crystal structure and mechanistic basis of a functional homolog of the antigen transporter TAP. Proc Natl Acad Sci U S A *114*, E438-E447.

Olsen, A., Jonsson, A., and Normark, S. (1989). Fibronectin binding mediated by a novel class of surface organelles on *Escherichia coli*. Nature *338*, 652-655.

Orban, T., and Tsybovsky, Y. (2015). Probing conformational changes in rhodopsin using hydrogen-deuterium exchange coupled to mass spectrometry. Methods Mol Biol *1271*, 113-121.

Ostolaza, H., Bakas, L., and Goni, F.M. (1997). Balance of electrostatic and hydrophobic interactions in the lysis of model membranes by *E. coli* alpha-haemolysin. J Membr Biol *158*, 137-145.

Ostolaza, H., Bartolome, B., Serra, J.L., de la Cruz, F., and Goni, F.M. (1991). Alpha-haemolysin from *E. coli*. Purification and self-aggregation properties. FEBS Lett *280*, 195-198.

Palmgren, M.G., Larsson, C., and Sommarin, M. (1990). Proteolytic activation of the plant plasma membrane H(+)-ATPase by removal of a terminal segment. J Biol Chem *265*, 13423-13426.

Palmgren, M.G., Sommarin, M., Serrano, R., and Larsson, C. (1991). Identification of an autoinhibitory domain in the C-terminal region of the plant plasma membrane H(+)-ATPase. J Biol Chem *266*, 20470-20475.

Panahandeh, S., Maurer, C., Moser, M., DeLisa, M.P., and Muller, M. (2008). Following the path of a twin-arginine precursor along the TatABC translocase of *Escherichia coli*. J Biol Chem *283*, 33267-33275.

Park, E., and Rapoport, T.A. (2012). Bacterial protein translocation requires only one copy of the SecY complex in vivo. J Cell Biol *198*, 881-893.

Parsot, C., Hamiaux, C., and Page, A.L. (2003). The various and varying roles of specific chaperones in type III secretion systems. Curr Opin Microbiol *6*, 7-14.

Patzlaff, J.S., van der Heide, T., and Poolman, B. (2003). The ATP/substrate stoichiometry of the ATP-binding cassette (ABC) transporter OpuA. J Biol Chem *278*, 29546-29551.

Pena, A., Ripoll-Rozada, J., Zunzunegui, S., Cabezon, E., de la Cruz, F., and Arechaga, I. (2011). Autoinhibitory regulation of TrwK, an essential VirB4 ATPase in type IV secretion systems. J Biol Chem *286*, 17376-17382.

Piddock, L.J. (2006). Multidrug-resistance efflux pumps - not just for resistance. Nat Rev Microbiol *4*, 629-636.

Pirrone, G.F., Emert-Sedlak, L.A., Wales, T.E., Smithgall, T.E., Kent, M.S., and Engen, J.R. (2015). Membrane-Associated Conformation of HIV-1 Nef Investigated with Hydrogen Exchange Mass Spectrometry at a Langmuir Monolayer. Anal Chem *87*, 7030-7035.

Poole, K. (2007). Efflux pumps as antimicrobial resistance mechanisms. Ann Med *39*, 162-176.

Porollo, A.A., Adamczak, R., and Meller, J. (2004). POLYVIEW: a flexible visualization tool for structural and functional annotations of proteins. Bioinformatics *20*, 2460-2462.

Poyraz, O., Schmidt, H., Seidel, K., Delissen, F., Ader, C., Tenenboim, H., Goosmann, C., Laube, B., Thunemann, A.F., Zychlinsky, A.*, et al.* (2010). Protein refolding is required for assembly of the type three secretion needle. Nat Struct Mol Biol *17*, 788-792.

Procko, E., Ferrin-O'Connell, I., Ng, S.L., and Gaudet, R. (2006). Distinct structural and functional properties of the ATPase sites in an asymmetric ABC transporter. Mol Cell *24*, 51-62.

Putman, M., van Veen, H.W., and Konings, W.N. (2000). Molecular properties of bacterial multidrug transporters. Microbiol Mol Biol Rev *64*, 672-693.

Reimann, S., Poschmann, G., Kanonenberg, K., Stuhler, K., Smits, S.H., and Schmitt, L. (2016). Interdomain regulation of the ATPase activity of the ABC transporter haemolysin B from *Escherichia coli*. Biochem J *473*, 2471-2483.

Rhodes, C.R., Gray, M.C., Watson, J.M., Muratore, T.L., Kim, S.B., Hewlett, E.L., and Grisham, C.M. (2001). Structural consequences of divalent metal binding by the adenylyl cyclase toxin of *Bordetella pertussis*. Arch Biochem Biophys *395*, 169-176.

Rich, D.P., Gregory, R.J., Anderson, M.P., Manavalan, P., Smith, A.E., and Welsh, M.J. (1991). Effect of deleting the R domain on CFTR-generated chloride channels. Science *253*, 205-207.

Riekhof, W.R., Naik, S., Bertrand, H., Benning, C., and Voelker, D.R. (2014). Phosphate starvation in fungi induces the replacement of phosphatidylcholine with the phosphorus-free betaine lipid diacylglyceryl-N,N,N-trimethylhomoserine. Eukaryot Cell *13*, 749-757.

Robinson, C., and Bolhuis, A. (2004). Tat-dependent protein targeting in prokaryotes and chloroplasts. Biochim Biophys Acta *1694*, 135-147.

Rogers, H.J., Perkins, H.R., and Ward, J.B. (1980). Microbial cell walls and membranes (London: Chapman and Hall).

Rollauer, S.E., Tarry, M.J., Graham, J.E., Jaaskelainen, M., Jager, F., Johnson, S., Krehenbrink, M., Liu, S.M., Lukey, M.J., Marcoux, J.*, et al.* (2012). Structure of the TatC core of the twin-arginine protein transport system. Nature *492*, 210-214.

Roman-Hernandez, G., Peterson, J.H., and Bernstein, H.D. (2014). Reconstitution of bacterial autotransporter assembly using purified components. Elife *3*, e04234.

Rose, T., Sebo, P., Bellalou, J., and Ladant, D. (1995). Interaction of calcium with *Bordetella pertussis* adenylate cyclase toxin. Characterization of multiple calcium-binding sites and calcium-induced conformational changes. J Biol Chem *270*, 26370-26376.

Rosenberg, O.S., Dovala, D., Li, X., Connolly, L., Bendebury, A., Finer-Moore, J., Holton, J., Cheng, Y., Stroud, R.M., and Cox, J.S. (2015). Substrates Control Multimerization and Activation of the Multi-Domain ATPase Motor of Type VII Secretion. Cell *161*, 501-512.

Russell, A.B., Hood, R.D., Bui, N.K., LeRoux, M., Vollmer, W., and Mougous, J.D. (2011). Type VI secretion delivers bacteriolytic effectors to target cells. Nature *475*, 343-347.

Russell, A.B., Peterson, S.B., and Mougous, J.D. (2014). Type VI secretion system effectors: poisons with a purpose. Nat Rev Microbiol *12*, 137-148.

Saier, M.H., Jr. (1994). Computer-aided analyses of transport protein sequences: gleaning evidence concerning function, structure, biogenesis, and evolution. Microbiol Rev *58*, 71-93.

Saier, M.H., Jr. (2000). A functional-phylogenetic classification system for transmembrane solute transporters. Microbiol Mol Biol Rev *64*, 354-411.

Saier, M.H., Jr., Reddy, V.S., Tsu, B.V., Ahmed, M.S., Li, C., and Moreno-Hagelsieb, G. (2016). The Transporter Classification Database (TCDB): recent advances. Nucleic Acids Res *44*, D372-379.

Sakamoto, K., Hayashi, A., Sakamoto, A., Kiga, D., Nakayama, H., Soma, A., Kobayashi, T., Kitabatake, M., Takio, K., Saito, K.*, et al.* (2002). Site-specific incorporation of an unnatural amino acid into proteins in mammalian cells. Nucleic Acids Res *30*, 4692-4699.

Sanchez-Magraner, L., Cortajarena, A.L., Garcia-Pacios, M., Arrondo, J.L., Agirre, J., Guerin, D.M., Goni, F.M., and Ostolaza, H. (2010). Interdomain Ca(2+) effects in *Escherichia coli* alpha-haemolysin: Ca(2+) binding to the C-terminal domain stabilizes both C- and N-terminal domains. Biochim Biophys Acta *1798*, 1225-1233.

Sanchez-Magraner, L., Viguera, A.R., Garcia-Pacios, M., Garcillan, M.P., Arrondo, J.L., de la Cruz, F., Goni, F.M., and Ostolaza, H. (2007). The calcium-binding C-terminal domain of *Escherichia coli* alpha-hemolysin is a major determinant in the surface-active properties of the protein. J Biol Chem *282*, 11827-11835.

Sandkvist, M., Michel, L.O., Hough, L.P., Morales, V.M., Bagdasarian, M., Koomey, M., DiRita, V.J., and Bagdasarian, M. (1997). General secretion pathway (eps) genes required for toxin secretion and outer membrane biogenesis in *Vibrio cholerae*. J Bacteriol *179*, 6994-7003.

Sargent, F., Stanley, N.R., Berks, B.C., and Palmer, T. (1999). Sec-independent protein translocation in *Escherichia coli*. A distinct and pivotal role for the TatB protein. J Biol Chem *274*, 36073-36082.

Sato, S., Mimasu, S., Sato, A., Hino, N., Sakamoto, K., Umehara, T., and Yokoyama, S. (2011). Crystallographic study of a site-specifically cross-linked protein complex with a genetically incorporated photoreactive amino acid. Biochemistry *50*, 250-257.

Sauna, Z.E., Kim, I.W., Nandigama, K., Kopp, S., Chiba, P., and Ambudkar, S.V. (2007). Catalytic cycle of ATP hydrolysis by P-glycoprotein: evidence for formation of the E.S reaction intermediate with ATP-gamma-S, a nonhydrolyzable analogue of ATP. Biochemistry *46*, 13787-13799.

Saurin, W., Hofnung, M., and Dassa, E. (1999). Getting in or out: early segregation between importers and exporters in the evolution of ATP-binding cassette (ABC) transporters. J Mol Evol *48*, 22-41.

Schiebel, E., Driessen, A.J., Hartl, F.U., and Wickner, W. (1991). Delta mu H+ and ATP function at different steps of the catalytic cycle of preprotein translocase. Cell *64*, 927-939.

Schindel, C., Zitzer, A., Schulte, B., Gerhards, A., Stanley, P., Hughes, C., Koronakis, V., Bhakdi, S., and Palmer, M. (2001). Interaction of *Escherichia coli* hemolysin with biological membranes. A study using cysteine scanning mutagenesis. Eur J Biochem *268*, 800-808.

Schmitt, L., Benabdelhak, H., Blight, M.A., Holland, I.B., and Stubbs, M.T. (2003). Crystal Structure of the Nucleotide-binding Domain of the ABC-transporter Haemolysin B: Identification of a Variable Region Within ABC Helical Domains. Journal of Molecular Biology *330*, 333-342.

Schneider, E., and Hunke, S. (1998). ATP-binding-cassette (ABC) transport systems: functional and structural aspects of the ATP-hydrolyzing subunits/domains. FEMS Microbiol Rev *22*, 1-20.

Schulein, R., Gentschev, I., Mollenkopf, H.J., and Goebel, W. (1992). A topological model for the haemolysin translocator protein HlyD. Mol Gen Genet *234*, 155-163.

Senior, A.E., and Bhagat, S. (1998). P-glycoprotein shows strong catalytic cooperativity between the two nucleotide sites. Biochemistry *37*, 831-836.

Shao, N., Singh, N.S., Slade, S.E., Jones, A.M., and Balasubramanian, M.K. (2015). Site Specific Genetic Incorporation of Azidophenylalanine in *Schizosaccharomyces pombe*. Sci Rep *5*, 17196.

Shevchik, V.E., Robert-Baudouy, J., and Condemine, G. (1997). Specific interaction between OutD, an *Erwinia chrysanthemi* outer membrane protein of the general secretory pathway, and secreted proteins. EMBO J *16*, 3007-3016.

Siarheyeva, A., Liu, R., and Sharom, F.J. (2010). Characterization of an asymmetric occluded state of P-glycoprotein with two bound nucleotides: implications for catalysis. J Biol Chem *285*, 7575-7586.

Simpson, B.W., Owens, T.W., Orabella, M.J., Davis, R.M., May, J.M., Trauger, S.A., Kahne, D., and Ruiz, N. (2016). Identification of Residues in the Lipopolysaccharide ABC Transporter That Coordinate ATPase Activity with Extractor Function. MBio *7*.

Simpson, R.J., and Greening, D.W. (2011). Serum/plasma proteomics: methods and protocols, Vol 728 (New York, N.Y.: Humana Press, c2011).

Slotboom, D.J. (2014). Structural and mechanistic insights into prokaryotic energy-coupling factor transporters. Nat Rev Microbiol *12*, 79-87.

Smith, P.C., Karpowich, N., Millen, L., Moody, J.E., Rosen, J., Thomas, P.J., and Hunt, J.F. (2002). ATP binding to the motor domain from an ABC transporter drives formation of a nucleotide sandwich dimer. Mol Cell *10*, 139-149.

Sohlenkamp, C., and Geiger, O. (2016). Bacterial membrane lipids: diversity in structures and pathways. FEMS Microbiol Rev *40*, 133-159.

Solomonson, M., Huesgen, P.F., Wasney, G.A., Watanabe, N., Gruninger, R.J., Prehna, G., Overall, C.M., and Strynadka, N.C. (2013). Structure of the mycosin-1 protease from the mycobacterial ESX-1 protein type VII secretion system. J Biol Chem *288*, 17782-17790.

Sotomayor Perez, A.C., Karst, J.C., Davi, M., Guijarro, J.I., Ladant, D., and Chenal, A. (2010). Characterization of the regions involved in the calcium-induced folding of the intrinsically disordered RTX motifs from the *Bordetella pertussis* adenylate cyclase toxin. J Mol Biol *397*, 534-549.

Spano, S., and Galan, J.E. (2013). A novel anti-microbial function for a familiar Rab GTPase. Small GTPases *4*, 252-254.

Stanley, P., Koronakis, V., and Hughes, C. (1991). Mutational analysis supports a role for multiple structural features in the C-terminal secretion signal of *Escherichia coli* haemolysin. Mol Microbiol *5*, 2391-2403.

Stanley, S.A., Raghavan, S., Hwang, W.W., and Cox, J.S. (2003). Acute infection and macrophage subversion by *Mycobacterium tuberculosis* require a specialized secretion system. Proc Natl Acad Sci U S A *100*, 13001-13006.

Stein, W.D. (1986). Transport and Diffusion Across Cell Membranes (Academic Press, San Diego).

Steinfels, E., Orelle, C., Fantino, J.R., Dalmas, O., Rigaud, J.L., Denizot, F., Di Pietro, A., and Jault, J.M. (2004). Characterization of YvcC (BmrA), a multidrug ABC transporter constitutively expressed in *Bacillus subtilis*. Biochemistry *43*, 7491-7502.

Sturm, A., Schierhorn, A., Lindenstrauss, U., Lilie, H., and Bruser, T. (2006). YcdB from *Escherichia coli* reveals a novel class of Tat-dependently translocated hemoproteins. J Biol Chem *281*, 13972-13978.

Su, C.C., Long, F., Zimmermann, M.T., Rajashankar, K.R., Jernigan, R.L., and Yu, E.W. (2011). Crystal structure of the CusBA heavy-metal efflux complex of *Escherichia coli*. Nature *470*, 558-562.

Sun, J., Deng, Z., and Yan, A. (2014). Bacterial multidrug efflux pumps: mechanisms, physiology and pharmacological exploitations. Biochem Biophys Res Commun *453*, 254-267.

Thanabalu, T., Koronakis, E., Hughes, C., and Koronakis, V. (1998). Substrate-induced assembly of a contiguous channel for protein export from *E.coli*: reversible bridging of an inner-membrane translocase to an outer membrane exit pore. EMBO J *17*, 6487-6496.

Thomas, S., Bakkes, P.J., Smits, S.H., and Schmitt, L. (2014a). Equilibrium folding of pro-HlyA from *Escherichia coli* reveals a stable calcium ion dependent folding intermediate. Biochim Biophys Acta *1844*, 1500-1510.

Thomas, S., Holland, I.B., and Schmitt, L. (2014b). The Type 1 secretion pathway - the hemolysin system and beyond. Biochim Biophys Acta *1843*, 1629-1641.

Thomas, S., Smits, S.H., and Schmitt, L. (2014c). A simple in vitro acylation assay based on optimized HlyA and HlyC purification. Anal Biochem *464*, 17-23.

Tikhonova, E.B., Dastidar, V., Rybenkov, V.V., and Zgurskaya, H.I. (2009). Kinetic control of TolC recruitment by multidrug efflux complexes. Proc Natl Acad Sci U S A *106*, 16416-16421.

Tikhonova, E.B., Yamada, Y., and Zgurskaya, H.I. (2011). Sequential mechanism of assembly of multidrug efflux pump AcrAB-TolC. Chem Biol *18*, 454-463.

Tosi, T., Pflug, A., Discola, K.F., Neves, D., and Dessen, A. (2013). Structural basis of eukaryotic cell targeting by type III secretion system (T3SS) effectors. Res Microbiol *164*, 605-619.

Trent, M.S., Worsham, L.M., and Ernst-Fonberg, M.L. (1998). The biochemistry of hemolysin toxin activation: characterization of HlyC, an internal protein acyltransferase. Biochemistry *37*, 4644-4652.

Trokter, M., Felisberto-Rodrigues, C., Christie, P.J., and Waksman, G. (2014). Recent advances in the structural and molecular biology of type IV secretion systems. Curr Opin Struct Biol *27*, 16-23.

Uchida, K., Mori, H., and Mizushima, S. (1995). Stepwise movement of preproteins in the process of translocation across the cytoplasmic membrane of *Escherichia coli*. J Biol Chem *270*, 30862-30868.

Vadas, O., Jenkins, M.L., Dornan, G.L., and Burke, J.E. (2017). Using Hydrogen-Deuterium Exchange Mass Spectrometry to Examine Protein-Membrane Interactions. Methods Enzymol *583*, 143-172.

Valent, Q.A., Kendall, D.A., High, S., Kusters, R., Oudega, B., and Luirink, J. (1995). Early events in preprotein recognition in *E. coli*: interaction of SRP and trigger factor with nascent polypeptides. EMBO J *14*, 5494-5505.

van der Heide, T., and Poolman, B. (2000). Osmoregulated ABC-transport system of *Lactococcus lactis* senses water stress via changes in the physical state of the membrane. Proc Natl Acad Sci U S A *97*, 7102-7106.

van der Heide, T., and Poolman, B. (2002). ABC transporters: one, two or four extracytoplasmic substrate-binding sites? EMBO Rep *3*, 938-943.

Vences-Guzman, M.A., Guan, Z., Bermudez-Barrientos, J.R., Geiger, O., and Sohlenkamp, C. (2013). *Agrobacteria* lacking ornithine lipids induce more rapid tumour formation. Environ Microbiol *15*, 895-906.

Verger, D., Miller, E., Remaut, H., Waksman, G., and Hultgren, S. (2006). Molecular mechanism of P pilus termination in uropathogenic *Escherichia coli*. EMBO Rep *7*, 1228-1232.

Verhalen, B., and Wilkens, S. (2011). P-glycoprotein retains drug-stimulated ATPase activity upon covalent linkage of the two nucleotide binding domains at their C-terminal ends. J Biol Chem *286*, 10476-10482.

Vollmer, W., and Bertsche, U. (2008a). Murein (peptidoglycan) structure, architecture and biosynthesis in *Escherichia coli*. Biochim Biophys Acta *1778*, 1714-1734.

Vollmer, W., Blanot, D., and de Pedro, M.A. (2008b). Peptidoglycan structure and architecture. FEMS Microbiol Rev *32*, 149-167.

Voulhoux, R., Bos, M.P., Geurtsen, J., Mols, M., and Tommassen, J. (2003). Role of a highly conserved bacterial protein in outer membrane protein assembly. Science *299*, 262-265.

Wagner, W., Vogel, M., and Goebel, W. (1983). Transport of hemolysin across the outer membrane of *Escherichia coli* requires two functions. J Bacteriol *154*, 200-210.

Wandersman, C., and Delepelaire, P. (1990). TolC, an *Escherichia coli* outer membrane protein required for hemolysin secretion. Proc Natl Acad Sci U S A *87*, 4776-4780.

Wang, B., Dukarevich, M., Sun, E.I., Yen, M.R., and Saier, M.H., Jr. (2009). Membrane porters of ATP-binding cassette transport systems are polyphyletic. J Membr Biol *231*, 1-10.

Wang, L., J., M.T., Liu, D.R., and Schultz, P.G. (2000). A new functional suppressor tRNA/aminoacyl-tRNA synthetase pair for the in vivo incorporation of unnatural amino acids into proteins. Journal of the American Chemical Society *122*, 5010-5011.

Wang, L., and Schultz, P.G. (2001). A general approach for the generation of orthogonal tRNAs. Chem Biol *8*, 883-890.

Wang, R.C., Seror, S.J., Blight, M., Pratt, J.M., Broome-Smith, J.K., and Holland, I.B. (1991). Analysis of the membrane organization of an *Escherichia coli* protein translocator, HlyB, a member of a large family of prokaryote and eukaryote surface transport proteins. J Mol Biol *217*, 441-454.

Wang, W., Takimoto, J.K., Louie, G.V., Baiga, T.J., Noel, J.P., Lee, K.F., Slesinger, P.A., and Wang, L. (2007). Genetically encoding unnatural amino acids for cellular and neuronal studies. Nat Neurosci *10*, 1063-1072.

Wang, Z., Fan, G., Hryc, C.F., Blaza, J.N., Serysheva, II, Schmid, M.F., Chiu, W., Luisi, B.F., and Du, D. (2017). An allosteric transport mechanism for the AcrAB-TolC Multidrug Efflux Pump. Elife *6*.

Ward, A., Reyes, C.L., Yu, J., Roth, C.B., and Chang, G. (2007). Flexibility in the ABC transporter MsbA: Alternating access with a twist. Proc Natl Acad Sci U S A *104*, 19005-19010.

Welch, R.A. (1991). Pore-forming cytolysins of Gram-negative bacteria. Mol Microbiol *5*, 521-528.

Welch, R.A. (2001). RTX toxin structure and function: a story of numerous anomalies and few analogies in toxin biology. Curr Top Microbiol Immunol *257*, 85-111.

Welch, R.A., Dellinger, E.P., Minshew, B., and Falkow, S. (1981). Haemolysin contributes to virulence of extra-intestinal *E. coli* infections. Nature *294*, 665-667.

Welch, R.A., Forestier, C., Lobo, A., Pellett, S., Thomas, W., Jr., and Rowe, G. (1992). The synthesis and function of the *Escherichia coli* hemolysin and related RTX exotoxins. FEMS Microbiol Immunol *5*, 29-36.

Wen, P.C., and Tajkhorshid, E. (2011). Conformational coupling of the nucleotide-binding and the transmembrane domains in ABC transporters. Biophys J *101*, 680-690.

Werner, J., and Misra, R. (2005). YaeT (Omp85) affects the assembly of lipid-dependent and lipid-independent outer membrane proteins of *Escherichia coli*. Mol Microbiol *57*, 1450-1459.

White, A.P., Collinson, S.K., Banser, P.A., Gibson, D.L., Paetzel, M., Strynadka, N.C., and Kay, W.W. (2001). Structure and characterization of AgfB from *Salmonella enteritidis* thin aggregative fimbriae. J Mol Biol *311*, 735-749.

Wickner, W., Driessen, A.J., and Hartl, F.U. (1991). The enzymology of protein translocation across the *Escherichia coli* plasma membrane. Annu Rev Biochem *60*, 101-124.

Worrall, L.J., Hong, C., Vuckovic, M., Deng, W., Bergeron, J.R., Majewski, D.D., Huang, R.K., Spreter, T., Finlay, B.B., Yu, Z.*, et al.* (2016). Near-atomic-resolution cryo-EM analysis of the *Salmonella* T3S injectisome basal body. Nature.

Wright, K.J., Seed, P.C., and Hultgren, S.J. (2007). Development of intracellular bacterial communities of uropathogenic *Escherichia coli* depends on type 1 pili. Cell Microbiol *9*, 2230-2241.

Wu, K.H., and Tai, P.C. (2004). Cys32 and His105 are the critical residues for the calcium-dependent cysteine proteolytic activity of CvaB, an ATP-binding cassette transporter. J Biol Chem *279*, 901-909.

Wu, T., Malinverni, J., Ruiz, N., Kim, S., Silhavy, T.J., and Kahne, D. (2005). Identification of a multicomponent complex required for outer membrane biogenesis in *Escherichia coli*. Cell *121*, 235-245.

Xu, Y., Lee, M., Moeller, A., Song, S., Yoon, B.Y., Kim, H.M., Jun, S.Y., Lee, K., and Ha, N.C. (2011a). Funnel-like hexameric assembly of the periplasmic adapter protein in the tripartite multidrug efflux pump in Gram-negative bacteria. J Biol Chem *286*, 17910-17920.

Xu, Y., Sim, S.H., Song, S., Piao, S., Kim, H.M., Jin, X.L., Lee, K., and Ha, N.C. (2010). The tip region of the MacA alpha-hairpin is important for the binding to TolC to the *Escherichia coli* MacAB-TolC pump. Biochem Biophys Res Commun *394*, 962-965.

Xu, Y., Song, S., Moeller, A., Kim, N., Piao, S., Sim, S.H., Kang, M., Yu, W., Cho, H.S., Chang, I.*, et al.* (2011b). Functional implications of an intermeshing cogwheel-like interaction between TolC and MacA in the action of macrolide-specific efflux pump MacAB-TolC. J Biol Chem *286*, 13541-13549.

Yen, M.R., Tseng, Y.H., Nguyen, E.H., Wu, L.F., and Saier, M.H., Jr. (2002). Sequence and phylogenetic analyses of the twin-arginine targeting (Tat) protein export system. Arch Microbiol *177*, 441-450.

Yin, Y., Zhang, F., Ling, V., and Arrowsmith, C.H. (1995). Structural analysis and comparison of the C-terminal transport signal domains of hemolysin A and leukotoxin A. FEBS Lett *366*, 1-5.

Young, T.S., Ahmad, I., Brock, A., and Schultz, P.G. (2009). Expanding the genetic repertoire of the methylotrophic yeast *Pichia pastoris*. Biochemistry *48*, 2643-2653.

Young, T.S., Ahmad, I., Yin, J.A., and Schultz, P.G. (2010). An enhanced system for unnatural amino acid mutagenesis in *E. coli*. J Mol Biol *395*, 361-374.

Yuan, Y.R., Blecker, S., Martsinkevich, O., Millen, L., Thomas, P.J., and Hunt, J.F. (2001). The crystal structure of the MJ0796 ATP-binding cassette. Implications for the structural consequences of ATP hydrolysis in the active site of an ABC transporter. J Biol Chem *276*, 32313-32321.

Zaitseva, J., Holland, I.B., and Schmitt, L. (2004). The role of CAPS buffer in expanding the crystallization space of the nucleotide-binding domain of the ABC transporter haemolysin B from *Escherichia coli*. Acta Crystallogr D Biol Crystallogr *60*, 1076-1084.

Zaitseva, J., Jenewein, S., Jumpertz, T., Holland, I.B., and Schmitt, L. (2005a). H662 is the linchpin of ATP hydrolysis in the nucleotide-binding domain of the ABC transporter HlyB. EMBO J *24*, 1901-1910.

Zaitseva, J., Jenewein, S., Wiedenmann, A., Benabdelhak, H., Holland, I.B., and Schmitt, L. (2005b). Functional characterization and ATP-induced dimerization of the isolated ABC-domain of the haemolysin B transporter. Biochemistry *44*, 9680-9690.

Zaitseva, J., Oswald, C., Jumpertz, T., Jenewein, S., Wiedenmann, A., Holland, I.B., and Schmitt, L. (2006). A structural analysis of asymmetry required for catalytic activity of an ABC-ATPase domain dimer. EMBO J *25*, 3432-3443.

Zhang, F., Sheps, J.A., and Ling, V. (1993). Complementation of transport-deficient mutants of *Escherichia coli* alpha-hemolysin by second-site mutations in the transporter hemolysin B. J Biol Chem *268*, 19889-19895.

Zhang, F., Yin, Y., Arrowsmith, C.H., and Ling, V. (1995). Secretion and circular dichroism analysis of the C-terminal signal peptides of HlyA and LktA. Biochemistry *34*, 4193-4201.

Zhang, Z., Smith, B.A., Wang, L., Brock, A., Cho, C., and Schultz, P.G. (2003). A new strategy for the site-specific modification of proteins in vivo. Biochemistry *42*, 6735-6746.

Zhou, Y., Blanco, L.P., Smith, D.R., and Chapman, M.R. (2012). Bacterial amyloids. Methods Mol Biol *849*, 303-320.

Zou, P., Bortolus, M., and McHaourab, H.S. (2009). Conformational cycle of the ABC transporter MsbA in liposomes: detailed analysis using double electron-electron resonance spectroscopy. J Mol Biol *393*, 586-597.

Zoued, A., Brunet, Y.R., Durand, E., Aschtgen, M.S., Logger, L., Douzi, B., Journet, L., Cambillau, C., and Cascales, E. (2014). Architecture and assembly of the Type VI secretion system. Biochim Biophys Acta *1843*, 1664-1673.

Zuccato, C., Valenza, M., and Cattaneo, E. (2010). Molecular mechanisms and potential therapeutical targets in Huntington's disease. Physiol Rev *90*, 905-981.

Zverev, V.V., and Khmel, I.A. (1985). The nucleotide sequences of the replication origins of plasmids ColA and ColD. Plasmid *14*, 192-199.

A. Curriculum vitae

Personal Data

Name	Sven Reimann
Date of birth	5 July 1985
Place of birth	Haan

University Education

since Sep 2012 — **Doctorate**
Heinrich-Heine-University Düsseldorf
Institute of Biochemistry
Prof. Dr. Lutz Schmitt
Regulation of the activity of the Escherichia coli ABC transporter haemolysin B

Oct 2010 – Sep 2012 — **Master of Science, Biochemistry**, grade 1.4
Heinrich-Heine-University Düsseldorf
Forschungszentrum Jülich
Prof. Dr. Karl-Erich Jaeger
Characterisation of both domains of the protease SprP of Pseudomonas aeruginosa (grade 1.0)

Oct 2006 - Sep 2010 — **Bachelor of Science, Biochemistry**, grade 2.4
Heinrich-Heine-University Düsseldorf
Forschungszentrum Jülich
Prof. Dr. Karl-Erich Jaeger
Construction and characterisation of a qspA-negative Pseudomonas aeruginosa strain (grade 1.0)

Civilian Service

Jul 2005 - Mar 2006 — Civilian Service, Krefeld
Malteser Hilfsdienst e.V
Patient Transport Ambulance

School Education

Aug 1996 - Jun 2005 — General qualification for university entrance, Abitur, grade 2.4
Ricarda-Huch-Gymnasium, Krefeld

Awards and Scholarships

Apr 2016 **Awarded best poster prize**

Reimann, S., Poschmann, G., Kanonenberg, K., Stühler, K., Smits, S. H. J., Schmitt, L., "Regulation of the ATPase activity of the T1SS ABC transporter HlyB", 10th Transporter Colloquium (GBM) in Rauischholzhausen, April 2016

Sep 2012 – Sep 2013 Scholarship of the NRW Research School BioStruct, granted by the Ministry of Innovation, Science and Research of the State North Rhine-Westphalia, the Heinrich-Heine-University Dusseldorf, and the Entrepreneur Foundation at the Heinrich-Heine-University of Dusseldorf

Conferences Attended

2016 **Reimann, S.**, Poschmann, G., Kanonenberg, K., Stühler, K., Smits, S. H.J., Schmitt, L., "Regulation of the ATPase activity of the T1SS ABC transporter HlyB", 10th Transporter Colloquium (GBM) in Rauischholzhausen, April 2016 (Presentation and Poster).

2014 Kanonenberg, K., **Reimann, S.**, Peherstorfer, S., Schwarz, C. K. W., Smits, S. H.J., Schmitt, L., "Functional characterisation of the HlyA type I secretion system in *E. coli*", ABC2014: Special Meeting in Innsbruck, Austria, March 2014 (Poster)

2013 **Reimann, S.**, Kanonenberg, K., Smits, S. H.J., Schmitt, L., "Functional and structural characterisation of the T1SS ABC transporter HlyB", BioStruct Symposium in Düsseldorf, Germany, November 2013 (Poster)

Reimann, S., Kanonenberg, K., Smits, S. H.J., Schmitt, L., "Functional and structural characterisation of the T1SS ABC transporter HlyB", Molecular Life Sciences: International Symposium of the GBM in Frankfurt am Main, Germany, October 2013 (Poster)

List of Publications

2016 Holland, I.B., Peherstorfer, S., Kanonenberg, K., Lenders, M., **Reimann, S.**, and Schmitt, L., "Type I Protein Secretion-Deceptively Simple yet with a Wide Range of Mechanistic Variability across the Family", *EcoSal Plus*, vol. 7, Dec. 2016

Reimann, S., Poschmann, G., Kanonenberg, K., Stuhler, K., Smits, S.H.J., and Schmitt, L., "Interdomain regulation of the ATPase activity of the ABC transporter haemolysin B from *Escherichia coli*," *Biochem. J.*, vol. 473, no. 16, pp. 2471–2483, Aug. 2016.

2014 Ciglia, E., Vergin, J., **Reimann, S.**, Smits, S.H., Schmitt, L., Groth, G., and Gohlke, H., "Resolving Hot Spots in the C-Terminal Dimerization Domain that Determine the Stability of the Molecular Chaperone Hsp90," *PLoS One*, vol. 9, no. 4, p. e96031, Apr. 2014

2013 Lenders, M.H.H.[a], **Reimann, S.**[a], Smits, S.H.J., and Schmitt, L., "Molecular insights into type I secretion systems.," *Biol. Chem.*, vol. 394, no. 11, pp. 1371–84, Nov. 2013
[a]contributed equally

B. Acknowledgements

An erster Stelle danke ich Prof. Dr. Lutz Schmitt. Vielen Dank, dass du es mir ermöglicht hast diesen Weg einzuschlagen und damit diese einmaligen Erfahrungen sammeln zu können. Ich danke dir für die zahlreichen Gespräche in denen du die richtigen Worte gefunden hast und damit, trotz vieler Herausforderungen für den nötigen Optimismus gesorgt hast. Ich habe mich immer wieder gefreut an deinem Enthusiasmus teilhaben zu können, der dir hoffentlich nie verloren gehen wird und der es mir ermöglichte die Forschung aus vielen faszinierenden Blickwinkeln wahrzunehmen. Lutz, danke für diese schöne Zeit!

Ein weiterer großer Dank geht an Dr. Sander Smits. Ich danke dir dafür, in brenzligen und wichtigen Situationen die nötige Ruhe und Zuversicht ausgestrahlt zu haben. Durch deine Fähigkeit die Sachen wunderbar unkompliziert auf den Punkt zu bringen, hast du mir oft die nötigen Denkanstöße gegeben um den roten Faden nicht aus den Augen zu verlieren. Ich bin dir auch ein riesiges Dankeschön schuldig für deine unendliche Geduld bei der Korrektur dieser Arbeit.

Ein großes Dankeschön möchte ich PD. Dr. Ulrich Schulte aussprechen. Deine sympathische und herzliche Art hat mir bereits meinen Start in Düsseldorf sehr angenehm gemacht und dadurch hast du auch meinen gesamten weiteren Weg unbewusst, positiv beeinflusst.

Ich bedanke mich bei Prof. Dr. Karl-Erich Jaeger für die Übernahme des Korreferats und dass ich meine ersten wissenschaftlichen Gehversuche/Abschlussarbeiten im Institut für molekulare Enzymtechnologie unternehmen durfte.
In diesem Zusammenhang bedanke ich mich auch bei Dr. Susanne Wilhelm, Dr. Alexander Pelzer und Marko Laschinski. Vielen Dank für eure wichtige Unterstützung und dass ihr meinen Einstieg in die wissenschaftliche Welt so angenehm gestaltet habt.

Dr. Cordula Kruse danke ich für die tolle Organisation und Betreuung während meines Einstiegs in die Promotion, die wunderbare Beratung während meiner Promotion, die stets offene Türe und die tiefsinnigen Gespräche.

Dr. Michael Lenders (the one and only), auch wenn es mir schwer fällt an dieser Stelle etwas seriöses zu schreiben, ich danke dir von Herzen für eine unvergessliche, verrückte Zeit im Labor, während des

Studiums und privat. Ich danke dir auch für die fachlichen und persönlichen Gespräche, die mich stets mindestens einen Schritt nach vorne gebracht haben. Die Welt braucht mehr ‚Michael'!
Marcel Lagedroste, ich danke dir dafür, dass ich an deinen wundervollen Emotionsausbrüchen teilhaben durfte, falls ein Experiment mal wieder nicht geklappt hat. Ich danke dir auch für den alltäglichen Wahnsinn der die Arbeit im Labor zu einer wahrhaft unvergesslichen Zeit gemacht hat. BÄM!
Vielen Dank Tobias Beer für die zahllosen, herrlich ausufernden Fachsimpeleien, die zu den abwegigsten und interessantesten Ideen geführt haben. Denke an dein tägliches Pensum!
Isabelle, ich wünsche dir viel Kraft und Ausdauer für die Zukunft um es mit diesen Chaoten im Labor auszuhalten und noch viel Erfolg für deine Promotion.
Ich danke Manuel Wagner dafür, dass er immer ein offenes Ohr hatte und mir durch seine Hilfsbereitschaft zur Seite stand. Vielen Dank für deine Unterstützung und deine dringend benötigte Gelassenheit an dem einen oder anderen Tag. Ach, hey Manuel …
Ich danke euch allen für die vielen konstruktiven Gespräche und die perfekte Laboratmosphäre in Lab29.

Katja Döhl, Rebecca Clemens und Martin Prescher danke ich für die ewig gute Stimmung die sie verbreitet haben und für ihre Ansprechbarkeit und Hilfsbereitschaft zu jeder Zeit. Martin, whoop! whoop!, ich finde du hast einen außergewöhnlich guten Büchergeschmack (hüstel) und ich wünsche dir noch weiterhin viel Erfolg für deine Promotion. Katja und Rebecca, ich danke euch für die kleinen Rituale des Alltags, die schönen Gespräche und das Aufzeigen meiner unentdeckten Talente, z.B. indem man mir in den Bauch piekst… Harry Potter lässt grüßen!

Vielen Dank Jens Reiners für deine Unterstützung und Feedback sowie für deine geduldige Einarbeitung bei der Betreuung des Praktikums. Ich danke dir auch, dass du Michael im Büro so gut unter Kontrolle hattest. Das hätte sonst ich ausbaden müssen…

Ich danke Dr. Diana Kleinschrodt vor allen Dingen für die vielen schönen Gespräche, für die Unterstützung in allen fachlichen Fragen und für ihre legendären Labor-Rezepte die den Alltag so viel einfacher gemacht haben.

Einen großen Applaus bitte für Iris Fey und Martina Wesemann. Vielen Dank für eure fabelhafte Unterstützung, euer know-how und eure Geduld. Ohne euren Einsatz wäre das ein oder andere Experiment (oder Praktikum) definitiv anders gelaufen oder hätte so nie statt gefunden.

I would also like to express my thanks to Sakshi Khosa for her generous help in the lab and for being such a kind person. I thank you for all your advices especially close to the final steps of my PhD and I really enjoyed the chats during our bus travels. I still regret having missed the Hogwarts Exhibition and ok, now it is official: I accept 'thingie'© is your word… but, if you have 'thingIE', I will get the patent for 'thingY', ok?!

Ein großer Dank geht an Kerstin Kanonenberg, Sandra Peherstorfer und Olivia Spitz, Leidensgenossen und Mitstreiter in dem EINEN Projekt. Ich danke euch für eure konstruktiven Gespräche, euer Feedback und eure Unterstützung. Sandra, schön dass du es am MALS mit Michael und mir ausgehalten hast, das solltest du dir eigentlich in den Lebenslauf schreiben dürfen. Bunt, verrückt und mit einem künstlerisch noch unentdeckten Talent, Olivia, danke für deine erfrischende und direkte Art. Dadurch hast du so manchem Moment die unnötige Anspannung geraubt. Einfach klasse!

I would like to mention my thanks to Tim Kroll and Eleanor Zhang for being a great company in the office and in the lab. I wish you all the best for your future steps, especially during the PhD (Tim) and your next career steps (Eleanor).

Ich danke den 'plant ladies' Kalpana Shanmugarajah und Katharina Gräfe für ihre Unterstützung im Labor und dass sie durch ihren Charme die Arbeitsatmosphäre zu etwas besonderem gemacht haben. Ich danke dir Kalpana für deine offene und herzliche Art. Katharina, dich einmal zu erschrecken war ein einschneidendes Erlebnis. Seitdem überlege ich mir immer gründlichst wie mein anschließender Fluchtplan aussieht. Aber es hat viel Spaß gemacht!

Vielen Dank an Frau Mathilde Blum für die Organisation und Verwaltung während der gesamten Promotion. Es war immer beruhigend zu wissen, dass die Dinge bei ihnen in den besten Händen sind.

Ich danke Isabell Wingartz für das herzliche Willkommen heißen im Institut und ihre geduldige Einarbeitung. Ich wünsche dir noch viel Erfolg auf deinem weiteren Weg.

Ein großes Dankeschön geht an Dr. Ricarda Moseler für ihre herzlichen, offenen Worte und ihre Unterstützung bei der Einfindung im Institut. (Wer verdammt nochmal hat die Nickel Lösung leer gemacht?) Schön, dass du es entdeckt hast, ich glaube nach diesem Vorfall haben wir uns erst so richtig kennen gelernt.

Ich danke der ‚alten Riege' Dr. Philipp Ellinger, Dr. Jan Stindt, Dr. Iris Gawarzeski, Dr. André Abts, Dr. Sabrina Thomas, Dr. Zainab AlKhatib, Dr. Nacera Infed, Dr. Susanne Przbylla, Sadber Rasid, Dr. Rakeshkumar Gupta, Dr. Nils Hanekop und explizit meinem ehemaligen Labornachbarn Dr. Christian Schwarz und Dr. Miroslav Kirov für die tolle Arbeitsatmosphäre, die beste Unterstützung und Einarbeitung im Labor.

Unseren Einsiedlern Dr. Andreas Uhde, Dr. José Montoya, Dr. Hilke Wobst und Dr. Janpeter Stock danke ich für die guten Gespräche, Tipps und dafür, dass sie sich die Zeit genommen haben mir wertvolles Feedback aus neuen Blickwinkeln zu geben.

Ich bedanke mich ebenfalls bei ‚meinen' Studentinnen/-en und aufstrebenden Wissenschaftlerinnen/-n Julia Zaschke-Kriesche, Antonio Hover, Caroline Heinrich und Nathalie Hönatsch. Vielen Dank für eure Arbeit die ihr in dieses Projekt gesteckt habt und ich wünsche euch viel Erfolg auf eurem weiteren Weg.

Ich bedanke mich bei der Internationalen NRW Forschungsschule BioStruct vom Ministerium für Innovation, Wissenschaft und Forschung des Landes Nordrhein-Westfalen, der Heinrich-Heine-Universität Düsseldorf und der Entrepreneur-Stiftung der Heinrich-Heine-Universität Düsseldorf für die finanzielle Unterstützung und Ausbildung im Rahmen meines Stipendiums.

Zu guter Letzt gilt mein Dank in besonderem Maße meinen Freunden, meiner Freundin und meiner Familie. Ich danke euch dafür, dass ihr mich immer bedingungslos dabei unterstützt habt meine Ziele zu erreichen. Ich bin dankbar dafür, euch an meiner Seite zu wissen. Ich bin dankbar für eure Rücksicht, eure Geduld und eure Liebe.

C. Declaration

Ich versichere an Eides Statt, dass die Dissertation von mir selbständig und ohne unzulässige fremde Hilfe unter Beachtung der „Grundsätze zur Sicherung guter wissenschaftlicher Praxis an der Heinrich-Heine-Universität Düsseldorf“ erstellt worden ist. Die Dissertation wurde in der vorgelegten oder in ähnlicher Form noch bei keiner anderen Fakultät eingereicht. Ich habe bisher keine erfolglosen und erfolgreichen Promotionsversuche unternommen.

(Ort, Datum) (Sven Reimann)